

**Structural Studies of Tetranortriterpenoids from the  
Congolese species of *Entandrophragma angolense***

And

**Efficient Short Step Synthesis of  
Corey's Tamiflu Intermediate**

A dissertation submitted to the Graduate School of Science and Engineering  
of Kagoshima University in partial fulfillment of the requirement for the degree of

DOCTOR OF PHILOSOPHIA

In

Nature System Sciences.

March 2008, Kagoshima

**Nsiama Tienabe Kipassa**

*To: Lydia, Timothée and Karel*

Minds are like parachutes: they only function when they're open.

Sir Thomas Robert Dewar

## Abstract

### 日本語-Japanese

本論文は二つの部分から成る。第一部は、天然物化学であり、リモノイドとして知られている有機化合物の単離および構造決定について述べる。第二部は有機合成であり、塩基触媒を用いた立体選択的な Diels-Alder 反応を利用した生理活性を持つ化合物の合成について述べる。

#### *Entandrophragma angolense* から得られたテトラノルテルペノイドの構造研究

アフリカで抗マラリア剤として使われているセンダン科 *Entandrophragma angolense* の抽出物は昆虫 *Spodoptera* に対して強い摂食阻害活性を示しました。そこで、この植物に含まれる生理活性化合物の調査を行った。植物のヘキサン、エーテル及びメタノール抽出物をクロマトグラフ法を用いて精製したところ、23 種の化合物が単離することができた。これらの化合物の構造は高分解マスペクトル、1D 及び 2D NMR などによって決定し、23 種のうち 21 種が protolimonoids、gedunin、mexicanolide、andirobin 及び phragmalin 誘導体に分類されるリモノイドであることが確認された。得られた化合物のうち 16 種は新規化合物であり、5 種は既知の methyl angolensante、methyl 6-acetoxiangolensante, secomahoganin, 3 $\beta$ -hydroxy-3-deoxycarapin 及び and xylocensin K であるとして同定された。

#### Corey のタミフル合成中間体の効率的な合成法の開発

当研究室で開発された塩基触媒 Diels-Alder 反応を利用し、タミフルの合成中間体の効率的な合成法の開発を行った。本研究では *N*-nosyl-3-hydroxy-2-pyridone と ethyl acrylate との塩基触媒 Diels-Alder 反応の付加体を出発原料とし、Corey らのタミフル合成中間体の合成法を確立した。この合成法は、わずか四段階の変換と三回の精製過程を経るだけで目的化合物を得られる効率的な法である。

## English-英語

This dissertation comprises two parts, one is the chemistry of natural products dealing with the isolation and structure elucidation of limonoids and the second part is synthetic organic chemistry dealing with the use of a stereoselective base-catalyzed Diels-Alder reaction for the synthesis of small biologically active compound ingredient.

### Structural Studies of Tetranortriterpenoids from the Congolese species of *Entandrophragma angolense*

The extracts of *E. angolense*, a Meliaceae plant used in African folk medicine against malaria, displayed considerable antifeedant activity against *Spodoptera* insects. Thus, the plant was selected for further fractionation of its extracts. The fractionation of the extracts has been carried out using chromatographic methods and resulted to the isolation of twenty-three compounds. The structure elucidation of these compounds was performed by spectroscopic methods including mass spectrometry, 1D and 2D NMR. Two compounds are not limonoids and the remaining ones are limonoids and could be classified as protolimonoid, gedunin, andirobin and phragmalin compound-types. Sixteen compounds have been found to be new rings and the five known compounds isolated have been identified as methyl angolensante, methyl 6-acetoxyangolensante, secmahoganin, 3 $\beta$ -hydroxy-3-deoxycarapin and xylocensin K.

### Efficient Short Step Synthesis of Corey's Tamiflu Intermediate

Catalysts have been used to facilitate the Diels-Alder reaction and almost catalysts developed are Lewis acids. Our lab developed a unique base-catalyzed diastereoselective Diels-Alder reaction of pyridone derivative as diene and electron deficient dienophiles. The unique poly-functionalized bicyclic lactam obtained from the reaction between *N*-nosyl-3-hydroxy-2-pyridone and ethyl acrylate has been used as building block for the synthesis of Corey's Tamiflu intermediate. This synthesis route is short and the production of different intermediates is simple. Only four chemical transformations and three purification steps are required to obtain the targeted compound, equivalent to the Tamiflu intermediate from the Diels-Alder adduct.

## Acknowledgments

I am so grateful to the Ministry of Education, Culture, Sports, Science and Technology of Japan for giving me the opportunity to do graduate studies at Kagoshima University/ Japan.

I wish to express my gratitude to Professor Nakatani, Department of Chemistry, Faculty of Science, Kagoshima University for his supervision. His patience and understanding helped me to improve this work.

I would like to express also my deepest sense of gratitude, sincere appreciation and profound regards to Associate Professor Hiroaki Okamura for his scholastic guidance, constant encouragement for the completion of my ph d studies.

It is my pleasure to express my sincerest gratitude to Professor Tetsuo Iwagawa for his understanding and I appreciated a lot the support he had given me in the accomplishment of my ph d studies.

Words cannot express the debt and love that me and family owe to Hiroshi, Shouko and Akiko Matsuda. They are our second family; their love, wisdom, attention warmed our hearts during painful moments and have been a great support for us.

A special thank to Professor Taba Kalulu (Faculty of Science/Kinshasa University) for his initial guidance to strengthen my research skills. He convinced and gave me motivation to do advanced studies especially at the ph d level.

I would like to thank also M. Yannick Vincendeau, the General Manager of Centre Hospitalier Monkole and M. Crispin Mulaji Kyela, Junior Lecturer at Faculty of Science/Chemistry Department/Kinshasa University for their contribution in the collection of Meliaceae plant samples used for this study. I would like to thank also M. Paul Kamba Malumba, Junior lecturer at Faculty of Agriculture/Kinshasa University for identification of the plant.

I am very thankful to Professor Maki Oshima, Director of the International Student Center, for her support and encouragement but most of all thank you for being concerned about me.

Finally, I expressed also my gratitude to all my labmates during the past five and half years to whom I would like to say these words in Japanese : 仲がよくしてくれてありがとうございました.

## Table of contents

<b>ABSTRACT</b> .....	<b>I</b>
<b>ACKNOWLEDGMENTS</b> .....	<b>III</b>
<b>TABLE OF CONTENTS</b> .....	<b>IV</b>
<b>LIST OF FIGURES</b> .....	<b>VII</b>
<b>LIST OF SCHEMES</b> .....	<b>IX</b>
<b>LIST OF TABLES</b> .....	<b>X</b>
<b>LIST OF ABBREVIATIONS</b> .....	<b>XI</b>

### *PART ONE*

<b>INTRODUCTION</b> .....	<b>1</b>
<b>CHAPTER I. LIMONIDS</b> .....	<b>3</b>
<b>I.1. Plant chemicals</b> .....	<b>3</b>
<b>I.2. Limonoids</b> .....	<b>6</b>
I.2.1. Definition .....	6
I.2.2. Biosynthesis of limonoids .....	6
<b>I.3. Classification of limonoids</b> .....	<b>8</b>
<b>I.4. Biological activity of limonoids</b> .....	<b>10</b>
I.4.1. Antimalarial activity .....	10
I.4.2. Antiviral activity .....	11
I.4.3. Cell adhesion inhibition .....	12
I.4.4. Antitumour .....	13
I.4.5. Antifeedant .....	16
I.4.6. Antifungal .....	17
I.4.7. Antibacterial .....	20
I.4.8. Antioxidant .....	20
I.4.9. Anti-ulcer .....	20
I.4.10. Spermicidal activity .....	20
I.4.11. Plant-growth inhibitory activities .....	21
I.4.12. Moulting inhibiting activity .....	22
I.4.13. Insect growth inhibition .....	22

<b>CHAPTER II. THE CHEMISTRY OF THE GENUS <i>ENTANDROPHRAGMA</i></b> -----	<b>23</b>
<b>II.1. Introduction</b> -----	<b>23</b>
<b>II.2. Uses</b> -----	<b>24</b>
<b>II.3. Chemistry of Meliaceae</b> -----	<b>24</b>
<b>II.4. Chemistry of the genus <i>Entandrophragma</i></b> -----	<b>26</b>
II.4.1. <i>Entandrophragma delevoyi</i> -----	27
II.4.2. <i>Entandrophragma excelsum</i> Sprague-----	28
II.4.3. <i>Entandrophragma macrophyllum</i> A. Chev.-----	28
II.4.4. <i>Entandrophragma bussei</i> Harms ex Engler-----	29
II.4.5. <i>Entandrophragma candollei</i> Harms-----	29
II.4.6. <i>Entandrophragma caudatum</i> Sprague-----	30
II.4.7. <i>Entandrophragma cylindricum</i> Sprague-----	32
II.4.8. <i>Entandrophragma palustre</i> Staner-----	32
II.4.9. <i>Entandrophragma spicatum</i> Sprague-----	33
II.4.10. <i>Entandrophragma utile</i> Sprague-----	33
II.4.11. <i>Entandrophragma angolense</i> -----	35
<b>II.5. Purpose of this work</b> -----	<b>37</b>
<b>II.6. Description of the plant under study<sup>108</sup></b> -----	<b>38</b>
<b>CHAPTER III. MATERIAL AND METHODS</b> -----	<b>39</b>
<b>III.1. General</b> -----	<b>39</b>
<b>III.2. Plant material</b> -----	<b>39</b>
<b>III.3. Extraction and isolation</b> -----	<b>39</b>
III.3.1. Preparation of extracts-----	39
III.3.2 Purification of the hexane extract-----	41
III.3.2. Purification of the ether extract-----	42
III.3.3. Purification of the methanol extract-----	42
<b>CHAPTER IV. STRUCTURE ELUCIDATION</b> -----	<b>47</b>
<b>IV.1. Introduction</b> -----	<b>47</b>
<b>IV.2. Classification of isolated compounds</b> -----	<b>47</b>
IV.2.1. Protolimonoids-----	47
IV.2.2. Gedunin derivatives-----	47
IV.2.3. Andirobin derivatives-----	48
IV.2.4. Mexicanolides derivatives-----	48
IV.2.5. Phragmalin derivatives-----	49
<b>IV.3. Structure determination</b> -----	<b>49</b>
IV.3.1. Protolimonoids-----	49
IV.3.2 Gedunin derivatives-----	54
IV.3.3. Mexicanolide derivatives-----	57
IV.3.4. Phragmalin derivatives-----	65
<b>CHAPTER V. SUMMARY</b> -----	<b>84</b>

## PART TWO

<b>INTRODUCTION</b> .....	<b>85</b>
<b>CHAPTER I. TAMIFLU DESIGN AND TOTAL SYNTHESIS</b> .....	<b>88</b>
<b>I.1. Introduction</b> .....	<b>88</b>
<b>I.1. Gilead drug design and synthesis.</b> .....	<b>89</b>
I.1.1. Drug design .....	89
I.1.2. Large scale production of compounds 6a-6f .....	93
I.1.3. Current industrial synthesis of oseltamivir phosphate .....	94
I.1.4. Azide-free transformations .....	96
I.1.5. Shikimic and quinic acids-independent routes .....	98
I.1.6. Academic chemists approaches on Tamiflu synthesis .....	100
<b>CHAPTER II. BASE-CATALYZED DIELS-ALDER APPROACH TO OSELTAMIVIR INTERMEDIATE</b> .....	<b>108</b>
<b>II.1. Introduction</b> .....	<b>108</b>
<b>II.2. Base catalyzed Diels-Alder reaction in our laboratory</b> .....	<b>109</b>
<b>II.3. Retrosynthesis of Tamiflu Intermediate</b> .....	<b>109</b>
<b>II.4. Synthesis of the Intermediate</b> .....	<b>110</b>
II.4.1. Preparation of the diene .....	110
II.4.2. Diels-Alder reaction of <i>N</i> -nosyl-3-hydroxy-2-pyridone .....	111
II.4.3. Synthesis of the targeted compound .....	112
II.4.4. Alternative route to the Corey's Tamiflu Intermediate .....	113
<b>II.5. Conclusion</b> .....	<b>114</b>
<b>CHAPTER III. EXPERIMENTAL SECTION</b> .....	<b>115</b>
<b>CHAPTER IV. SUMMARY</b> .....	<b>119</b>
<b>REFERENCES</b> .....	<b>120</b>



## List of figures

- Figure 1. Isolated tetranortriterpenoids from *E. angolense*
- Figure 2. COSY and selected HMBC correlations in **12**
- Figure 3. Computer-generated energy minimized model of **12** with key NOE correlations observed.
- Figure 4. COSY and selected HMBC correlations in **3**
- Figure 5. Computer-generated energy minimized model of **3** with key NOE correlations observed
- Figure 6. COSY and selected HMBC correlations in **4**
- Figure 7. Computer-generated energy minimized model of **4** with key NOE correlations observed
- Figure 8. COSY and selected HMBC correlations in **8**
- Figure 9. Computer-generated energy minimized model of **8** with key NOE correlations observed
- Figure 10. COSY and selected HMBC correlations in **14**
- Figure 11. Computer-generated energy minimized model of **14** with key NOE correlations observed
- Figure 12. COSY and selected HMBC correlations in **2**
- Figure 13. Computer-generated energy minimized model of **2** with key NOE correlations observed
- Figure 14. COSY and selected HMBC correlations in **16**
- Figure 15. Computer-generated energy minimized model of **16** with key NOE correlations observed
- Figure 16. COSY and selected HMBC correlations in **18**
- Figure 17. Computer-generated energy minimized model of **18** with key NOE correlations observed
- Figure 18. COSY and selected HMBC correlations in **9**
- Figure 19. Computer-generated energy minimized model of **9** with key NOE correlations observed
- Figure 20. COSY and selected HMBC correlations in **15**
- Figure 21. Computer-generated energy minimized model of **15** with key NOE correlations observed
- Figure 22. COSY and selected HMBC correlations in **7**
- Figure 23. Computer-generated energy minimized model of **7** with key NOE correlations observed
- Figure 24. COSY and selected HMBC correlations in **6**
- Figure 25. Computer-generated energy minimized model of **6** with key NOE correlations observed
- Figure 26. COSY and selected HMBC correlations in **11**
- Figure 27. Computer-generated energy minimized model of **11** with key NOE correlations observed
- Figure 28. COSY and selected HMBC correlations in **17**
- Figure 29. Computer-generated energy minimized model of **17** with key NOE correlations observed

- Figure 30. COSY and selected HMBC correlations in **22**
- Figure 31. Computer-generated energy minimized model of **22** with key NOE correlations observed
- Figure 32. COSY and selected HMBC correlations in **23**
- Figure 33. Computer-generated energy minimized model of **23** with key NOE correlations observed

## List of schemes

- Scheme 1. Terpenoid groups
- Scheme 2. Cyclization of oxidosqualene to form bicyclic compounds
- Scheme 3. Biosynthesis of limonoids
- Scheme 4. The relationship between limonoids
- Scheme 5. Preparation of crude extracts from the root bark of *E. angolense*
- Scheme 6. Isolation of limonoids from the *n*-hexane extract
- Scheme 7. Purification of the ether extract
- Scheme 8. Isolation of limonoids from the methanol extract
- Scheme 9. Rational design of carbocyclic Transition-State Analogues
- Scheme 10. Synthetic pathway of NA carbocyclic inhibitors
- Scheme 11. Large-scale production of oseltamivir for clinical studies
- Scheme 12. Quinic acid route to industrial production of epoxide **22**
- Scheme 13. Shikimic acid route to industrial production of epoxide **22**
- Scheme 14. Azide-free allylamine route to oseltamivir phosphate
- Scheme 15. Azide-free *t*-butylamine-diallylamine route to oseltamivir phosphate
- Scheme 16. Diels-Alder concept in the synthesis of oseltamivir
- Scheme 17. Aromatic rings transformation route to oseltamivir
- Scheme 18. Shibasaki route 1 to oseltamivir phosphate
- Scheme 19. Shibasaki route 2 to oseltamivir phosphate
- Scheme 20. Shibasaki route 3 to oseltamivir phosphate
- Scheme 21. Cong route to oseltamivir phosphate active ingredient
- Scheme 22. Corey synthesis of oseltamivir phosphate
- Scheme 23. Fukuyama synthesis of oseltamivir phosphate
- Scheme 24. Bromfield approach to oseltamivir synthesis
- Scheme 25. Discovery of Diels-Alder reaction
- Scheme 26. Retrosynthesis of Corey's oseltamivir phosphate intermediate
- Scheme 27. Production of the diene **138**
- Scheme 28. Preparation of Corey's oseltamivir phosphate intermediate equivalent **143**
- Scheme 29. Alternative route to the Corey's oseltamivir phosphate intermediate **103**

## List of tables

Table 1. Classification of Protolimonoids and Limonoids

Table 2. The Meliaceae subdivision

Table 3.  $^1\text{H}$  and  $^{13}\text{C}$  NMR spectroscopic data of compounds **12**, **3** and **4**.

Table 4.  $^1\text{H}$  and  $^{13}\text{C}$  NMR spectroscopic data of compounds **8** and **14**.

Table 5.  $^1\text{H}$  and  $^{13}\text{C}$  NMR spectroscopic data of angolensins A (**2**), B (**16**) and C (**18**)

Table 6.  $^1\text{H}$  and  $^{13}\text{C}$  NMR spectroscopic data angolensins D (**9**), E (**15**) and F (**7**)

Table 7.  $^1\text{H}$  and  $^{13}\text{C}$  NMR spectroscopic data of compounds **6**, **11** and **17**

Table 8.  $^1\text{H}$  and  $^{13}\text{C}$  NMR spectroscopic data of compounds **22** and **23**

Table 9. Structure-activity relationship among analogue with various alkyl chains

## List of abbreviations

DEPT	Distortionless Enhancement by Polarization Transfer
FABMS	Fast Atom Bombardment Mass Spectrometry
HMBC	Heteronuclear Multiple Bond Correlation
HMQC	Heteronuclear Multiple Quantum Correlation
MPC	Middle Pressure Chromatography
HPLC	High Performance Liquid Chromatography
HRFABMS	High Resolution Fast Atom Bombardment Mass Spectrometry
MeCN	Acetonitrile
MeOH	Methanol
NMR	Nuclear Magnetic Resonance
NOE	Nuclear Overhauser Effect
CC	Column Chromatography
VCC	Vacuum Column Chromatography
NA	Neuraminidase
H	Haemagglutinin
AIBN	2,2'-azobisisobutyronitrile
Alloc	allyloxycarbonyl
BBN	borabicyclo[3.3.1]nonane
Boc	<i>tert</i> -butoxycarbonyl
DMAP	4-dimethylaminopyridine
DMF	<i>N,N</i> -dimethylformamide
dppp	1,3-bis(diphenylphosphanyl)propane
EWG	electron withdrawing group
imid.	imidazole
MOM	methoxymethyl
PMB	<i>p</i> -methoxybenzyl
pyr	pyridine
TBAF	tetra- <i>n</i> -butylammonium fluoride
TBDPS	<i>tert</i> -butyldiphenylsilyl
TBS	<i>tert</i> -butyldimethylsilyl
Tf	trifluoromethanesulfonyl
DIPEA	<i>N,N'</i> -Diisopropylethylamine
DPPA	Diphenylphosphorylazide
DEPC	Diethyl pyrocarbonate
THF	tetrahydrofuran
EtOH	ethanol

rt	room temperature
DME	Dimethoxyethane
PCC	Pyridinium chlorochromate
DBU	1,8-Diazobicyclo[5.4.0]undec-7-ene
NBA	<i>N</i> -bromoacetamide
DMP	Dimethoxypropane
KHDMS	Hexamethyl disilylazane potassium
NaHDMS	Hexamethyl disilylazane sodium
NBS	<i>N</i> -bromosuccinimide
NsCl	Nosyl, 2-nitrobenzenesulfonyl

## **Introduction**

Plant chemicals are often classified as either primary or secondary metabolites. Primary metabolites are substances widely distributed in nature, occurring in one form or another in virtually all organisms. In higher plants such compounds are often concentrated in seeds and vegetative storage organs and are needed for physiological development because of their role in basic cell metabolism. (Examples: carbohydrates, lipids, proteins...)<sup>1</sup>.

Secondary metabolites are compounds biosynthetically derived from primary metabolites. Contrary to primary metabolites these compounds are not ubiquitous in the living organisms that produce them nor are they necessarily expressed continuously. Although plants are better known as a source of secondary metabolites, bacteria, fungi and many marine organisms (sponges, tunicates, corals, snails) are very interesting sources, too. Secondary metabolites, also known as natural products are not essential for normal growth, development or reproduction of an organism. In this sense they are "secondary". The function or importance of these compounds to the organism's development is usually of ecological nature as they are used as defence against predators (herbivores, pathogens etc.), for interspecies competition, and to facilitate the reproductive processes<sup>2</sup>.

Secondary metabolites can be classified by their chemical structure or physical properties into one or more of the following groups: alkaloids, terpenoids, polyketides, aliphatic, aromatic, and heteroaromatic organic acids, phenols, iridoids, steroids, saponins, peptides, ethers, oils, resins and balsams. The terpenoids constitute the largest family of natural products derived from C<sub>5</sub> isoprene units and one of the typical structures contains 30 carbons in its basic skeleton and it is known as triterpenoid<sup>2</sup>.

The triterpenoid skeleton may be subjected to a variety of structural modifications. A particular modification leads to loss of several skeletal carbon atoms. Pre-eminent among such degraded triterpenoids are the steroids (containing the tetracyclic ring system of lanosterol, but lacking the three methyl groups at C-4, and C-14), quassinoids (which have lost ten carbons, including one of the C-4 methyls) and limonoids (in which four terminal carbons from the side chain are removed, tetranortriterpenoids).

Limonoids production is confined to plants in the order of Rutales. In particular, they characterize members of the family Meliaceae, where they are diverse and abundant. And thus, their presence can be used for chemotaxonomic purpose<sup>3</sup>.

Several preparations from leaves, seeds, stem bark and roots of many plants belonging to the Meliaceae family have been also widely used in traditional medicine and limonoids are believed to be the most important active principle of the plants of this family. Indeed, several studies have established a wide range of biological activities for these compounds, including insect antifeedant and growth regulating properties, a variety of medicinal effects in animals and humans, and antifungal, bacteriocidal and antiviral activities<sup>4</sup>.

Chemically, limonoids have been classified on the basis of which the four rings, designated as A, B, C and D in the intact triterpene nucleus, have been subjected to oxidative changes which could be also accompanied by some molecular rearrangements.

Protolimonoids appear to be biochemical precursors of the limonoids and can have an oxidised side chain, which may or may not have been cyclised. Ring *D-seco* compounds (gedunin, III) are commonly found in the African mahogany plants together with rings *B,D-seco* compounds. Rings *B,D-seco* compounds are divided into 4 subgroups depending on whether further transformations have occurred. The first subgroup is having the rings B cleaved and D oxidatively opened (andirobins IVa). A second subgroup, derived from andirobin by contraction of ring C (trijuginin IVb) while in the third subgroup a new ring has been formed between C-2 and C-30 (mexicanolide, IVc). The fourth subgroup observed is the one derived for further modification of mexicanolide by bridging of ring A (phragmalin, IVd).

During an investigation on antifeedant limonoid compounds from Meliaceae plants, the root bark extract of *Entandrophragma angolense*, a plant used in African folk medicine as febrifuge for malarial fever, displayed considerable activity against *Spodoptera* insects and has been selected for further investigations.

In the past, the very first phytochemical studies of this plant led to the isolation of rings *B,D-seco* compounds methyl angolensate (major component)<sup>5</sup> and gedunin<sup>6</sup>. Interestingly, the discovery of gedunin in this plant gave a start to the chemical development of limonoids<sup>7</sup>.

The protolimonoid entandrolide was isolated from the seeds<sup>8</sup>. In the last decade, two phytochemical studies have been reported. One led to the isolation of triterpenoids compounds, 3,23-dioxotirucalla-7,24-dien-21-al, 3,4-secotirucalla-23-oxo-4,7,24-trien-21-al-3-oic acid and 3,4-secotirucalla-23-oxo-4(28),7,24-trien-3,21-dioic acid (21-methyl ester)<sup>9</sup>. The other described the isolation of ring *A,D-seco* compounds 7 $\alpha$ -acetoxydihydnomilin, and 7 $\alpha$ -obacunyl acetate, along with 22-hydroxyhopan-3-one, 24-methylene-cycloartenol, tricosanoic acid, methyl angolensate, methyl oleanate and betulinic acid<sup>10</sup>.

A series of experiments have been carried out on the limonoid constituents of the hexane, ether and methanol extracts of the root bark of this plant. The extracts were fractionated using mainly chromatographic methods. Successfully, some limonoids compounds were isolated and their structures have been elucidated by spectroscopic means. In this dissertation, the results of this investigation are described.

Thus, for a better understanding, the present work is broken up into five chapters. The first chapter describes the limonoids chemistry with some examples of reported active compounds. The second is a review exploring the chemistry of the genus *Entandrophragma*. The third chapter is centered in the description of material and methods. The fourth chapter is a discussion on the structure elucidation and the fifth and last chapter summarized results obtained during these studies.



## **Chapter I. Limonoids**

### **I.1. Plant chemicals**

Plant chemicals are often classified as either primary or secondary metabolites. Primary metabolites are substances widely distributed in nature, occurring in one form or another in virtually all organisms. In higher plants such compounds are often concentrated in seeds and vegetative storage organs and are needed for physiological development because of their role in basic cell metabolism. (Examples: carbohydrates, lipids, proteins...)<sup>1</sup>.

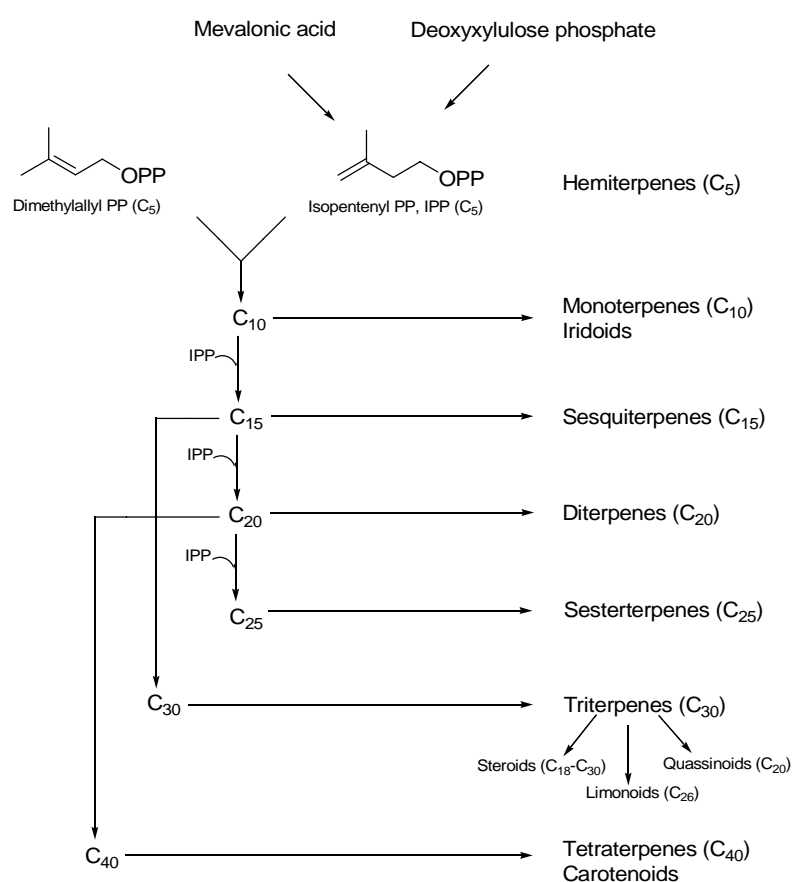
Secondary metabolites are compounds biosynthetically derived from primary metabolites. Contrary to primary metabolites these compounds are not ubiquitous in the living organisms that produce them nor are they necessarily expressed continuously. Although plants are better known as a source of secondary metabolites, bacteria, fungi and many marine organisms (sponges, tunicates, corals, and snails) are very interesting sources, too. Secondary metabolites, also known as natural products are not essential for normal growth, development or reproduction of an organism. In this sense they are "secondary". The function or importance of these compounds to the organism's development is usually of ecological nature as they are used as defence against predators (herbivores, pathogens etc.), for interspecies competition, and to facilitate the reproductive processes<sup>1,2</sup>.

Secondary metabolites can be classified by their chemical structure or physical properties into one or more of the following groups: alkaloids, terpenoids, polyketides, aliphatic, aromatic, and heteroaromatic organic acids, phenols, iridoids, steroids, saponins, peptides, ethers, oils, resins and balsams. The terpenoids constitute the largest family of natural products derived from C<sub>5</sub> isoprene units. Typical structures contain carbon skeletons represented by (C<sub>5</sub>)<sub>n</sub>, and are classified as hemiterpenes (C<sub>5</sub>), monoterpenes (C<sub>10</sub>), sesquiterpenes (C<sub>15</sub>), diterpenes (C<sub>20</sub>), sesterterpenes (C<sub>25</sub>), triterpenes (C<sub>30</sub>) and tetraterpenes (C<sub>40</sub>). Many other natural products such as alkaloids, phenolics, and vitamins contain terpenoid elements in their molecules also<sup>2</sup>.

An unusually complex and flexible reaction mechanism generates these ring systems. In the early 1950s, Ruzicka and co-workers deduced that all C<sub>30</sub>H<sub>50</sub>O triterpene alcohols known by that time were biosynthesized similarly, and they proposed the biogenetic isoprene rule, a set of governing principles that could explain the biosynthesis of these compounds<sup>11</sup>.

However isoprene, considered as building block for these compounds, is produced naturally but is not involved in the formation of terpenoids. The biochemically active isoprene units were identified as the diphosphate (pyrophosphate) esters dimethylallyl diphosphate (DMAPP) and isopentenyl diphosphate (IPP) which may be derived by two pathways, by way of intermediates mevalonic acid or 1-deoxy-D-xylulose 5-phosphate (deoxyxylulose phosphate)<sup>2</sup>.

Terpenoids play diverse functional roles in plants as hormones (gibberellins, abscisic acid), photosynthetic pigments (phytol, carotenoids), electron carriers (ubiquinone, plastoquinone), mediators of polysaccharide assembly (polyprenyl phosphates), and structural components of membranes (phytosterols). In addition to these universal physiological, metabolic, and structural functions, many specific terpenoid compounds (commonly in the C<sub>10</sub>, C<sub>15</sub>, and C<sub>20</sub> families) serve in communication and defense, for example, as attractants for pollinators and seed dispersers, competitive phytotoxins, antibiotics, and herbivore repellents and toxins. Terpenoids available in relatively large amounts as essential oils, resins, and waxes are important renewable resources and provide a range of commercially useful products, including solvents, flavorings and fragrances, adhesives, coatings, and synthetic intermediates. Members of the terpenoid group also include industrially useful polymers (rubber, chicle) and a number of pharmaceuticals (artemisinin, taxol) and agrochemicals (pyrethrins, azadirachtin)<sup>12</sup>.

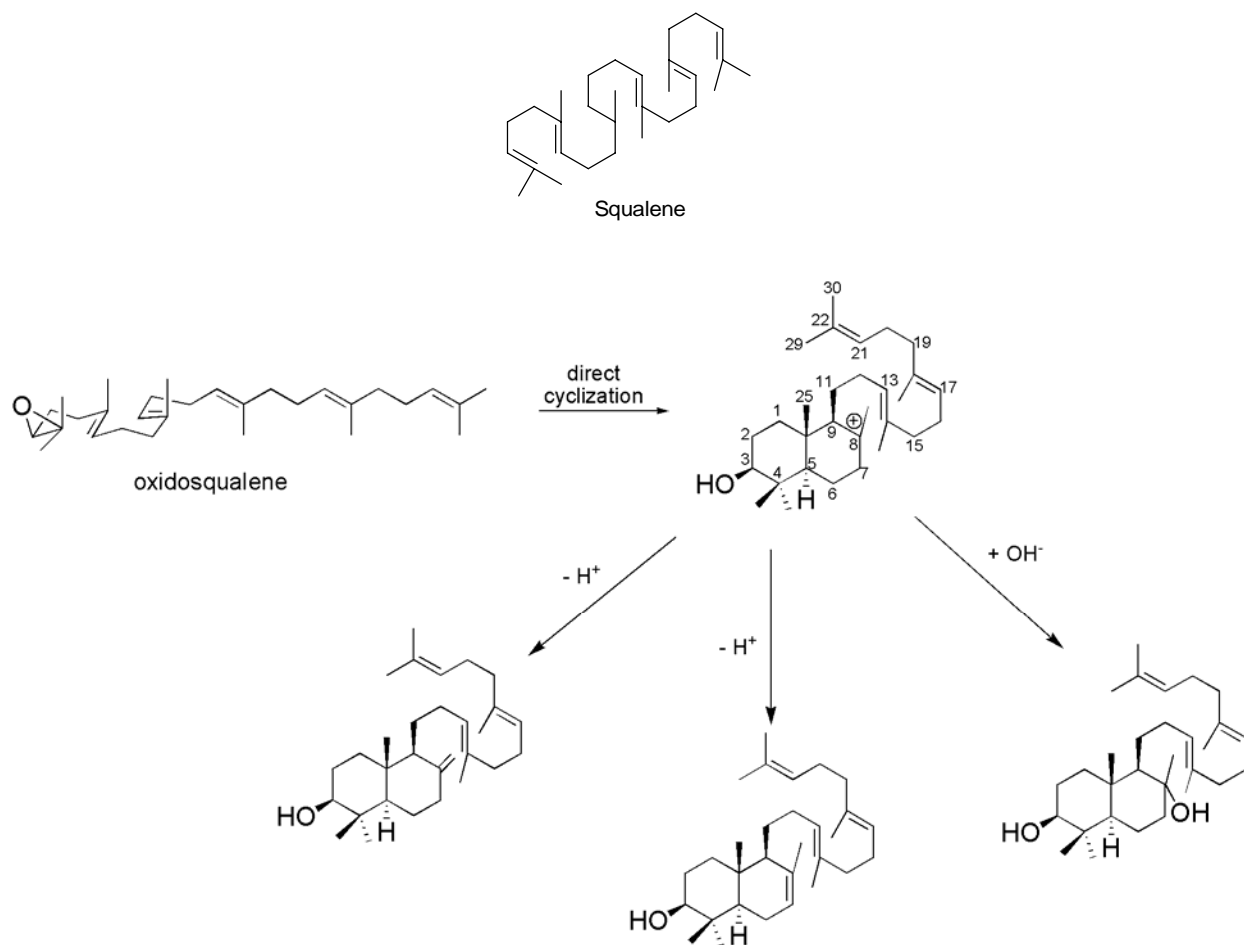


**Scheme 1.** Terpenoid groups

The triterpenoids are a large and structurally diverse group of natural products derived from squalene or related acyclic 30-carbon precursors.

As a general mechanism of production of triterpenoids, all-trans squalene or oxidosqualene is activated by cationic attack. A cascade of cation-olefin cyclizations then generates a cyclic carbocation, which can rearrange and cyclize further. Antiperiplanar shifts terminated by proton loss then yield a neutral species. Scheme 2 depicted the formation of a bicyclic triterpenes compounds<sup>11</sup>.

Several decades of research have refined the biogenetic isoprene rule. Extensive efforts in natural product isolation provided numerous additional triterpenoids, which consistently had structures that could be rationalized by the biogenetic isoprene rule, providing further support for these guidelines. Consequently, although the formation of only a minority of triterpenoid ring systems has been experimentally investigated, enzyme-mediated cyclization of squalene or oxidosqualene under the biogenetic rule is the most credible origin of these triterpenoids. The biogenetic isoprene rule predicts product structures so consistently that the plausibility of a newly assigned structure can be assessed based on whether its formation can be deduced according to the isoprene rule<sup>11</sup>.



**Scheme 2.** Cyclization of oxidosqualene to form bicyclic compounds

Triterpenoids display well over 100 distinct skeletons. Most are 6-6-6-5 tetracycles, 6-6-6-6-5 pentacycles, or 6-6-6-6-6 pentacycles, but acyclic, monocyclic, bicyclic, tricyclic, and hexacyclic triterpenoids have also been isolated from natural sources.

The triterpenoid skeletons may be subjected to a variety of structural modifications. A particular modification leads to loss of several skeletal carbon atoms. Pre-eminent among such degraded triterpenoids are the steroids (containing the tetracyclic ring system of lanosterol, but lacking the three methyl groups at C-4, and

C-14), quassinoids (which have lost ten carbons, including one of the C-4 methyls) and limonoids (in which four terminal carbons from the side chain are removed, tetranortriterpenoids)<sup>2</sup>.

Limonoids production is confined to plants in the order of Rutales. In particular, they characterize members of the family Meliaceae, where they are diverse and abundant. A more limited range of structures is found in the families Rutaceae and Cneoraceae. In the family Simabouraceae, only *Harrisonia abyssinica* is known to produce limonoids, although other species commonly contain the biosynthetically related quassinoids<sup>13</sup>.

Currently limonoids are under investigation for a wide variety of therapeutic effects such as antiviral, antifungal, antibacterial, antineoplastic and antimalarial. They also show effectiveness as insecticides.

## **I.2. Limonoids**

### **I.2.1. Definition**

Limonoids are derived from tetracyclic triterpenes similar to euphol (H-20 $\beta$ ) or tirucallol (H-20 $\alpha$ ) by a series of oxidative changes, interspersed with molecular rearrangements. In the course of these changes, the side chain is oxidized eventually to a  $\beta$ -substituted furan ring by the loss of four carbon atoms; hence an alternative name, tetranortriterpenoids with 4,4,8-trimethyl-17-furanylsteroidal skeleton.

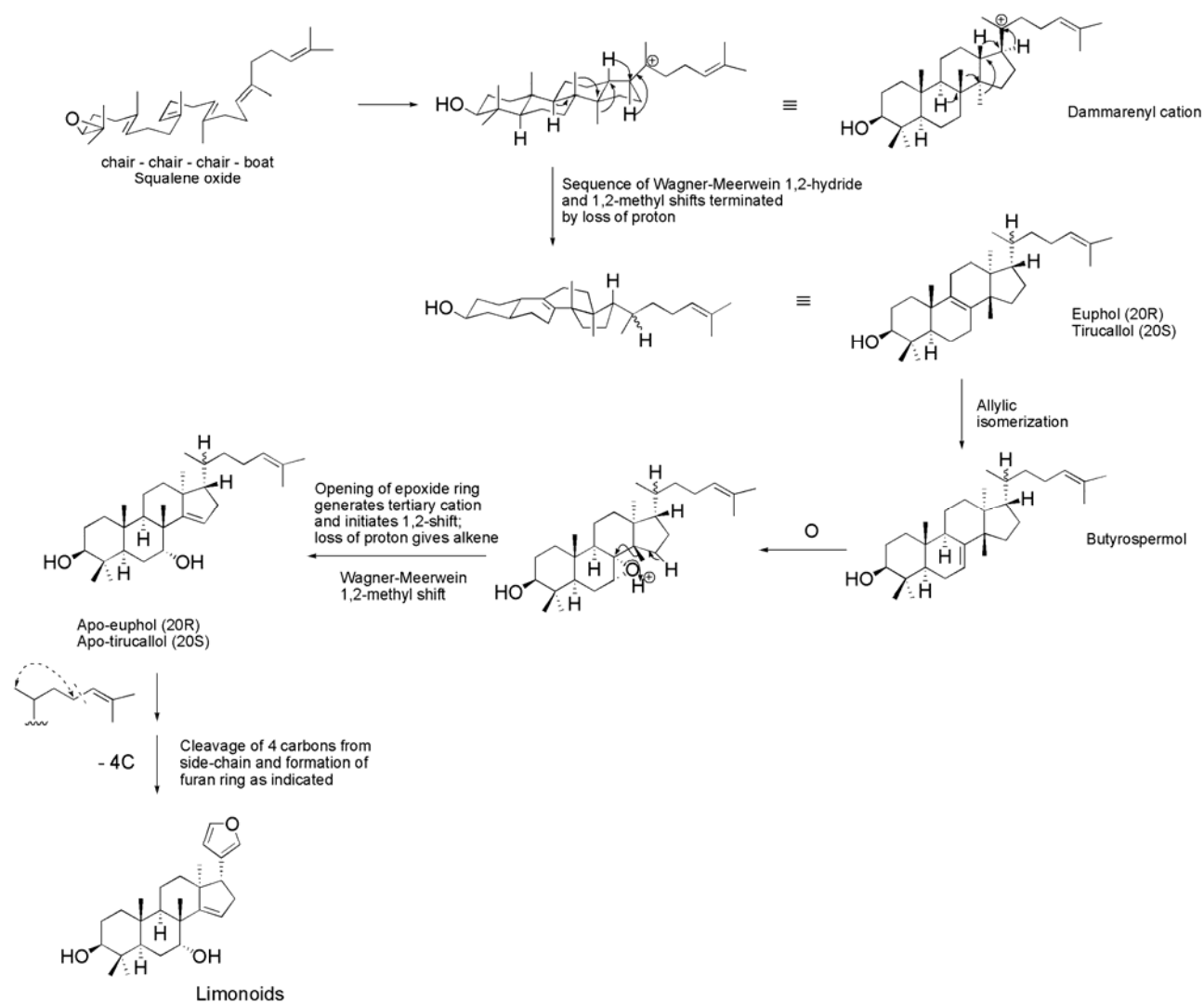
Protolimonoids appear to be biochemical precursors of the limonoids. Protolimonoids that have an oxidized side chain, which may or may not have been cyclised, have either a double bond between C7 and C8, or have undergone an apo-euphol rearrangement to give a methyl group at C-8 and a C-14, C-15 double bond, or are intermediate as in the glabretal-type compounds which have a C-13, C-14, C-18 cyclopropane ring<sup>14</sup>.

Limonoids show a high degree of structural variation which can easily be rationalized by simple biogenetic arguments.

### **I.2.2. Biosynthesis of limonoids**

Limonoids are thought to arise from euphol (H-20 $\beta$ ) or tirucallol (H-20 $\alpha$ ). The stereochemistry of the precursor is unknown. Most quassinoids and C30 triterpenes in the Rutales have the C-20 (*R*) configuration, suggesting tirucallol as the precursor, it was found that in *Azadirachta indica* leaves the C-20(*S*) euphol is converted to the limonoid nimbolide more efficiently than is tirucallol. According to the generally accepted scheme, the double bond between C-7/C-8 is epoxidized to a 7-epoxide, which is then opened inducing a Wagner-Meerwein shift of Me-14 to C-8, formation of the OH-7, and introduction of a double bond at C-14/C-15. Subsequently, the side chain is cyclized with the loss of four carbons to form the 17 $\beta$ -furan ring (Scheme 3). That the latter step is accomplished after the formation of 4,4,8-trimethylsteroid skeleton is indicated by the

occurrence of several protolimonoids, 4,4,8-trimethylsteroid compounds with an intact C-8 side chain, such as meliantriol and melianone<sup>13</sup>.



**Scheme 3.** Biosynthesis of limonoids (modified from ref. 2)

The specialization of the basic limonoid skeleton through oxidations, ring-opening and rearrangements, and cyclizations lead to the structural diversity of limonoids. Limonoids are classified according to their chemical structure.

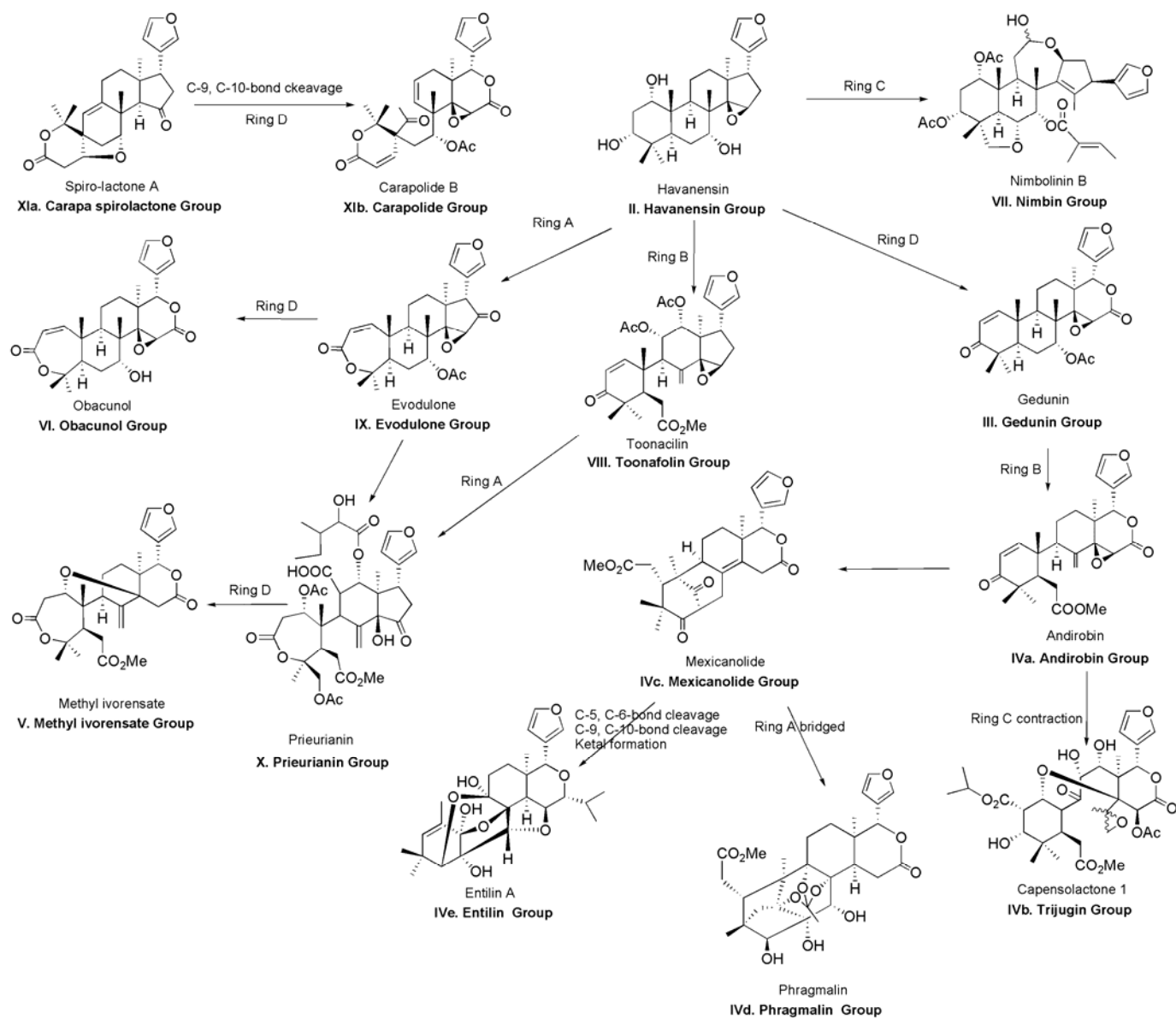
### I.3. Classification of limonoids

Taylor classified compounds from the Meliaceae into protolimonoids and nine classes of limonoids based on which of the four rings, designated as A, B, C, and D in the intact triterpene nucleus have been oxidatively opened<sup>7</sup>.

In a review on the chemistry of Meliaceae, Mulholland added two further subgroups the trijugins and entilins and the carapolide group, and modified the criterion for grouping compounds into the phragmalin group. The relationship between the groups is shown in Scheme 4<sup>15</sup>.

**Table 1.** Classification of Protolimonoids and Limonoids

Class	Group	Side chain	Ring A	Ring B	Ring C	Ring D
<b>I</b>	Protolimonoids	intact	Usually intact	Intact	Intact	Intact
<b>II</b>	Havenensin	Furan	Intact	Intact	Intact	Intact
<b>III</b>	Gedunin	Furan	Intact	Intact	Intact	Lactone
<b>IVa</b>	Andiborin	Furan	Intact	Open	Intact	Lactone
<b>IVb</b>	Trijugin	Furan	Intact	Open	Contracted	Lactone
<b>IVc</b>	Mexicanolide	Furan	Intact	Opened and recycled	Intact	Lactone
<b>IVd</b>	Phragmalin	Furan	Intact	Opened and recycled with C-4, C-29, C-1 bridge	Intact	Lactone
<b>IVe</b>	Entilin	Furan	Modified	Cleavage of C-9, C-10-bond	Intact	Lactone
<b>V</b>	Methyl ivorensate	Furan	Open or Lactone	Open	Intact	Lactone
<b>VI</b>	Obacunol	Furan	Open or Lactone	Intact	Intact	Lactone
<b>VII</b>	Nimbin	Furan	Intact	Intact	Open	Intact
<b>VIII</b>	Toonafolin	Furan	Intact	Open or Lactone	Intact	Intact
<b>IX</b>	Evoludone	Furan	Open or Lactone	Intact	Intact	Intact
<b>X</b>	Prieurianin	Furan	Open or Lactone	Open	Intact	Intact
<b>XIa</b>	Carapa spiro lactone	Furan	Contracted	Intact	Intact	Intact
<b>XIb</b>	Carapolide	Furan	Contracted	Cleavage of C-9, C-10-bond	Intact	Lactone



Scheme 4. The relationship between limonoids

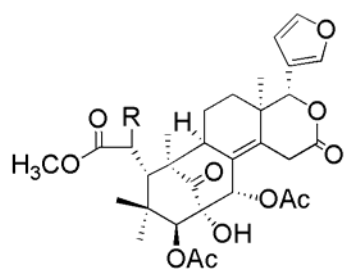
## I.4. Biological activity of limonoids

### I.4.1. Antimalarial activity

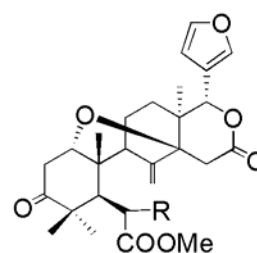
More recently only, limonoids have been investigated for their antimalarial activity. Up to now, the most potent antimalarial limonoid to be reported is gedunin which was isolated from several Meliaceae plants used to treat malaria in folk medicine.

22 species of Meliaceae extracts were examined for antimalarial activity using *in vitro* tests with two clones of *Plasmodium falciparum*, one sensitive to chloroquine (W2) and one chloroquine-resistant (D6). Among the active extracts, *Cedrela odorata* wood and *Azadirachta indica* leaves were recorded. These plants contained the limonoid gedunin. The purification and antimalarial assessment of gedunin against the W2 and D6 clones showed that it was more effective against the W2 clone than the D6 clone (the respective  $IC_{50}$  are 20 and 39 ng/ml). And gedunin had better activity than chloroquine against the W2 clone<sup>16</sup>.

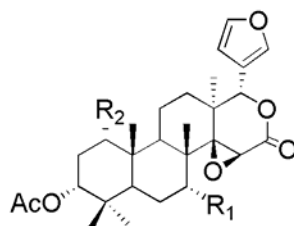
The crude extract from the bark and seeds of *Khaya grandifoliola* was active *in vitro* against the chloroquine-resistant *Plasmodium falciparum* W2/Indochina clone isolates with an  $IC_{50}$  value of 13.23  $\mu$ g/ml. The purification of the extract yielded seven limonoids: methyl angolensate, methyl 6-hydroxyangolensate, gedunin, 7-deacetylkhivorin, 1-deacetylkhivorin, swietenolide, and 6-acetylswietenolide. The determination of the antimalarial activity of these compounds gave respectively the following  $IC_{50}$  5.34, 21.59, 1.25, 5.08, 9.63, 18.56 and 7.46  $\mu$ g/ml while the  $IC_{50}$  of chloroquine was 0.61. Methyl angolensate, gedunin, 7-deacetylkhivorin, 1-deacetylkhivorin and 6-acetylswietenolide exhibited moderate antimalarial activity (with  $IC_{50}$  values between 1.25 – 9.63  $\mu$ g/ml) while the remaining two compounds showed weak activity ( $IC_{50}$  = 10 – 50  $\mu$ g/ml)<sup>17</sup>.



R = OH; swietenolide  
R = COOCH<sub>3</sub>; 1-deacetylkhivorin



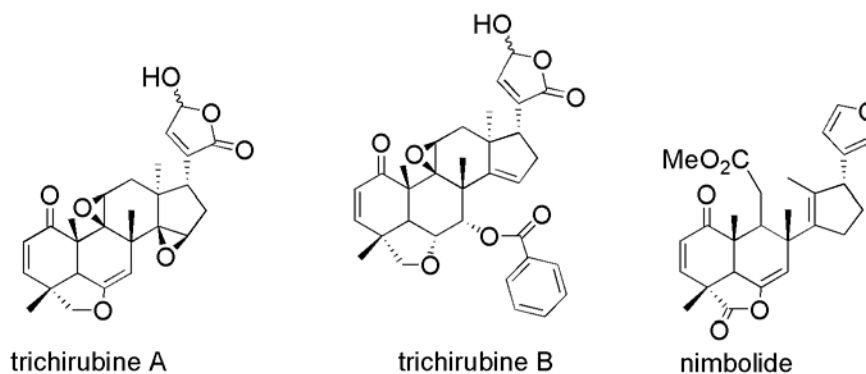
R = H; methyl angolensate  
R = OH; methyl 6-hydroxyangolensate



R<sub>1</sub> = OH, R<sub>2</sub> = COOCH<sub>3</sub>; 7-Deacetylkhivorin  
R<sub>1</sub> = COOCH<sub>3</sub>, R<sub>2</sub> = OH; 1-Deacetylkhivorin



Following a veterinary and behavioral survey of chimpanzees from a natural population in Uganda, leaf samples of *Trichilia rubescens* were collected because of the unusual method of ingestion observed. The methanolic crude extract of *T. rubescens* leaves exhibited significant antimalarial activity *in vitro* with an  $IC_{50} = 12 \mu\text{g/ml}$  against intraerythrocytic asexual forms of *P. falciparum*. The chloroquine-resistant strain FcB1 of *P. falciparum* ( $IC_{50}$  of chloroquine = 62 ng/ml). Bioassay directed fractionation provided two limonoids, trichirubines A and B. Trichirubine A exhibited a significant antimalarial activity with an  $IC_{50} = 0.3 \mu\text{g/ml}$  while the isolated amount of trichirubine B did not allow the evaluation of its antimalarial activity<sup>18</sup>.



Nimbolide, a limonoid isolated from the leaves of *Azadirachta indica* inhibited the growth of *P. berghei in vitro* with  $ED_{50} = 2.0 \mu\text{M}$ <sup>19</sup>. The presence of the conjugated system on ring A seems to be critical for the antimalarial activities.

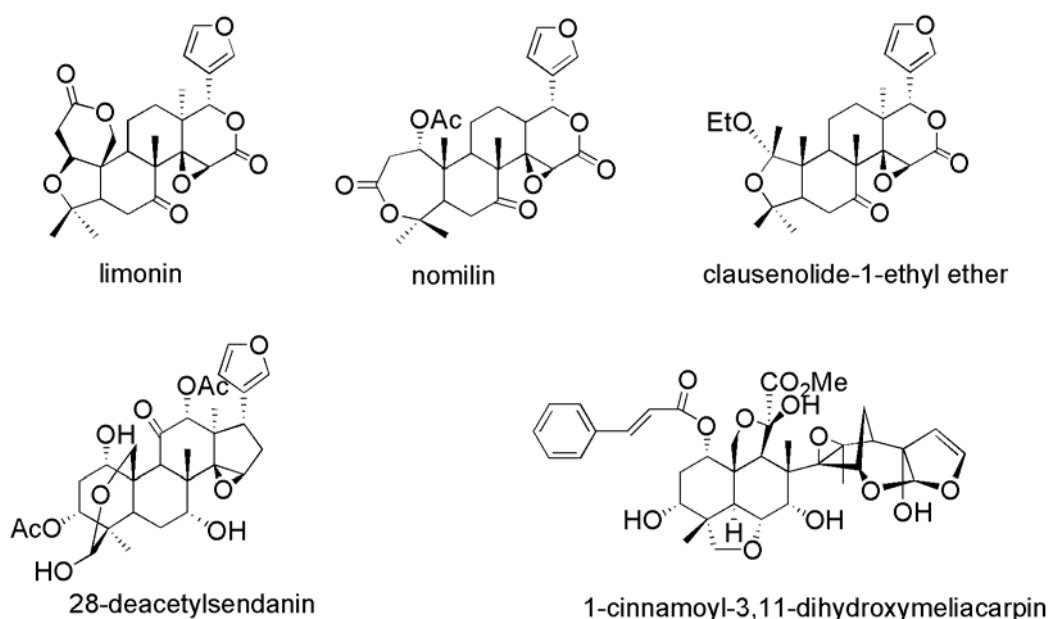
#### I.4.2. Antiviral activity

Limonin and nomilin have been reported for their antiviral activity. These terpenoids inhibited the HIV-1 replication in culture of human peripheral blood mononuclear cells and on monocytes/macrophages ( $EC_{50}$  values: 60.0  $\mu\text{M}$  and 52.2  $\mu\text{M}$ , respectively). They inhibited also at all concentrations studied the production of HIV-p24 antigen even when the peripheral blood mononuclear cells employed were chronically infected ( $EC_{50}$  values of 61.0  $\mu\text{M}$  for limonin and 76.2  $\mu\text{M}$  for nomilin). Regards the mechanism of action, limonin and nomilin inhibit *in vitro* HIV-1 protease activity<sup>20</sup>.

Clausenolide-1-ethyl ether is a limonoid isolated from ethanol extract of rhizomes of *Clausena excavate* (family Rutaceae), exhibited HIV inhibitory activity in 1A2 cell line in syncytium assay with an  $EC_{50}$  value of  $3.44 \times 10^{-5} \text{ M}$ , while having a much lower cytotoxicity, i.e. an  $IC_{50}$  value  $5.48 \times 10^{-4} \text{ M}$  for inhibition of tetrazolium conversion to formazan. This compound was also tested using a reverse transcriptase assay. It was found that the compound, at 200  $\mu\text{g/mL}$ , inhibited <30% HIV-1 reverse transcriptase activity. It was concluded that its anti-HIV-1 activity is probably not due to inhibition of reverse transcriptase, but rather to inhibition at other stages in the replication cycle of HIV-1<sup>21</sup>.

28-deacetylsendanin (28-DAS), a compound purified from the fruit of *Melia azedarach* exerted an antiviral effect on herpes simplex virus-1 (HSV-1) in Vero cells. The 50% inhibitory concentration ( $IC_{50}$ ) of 28-DAS was 1.46  $\mu\text{g/ml}$  without cytotoxicity at 400  $\mu\text{g/ml}$  on Vero cells. 28-DAS inhibited the replication of HSV-1, reduced the synthesis of HSV-1 TK, and led to the formation of defective nucleocapsids<sup>22</sup>.

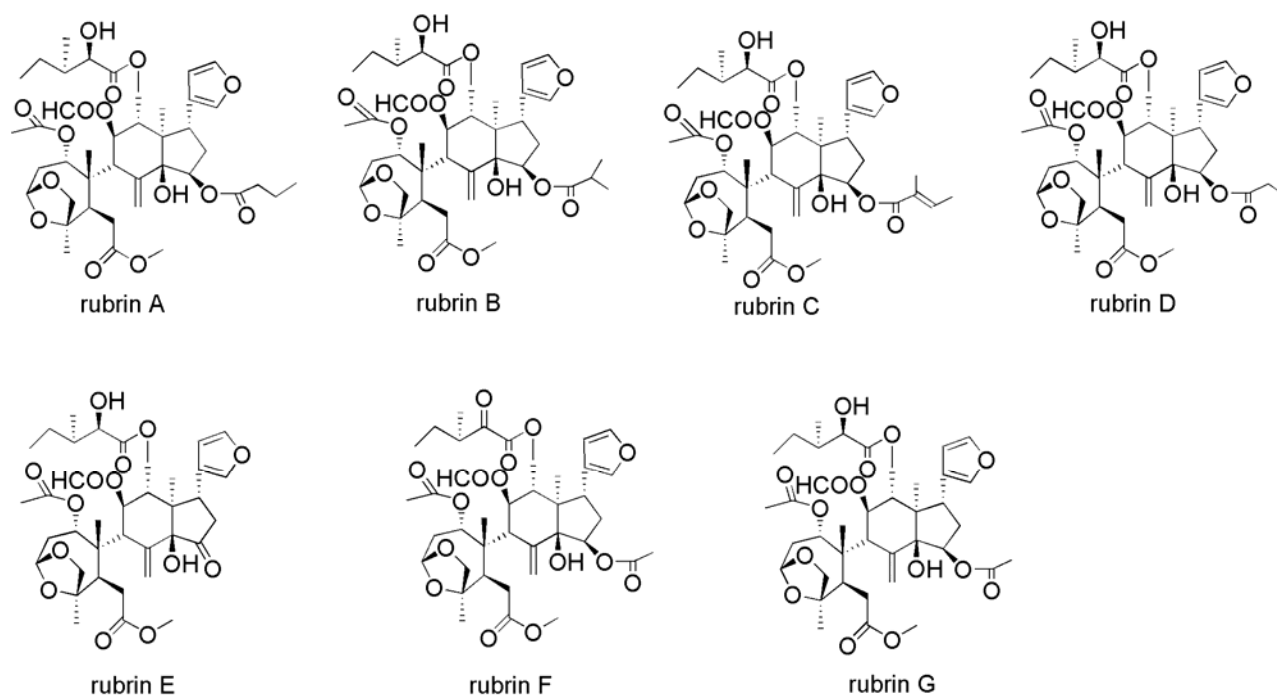
The limonoid 1-cinnamoyl-3,11-dihydroxymeliacarpin, isolated from the leaves of *Melia azedarach*, inhibits vesicular stomatitis (VSV) and herpes simplex (HSV-1) viruses multiplication in vitro when added after infection with low cytotoxicity. It showed an  $IC_{50}$  values of 6  $\mu\text{M}$  and 20  $\mu\text{M}$  for vesicular stomatitis (VSV) and herpes simplex (HSV-1) viruses, respectively<sup>23</sup>.



#### I.4.3. Cell adhesion inhibition

In the course of search for natural compounds that inhibit cell adhesion, the extract from the root of *Trichilia rubra* was identified as having potent inhibitory activity in a bioassay for lymphocyte function associated antigen-1 to intercellular adhesion molecule-1 (LFA-1:ICAM-1) mediated adhesion of JY and HeLa cells, developed and automated in-house for large throughput screening. The bioassay fractionation of the dichloromethane extract led to the isolation of seven bioactive compounds: rubrin A-G with hemioortho ester A-ring. These compounds exhibited potent inhibitory activity in the LFA-1:ICAM-1 mediated cell adhesion assay with  $IC_{50}$  values 10-25 nM and showed no cytotoxicity at concentration up to 20  $\mu\text{M}$  in either a 5-hour or 24-hour tritiated thymidine uptake assay or on MTT assay. The presence of the unique hemioortho ester A-ring is crucial to potency. Indeed, the inhibitory activity of the closest structurally related priurianin and epoxypriurianin were 10-20  $\mu\text{M}$  while the more distantly related displayed no activity up to 20  $\mu\text{M}$ .

Cell adhesion inhibitors may have therapeutic potential as anti-inflammatory and antimetastatic agents<sup>24</sup>.



#### I.4.4. Antitumour

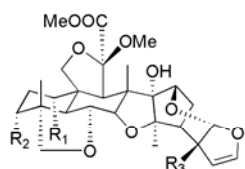
A series of methoxymeliacarpinins derivatives isolated from *Melia azedarach* were tested for their cytotoxic activity against the P388 lymphocytic leukemia cells. The following  $IC_{50}$  values 100, 48.0, 47.0, 10.5 and 1.5 were exhibited respectively by compounds 1-tigloyl-3,20-diacetyl-11-methoxymeliacarpinin, 3-tiglyol-1,20-diacetyl-11-methoxymeliacarpinin, 1-deoxy-3-methacrylyl-11-methoxymeliacarpinin, 1-cinnamoyl-3-acetyl-11-methoxymeliacarpinin and 1-cinnamoyl-3-hydroxy-11-methoxymeliacarpinin. 1-cinnamoyl-3-hydroxy-11-methoxymeliacarpinin showed significant cytotoxicity while in its acetate (1-cinnamoyl-3-acetyl-11-methoxymeliacarpinin), the activity decreased<sup>25</sup>. This suggests that the acetylation, might be the cause of decrease of activity.

However 1-tigloyl-3,20-diacetyl-11-methoxymeliacarpinin and 3-tiglyol-1,20-diacetyl-11-methoxymeliacarpinin are also C-20 acetate and their cytotoxicity is almost zero, they are also acetylated methoxymeliacarpinins derivatives of 1-tiglyol-3-acetyl-11-methoxymeliacarpinin and 3-acetyl-3-tiglyol-11-methoxymeliacarpinin which exhibited  $IC_{50}$  of 3.2 and 3.3  $\mu\text{g/ml}$ .

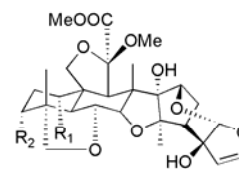
A bioassay guided isolation of extraction from *Melia azedarach* led to isolation of five cytotoxic tetranortriterpenoids. These compounds which have the characteristics of sendanin and azedarachtin types, exhibited significant inhibition of P388 cells in vitro. The three sendanin-type limonoids 29-isobutylsendanin, 12-hydroxyamoorastin and 29-deacetylsendanin exhibited strong cytotoxic activity against P388 lymphocytic leukemia cells with the  $IC_{50}$  of 0.034, 0.090 and 0.026  $\mu\text{g/ml}$  respectively. The azedarachtin type compounds 1-tigloyl-3-acetyl-11-methoxymeliacarpinin and 1-acetyl-3-tiglyol-11-methoxymeliacarpinin have  $IC_{50} = 3.2$  and 3.3  $\mu\text{g/ml}$  respectively. It was also notice that the acetylation of  $1\alpha$  or  $7\alpha$ -OH of 12-hydroxyamoorastin decreased the cytotoxic activity while the acetylation of both positions led to the loss of the cytotoxicity<sup>26</sup>.

Aphanastatin, a limonoid isolated from the  $\text{CH}_2\text{Cl}_2$  soluble part of the water extract of the seed of *Aphanamixis grandifolia*. This compound inhibited the growth of the murine lymphocytic leukemia P388 with an  $\text{ED}_{50} = 0.065 \mu\text{g/ml}^{27}$ .

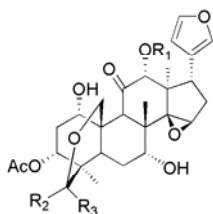
Amoorastatin, isolated from the same extract has even a greater cells growth inhibitory effect with  $\text{ED}_{50} < 0.001 \mu\text{g/ml}^{28}$ .



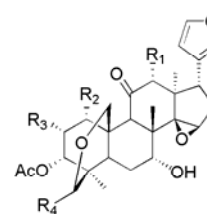
$\text{R}_1 = \text{OTig}$ ,  $\text{R}_2 = \text{R}_3 = \text{OCOCH}_3$ ; 1-tigloyl-3,20-diacetyl-11-methoxymeliacarpinin,  
 $\text{R}_1 = \text{R}_3 = \text{OCOCH}_3$ ,  $\text{R}_2 = \text{OTig}$ ; 3-tiglyol-1,20-diacetyl-11-methoxymeliacarpinin,  
 $\text{R}_1 = \text{OCin}$ ,  $\text{R}_2 = \text{R}_3 = \text{OH}$ ; 1-deoxy-3-methacrylyl-11-methoxymeliacarpinin,  
 $\text{R}_1 = \text{H}$ ,  $\text{R}_2 = \text{OCOC}(\text{CH}_3)$ ,  $\text{R}_3 = \text{OH}$ ; 1-cinnamoyl-3-acetyl-11-methoxymeliacarpinin and  
 $\text{R}_1 = \text{OCin}$ ,  $\text{R}_2 = \text{OCOCH}_3$ ,  $\text{R}_3 = \text{OH}$ ; 1-cinnamoyl-3-hydroxy-11-methoxymeliacarpinin.



$\text{R}_1 = \text{OTig}$ ,  $\text{R}_2 = \text{OCOCH}_3$ ; 1-tigloyl-3-acetyl-11-methoxymeliacarpinin  
 $\text{R}_1 = \text{OCOCH}_3$ ,  $\text{R}_2 = \text{OTig}$ ; 1-acetyl-3-tiglyol-11-methoxymeliacarpinin



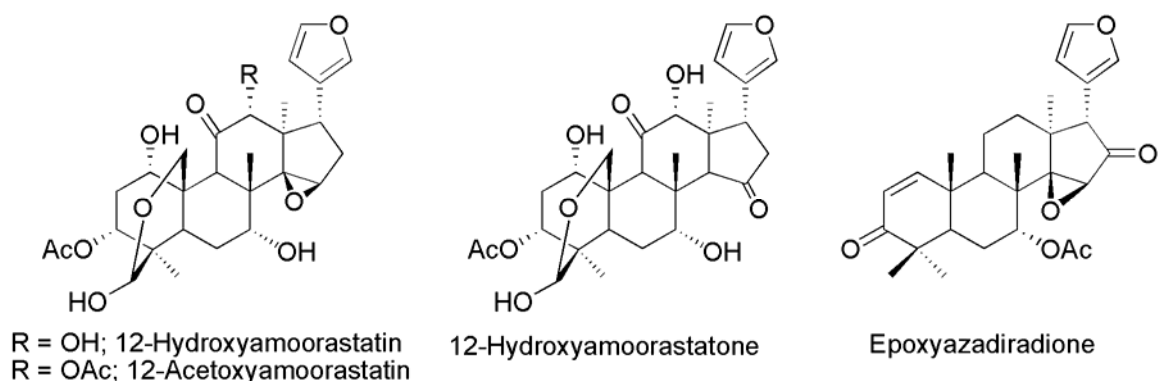
$\text{R}_1 = \text{COCH}_3$ ,  $\text{R}_2 = \text{Isobutyryl}$ ,  $\text{R}_3 = \text{H}$ ; 29-isobutylsendanin  
 $\text{R}_1 = \text{H}$ ,  $\text{R}_2 = \text{OH}$ ,  $\text{R}_3 = \text{H}$  (or  $\text{R}_2 = \text{H}$ ,  $\text{R}_3 = \text{OH}$ ); 12-hydroxyamoorastatin  
 $\text{R}_1 = \text{COCH}_3$ ,  $\text{R}_2 = \text{OH}$ ,  $\text{R}_3 = \text{H}$  (or  $\text{R}_2 = \text{H}$ ,  $\text{R}_3 = \text{OH}$ ); 29-deacetyl-sendanin



$\text{R}_1 = \text{H}$ ,  $\text{R}_2 = \text{OH}$ ,  $\text{R}_3 = \text{H}$ ,  $\text{R}_4 = \text{OH}$ ; amoorastatin  
 $\text{R}_1 = \text{OH}$ ,  $\text{R}_2 = \text{OAc}$ ,  $\text{R}_3 = \text{OH}$ ,  $\text{R}_4 = \text{OCOCH}(\text{CH}_3)\text{CH}_2\text{CH}_3$ ; aphanastatin

Three cytotoxic limonoids 12-hydroxyamoorastatin, 12-hydroxyamoorastatin and 12-acetoxyamoorastatin were isolated from the stem bark of *Melia azedarach* var Japonica. These compounds were significantly cytotoxic to human tumour cell lines of A-549 (human lung adenocarcinoma), SK-OV-3 (human ovarian adenocarcinoma), SK-MEL-2 (human malignant melanoma), XF-498 (human CNS carcinoma) and HCT-15 (human colon adenocarcinoma). The  $\text{ED}_{50}$  values observed are  $9.2 \times 10^{-1}$ , 13.7,  $3.8 \times 10^{-1}$ , 2.0 and  $1.6 \mu\text{gml}^{-1}$  for 12-hydroxyamoorastatin;  $4.0 \times 10^{-2}$ ,  $2.5 \times 10^{-1}$ ,  $1.0 \times 10^{-2}$ ,  $2.0 \times 10^{-2}$  and  $8.0 \times 10^{-2} \mu\text{gml}^{-1}$  for 12-hydroxyamoorastatin and  $1.0 \times 10^{-2}$ ,  $2.0 \times 10^{-2}$ ,  $7.0 \times 10^{-4}$ ,  $7.0 \times 10^{-3}$  and  $4.0 \times 10^{-2} \mu\text{gml}^{-1}$  for 12-acetoxyamoorastatin for A-549, SK-OV-3, SK-MEL-2, XF-498 and HCT-15 respectively.

12-hydroxyamoorastatin was less active, suggesting that the 14,15 $\beta$ -epoxide is an important factor for cytotoxicity. 12-acetoxyamoorastatin is the most active, having  $\text{ED}_{50}$  values ranging from 0.0007 to  $0.04 \mu\text{g/ml}$  which indicates that it has stronger cytotoxic potential than reference antimycin A ( $\text{ED}_{50} = 0.27 - 5.5 \mu\text{gml}^{-1}$ )<sup>29</sup>.



Three limonoids of the neem were found to be toxic to mammalian and insect cell cultures. N1E-115 neuroblastoma (mouse), 143.TK- osteosarcoma (human) and Sf9 (insect) were sensitive to nimbolide, epoxyazadiradione, salanin and nimbin. The most potent of these limonoids is nimbolide with an  $IC_{50}$  ranging from 4 to 10  $\mu M$  and averaging 6  $\mu M$  for the three cell lines. Other limonoids average  $IC_{50}$  values are epoxyazadiradione 27  $\mu M$ , salannin 112  $\mu M$ , and nimbin, deacetylnimbin and azadirachtin each > 200  $\mu M$  (practically nontoxic)<sup>30</sup>.

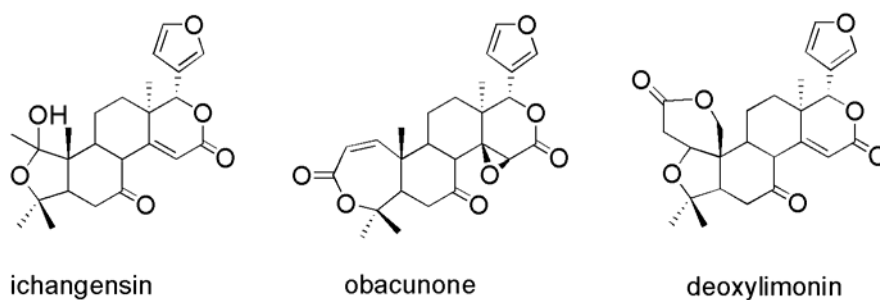
*Citrus* taxa and their hybrids yielded 36 limonoids which are commonly called citrus limonoids. Among, these limonoids, limonin is known to be the predominant limonoid in all citrus species. However in *Citrus ichangensis*, ichangensin is the predominant<sup>31</sup>.

Several studies have been carried out especially about the anticancer activity of *citrus* limonoids. A number of citrus limonoids were tested for their ability to inhibit the proliferation of MDA-MB-435 ER- and MCF-7 ER+ human breast cancer cells. In ER-cells, limonin methoxime and deacetylnomilin were the most effective inhibitors having  $IC_{50}$ s of 0.02 and 0.07  $\mu g/mL$  respectively. In ER+ cells, deacetylnomilin, obacunone and methyl nomilate were the most effective inhibitors of proliferation having  $IC_{50}$ s of 0.005, 0.009 and 0.01  $\mu g/mL$  respectively. These results suggest that citrus limonoids have important anti-cancer activity<sup>32</sup>.

*Citrus* limonoids, including obacunol, isolated also from some Meliaceae species, have been found to be potent inducers of Glutathione S-transferase activity in mice. Glutathione S-transferase enzymes are one the major enzyme systems responsible for the removal of complex chemical waste including carcinogens from cell<sup>33</sup>.

Among the studied *citrus* limonoids, limonin and nomilin have been showed to inhibit the development of carcinogen-induced cancers in a variety of different animal models, including models for stomach, lung and skin cancer. In the two-stage model for skin carcinogenesis, the data showed that nomilin was more effective as an inhibitor during the initiation stage of carcinogenesis, whereas limonin was more active during the promotional phase of carcinogenesis. These data suggested that the two limonoids, although structurally similar, may be operating by different mechanisms of action<sup>34</sup>.

Ichangensin, deoxylimonin and obacunone inhibited the development of 7,12-dimethylbenz[a]anthracene-induced oral tumors. Using the hamster cheek pouch model, these compounds have been tested for cancer chemopreventive activity. Ichangensin had no effect on tumor number or burden. In the other hand, obacunone reduced tumor number and burden by 25 and 40%, respectively, whereas deoxylimonin reduced tumor number and burden by 30 and 50%, respectively. The data obtained indicated that changes in the A ring of the limonoid nucleus can lead to loss of anticancer activity, whereas changes in the D ring can be tolerated without any apparent loss of biological activity<sup>34</sup>.

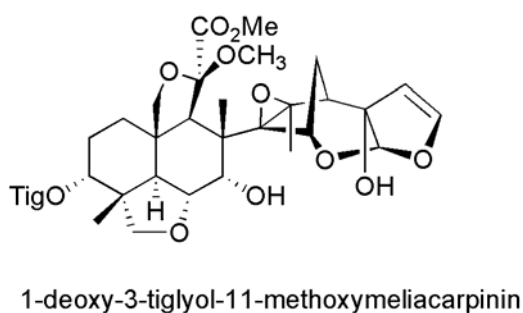


#### I.4.5. Antifeedant

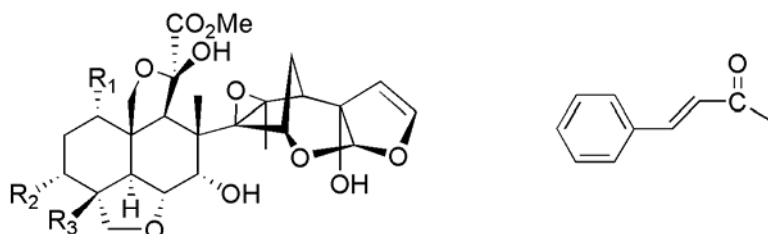
Antifeedant activity of the limonoids has been well studied. Azadirachtin and related highly oxidized C-seco limonoids are known to be the most potent.

Azadirachtin is known to affect over 200 species of insects and mites<sup>13</sup>. Azadirachtin exhibits antifeeding against the larvae of the voracious insects *Epilachna varivestis* and *Spodoptera littoralis* with  $ED_{50} = 1.7$  and  $< 1$  ppm respectively<sup>35</sup>. As an insecticide, azadirachtin-based products control more than 400 species of insects<sup>36</sup>.

The root bark of *Melia azedarach* yielded an azadirachtin related compound 1-deoxy-3-tiglyol-11-methoxymeliacarpinin which inhibited completely the feeding of the larvae of *Spodoptera exigua* at concentration of  $3 \mu\text{g}/\text{cm}^2$ <sup>(37)</sup>.

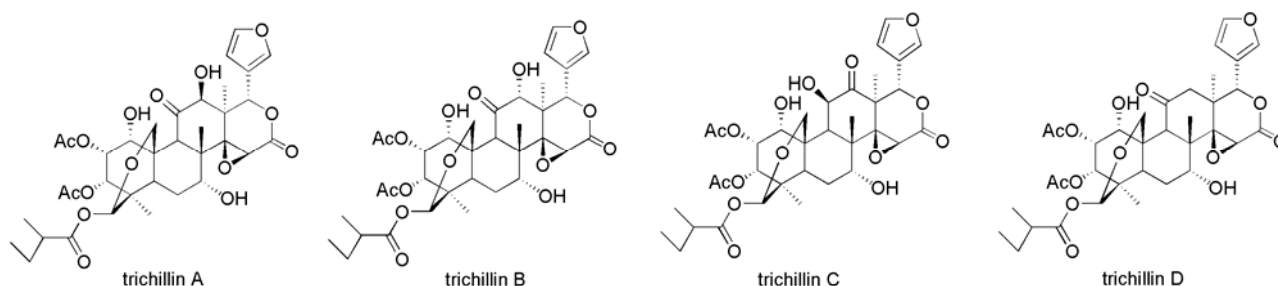


Three meliacarpin having the same ring with azadirachtin were isolated as potent insecticide against *S. littoralis* from the leaves of *Melia azedarach*. The three meliacarpins derivatives, namely 1,3-dicinnamoyl-11-hydroxymeliacarpin, 1-cinnamoyl-3-methacrylyl-11-hydroxymeliacarpin and 1-cinnamoyl-3-acetyl-11-hydroxymeliacarpin exhibited an  $EC_{50}$  of 0.57, 0.57 and 0.48 ppm respectively towards the neonate of larvae of *Spodoptera littoralis*<sup>38</sup>.



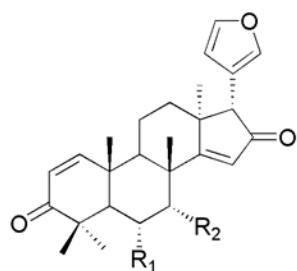
R<sub>1</sub> = OCin, R<sub>2</sub> = OCin, R<sub>3</sub> = CH<sub>3</sub>; 1,3-dicinnamoyl-11-hydroxymeliacarpin  
 R<sub>1</sub> = OCin, R<sub>2</sub> = OCOC(CH<sub>3</sub>)=CH<sub>2</sub>, R<sub>3</sub> = CH<sub>3</sub>; 1-cinnamoyl-3-methacrylyl-11-hydroxymeliacarpin  
 R<sub>1</sub> = OCin, R<sub>2</sub> = OCin, R<sub>3</sub> = CH<sub>3</sub>; 1-cinnamoyl-3-acetyl-11-hydroxymeliacarpin  
 R<sub>1</sub> = OTig, R<sub>2</sub> = OAc, R<sub>3</sub> = CO<sub>2</sub>CH<sub>3</sub>; azadirachtin

A series of trichilins A-D, isolated from the root bark of *Trichilia roka*, exhibited also antifeedant activity. The most potent antifeedants in this group was trichillins B which is active at 200 ppm, followed by trichillin A at 300 ppm and trichillin D at 400 ppm. The antifeedant test was conducted against the voracious *Spodoptera eridania*<sup>39</sup>.

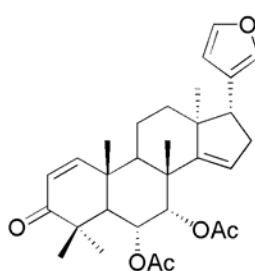


#### I.4.6. Antifungal

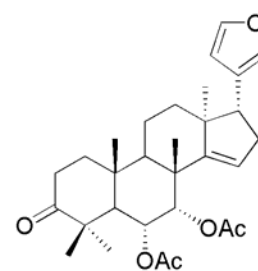
The plant *Chisocheton paniculatus* Hiern, yielded 4 limonoids possessing the intact apo-euphol skeleton, (1, 2, 3, and 1,2-dihydro-6 $\alpha$ -acetoxyazadirone). These compounds exhibited strong inhibitory properties against pathogenic fungi *Curvularia verruciformis* (lemon grass), *Dreschleva oryzae* (rice) and *Alternaria solani* (tomato)<sup>40</sup>.



$R_1 = R_2 = \text{OAc}$ ; 6 $\alpha$ -acetoxyazadiradione  
 $R_1 = R_2 = \text{OH}$ ; 6 $\alpha$ -hydroxydeacetylazadiradione



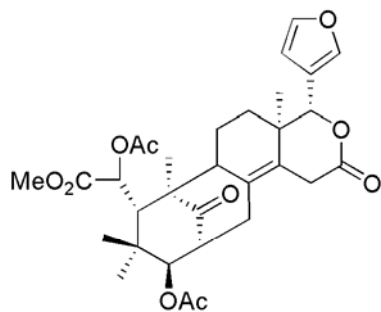
6 $\alpha$ -acetoxyazadirone



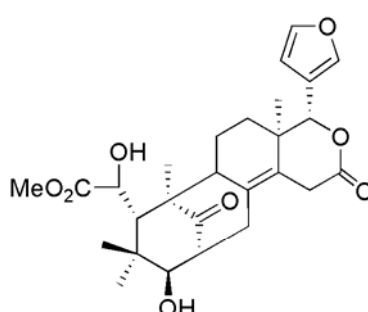
1,2-dihydroxy-6 $\alpha$ -acetoxyazadirone

Unfortunately, data on the method of evaluation and concentration were not reported

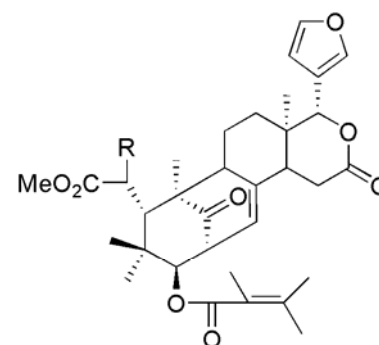
A series of mexicanolide derivatives 2 $\alpha$ ,3 $\beta$ -dihydroxmexicanolide, 3 $\beta$ -acetoxymexicanolide, 3 $\beta$ -hydroxmexicanolide and 2 $\alpha$ -hydroxmexicanolide from *Khaya senegalensis*, and februgin, hydroxylated februgin, swietenine, 6-acetylswietenine, swietenolide, 3,6-Di-*O*-acetylswietenolide, 6-acetyl-3-tigloyl swietenolide and 3-tigloylswietenolide from *Swietenia mahogany* were tested for their antifungal activity against the groundnut rust *Puccinia arachidis*.



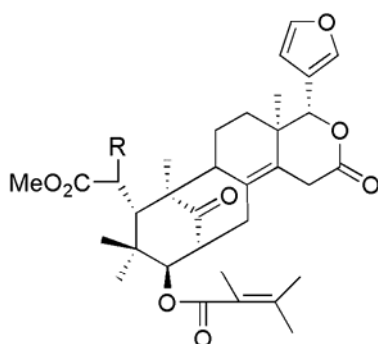
3,6-di-*O*-acetylswietenolide



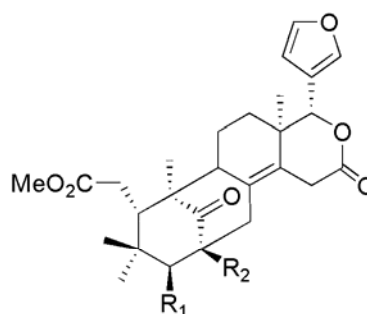
swietenolide



$R = \text{OH}$ ; swietenine  
 $R = \text{H}$ ; februgin  
 $R = \text{OCOCH}_3$ ; 6-acetylswietenine



$R = \text{OH}$ ; 3-tigloylswietenolide  
 $R = \text{OCOCH}_3$ ; 6-acetyl-3-tigloylswietenolide

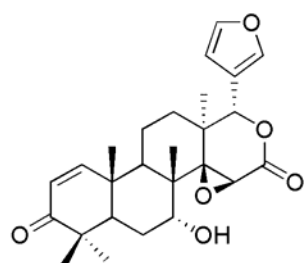


$R_1 = \text{O}$ ,  $R_2 = \text{OH}$ ; 2 $\alpha$ -hydroxmexicanolide  
 $R_1 = \text{OH}$ ,  $R_2 = \text{OH}$ ; 2 $\alpha$ ,3 $\beta$ -dihydroxmexicanolide  
 $R_1 = \text{OH}$ ,  $R_2 = \text{H}$ ; 3 $\beta$ -hydroxmexicanolide  
 $R_1 = \text{OAc}$ ,  $R_2 = \text{H}$ ; 3 $\beta$ -acetoxymexicanolide  
 $R_1 = \text{O}$ ,  $R_2 = \text{H}$ ; mexicanolide

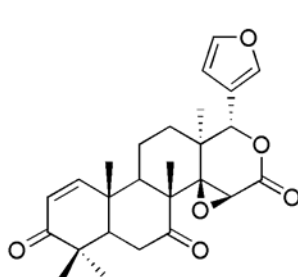


Mexicanolide, 3 $\beta$ -acetoxy-mexicanolide, 3 $\beta$ -hydroxymexicanolide and 2 $\alpha$ ,3 $\beta$ -dihydroxymexicanolide from *Khaya senegalensis*, and 6-acetylswietenine and 6-acetyl-3-tigloylswietenolide from *Swietenia mahogany* showed an effective reduction the number of rust pustules on detached groundnut leaves. At 10  $\mu\text{g}/\text{cm}^2$  leaflet area, over 80% reduction in pustule number was observed in treated leaflets. Surprisingly, while 3,6-di-*O*-acetylswietenolide and swietenolide were moderately active, swietenine and 2 $\alpha$ -hydroxymexicanolide increased disease severity considerably at lower concentrations relative to controls. From these results, some relation structure –reactivity conclusions have been proposed. Swietenine and its derivatives have a characteristic 8,30-double bond, while swietenolide and mexicanolide-type compounds have an 8,14-double bond. Other than the double bond position, the individual compounds differed in the substitutions at the C-2, C-3, and C-6 positions. The results indicated that the double bond-position does not influence to the antifungal activity but suggested that functional group substitutions may be critical for the antifungal activity<sup>41</sup>.

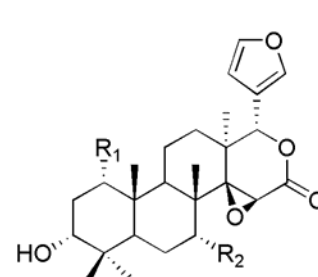
Several antifungal limonoids compounds have been isolated from the stem bark of *Khaya ivorensis*. Among these compounds, methyl angolensate and 1,3,7-trideacetylkhivirin displayed the highest antifungal activity against *Botrytis cinerea*, a plant pathogen fungus, with respectively 62.8 and 64.0% mycelial growth inhibition at 1000mg/litre, and 73.3 and 68.6% mycelial growth inhibition at 1500mg/litre. The mycelial growth inhibition of other compounds (methyl 6-hydroxyangolensate, 3-deacetylkhivirin, 3,7-dideacetylkhivirin, 7-deacetoxy-7-oxogedunin, 3-*O*-detigloyl-3-*O*-acetylswietenine and 3-*O*-acetylswietenolide) varied between 56.7 and 68.5 at 1500 mg/litre. At the same concentration, 7-deacetylgedunin exhibited a mycelial growth inhibition of 20.0 making it to be the weakest antifungal compounds of this group<sup>42</sup>.



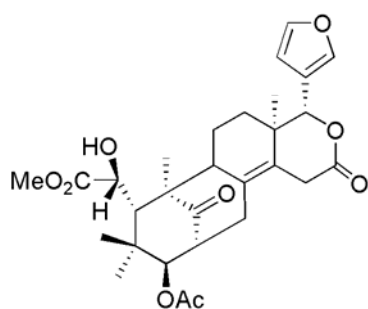
7-deacetylgedunin



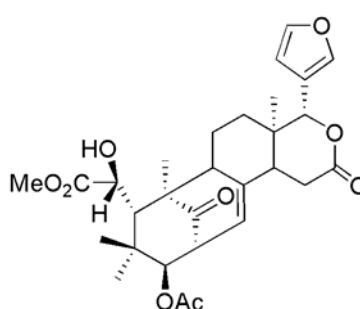
7-deacetoxy-7-oxogedunin



R<sub>1</sub> = OAc, R<sub>2</sub> = OAc; 3-deacetylkhivirin  
R<sub>1</sub> = OAc, R<sub>2</sub> = OH; 3,7-dideacetylkhivirin  
R<sub>1</sub> = OH, R<sub>2</sub> = OH; 1,3,7-trideacetylkhivirin



3-*O*-acetylswietenolide



3-*O*-detigloyl-3-*O*-acetylswietenine

#### I.4.7. Antibacterial

Salannin displayed antibacterial activity towards both gram+ve and gram-ve agents<sup>43</sup>.

Rutaevin, a limonoid isolated from the root bark of *Evodia glauca* Miq. has been reported to be active against the bacterium *Bacillus subtilis* at 100 µg/ml<sup>44</sup>.

The limonoid 3,7-dideacetylkhivorin, isolated also from the stem bark of *Khaya ivorensis*, inhibited completely the growth of *Salmonella enteritidis* at 1 and 2 mg/ml, and *Bacillus subtilis* at 2 mg/ml. However, the antibacterial activity of this compound was weaker than that of the antibiotic chloramphenicol, which showed complete inhibition of bacterial growth at 2.5 mg/l<sup>42</sup>.

#### I.4.8. Antioxidant

At concentration of 10 µM, the antioxidant activity of limonin and limonin 17-β-D-glucopyranoside were measured using a variety of *in vitro* models such as β-carotene-linoleic acid, 1,1-diphenyl-2-picryl hydrazyl (DPPH), superoxide, and hamster low-density lipoprotein (LDL). Limonin and limonin 17-β-D-glucopyranoside inhibitions were < 7% using the β-carotene-linoleate model system, and showed 0.5% and 0.25% of inhibition in the free radical scavenging activity using the DPPH method. In the superoxide model, limonin and limonin 17-β-D-glucopyranoside inhibited the production of superoxide radicals by 2.5-10%<sup>45</sup>.

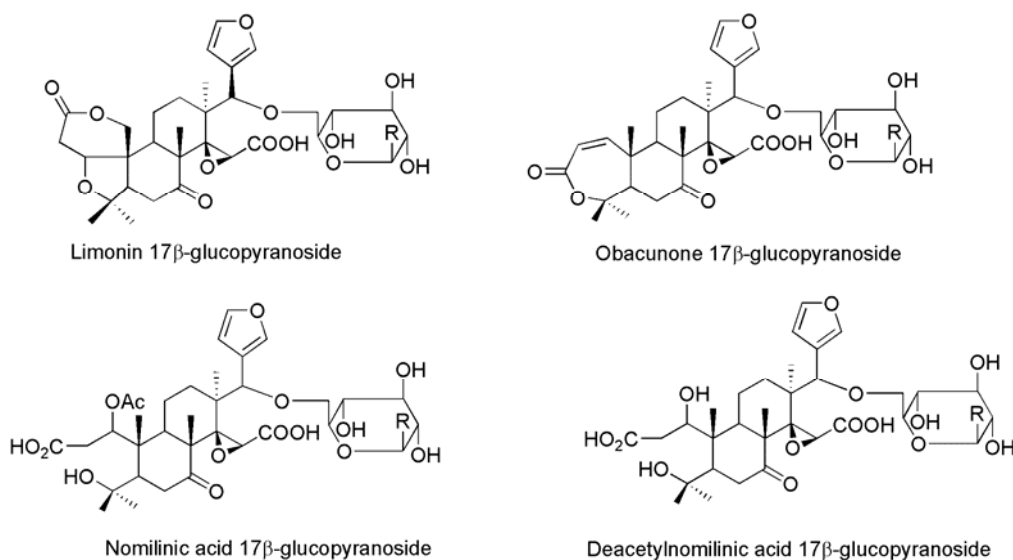
Another study showed the evidence that specific limonoid glucosides have the capacity to quench superoxide radicals. Indeed, the following limonoid glucosides, limonin 17β-D-glucopyranoside (LG), obacunone 17β-D-glucopyranoside (OG), nomilinic acid 17β-D-glucopyranoside (NAG), and deacetylnomilinic acid 17β-D-glucopyranoside (DNAG) were tested to quench free radicals against pyrogallol in a slightly alkaline solution. LG was the weakest (IC<sub>50</sub> = 7.88 mmol/L) and NAG the strongest (IC<sub>50</sub> = 3.11 mmol/L) (O<sup>2-</sup>) quencher while OG and DNAG had respectively IC<sub>50</sub> of 4.62 and 3.53 mmol/L. During this study, Poulose et al. noticed a second facet of their action which is to induce apoptosis<sup>46</sup>.

#### I.4.9. Anti-ulcer

Salannin, a limonoid bitter principle of the seed oil of *Azadirachta indica*, showed a significant protective activity on aspirin induced gastric lesions at oral doses of 10, 20, 50 mg/kg<sup>47</sup>. Methyl angolesante, the most abundant limonoid found in *Entandrophragma angolense* has anti-ulcer properties<sup>48</sup>.

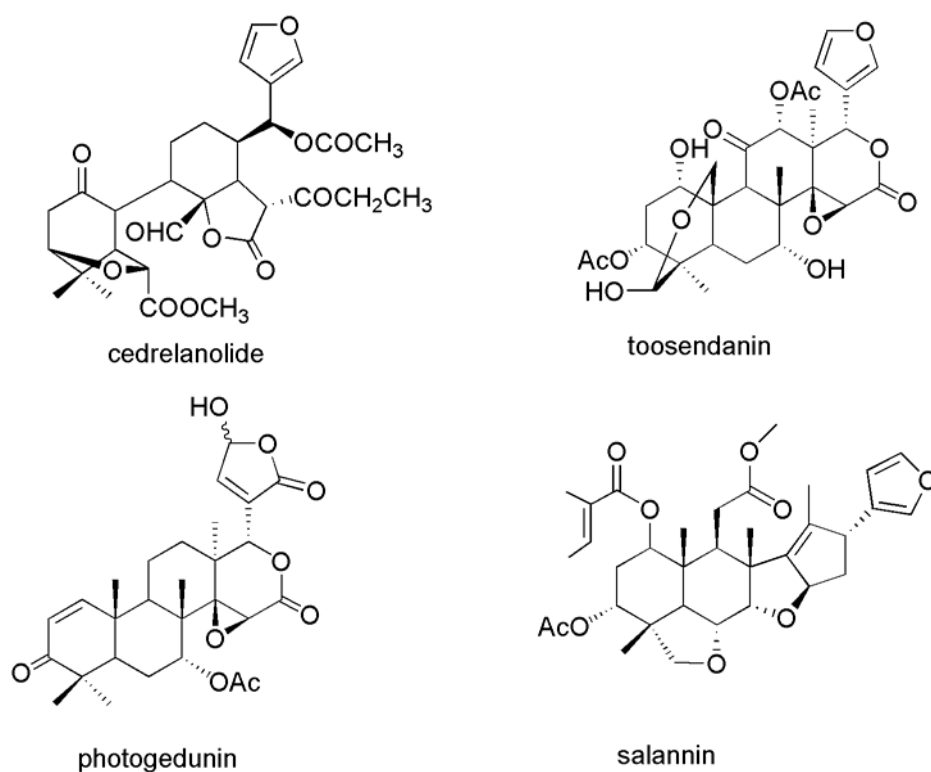
#### I.4.10. Spermicidal activity

Salannin exhibited such activity on human spermatozoa at 0.5 and 0.25% concentrations<sup>47</sup>.



#### I.4.11. Plant-growth inhibitory activities

Cedrelanolide inhibited seed germination of *Lolium multiflorum*, var. Hercules, *Triticum vulgare*, var. Salamanca, *Physalis ixocarpa*, and *Trifolium alexandrinum*, the concentration inhibiting 50% germination GI50 observed was 125.0, 157.0, 370.0 and 289.0  $\mu\text{M}$  respectively. This compound inhibited not only germination but also seed respiration, and seedling dry weights of these plant species. Further studies showed that cedrelanolide interferes with monocot preemergence properties, mainly energy metabolism of the seeds at the level of respiration. In addition, the compound inhibits photophosphorylation,  $\text{H}^+$  uptake, and noncyclic electron flow. This behavior might be responsible for its plant-growth inhibitory properties and its possible role as an allelopathic agent<sup>49</sup>.



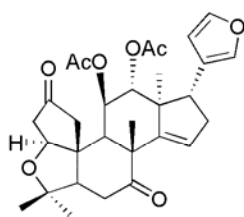
#### I.4.12. Moulting inhibiting activity

The citrus limonoids limonin, nomilin and obacunone exhibited moulting inhibiting activity against the 4<sup>th</sup> instar larvae of mosquito *Culex quinquefasciatus*. The EC<sub>50</sub> for inhibition of adult emergence was 6.31, 26.61 and 59.57 ppm for obacunone, nomilin and limonin, respectively<sup>50</sup>.

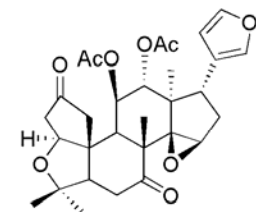
#### I.4.13. Insect growth inhibition

Using Toosendanin, a limonoid isolated from *Melia azadarach*, with a potent insect growth inhibition, as control photogedunin epimeric mixture, gedunin and cedrelanolide were evaluated against *Spodoptera frugiperda*. When tested for activity on neonate larvae into the no-choice bioassays, gedunin, photogedunin epimeric mixture, and photogedunin acetates mixture caused significant larval mortality with LC<sub>50</sub> of 39.0, 10.0, and 8.0 ppm at 7 days, respectively, as well as growth reduction which was clearly significant at 21 days. For the growth activity, gedunin was more active than toosendanin at low concentrations (50 ppm) but photogedunin epimeric mixture (1 + 2) and photogedunin acetates (3 + 4) showed the highest larval growth inhibition at high concentrations (52.0 ppm)<sup>51</sup>.

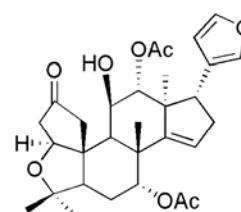
Using a standard bioassays test on late third or early fourth-instar larvae of the mosquito *Anopheles gambiae* s.s., three limonoids 11 $\beta$ ,12 $\alpha$ -Diacetoxyneotectleanin, 11 $\beta$ ,12 $\alpha$ -Diacetoxy-14 $\beta$ ,15 $\beta$ -epoxyneotectleanin et 7 $\alpha$ ,12 $\alpha$ -Diacetoxy-11 $\beta$ -hydroxynectleanin isolated from the root bark of *Turraea wakefieldii* exhibited strong mosquito larvicidal activity: 11 $\beta$ ,12 $\alpha$ -Diacetoxyneotectleanin (LD<sub>50</sub> = 7.83 ppm), 11 $\beta$ ,12 $\alpha$ -Diacetoxy-14 $\beta$ ,15 $\beta$ -epoxyneotectleanin (LD<sub>50</sub> = 7.07 ppm) and 7 $\alpha$ ,12 $\alpha$ -Diacetoxy-11 $\beta$ -hydroxynectleanin (LD<sub>50</sub> = 7.05 ppm), which shows that epoxidation of the C-14, C-15 double bond or de-acetylation of the 11-acetate group does not alter mosquito larvicidal activity<sup>52</sup>.



11 $\alpha$ ,12 $\beta$ -Diacetoxyneotectleanin



11 $\beta$ ,12 $\alpha$ -Diacetoxy-14 $\beta$ ,15 $\beta$ -epoxyneotectleanin



7 $\alpha$ ,12 $\alpha$ -Diacetoxy-11 $\beta$ -hydroxynectleanin

## Chapter II. The chemistry of the genus *Entandrophragma*

### II.1. Introduction

Meliaceae are woody family widely distributed throughout the tropics and subtropics, with only slight penetration into temperate zones; they occur in a variety of habitats from rain forests and mangrove swamps to semi-deserts<sup>53</sup>. The family Meliaceae, comprising about 51 genera and about 1400 species, forms a large botanical family<sup>54</sup>.

This family is extremely useful to man for the high quality of timbers and ease with which some species can be grown in plantations. Style and Pennington classified Meliaceae plant into four subfamilies<sup>55</sup> which are shown in Table 2<sup>15</sup>.

**Table 2.** The Meliaceae subdivision

<b>MELICEAE</b>	
<b>SUBFAMILY 1</b>	<b>Melioideae</b>
<b>Tribe</b>	<b>Genus</b>
1. Turraeeae	<i>Munronia, Naregamia, Turraea, Humbertioturraea, Calodecaryia, Nymania</i>
2. Melieae	<i>Melia, Azadirachta</i>
3. Vavaeeae	<i>Vavaeeae</i>
4. Trichilieae	<i>Trichilia, Pseudobersama, Pterorhachis, Walsura, Lepidotrichilia, Malleastrum, Ekebergia, Astrotrichilia, Owenia, Cipadessa</i>
5. Aglaieae	<i>Aglaia, Lansium, Aphanamixis, Reinwardtiodendron, Sphaerosacme</i>
6. Guareeae	<i>Heckeldora, Cabrarea, Ruagea, Turraeanthus, Guarea, Chisocheton, Megaphyllaea, Synoum, Anthocarapa, Pseudocarapa, Dysoxylum</i>
7. Sandoriceae	<i>Sandoricum</i>
<b>SUBFAMILY 2</b>	<b>Quivisiantoideae</b>
	<i>Quivisianto</i>
<b>SUBFAMILY 3</b>	<b>Capuroniantoideae</b>
	<i>Capuronianthus</i>
<b>SUBFAMILY 4</b>	<b>Swietenioideae</b>
1. Cedreleae	<i>Cedrela, Toona</i>
2. Swietenieae	<i>Khaya, Neobeguea, Soymida, Entandrophragma, Chukrasia, Pseudocedrela, Schmardaea, Swietenia, Lovoa</i>
3. Xylocarpeae	<i>Carapa, Xylocarpus</i>

## II.2. Uses

The timbers of certain Meliaceae are some of the most sought-after in the world, such that natural stands have been depleted. Other uses of Meliaceae included shade and street trees, fruit trees and the last but not the least, sources of biologically active compounds<sup>53</sup>.

The last use of Meliaceae plants can be justified by the fact that several preparations from leaves, seeds, stem bark and roots of many plants belonging to this family have a history of use in traditional medicine for treatment of various diseases. For example, in South Africa, most of Meliaceae species are used in a variety of ways in traditional medicine, including the treatment of stomach complaints, backache, fever, kidney complaints, rheumatism, dropsy and heart disease, and by diviners to put themselves into a trance prior to performing divining dances<sup>56</sup>. *Cedrela odorata* is used to procure abortions and also as fish poison in Cote d'Ivoire<sup>57</sup>. *Trichilia emetica* is employed for the treatment of various disorders in folk medicine of Mali: it is used in hepatic diseases, as a purgative, antiepileptic, antipyretic and antimalarial agent<sup>58</sup>.

## II.3. Chemistry of Meliaceae

The chemical studies on the Meliaceae lead to isolation of wide range of secondary metabolites. Sterols of the pregnane and stigmastanes classes and triterpenoids of the dammarane, lupine, oleanane and squalene classes; flavonoids, chromones, coumarins, benzofurans, mono-, sesqui-, di- and triterpenoids and alkaloids have been reported.

Methyl rocaglate is a benzofuran type compound isolated from *Aglaia odorata* and exhibited toxicity against 4th instar *Peridroma saucia* with a LD<sub>50</sub> of 0.33 µg per larva. Against neonate *P. saucia*, it inhibited its growth with an EC<sub>50</sub> = 0.90 ppm<sup>59</sup>. *Cedrelopsis grevei* yielded a coumarin compound, 7-methoxy-5-prenylcoumarin<sup>60</sup>.

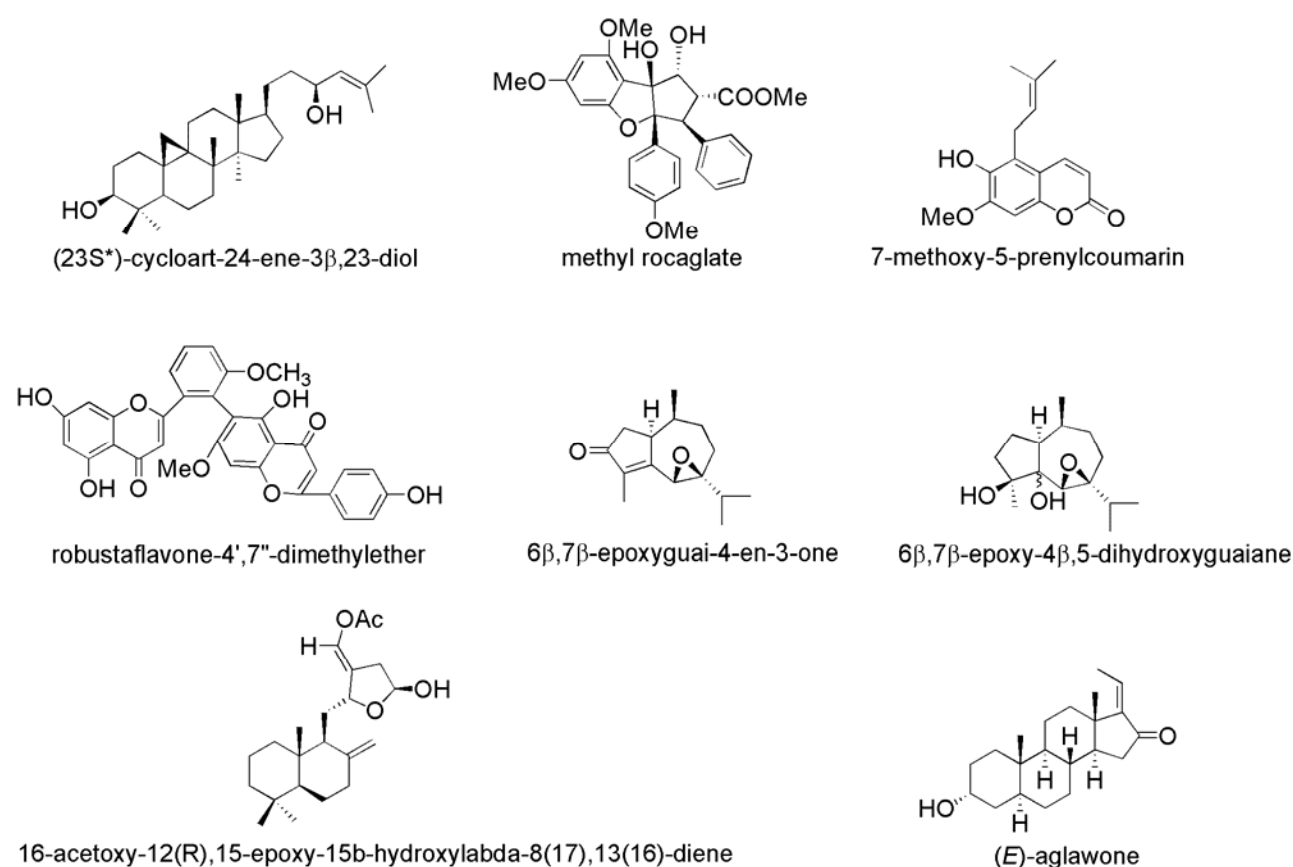
16-acetoxy-12(R),15-epoxy-15β-hydroxyabda-8(17),13(16)-diene is a diterpenoid isolated from *Turreanthus africanus*<sup>61</sup>. The stem bark of *Amoora rohituka* afforded two guaiane-derived sesquiterpenoids, 6β,7β-epoxyguai-4-en-3-one and 6β,7β-epoxy-4β,5-dihydroxyguaiane<sup>62</sup>.

*Guarea guidonia* yield the triterpenoid (23S\*)-cycloart-24-ene-3β,23-diol<sup>63</sup> and the biflavonoid robustaflavanone-4',7''-dimethylether was isolated from *Dysoxylum lenticellare*<sup>64</sup>. (E)-Aglawone is a pregnane steroid isolated from the bark of *Aglaia lawii*<sup>65</sup>.

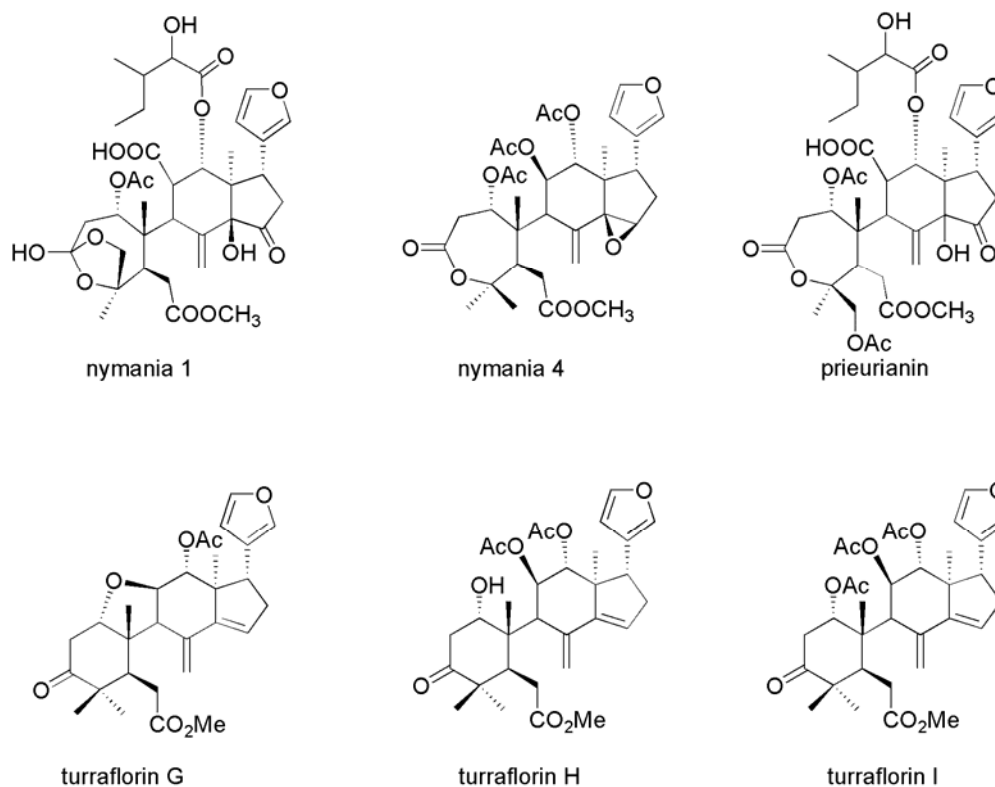
However, Meliaceae are best known for the synthesis and accumulation of bitter tetranortriterpenoids, which are known as limonoids or meliacins. And several phytochemical studies of Meliaceae established that limonoids are responsible of most of their biological activities. Indeed, limonoids have a wide range of

bioactivity including insect antifeedant and growth regulating properties, a variety of medicinal effects in animals and humans, and antifungal, bacteriocidal and antiviral activities.

The occurrence of limonoids (or meliacins) might offer possibilities for taxonomic purposes. The taxonomic position of *Nymania capensis* has been much disputed because of its external appearance but it is now considered to belong to the Meliaceae, where it is placed in the subfamily Melioideae and the tribe Turraeae. Chemical work on *N. capensis* showed that it produces limonoids having the ring A cleaved or lactonized, the ring B cleaved and both rings C and D intact. These features are encountered in the prieurianin group. Compounds such as nymania 1 and nymania 4 were isolated along with prieurianin from its bark and timber<sup>66</sup>.



Another plant belonging to this tribe which has been extensively investigated for its chemical components is *Turraea floribunda*. This plant produces limonoids which can be classified into toonafofin group such as turraflorins G, H and I isolated from its seeds<sup>67</sup>.



According to the generally accepted biosynthesis scheme of different groups of limonoids, prieurianin derived from toonafolin by the cleavage or lactonization of the ring A. This confirms the close relationship between *N. capensis* and *Turraea obtusifolia*.

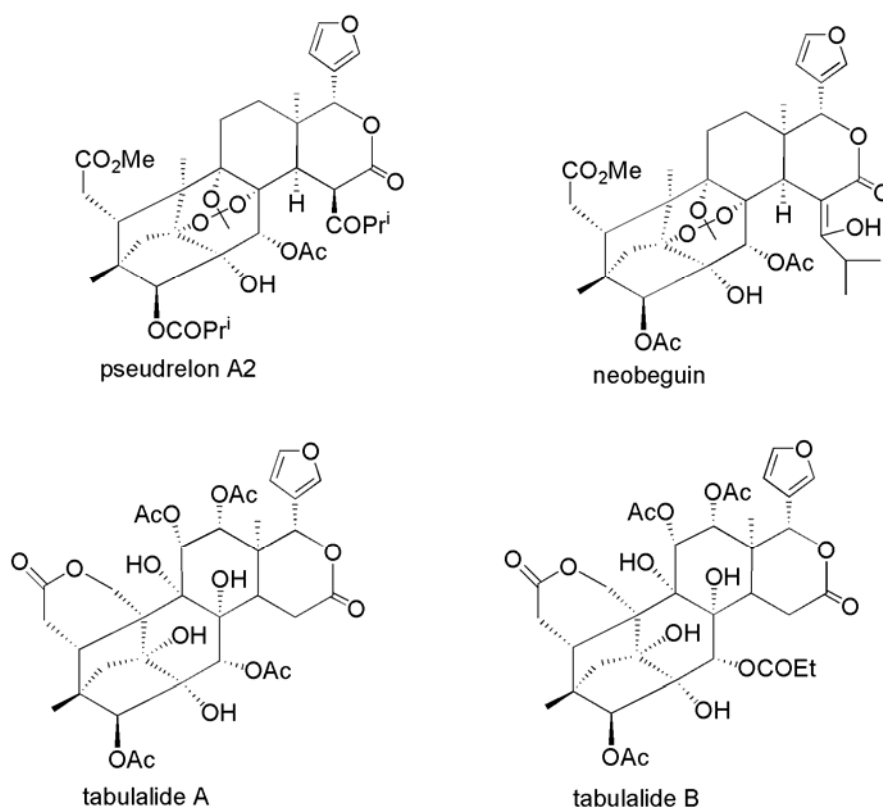
The subfamily 4, Swietenioideae, produces complex limonoids of mexicanolide and phragmalin groups where D ring has been oxidized and B ring opened and recycled. Phragmalins compounds have been isolated from plants such as *Neobeguea mahafalensis* from which pseudrelon A2 and a related compound neobeguine have been isolated<sup>68</sup>. Another plant belongs to this subfamily and produces phragmalin compound is *Chukrasia tabularis*, among isolated compounds there are tabulalides A and B<sup>69</sup>. However, these considerations are still extremely fragmentary so that phylogenetic conclusions have been premature and often conflicting<sup>53</sup>.

#### II.4. Chemistry of the genus *Entandrophragma*

*Entandrophragma* is a genus of eleven species of deciduous trees in the mahogany family Meliaceae, restricted to tropical Africa. At least some of the species attain large sizes, reaching 40-50 m tall, exceptionally 60 m, and 2 m in trunk diameter. The leaves are pinnate, with 5-9 pairs of leaflets, each leaflet 8-10 cm long with an acuminate tip. The flowers are produced in loose inflorescences, each flower small, with five yellowish petals about 2 mm long, and ten stamens. The fruit is a five-valved capsule containing numerous winged seeds<sup>70</sup>.

African mahoganies of the genus *Entandrophragma* are among the most valuable and intensively harvested timber species in central Africa. The wood of this genus has long been appreciated by international markets<sup>71</sup>.





From a discussion on chemical components of the heartwood of species of the genus *Entandrophragma*, the species fall into two groups. The first group consisted of *E. angolense* C. DC., *E. delevoyi* De Wild, *E. excelsum* Sprague and *E. macrophyllum* A. Chev. which yielded simple meliacins of – gedunin and andirobin groups. The other group consisting of *E. bussei* Harms ex Engler, *E. candollei* Harms, *E. caudatum* Sprague, *E. cylindricum* Sprague and *E. palustre* Staner, *E. spicatum* Sprague and *E. utile* Sprague yielded the more complex compounds of the phragmalin group<sup>72</sup>.

Since then, much chemical work has been done on the genus and several new compounds with new structural features have been isolated. In this section, the chemistry of investigated species is presented and chemical structures of isolated compounds are given.

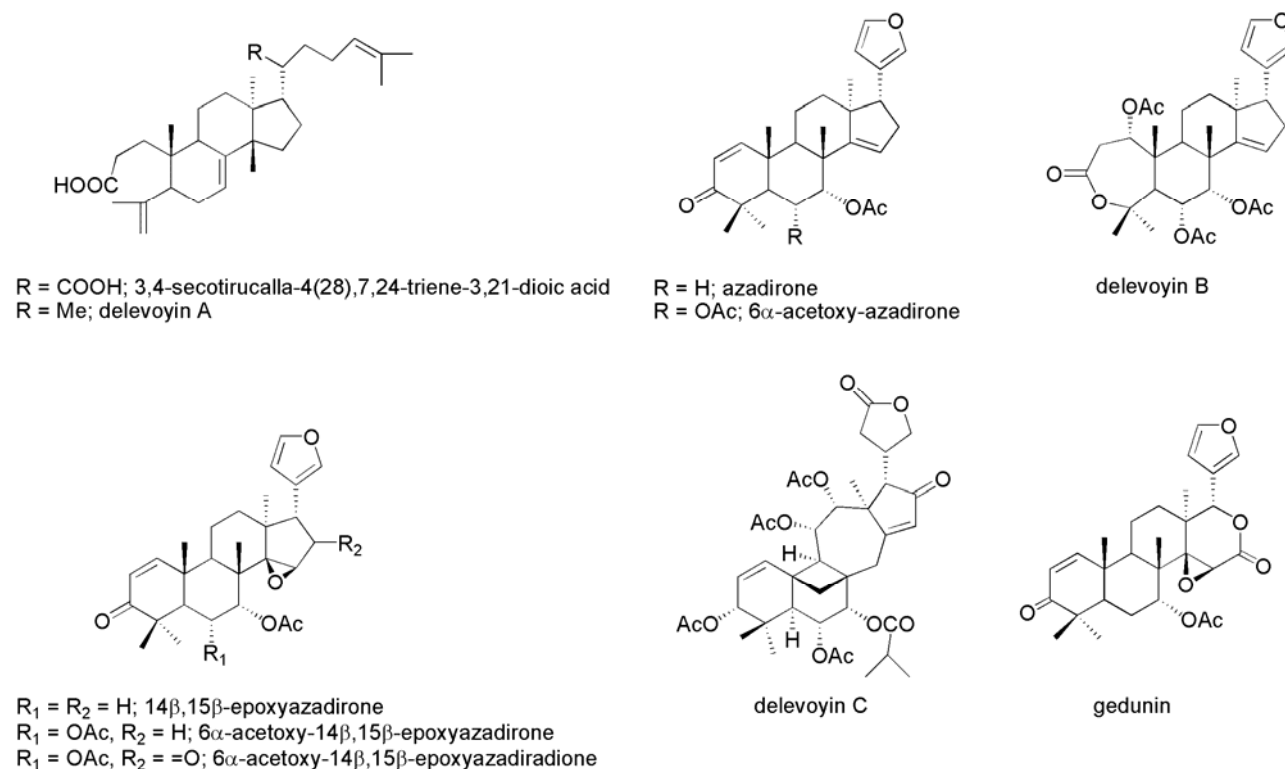
#### II.4.1. *Entandrophragma delevoyi*

The first compounds reported from this species are gedunin and  $\beta$ -sitosterol<sup>73</sup>. Their presence was confirmed later on by an investigation of the wood extract<sup>72</sup>.

More recently, a phytochemical investigation of this plant was carried out and led to the isolation of protolimonoids (3,4-secotirucalla-4(28),7,24-triene-3,21-dioic acid and Delevoyin A (3,4-secotirucalla-4(28),7,24-trien-3oic acid) and limonoids of the havanensin group (azadirone, 6 $\alpha$ -acetoxy-azadirone, 14 $\beta$ ,15 $\beta$ -

epoxyazadirone, 6 $\alpha$ -acetoxy-14 $\beta$ ,15 $\beta$ -epoxyazadirone and 6 $\alpha$ -acetoxy-14 $\beta$ ,15 $\beta$ -epoxyazadiradione) and evodulone group (Delevoyin B)<sup>74</sup>.

A tetranortriterpenoid derivative named Delevoyin C which possesses C-9, C-10, C-19, C-30-cyclobutanyl ring and seven membered ring C has been also reported<sup>75</sup>.



#### II.4.2. *Entandrophragma excelsum* Sprague

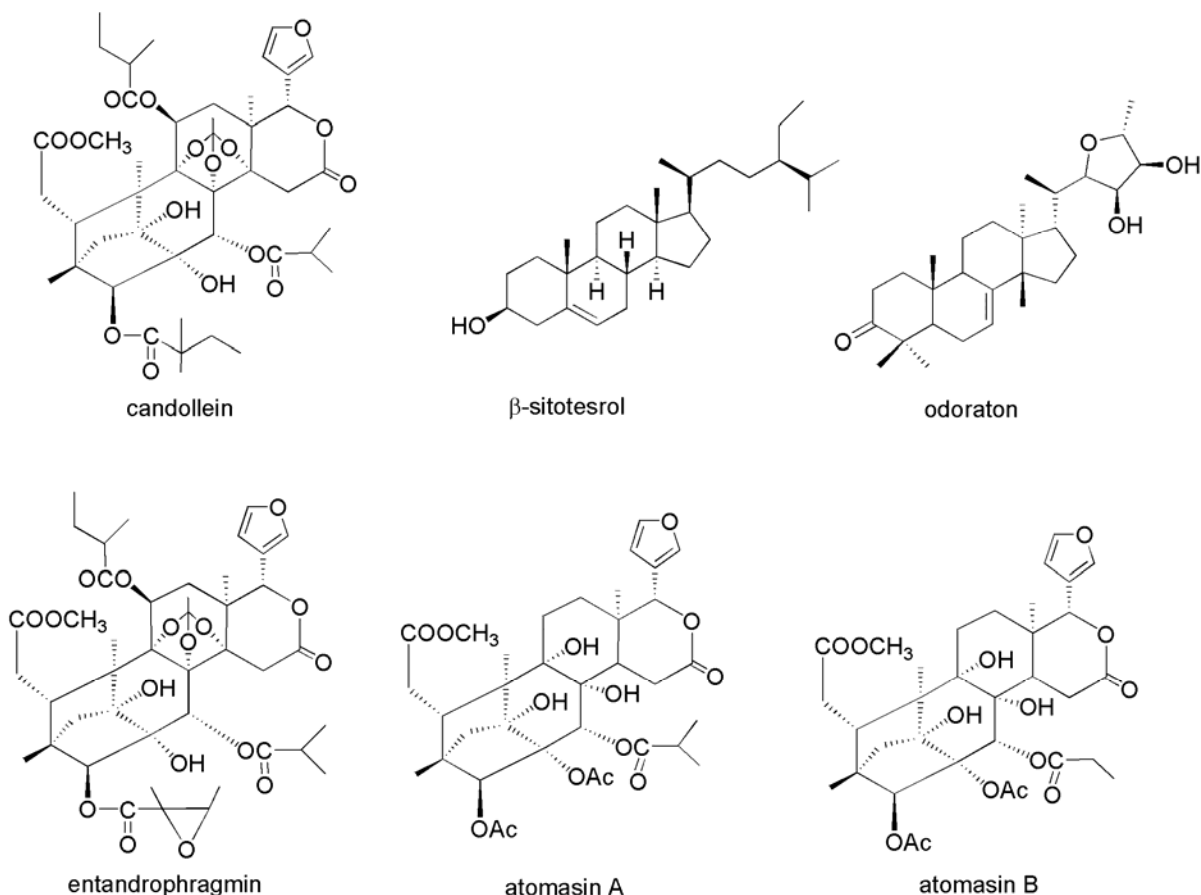
To our knowledge, the only chemical study on this species has been carried out by Taylor D. A. H. in 1964. This investigation, based on the isolation of oxidized triterpenoids derivatives of similar structure to limonin, did not give any crystalline product<sup>73</sup>. With the progress on isolation and separation methods, re-investigation on this species might clarify its phytochemical components.

#### II.4.3. *Entandrophragma macrophyllum* A. Chev.

This species contains mainly gedunin, besides this, methyl angolensate also has been reported<sup>72</sup>.

#### II.4.4. *Entandrophragma bussei* Harms ex Engler

Entandrophragmin and bussein, a series of phragmalin type compounds have been isolated from this species. Firstly, bussein A and B were isolated as a mixture from the timber of *E. bussei*<sup>73</sup> and their structures have been revised<sup>76</sup>. Later on, ten other busseins, C-G, J-M were isolated from the petroleum ether extract of the timber of this species<sup>77</sup>.



#### II.4.5. *Entandrophragma candollei* Harms

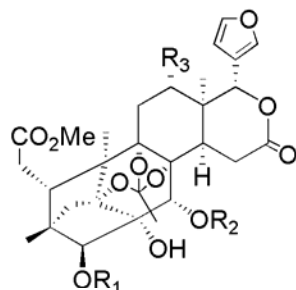
The investigation of the trunk bark of *E. candollei* led to the isolation of β-sitosterol, methyl angolensate, odoraton, candollein, atomasin A and atomasin B<sup>78</sup>. β-Sitosterol and candollein were previously reported from this plant<sup>72</sup>.

In searching for antifeedants of natural origin, Koul et al. selected *E. candollei* for investigation against a lepidopteran pest. From the bark of this tree, epoxiprieurianin and prieuranin were isolated as antifeedant compounds<sup>79</sup>. Prieurianin and epoxy prieurianin have been previously reported from *Trichilia prieuriana*<sup>80</sup> and *Guarea guidona*<sup>81</sup> respectively.

#### II.4.6. *Entandrophragma caudatum* Sprague

The timber of this plant yielded bussein A and B along with entandrophragmin, both phragmalin type compounds<sup>73</sup>. Another chemical investigation on this species led to the purification and structure elucidation of a compound known as phragmalin<sup>82</sup>.

The seed of the genus *Entandrophragma* were not reported to contain any limonoids only protolimonoids have been found in species such as *E. angolense*, *E. cylindricum* and *E. utile*<sup>8</sup>. Surprisingly, the seed of *E. caudatum* yielded limonoids, mainly phragmalin esters. Indeed, the investigation of the seed led to the isolation of the protolimonoids melianone and turreanthin (3-epimelianol acetate), previously isolated from *Turraeanthus africanus*<sup>83</sup>, and the limonoids phragmalin 3,30-di-sobutyrate, phragmalin 3-isobutyrate-30-propionate which has been previously isolated from *Chukrasia tabularis*<sup>84</sup>, 12 $\alpha$ -acetoxyphragmalin 3-nicotinate-30-isobutyrate and  $\Delta^{14,15}$ 12 $\alpha$ -butyryloxyphragmalin 3-nicotinate 30-isobutyrate<sup>85</sup>.

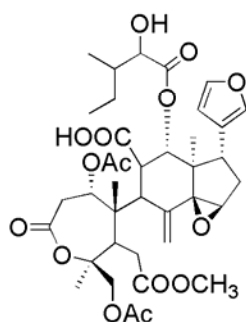


phragmalin 3,30-di-isobutyrate, R<sub>1</sub> = R<sub>2</sub> = isoPrCO, R<sub>3</sub> = H

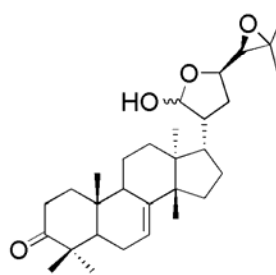
phragmalin 3-isobutyrate-30-propionate, R<sub>1</sub> = isoPrCO, R<sub>2</sub> = EtCO, R<sub>3</sub> = H

12 $\alpha$ -acetoxyphragmalin 3-nicotinate-30-isobutyrate R<sub>1</sub> = mC<sub>5</sub>H<sub>5</sub>NCO, R<sub>2</sub> = isoProCO, R<sub>3</sub> = MeCO

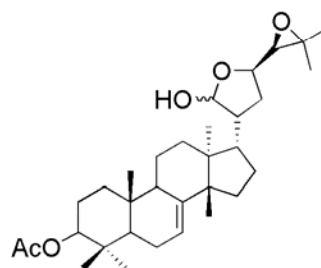
$\Delta^{14,15}$ 12 $\alpha$ -butyryloxyphragmalin 3-nicotinate 30-isobutyrate R<sub>1</sub> = mC<sub>5</sub>H<sub>5</sub>NCO, R<sub>2</sub> = R<sub>3</sub> = isoProCO



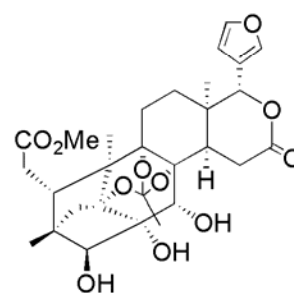
epoxyrieurianin



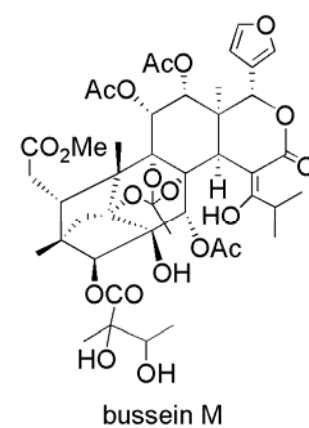
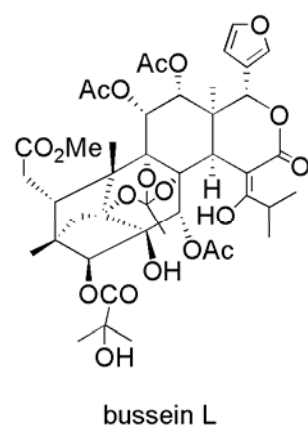
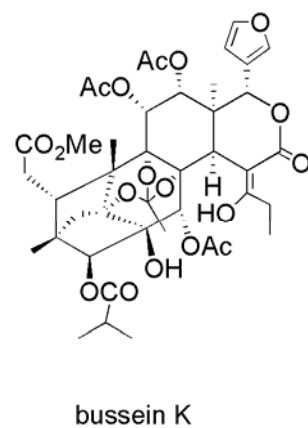
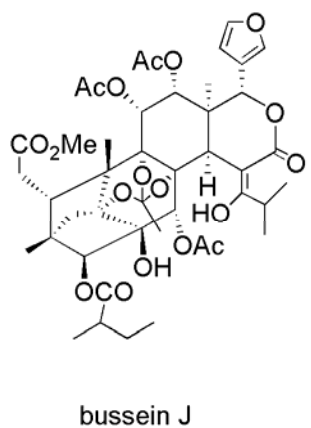
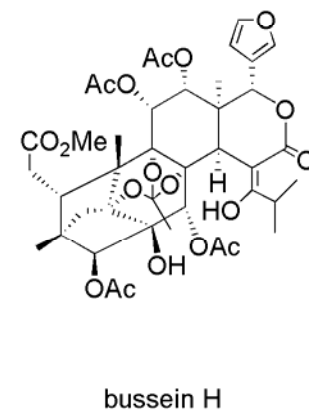
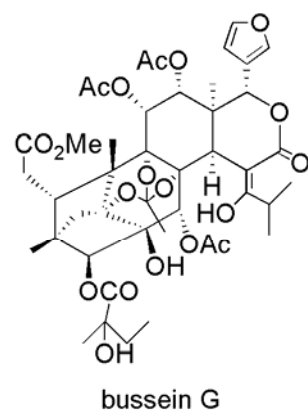
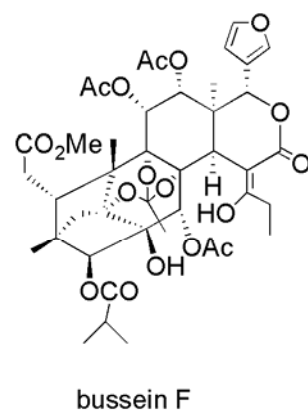
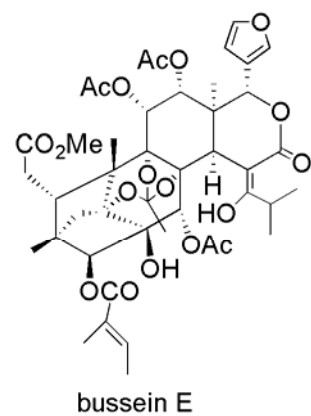
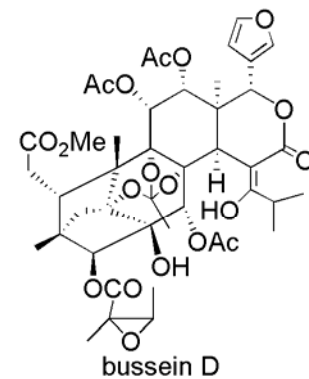
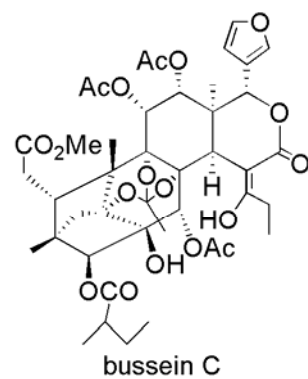
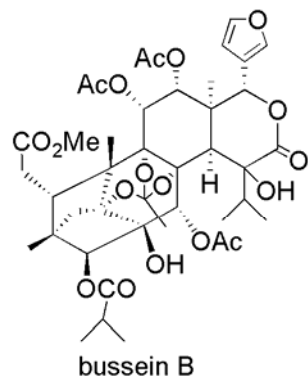
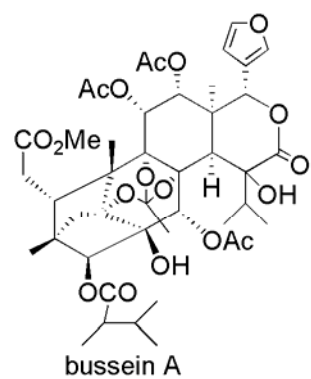
melianone



turreanthin



phragmalin

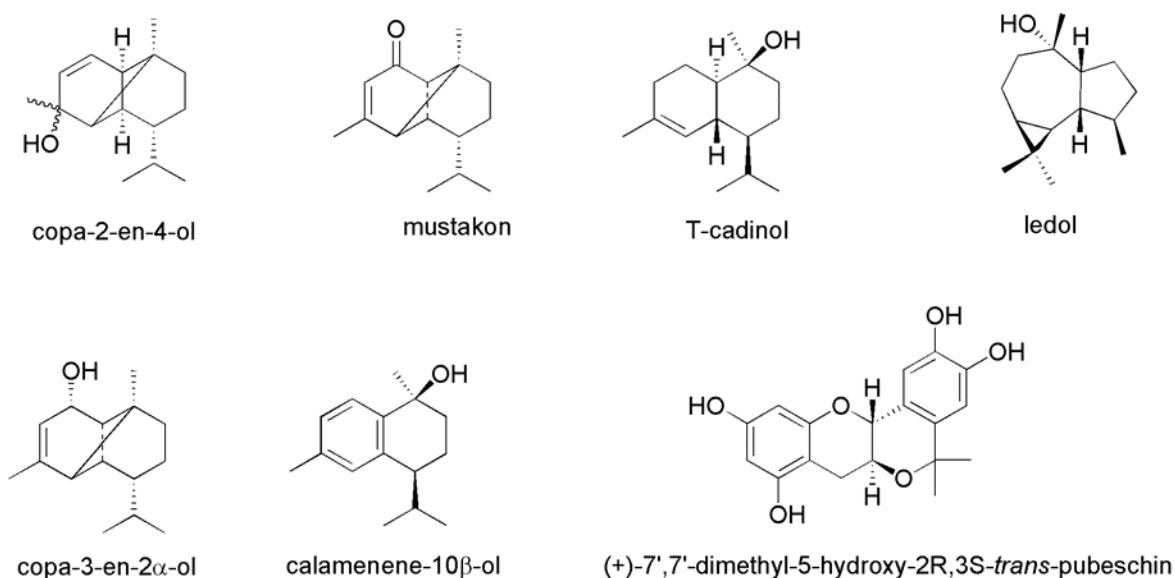


#### II.4.7. *Entandrophragma cylindricum* Sprague

This plant is the most valuable timber of this genus and its chemistry has been extensively studied. Several terpenoids compounds have been isolated from sesquiterpenoid to triterpenoids with also triterpenoid derivatives, flavonoid and alkaloid.

Firstly, the report of  $\beta$ -sitosterol and entandrophragmin was done<sup>6</sup>. Another investigation on the plant confirmed the presence of entandrophragmin which has been detected together with candollein<sup>72</sup>. Some sesquiterpenoids isolated from the bark of *E. cylindricum* exhibited antifeedant activity. These compounds are 3-hydroxy-copa-2-en, 2 $\alpha$ -hydroxy-copa-3-en, 10-Hydroxy-trans-calamenene, T-cadinol, ledol and mustakon<sup>86</sup>.

The peltogynoid 7',7'-Dimethyl-5-hydroxy-2R,3S-trans-pubeschin has been isolated from the wood of the plant<sup>87</sup>. The peltogynoids are a series of flavonoid compounds actively investigated during the mid-1970s<sup>88</sup>.



A commercial sample of the wood *E. cylindricum* contains a series of triterpenoids named Sapelins A-F. Sapelins A and B are tirucall-7-ene triterpene while Sapelins C, D and E are derivatives of 7 $\alpha$ -hydroxyapotirucall-14ene and Sapelin F is a pentahydroxy tirucall-7-ene<sup>89</sup>.

The stem bark of *E. cylindricum* yielded non carbocyclic triterpenoids called Sapelenins A-C<sup>90</sup>. Recently, two other acyclic triterpenoids named Sapelenins D-E have been reported<sup>91</sup>.

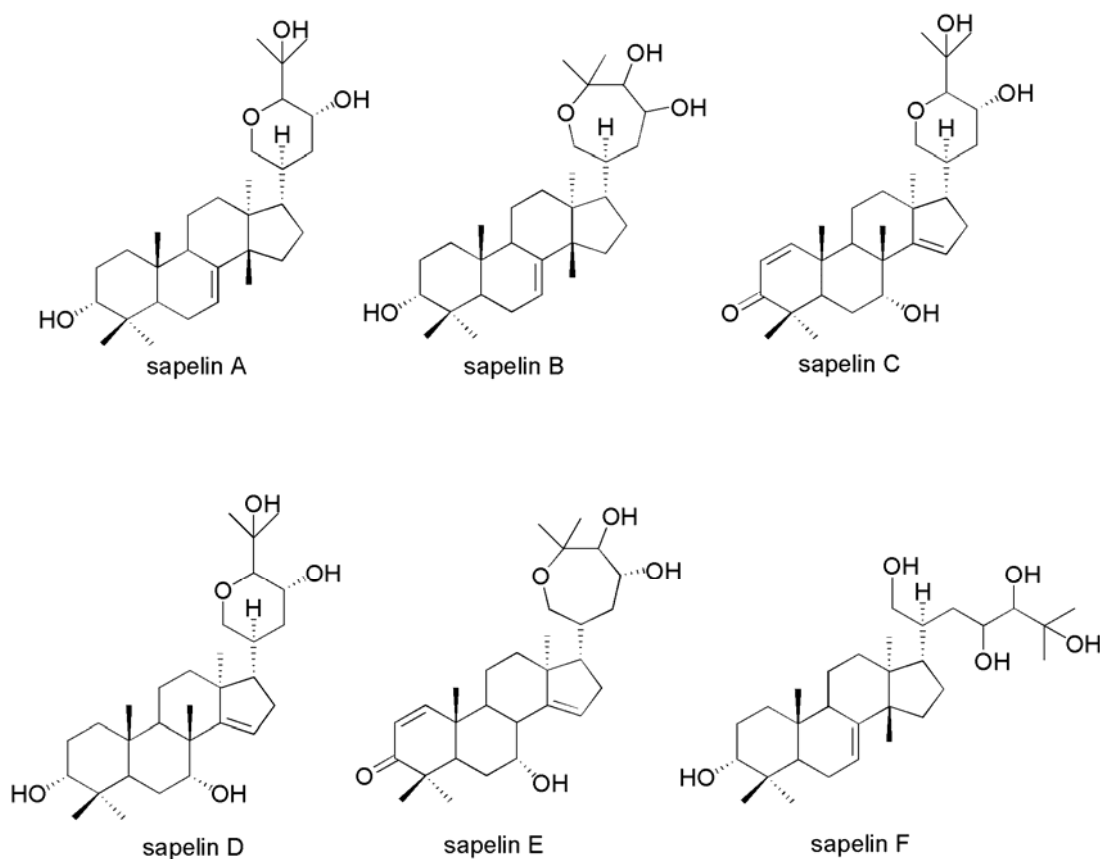
#### II.4.8. *Entandrophragma palustre* Staner

A study on limonoids components based on crystallization of the crude extract solution obtained from the timber, gave no crystal. However, the spectrum of the crude extract suggested it might contain

entandrophragmin or a similar compound<sup>72</sup>. Of course entandrophragmin is a common limonoid of this genus but further studies are required to confirm this observation.

#### II.4.9. *Entandrophragma spicatum* Sprague

The chemical study of *E. spicatum* led to the characterization of entandrophragmin and another compound similar to bussein<sup>72</sup>. A recent study on the components of this plant, confirmed these observations with the isolation of entandrophragmin, spicata-2, a compound similar to bussein, and furthermore a protolimonoid named spicatin (24-hydroxygrandifoliolenone)<sup>92</sup>.

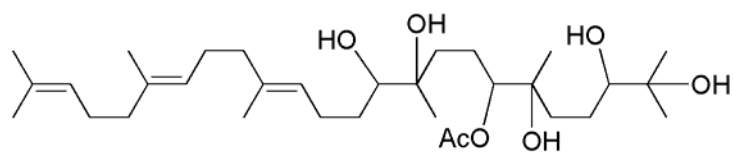


#### II.4.10. *Entandrophragma utile* Sprague

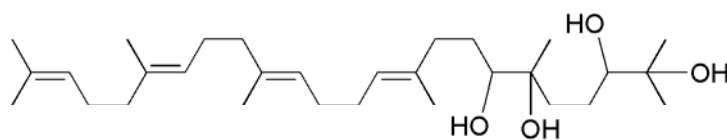
The most ancient investigation of *E. utile* was carried on the timber and yielded methyl angolensate, entandrophragmin and utilin<sup>6</sup>. The structure of Utilin was eventually determined by using X-ray crystallography<sup>93</sup>.

The phytochemical study of the seed of *E. utile* showed that it contains the protolimonoids Sapelin A, a compound previously isolated from *E. cylindricum* and an epoxytriol compound (3 $\alpha$ -21,23*R*-trihydroxy-

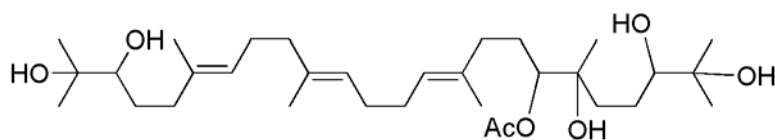
24*S*,25epoxy, 20 $\alpha$ H, which has been revealed later to be a derivative of Sapelin F), which is the hypothetical biogenetic precursor of Sapelin A<sup>94</sup>.



sapelenin A



sapelenin B



sapelenin C

The stem bark of *E. utile* contains also highly-oxygenated tetranortriterpenoid derivatives. The first two to be isolated were entilin A and its acetate entilin B<sup>95</sup>. Followed by the report of the isolation of entilin C<sup>96</sup> and entilin D<sup>97</sup>.

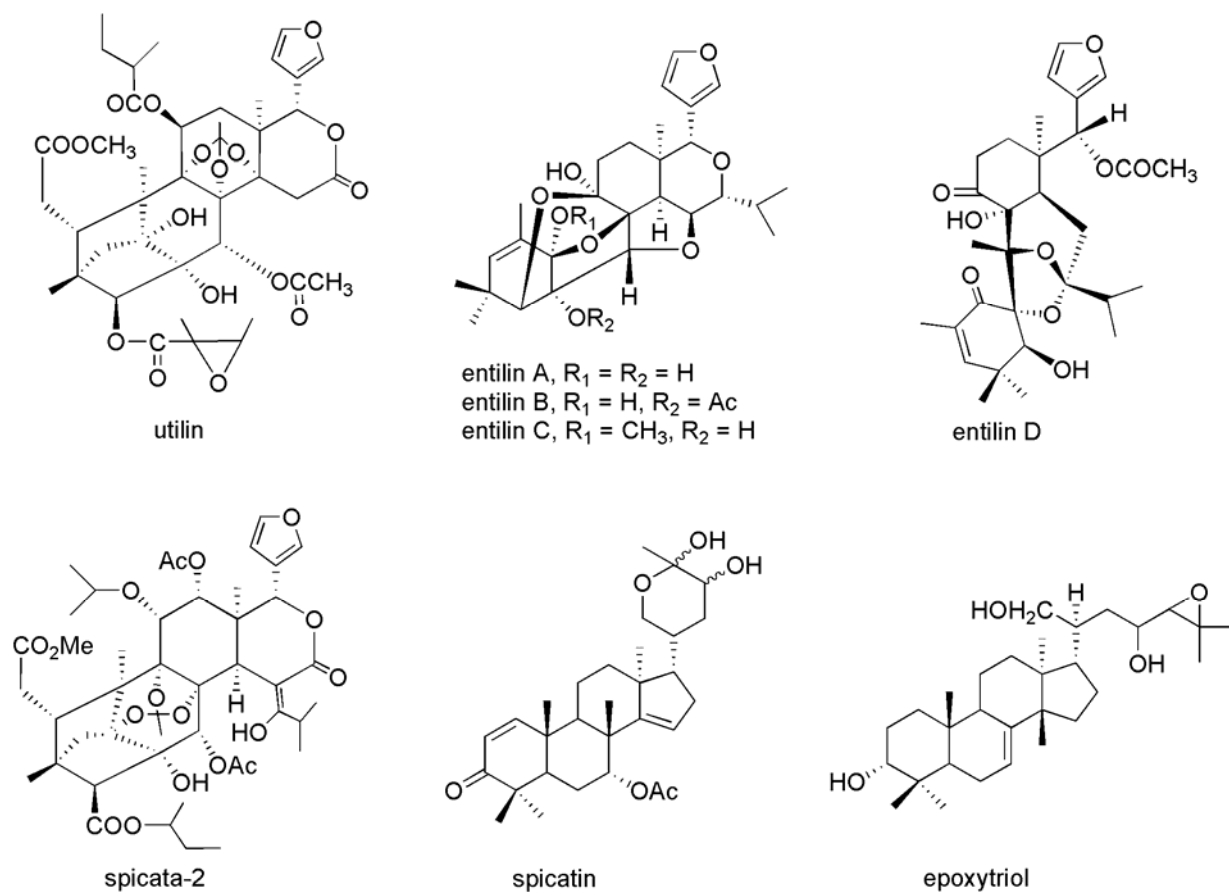
These compounds derived from mexicanolide which loses the side chain at C-5 and cleavage of the C-9, C-10-bond, to give a C5—C-10-double bond. Further modification of the ring D lactone and ketal formation occurs to give extremely complex compounds.

A series of sterol compound, all ergostane derivatives are also present in the stem bark. One identified as 3 $\beta$ ,7 $\alpha$ ,20 $\beta$ -trihydroxy ergosta-5,24(24')diene was isolated as mixture with another sterol compound<sup>98</sup>. Another sterol has been isolated from the stem bark, 3 $\beta$ ,7 $\alpha$ -dihydroxyergosta-5,24(28)-diene<sup>99</sup>.

Finally, 7 $\alpha$ ,20(S)-dihydroxy-4,24(28)-ergotadien-3-one another ergostane derivatives have been isolated as a crystalline solid from the same source<sup>100</sup>.

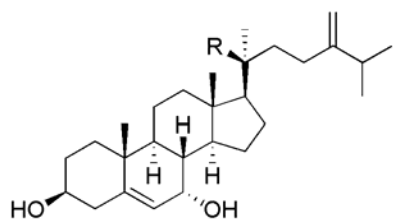
A mexicanolide type compound and its derivative have been isolated from the bark of *E. utile*. These compounds are respectively utilin B<sup>101</sup> and utilin C<sup>102</sup>.



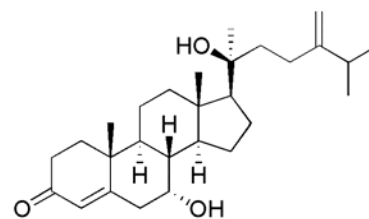


#### II.4.11. *Entandrophragma angolense*

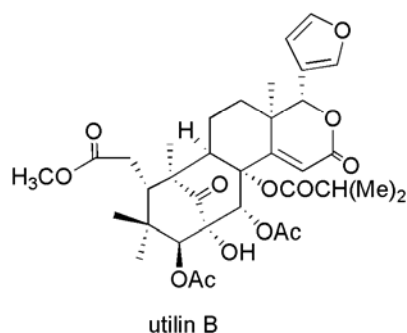
The limonoids isolated from *E. angolense* are gedunin and methyl angolensate together with  $\beta$ -sitosterol<sup>6</sup>. The occurrence of methyl angolensate was also confirmed by other investigations such as the one conducted by Bevan et al.<sup>103</sup>. The protolimonoid entandrolide was isolated from the seeds<sup>83</sup>.



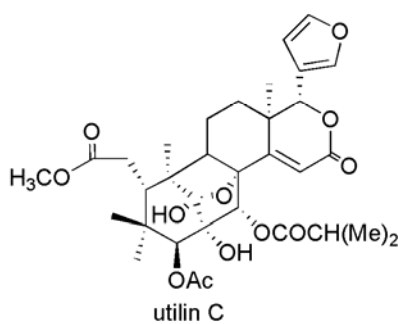
R = H; A sterol compound  
R = OH; 3 $\beta$ ,7 $\alpha$ ,20 $\beta$ -trihydroxy ergosta-5,24(24') diene



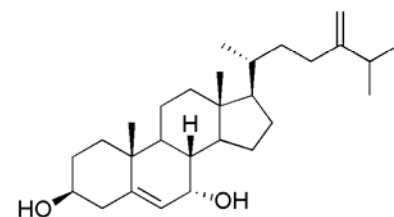
7 $\alpha$ ,20(S)-dihydroxy-4,24(28)-ergostadien-3-one



utilin B

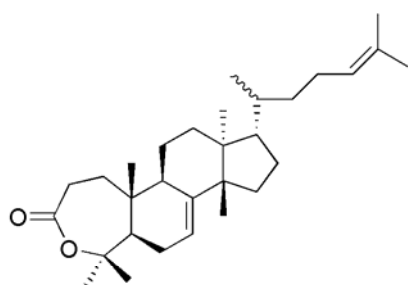


utilin C

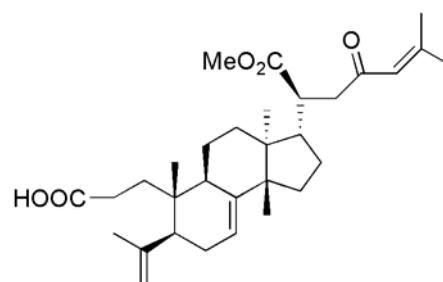


3 $\beta$ ,7 $\alpha$ -dihydroxyergosta-5,24(28)-diene

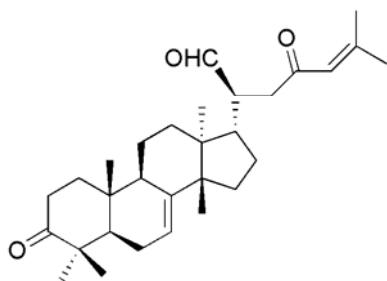
Recently, a chemical study on the leaves yielded 3,23-dioxotirucalla-7,24-dien-21-al, 3,4-secotirucalla-23-oxo-4(28),7,24-trien-21-al-3-oic acid and 3,4-secotirucalla-23-oxo-4(28),7,24-trien-3,21-dioic acid (21-methyl ester)<sup>104</sup>.



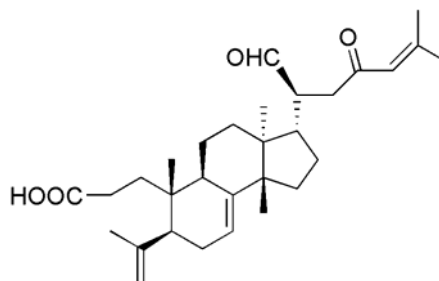
entandrolide



3,4-secotirucalla-23-oxo-4(28),7,24-trien-3,21-dioic acid (21-methyl ester)

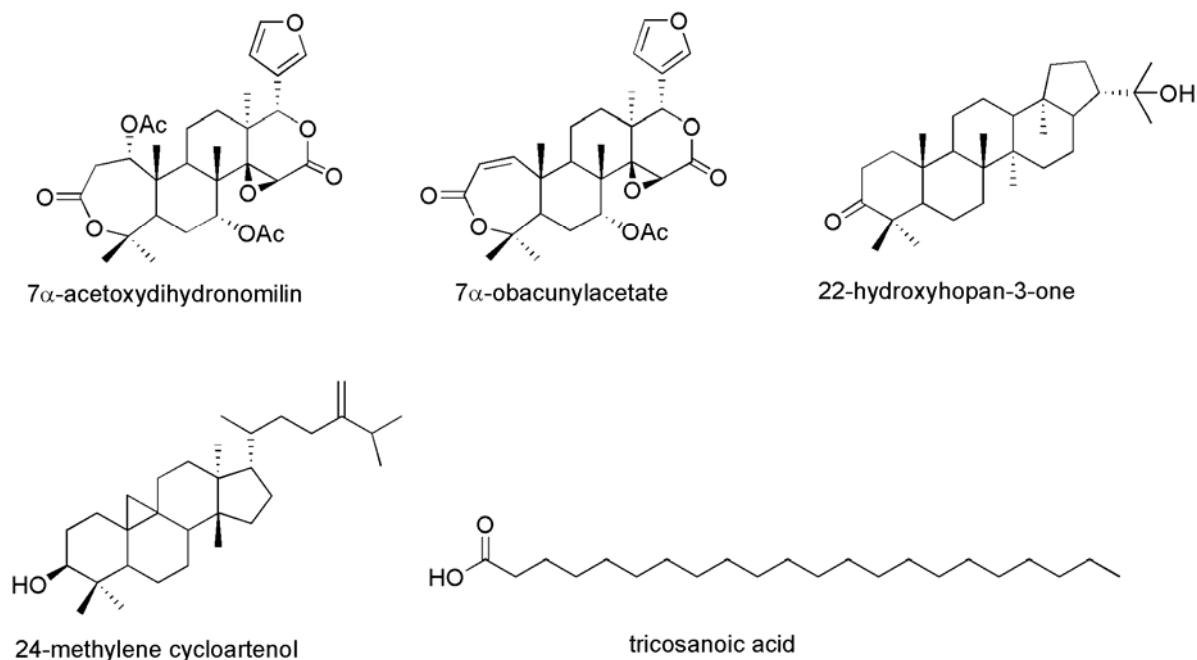


3,23-dioxotirucalla-7,24-dien-21-al



3,4-secotirucalla-23-oxo-4(28),7,24-trien-21-al-3-oic acid

Most recent phytochemical study of the stem bark of *E. angolense*, in addition to methyl angolensate, revealed the occurrence of the  $7\alpha$ -acetoxydihydromilin,  $7\alpha$ -obacunylacetate, 22-hydroxyhopan-3-one, 24-methylene cycloartenol and tricosanoic acid<sup>105</sup>.



Indeed, up to date, chemical differences between the species of *Entandrophragma* are noticeable. Some species such as *E. utile* and *E. cylindricum* have been extensively studied and a rich panel of compounds reported. Re-investigation of species such as *E. angolense*, *E. palustre* and *E. excelsum* can lead to a better knowledge of the chemistry of this genus.

## II.5. Purpose of this work

The chemistry of the genus *Entandrophragma* attracted the great interest in the past, because the knowledge of the chemistry of these plants could help to establish the relation of plant chemistry and phylogeny. Actively, an important number of investigations were carried out on different parts of plants. Especially bark, heartwood and seeds. And this genus yields compounds with fascinating chemical structure (triterpenoids derivatives highly oxidative of phragmalin type compound) and their biological activities. During this period, the isolation scheme was based generally on the crystallization of the compound in its solution with an appropriate solvent or mixture of solvents and/or by comparison of the  $R_f$  obtained by TLC of a known sample and the sample under study. Nowadays, the development of sensitive chromatographic and spectroscopic techniques for the isolation and structure determination of natural products has greatly facilitated phytochemical investigations.

During the past decade, the chemical investigations of *E. cylindricum* and *E. utile* brought to light the occurrence of terpenoid antifeedants with new structure features. Re-investigations of other species using modern separation techniques and spectroscopic methods are highly desired.

In a series of experiments carried out in our lab on Meliaceae species, several limonoids have been isolated and reported. In continuous of these investigations, phytochemical studies on the Congolese species of *Entandrophragma angolense* have been carried out, after the extracts of this plant have displayed a considerable antifeedant activity against *Spodoptera* insects.

*E. angolense* is widely used in ethnomedical treatment of various gastrointestinal disorders including peptic ulcers in humans<sup>106</sup> and in treatment of malaria<sup>48</sup>.

In this plant, the occurrence of gedunin and methylangolensate has been reported. The plant contains mainly methyl angolensate (in the timber of the Nigerian *Entandrophragma angolense*, it occurs in about 10%<sup>107</sup>).

The phytochemical study this plant has been limited to the determination of the biological activity of this compound and its ulcer activity has been established. The goal of this study is to clear up the existence of other secondary metabolites (limonoids) in this plant and the determination of their structures.

## II.6. Description of the plant under study<sup>108</sup>

**Scientific name:** *Entandrophragma. angolense*

**Other Common Names:** Mukusu (Uganda), Tiama (Ivory Coast), Edinam (Ghana), Kalungi (DR Congo).

**Distribution:** West, Central, and East Africa; occurs in rain forests, deciduous forests, and transitional formations. Coppices freely at the pole stage.

**The Tree:** Reaches a height of 160 ft, bole moderately straight, cylindrical, clear to 60 to 80 ft; trunk diameters 4 to 7 ft over large buttresses; wide-spreading root ridges.

The Wood:

**General Characteristics:** Heartwood pink brown or a dull uniform red, usually darkening on exposure to a deep red brown; sapwood creamy white or pale pink, up to 4 in. wide, sometimes not sharply demarcated. Grain interlocked, producing rather broad stripes; texture medium to rather coarse; without taste and almost without odor.

**Weight:** Basic specific gravity (ovendry weight/green volume) 0.45; air-dry density 34 pcf.

**Drying and Shrinkage:** Dries rapidly but with a marked tendency to warp. Kiln schedule T2-D4 is suggested for 4/4 stock and T2-D3 for 8/4. Shrinkage green to ovendry: radial 4.7%; tangential 6.6%; volumetric 11.8%. Movement in service is rated as small.

**Working Properties:** Works rather easily with hand and machine tools, but there is tearing of interlocked grain, otherwise a good finish is obtained in most operation. Good gluing properties.

**Durability:** Heartwood is rated as moderately durable, termite resistance is variable. Sapwood liable to attack by powder-post beetle.

**Preservation:** Heartwood is rated as extremely resistant to preservative treatments, sapwood is resistant.

**Uses:** Furniture, joinery, cabinetmaking, boat construction, decorative veneers and plywood.

## Chapter III. Material and Methods

### III.1. General

All solvents used in this study were distilled before use and the hplc solvents were filtered after distillation (Filters used for water, polymer: mixed cellulose ester, 0.45  $\mu\text{m}$ , 47 mm, Advantec; for methanol and acetonitrile, polymer: ptfе, 0.5  $\mu\text{m}$ , Advantec).

Chromatographic separations (CC, VCC, MPC) were carried out on Silica gel 60 (70-230 mesh). Analytical TLC was performed on precoated silica gel 60F<sub>254</sub> plates (Merck), spots were visualized under UV light (254 nm) and by spraying concentrated HCl after soaking the plate in Ehrlich reagent (a saturated solution of *p*-dimethyl amino benzaldehyde in ethanol), the appearance of a pink color indicates the presence of limonoids.

Preparative HPLC was carried out with a UV detector (Waters 2487 dual wavelength UV detector) at 225 nm under the following condition: column, 19 x 150 mm, packed with  $\mu$ Bondasphere 5 $\mu\text{m}$  C<sub>18</sub> – 100 Angstrom; solvent system, isocratic mode using MeOH or CH<sub>3</sub>CN containing water at 4 ml min<sup>-1</sup>.

NMR spectra were recorded at room temperature on a 600 MHz a JEOL FX-600 spectrometer. Chemical shifts ( $\delta$ ) are expressed in ppm relative to tetramethylsilane (TMS) as internal standard and coupling constants are given in Hz. <sup>1</sup>H NMR spectra were referenced against the CHCl<sub>3</sub> signal at  $\delta_{\text{H}}$  7.27, and <sup>13</sup>C NMR spectra to the corresponding signal at  $\delta_{\text{C}}$  77.0. Multiplicities were determined from DEPT experiments

IR (Film) and UV (MeOH) spectra were recorded respectively on JASCO FT/IR 5300 and Shimadzu UV-210A spectrophotometers. Melting points were determined on a Micro Melting Point apparatus and are uncorrected. HR-FABMS was acquired on a JEOL JMS XD-303 instrument. Optical rotations were measured at room temperature in CHCl<sub>3</sub> on a JASCO DIP-370S.

### III.2. Plant material

The root bark of *E. angolense* was collected in July 2002 at Jardin Botanique de Kisantu located in the province of Bas-Congo, Democratic Republic of Congo. A voucher specimen has been deposited in the Institut National pour la Recherche Agronomique (INERA) of Kinshasa University.

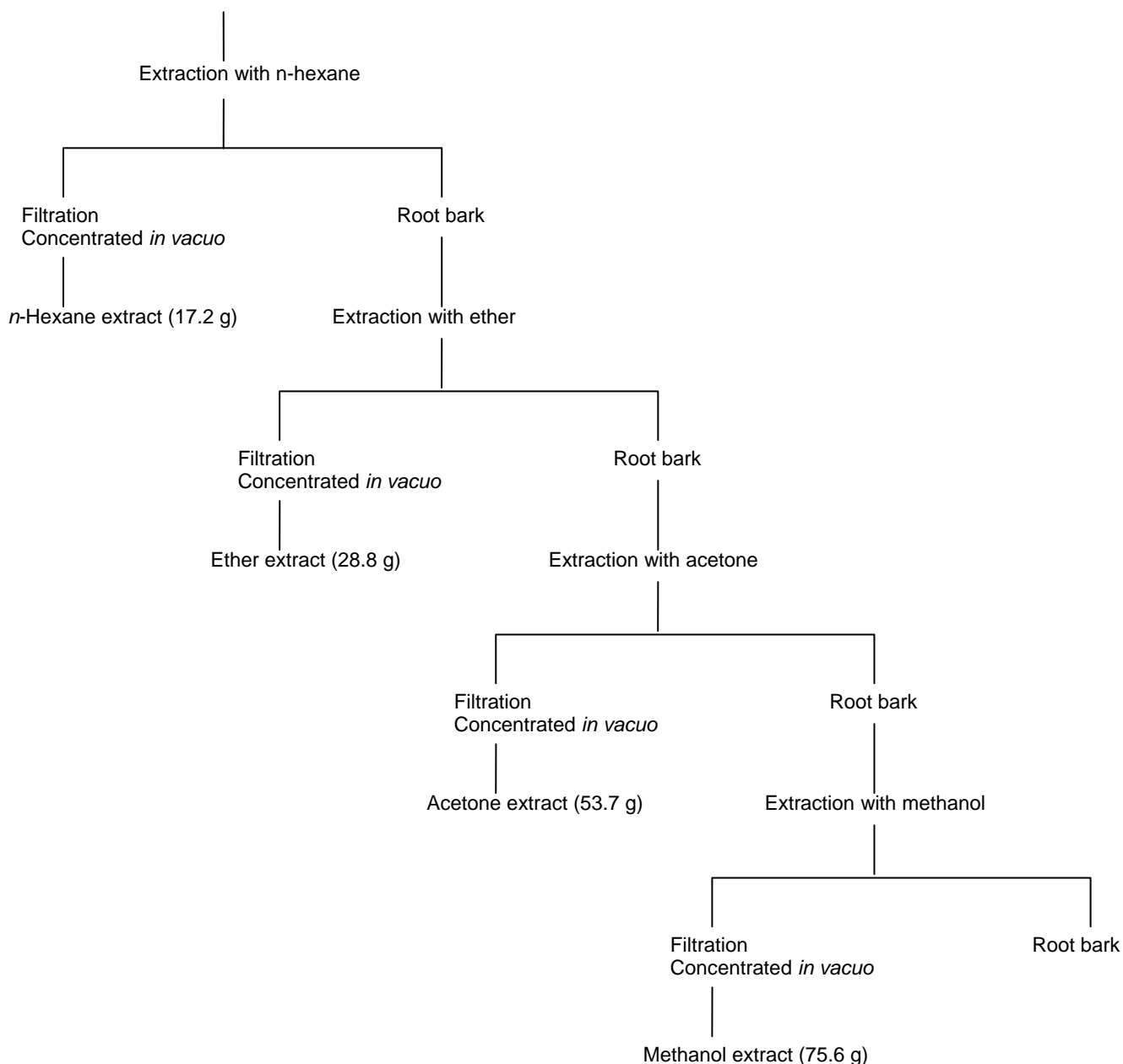
### III.3. Extraction and isolation

#### III.3.1. Preparation of extracts

The air-dried (1kg) was soaked successively with increasing polarity solvents: hexane, ether, acetone and methanol at room temperature using 3 liters of each for four weeks. The extracts were filtered two times and solvents removed under reduced pressure at 40°C to afford different crude extracts. These extracts were

obtained as depicted in figure. The appearance of a characteristic color upon treatment with Ehrlich's reagent on TLC showed that all these extracts contained a variety of limonoids. However, the TLC profile of the acetone extract was similar to this of methanol extract but the later seemed to be more concentrated in limonoids. So, for this study, the methanol extract was chosen instead of the acetone extract. Each extract was fractionated by a combination of chromatographic to yield different compounds.

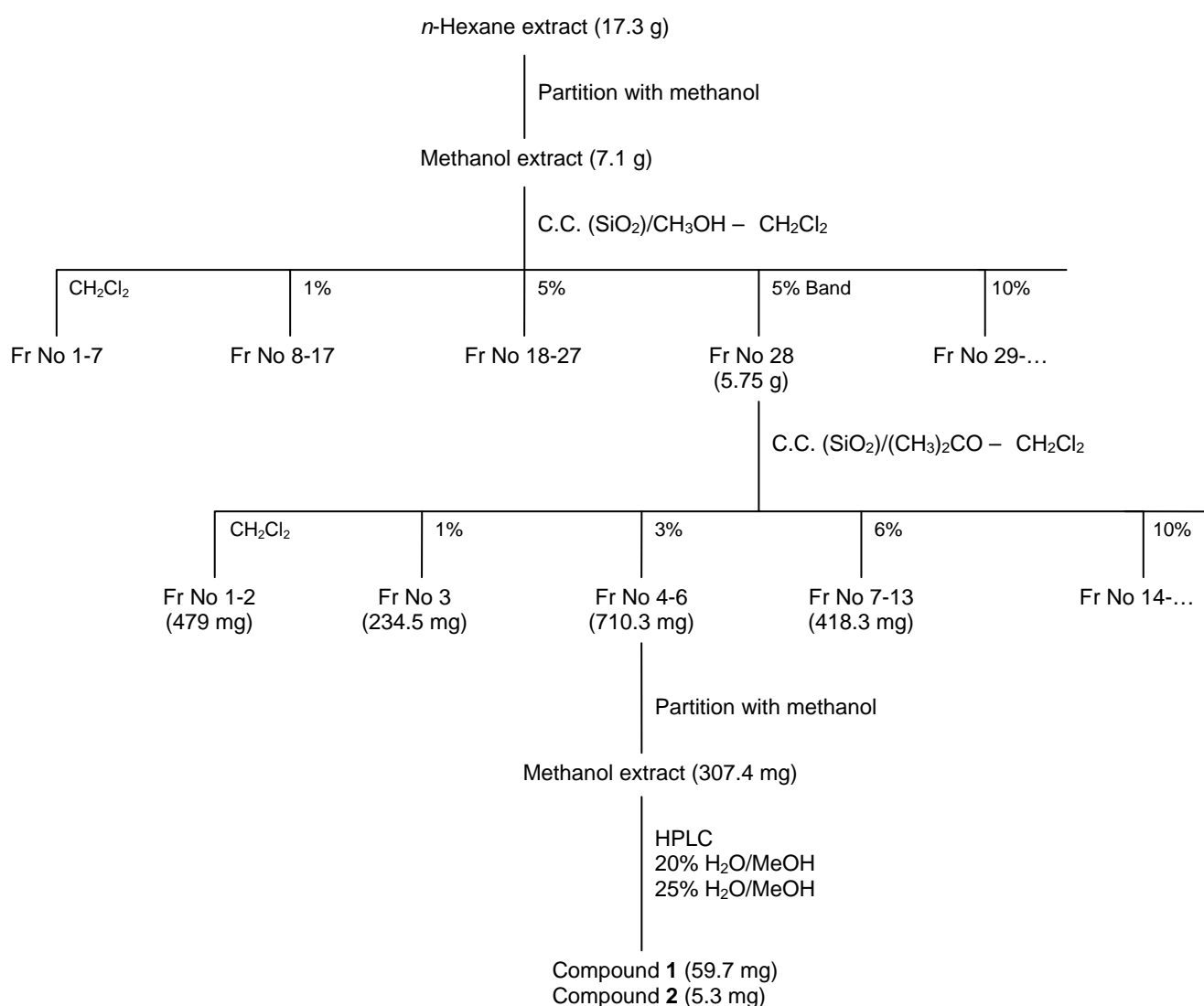
*Entandrophragma angolense* (Root bark, 1kg)



**Scheme 5.** Preparation of crude extracts from the root bark of *E. angolense*.

### III.3.2 Purification of the hexane extract

The *n*-hexane extract obtained as described in Scheme 5 was partitioned in methanol. The methanol extract (7.1 g) was subjected to CC on silica gel, eluted with increasing amount of methanol in dichloromethane. The only the fraction, fraction 28, which gave a positive test upon the Ehrlich reagent was retained. It was a band collected when eluting the column with 5% MeOH-CH<sub>2</sub>Cl<sub>2</sub> as solvent system. This fraction was rechromatographed on silica gel using acetone-CH<sub>2</sub>Cl<sub>2</sub> as solvent system. The fraction eluted with 3% of the solvent system gave a positive Ehrlich test and was used for the next step. The treatment of this fraction with methanol, led to a methanol extract which has been purified by HPLC with 20-25% MeOH-H<sub>2</sub>O to afford compounds **1** (59.7 mg) and **2** (5.3 mg). The extraction operations are depicted in Scheme 6.



**Scheme 6.** Isolation of limonoids from the *n*-hexane extract

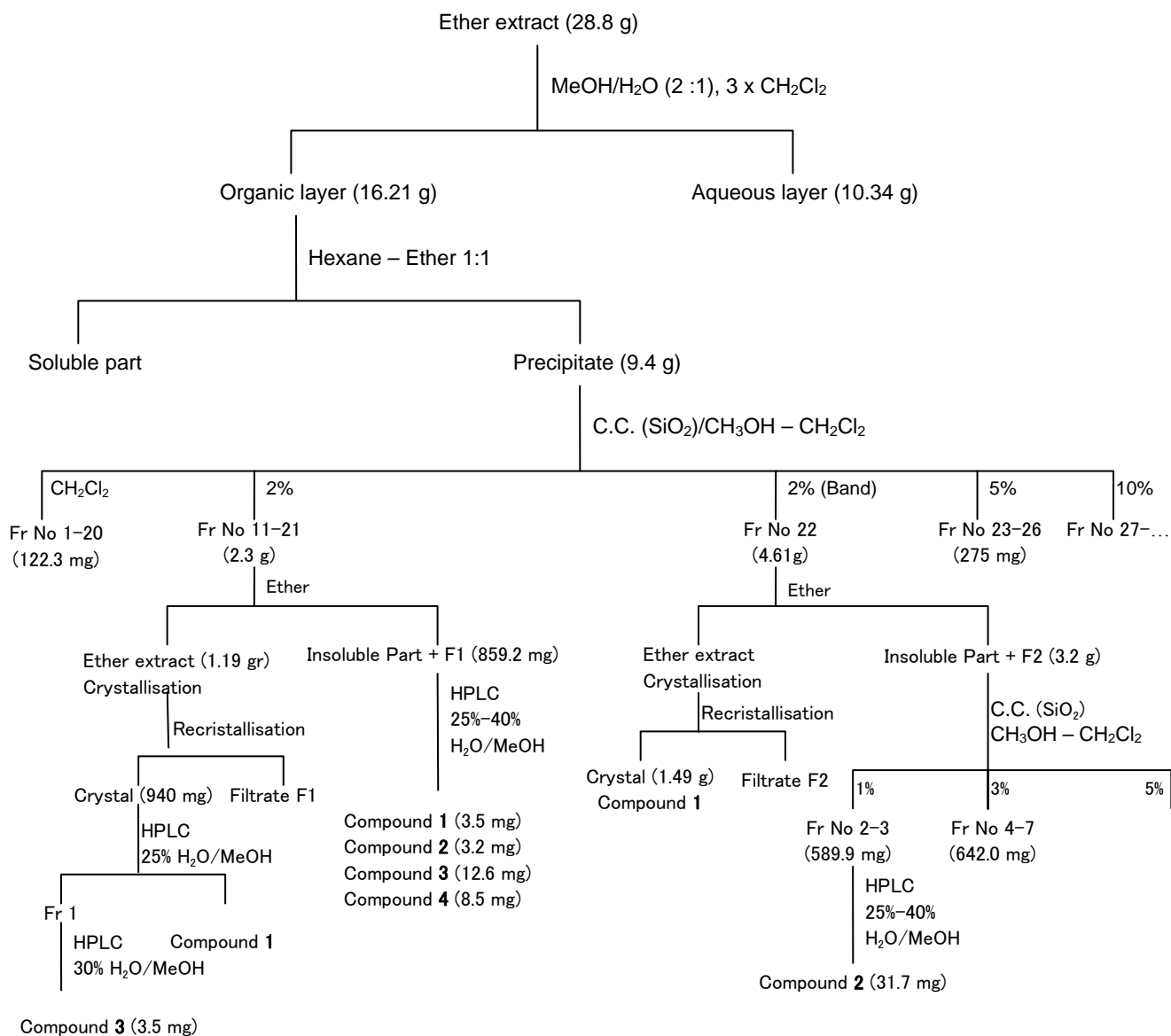
### III.3.2. Purification of the ether extract

The ether extract was dissolved in 1.5 l of MeOH–H<sub>2</sub>O (2:1) and then extracted with CH<sub>2</sub>Cl<sub>2</sub> (3 x 750 ml). The CH<sub>2</sub>Cl<sub>2</sub> layer (16.21 g) was treated with a mixture of hexane – ether (1:1) and the precipitate was removed and fractionated by column chromatography on silica gel using a CH<sub>2</sub>Cl<sub>2</sub>–MeOH solvent system. The elution with 2% MeOH- CH<sub>2</sub>Cl<sub>2</sub> afforded fractions which could be easily separated into two groups using Ehrlich reagent. The first group, fractions 11-21 (2.3 g), was extracted using ether. The ether extract crystallized, and the crystal was recrystallized and submitted to purification by preparative HPLC using 25% H<sub>2</sub>O-MeOH as solvent system to yield two fractions, one was compound **1** and the second fraction was further purified by HPLC using 30% H<sub>2</sub>O-MeOH solvent system to give compound **3** (3.5 mg). The ether insoluble extract was purified by HPLC using successively 25% and 40% of H<sub>2</sub>O-MeOH solvent system to yield compounds **1** (3.5 mg), **2** (3.2 mg), **3** (12.6 mg) and **4** (8.5 mg). The second group, fraction 22, collected as a band, was also treated with ether. The ether extract crystallized and the recrystallisation led to compound **1** (1.49 g). The HPLC of the ether insoluble part using 25% and 40% of H<sub>2</sub>O-MeOH as solvent system led to isolation of compound **2** (31.7 mg) (Scheme 7).

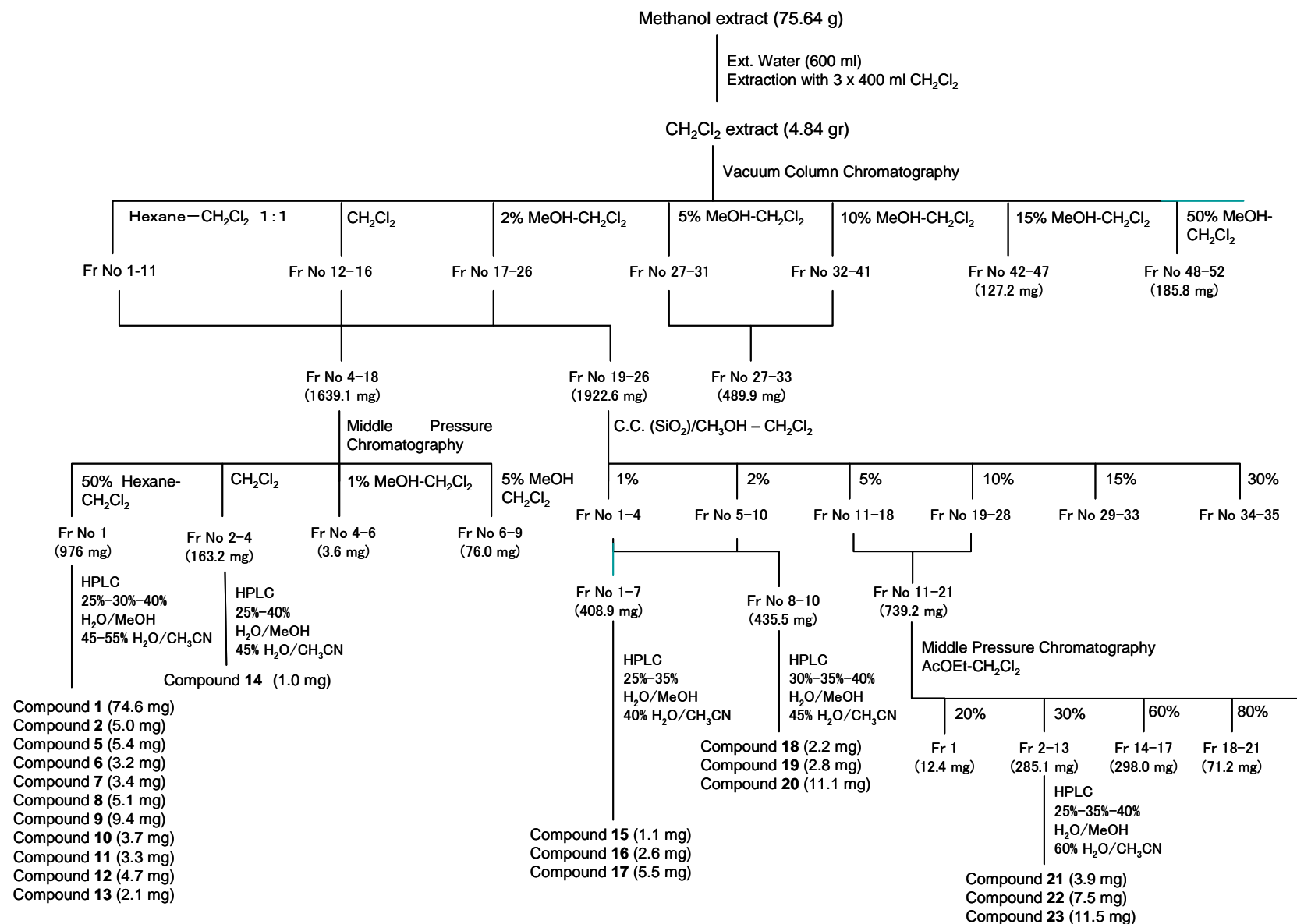
### III.3.3. Purification of the methanol extract

The methanol extract was suspended in water (600 ml) and extract three times with CH<sub>2</sub>Cl<sub>2</sub> (400 ml, each). The organic layer (4.84 gr) was fractioned on silica gel vacuum column chromatography using successively Hexane-CH<sub>2</sub>Cl<sub>2</sub> (1:1), CH<sub>2</sub>Cl<sub>2</sub> and a gradient MeOH-CH<sub>2</sub>Cl<sub>2</sub> as solvent systems. According to the TLC profiles, the fractions were rearranged in three parts as follows fractions 4-18 (1.6 g), fractions 19-26 (1.9 g) and fractions 27-33 (489.9 mg). The first part, was rechromatographed on silica gel MPC using successively Hexane-CH<sub>2</sub>Cl<sub>2</sub> (1:1), CH<sub>2</sub>Cl<sub>2</sub> and 1% and 5% MeOH-CH<sub>2</sub>Cl<sub>2</sub> to afford two limonoids fractions: fractions 1 (976 mg) and fractions 2-4 (163.2 mg). These fractions were purified by HPLC using 25-30%, 45% H<sub>2</sub>O-MeOH gradient as solvent system followed by 45-55% H<sub>2</sub>O/MeCN and yielded compounds **1-2**, **5-13** and **14**. The second part was fractioned also by silica gel column chromatography using MeOH-CH<sub>2</sub>Cl<sub>2</sub> as solvent system and three limonoid fractions were obtained. The first (fractions 1-7, 408.9 mg) and the second (fractions 8-10, 435.5 mg) were purified through HPLC with 25-35% H<sub>2</sub>O-MeOH followed by 40-45% H<sub>2</sub>O-MeCN gradient as eluent to give successively compounds **15-17** and compounds **18-20**. Finally, the third and last part (739.2) was separated by MPC using AcOEt-CH<sub>2</sub>Cl<sub>2</sub> as solvent system to afford one limonoid fraction which were subjected to HPLC purification to give compounds **21-23** (Scheme 8).





**Scheme 7.** Purification of the ether extract



Scheme 8. Isolation of limonoids from the methanol extract

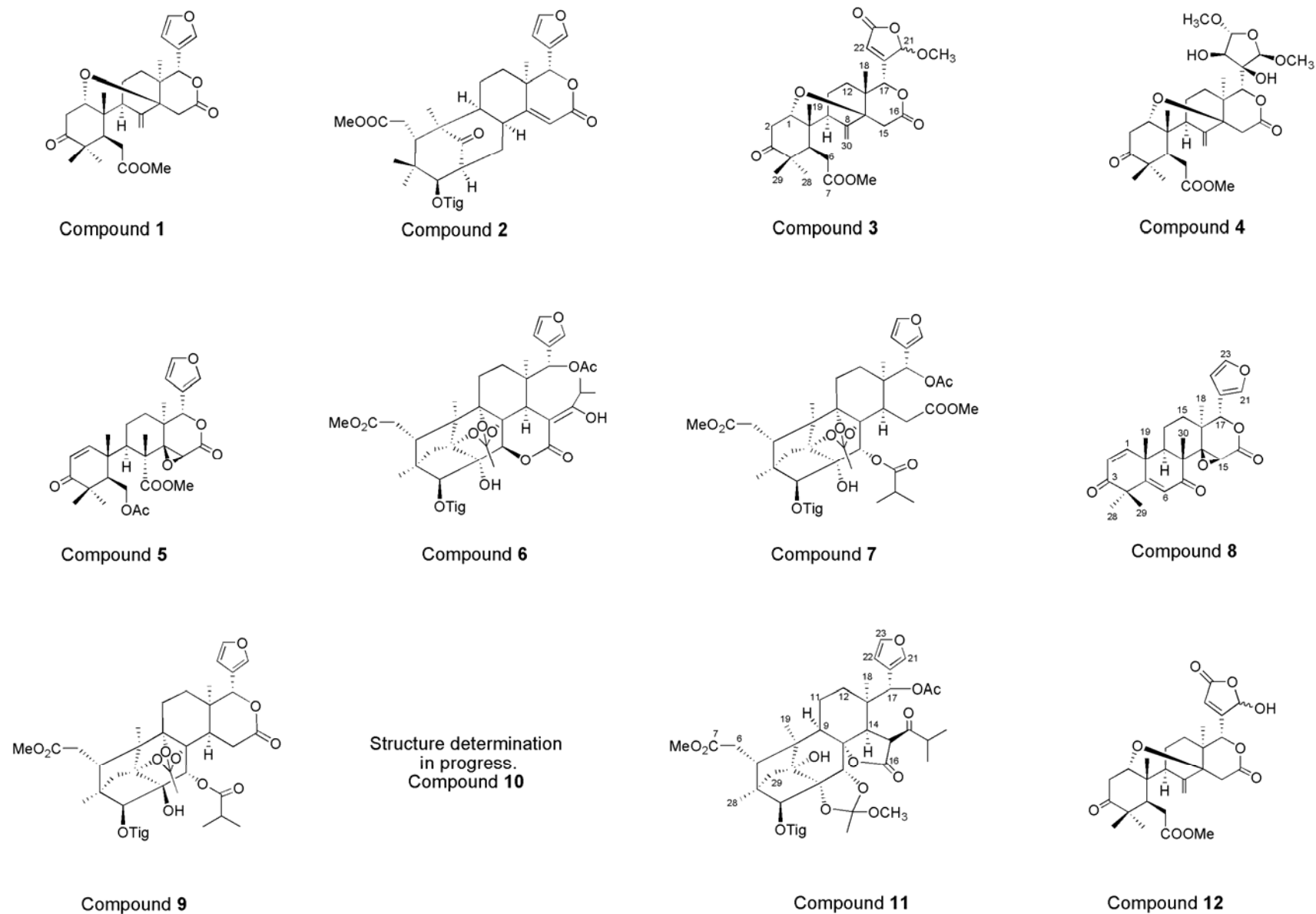


Figure 1. Isolated tetranortriterpenoids from *E. angolense*

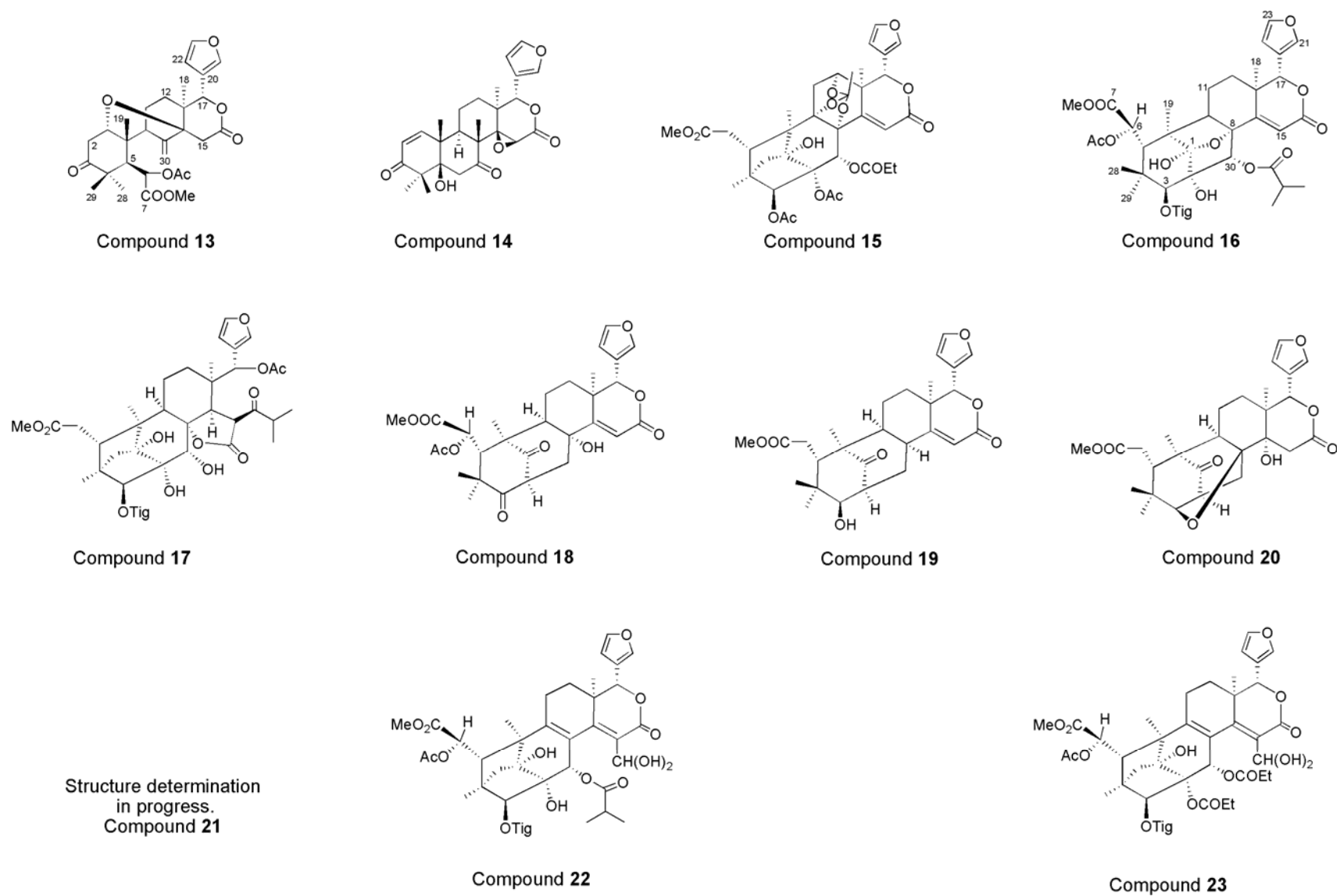


Figure 1 (continued). Isolated tetranortriterpenoids from *E. angolense*

## Chapter IV. Structure elucidation

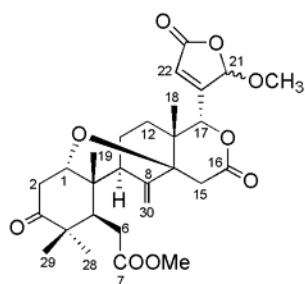
### IV.1. Introduction

The structure of these news compounds was determined using mass spectrometry and 1D and 2D NMR. The known compounds were identified by comparison of their spectroscopic data with these reported in the literature and they are: methyl angolensate (**1**)<sup>6</sup>, methyl 6-acetoxiangolensate (**13**)<sup>109</sup>, secmahoganin (**5**)<sup>110</sup>, xyloccensin K (**20**)<sup>111</sup> and 3 $\beta$ -hydroxy-3-deoxycarapin (**19**)<sup>112</sup>. Except methyl angolensate, this is the first isolation of the remaining known compounds from this plant. According their data, the isolated unknown compounds have been classified and the structure elucidation is discussed according to.

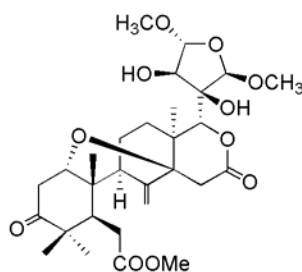
### IV.2. Classification of isolated compounds

The isolated compounds have been grouped according to the classification presented in Table 1. In this section, different groups are displayed.

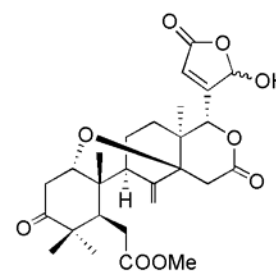
#### IV.2.1. Protolimonoids



Compound 3

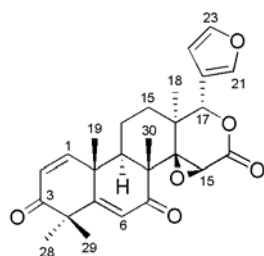


Compound 4

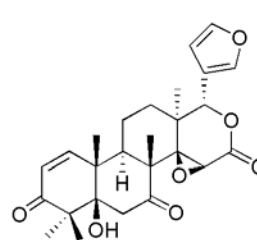


Compound 12

#### IV.2.2. Gedunin derivatives

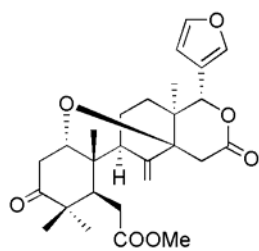


Compound 8

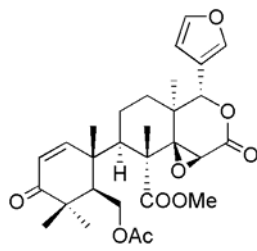


Compound 14

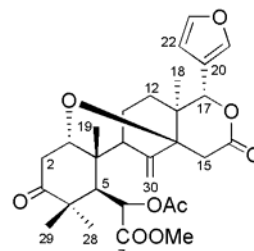
#### IV.2.3. Andirobin derivatives



Compound 1

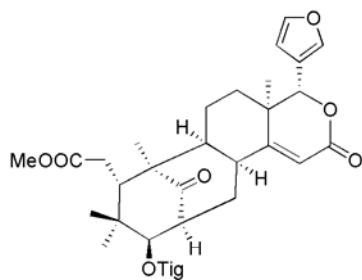


Compound 5

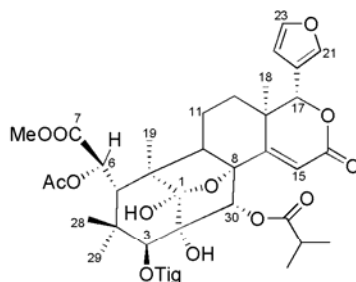


Compound 13

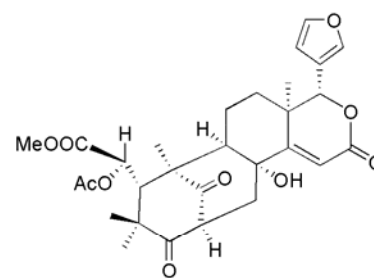
#### IV.2.4. Mexicanolides derivatives



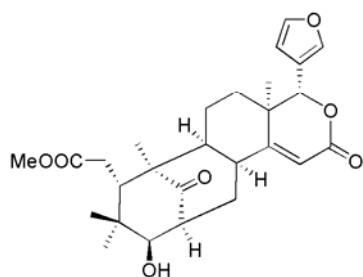
Compound 2



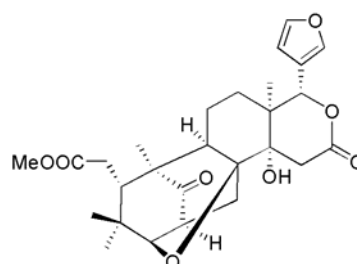
Compound 16



Compound 18

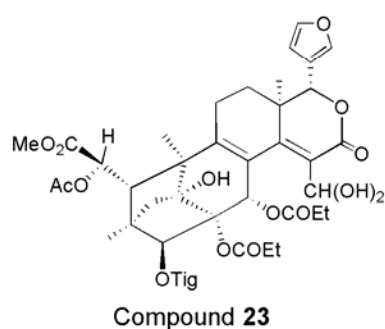
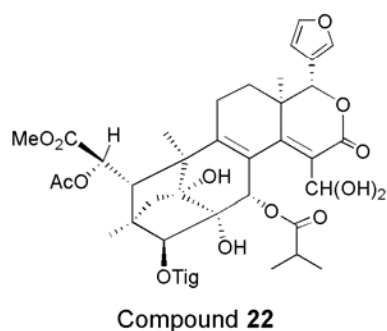
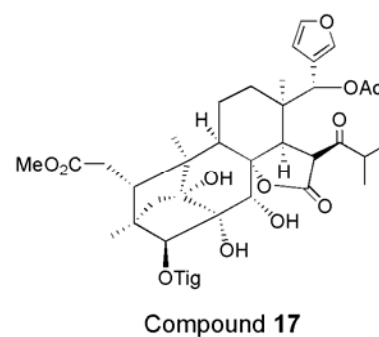
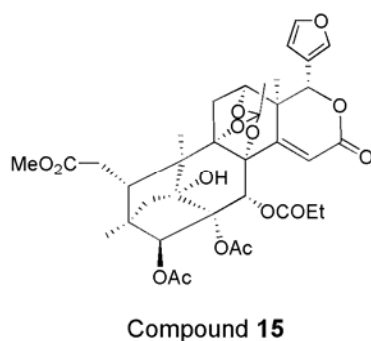
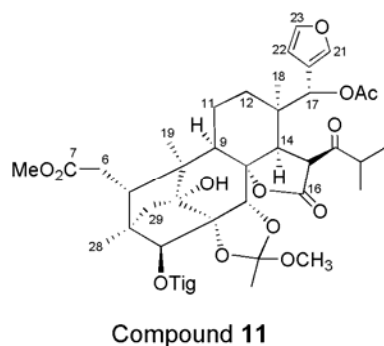
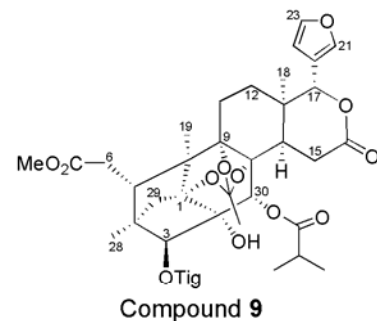
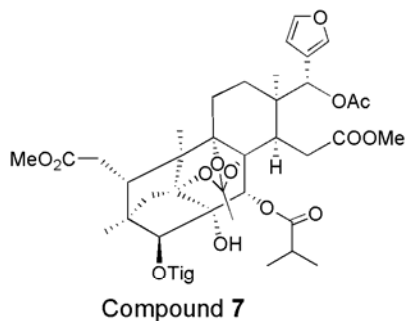
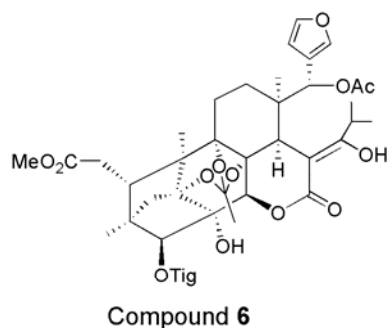


Compound 19



Compound 20

#### IV.2.5. Phragmalin derivatives



### IV.3. Structure determination

#### IV.3.1. Protolimonoids

Compound **12**, named entangosin A was obtained as an amorphous powder. Its HRFAB-MS spectrum showed molecular ion at  $m/z$ : 503.2286  $[M + H]^+$  in accordance with the molecular formula,  $C_{27}H_{34}O_9$ , indicating 11 degrees of unsaturation. The IR spectrum showed absorptions due to hydroxyl ( $3300\text{ cm}^{-1}$ ) and several carbonyls ( $1736\text{-}1753\text{ cm}^{-1}$ ). The UV spectrum exhibited a maximum at 216 nm consistent with a conjugated system. The  $^{13}\text{C}$  NMR data (Table 3) revealed that **12** contains one ketone, three ester carbonyls and four vinyl groups taking into account six unsaturations. Hence, the five remainders were attributed to five saturated rings. The  $^1\text{H}$  and  $^{13}\text{C}$  NMR spectra also indicated the presence of four quaternary methyls, six methylenes, six methines and eight quaternary carbons.

The NMR spectroscopic data of this compound were closely similar to those of methyl angolensate<sup>6</sup>. Thus, the H<sub>2</sub>-6 methylene protons observed at  $\delta_{\text{H}}$  2.63 and 2.24 which coupled with H-5 broad doublet showed HMBC correlation with an ester carbonyl carbon (C-7) at  $\delta_{\text{C}}$  174.0. A 8,30-exocyclic double bond resonance at  $\delta_{\text{H}}$  5.20 and 4.92 (H<sub>2</sub>-30) in the <sup>1</sup>H NMR spectrum and  $\delta_{\text{C}}$  144.8 (C-8) and 112.3 (C-30) in the <sup>13</sup>C NMR spectrum, the presence of a characteristic low-field singlet proton at  $\delta_{\text{H}}$  5.62 (H-17) also reinforce the suggestion of the closely relationship between **12** and methyl angolensate. However, **12** lacks signals of  $\beta$ -substituted furan ring and showed the characteristic 21-hydroxy-21-23-butenolide with an hemiacetal carbon at  $\delta_{\text{C}}$  98.1 (C-21) and an esteric carbonyl carbon at  $\delta_{\text{C}}$  169.3 (C-23) as observed also in domesticulide D<sup>113</sup>. Thus, **12** was assigned to 6-deacetoxydomesticulide D.

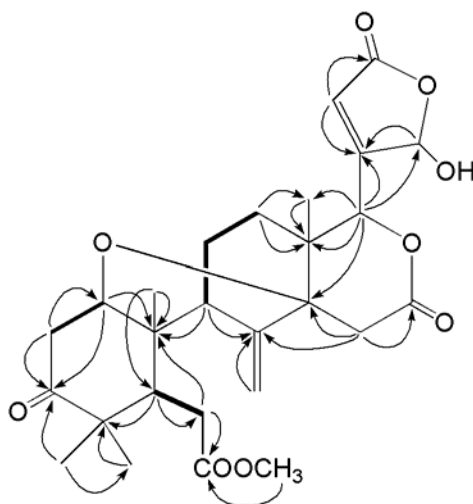


**Figure 2.** COSY and selected HMBC correlations in **12**

The relative stereochemistry of **12** was clarified by both the coupling constants and the NOE experiments (Figure 3). The H-9 proton exhibited NOE correlations with Me-18, H-11 $\alpha$ , and H-15 $\alpha$ ; H-5 correlated also with Me-28. Thus, the  $\alpha$ -orientation of these protons can be explained. The NOE cross-peaks were also observed between H-17 and H-12 $\beta$ , H-11 $\beta$  with H-15 $\beta$  indicated the  $\beta$ -orientation these protons. The NOE cross peak between H-1 and Me-29 indicated the  $\beta$ -orientation of H-1.

Entangosin B (**3**), showed no molecular-ion peak in the mass spectra but fragment ion peak was observed at  $m/z$ : 485.3 [ $\text{M}^+$ -CH<sub>3</sub>OH], due probably to the labile nature of methoxy acetal group. The molecular formula of C<sub>28</sub>H<sub>36</sub>O<sub>9</sub> was deduced from the mass spectrum in conjugation with the <sup>13</sup>C NMR and DEPT spectra. The IR spectrum showed absorption bands for carbonyl groups (1762, 1750, 1720 cm<sup>-1</sup>) and double bonds (1652 cm<sup>-1</sup>) and the UV spectrum exhibited maximum absorption at 216 nm ( $\alpha,\beta$ -unsaturated lactone).



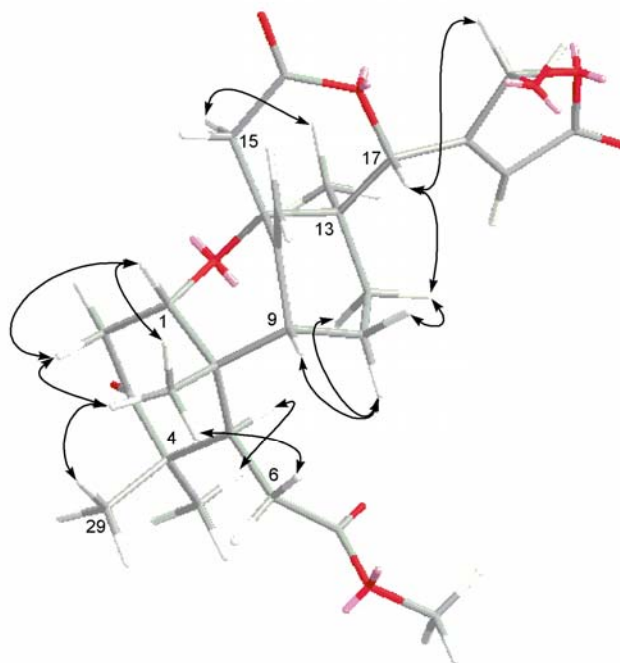


**Figure 3.** Computer-generated energy minimized model of **12** with key NOE correlations observed.

The NMR spectral data of **3** (Table 3) showed close similarities to those of **12** except for the observation of additional NMR signals ( $\delta_C$  57.4 and  $\delta_H$  3.59) due to a methoxy group. These observations suggested that **3** possesses the same basic skeleton with **12**.

The location of the methoxy group was established by the HMBC correlation of methoxy methyl protons to the hemiacetal carbon signal at  $\delta_C$  102.3 (C-21). Thus, **3** has been assigned as seco-tetranortriterpenoid bearing a  $\gamma$ -methoxybutenolide at C-17. Similarly to **12**, the relative stereochemistry of **3** (Figure 5) was determined by NOE experiments. The structure **3** has been determined as shown.

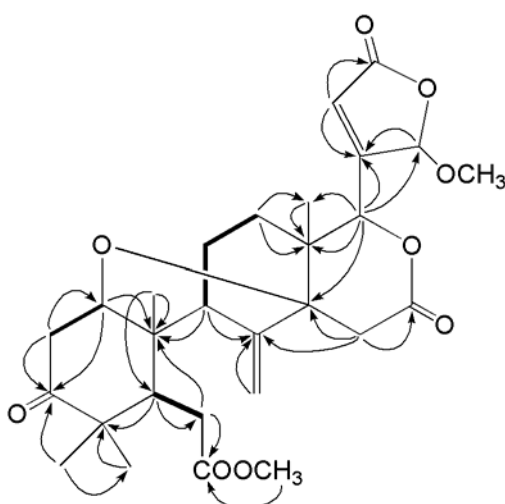


**Figure 4.** COSY and selected HMBC correlations in **3**

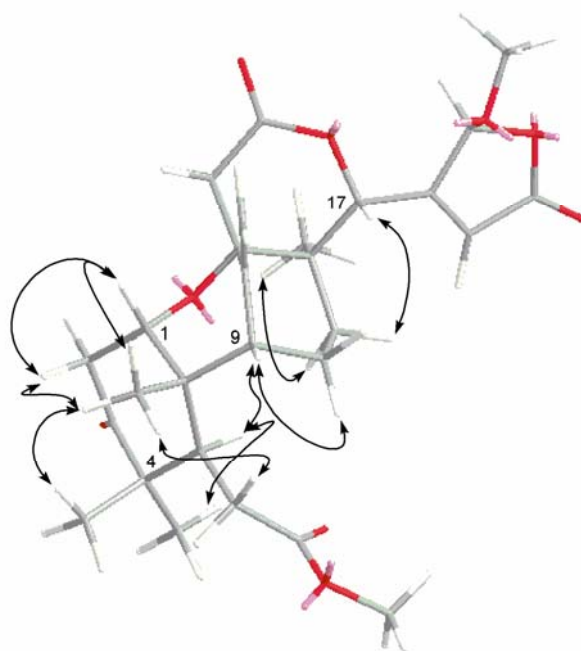


**Figure 5.** Computer-generated energy minimized model of **3** with key NOE correlations observed

Entangosin C (**4**) was isolated as an amorphous solid. In the FABMS, as for **3**, the molecular ion was not seen but fragment ion due to the loss of methanol was detected at  $m/z$ : 535.4. Thus the molecular formula was deduced as  $C_{29}H_{42}O_{11}$  from these mass spectrum data in conjunction with the  $^{13}C$  NMR and DEPT spectra. The IR spectrum showed absorption bands for carbonyl groups ( $1762$ - $1720\text{ cm}^{-1}$ ) and double bonds ( $1652\text{ cm}^{-1}$ ) while no characteristic absorption was observed in the UV spectrum.

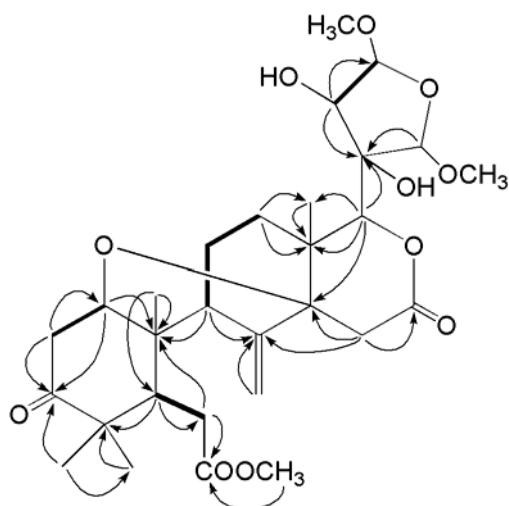


**Figure 6.** COSY and selected HMBC correlations in **4**

The  $^1H$  and  $^{13}C$  NMR spectral data of **4** (Table 3) showed close similarities to those of **12** and **3** besides the resonances of the C-17 side chain.  $^{13}C$  NMR spectrum of **4** indicated two hemiacetal carbon signals at  $\delta_C$  109.9

and 112.6, two oxygenated carbons at 82.1 and 76.1 (instead of tri-substituted double as observed in **12** and **3**) while  $^1\text{H}$  NMR spectrum indicated two methoxy methyl groups at  $\delta_{\text{H}}$  3.51 and 3.45. The proton at  $\delta_{\text{H}}$  4.99 (H-23), coupled with the proton at  $\delta_{\text{H}}$  4.20 (H-22) in the COSY, showed HMBC cross peak with an hemiacetal carbon signal at  $\delta_{\text{C}}$  109.9 (C-21), the quaternary oxygenated carbon at  $\delta_{\text{C}}$  82.1 (C-20) and the methoxy carbon at  $\delta_{\text{C}}$  55.5 ( $\delta$  3.51), permitting also the location of the methoxy group at C-23. The remaining methoxy group was placed at C-21 by its coupling with the hemiacetal carbon at  $\delta_{\text{C}}$  109.9 (C-21) bearing the proton observed as a single at  $\delta_{\text{H}}$  4.92 (H-21). HMBC cross-peak of the methoxy methyl protons to C-20 also supported the above mentioned location. Thus, it was concluded that the C-17 side chain is a 20,22-dihydroxy-21,23-dimethoxytetrahydrofuran. Such side chains have been found in Salvinicins A and B, two natural products from a Lamiaceae family plant<sup>115</sup>. The relative stereochemistry of **4** was determined by NOE experiments (Figure 7) as for **12** and **3**. In the NOE spectrum, H-17 correlated with H-21, H-22 and OMe-23. These correlations could suggest that these protons and the methoxy are oriented in the same face of the tetrahydrofuran ring. The NOE connectivity between OMe-21 and H-23 leading to the conclusion they are on the other face of tetrahydrofuran ring. Thus, the structure of **4** is proposed as shown.

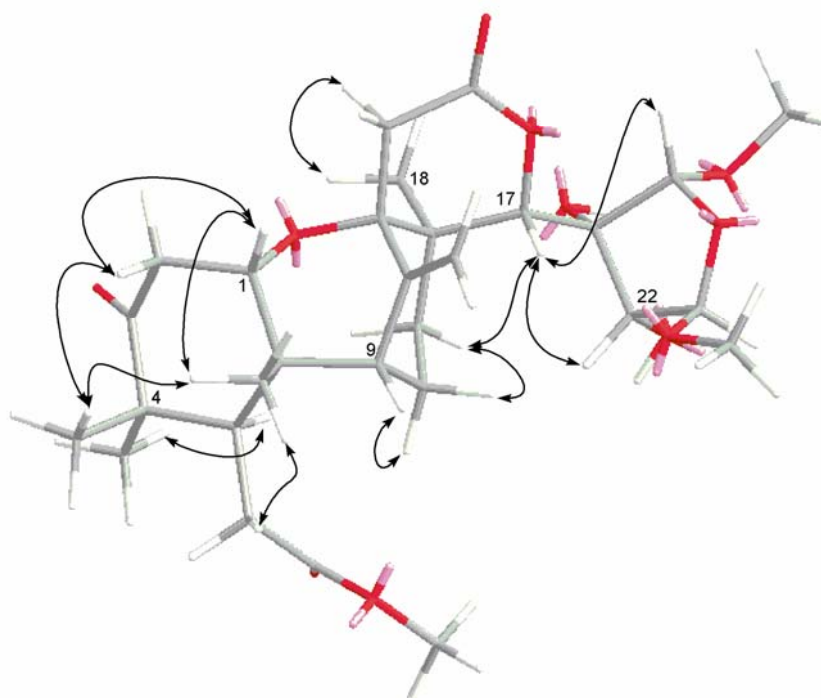


**Figure 7.** Computer-generated energy minimized model of **4** with key NOE correlations observed

### IV.3.2 Gedunin derivatives

Compound **8** was obtained as white amorphous solid. Its molecular formula  $C_{26}H_{28}O_6$ , deduced from the HRFAB-MS spectrum (pseudomolecular ion at  $m/z$  437.1971,  $[M+H]^+$ ;  $\Delta \pm 0.3$  mmu) and  $^{13}C$  NMR and DEPT spectra, corresponds to 12 degrees of unsaturation. The IR spectrum displayed bands at 1736-1750 (carbonyls), 1650 (carbon-carbon double) and  $873\text{ cm}^{-1}$  (furan ring). The UV spectrum band at 239 nm suggested the presence of conjugated system. The analysis of  $^1H$  and  $^{13}C$  NMR data fully explained that seven elements of unsaturation are present as double bonds (four carbon-carbon including furan ring, two ketone and one ester), therefore the molecule is pentacyclic.

The NMR spectroscopic data of **8** (Table 4) showed signals of five tertiary methyl groups, two methylenes, nine methines (six olefinics) and nine non-hydrogenated carbons (two olefinics), and the presence of one  $\beta$ -furanly moiety ( $\delta_H$  6.38, 7.39 and 7.42; each one proton). All the protons directly bonded to carbon atoms were assigned by  $^1H$ - $^{13}C$  shift-correlated measurements (HMQC). The data from decouplings and the subsequent 2D NMR studies using the COSY, HMBC and NOESY, suggested that compound **8** was gedunin-type limonoid<sup>114,115</sup>. Thus, two olefinic protons at  $\delta_H$  6.89 (d,  $J = 10.0$  Hz) and 6.00 (d,  $J = 10.0$  Hz) assigned to H-1 and H-2 correlated with a ketonic carbonyl carbon at  $\delta_C$  200.8 assigned to C-3 in the HMBC spectrum. The HMBC correlations of H-1 to Me-19 ( $\delta_C$  22.6), C-5 ( $\delta_C$  166.2) and C-10 ( $\delta_C$  41.4) and those of two methyl protons, Me-28 ( $\delta_H$  1.40) and Me-29 ( $\delta_H$  1.45) to the quaternary carbon signal, C-4 ( $\delta_C$  49.4) and C-3 were also observed. These observations fully assigned the ring A as possessing a 1-en-3-one system.

The downfield chemical shift of a signal at  $\delta_H$  5.44 observed as a singlet and assigned to H-17, showed  $^1H$ - $^{13}C$  correlations to two quaternary carbons at  $\delta_C$  37.4 (C-13) and  $\delta_C$  64.9 (C-14), a methyl carbon at  $\delta_C$  20.6 (Me-18), and a furan carbon at  $\delta_C$  120.1 (C-20) in the HMBC spectrum confirming then the location of the furan group at C-17 position. On the other hand, the observation of HMBC cross-peaks between a characteristic epoxy proton singlet at  $\delta_H$  3.95 (H-15) and the carbon signals at  $\delta_C$  64.9 (C-14),  $\delta_C$  166.7 (C-16, lactonic carbonyl) and  $\delta_C$  37.4 (C-13) revealed that the D-ring of **8** was in the form of  $\delta$ -lactone with a C-14/15 epoxy substituent. These findings strongly supported that **8** is a gedunin-type limonoid.

Also, the presence of one tri-substituted double bond at  $\delta$  166.2 and 123.5 was recognized and the olefinic proton signal of this bond ( $\delta_H$  6.03, H-6) showed HMBC correlations to the carbon signals of C-4, C-5, C-7 ( $\delta_C$  198.6), C-8 ( $\delta_C$  48.5) and C-10. The 12-methylene protons at  $\delta_H$  1.45 and 1.92 attached to the carbon at  $\delta_C$  32.8 showed HMBC correlations to C-9, C-11 ( $\delta_C$  18.9), C-13, C-14 and C-17. These correlations characterized rings B and C, and then the gross structure of this compound.

The relative stereochemistry of **8**, as shown, was established by NOE experiments (Figure 9) and also by some similarities observed with the reported NOE data of the molecule parent gedunin<sup>114</sup>. The NOE cross-peaks observed between H-17 and H-12 $\beta$ , between H-11 $\beta$  and Me-30, between H-17 and Me-30, and between Me-19 and Me-30 indicated the  $\beta$ -orientation these protons. The  $\alpha$ -orientation of H-9 signal was deduced by a NOE cross-peak shared with the Me-18. The  $\beta$ -orientation of the 14,15-epoxide moiety was determined by the weak NOE correlations of H-15/ Me-18 which was also observed in the NOESY of gedunin. Thus, compound **8** was assigned as 5,6-dehydro-7-oxogedunin.

**Table 3.**  $^1\text{H}$  and  $^{13}\text{C}$  NMR spectroscopic data of compounds **12**, **3** and **4**.

Position	Entangosin A ( <b>12</b> )		Entangosin B ( <b>3</b> )		Entangosin C ( <b>4</b> )	
	$\delta_{\text{C}}$ mult.	$\delta_{\text{H}}$ ( $J$ in Hz)	$\delta_{\text{C}}$ mult.	$\delta_{\text{H}}$ ( $J$ in Hz)	$\delta_{\text{C}}$ mult.	$\delta_{\text{H}}$ ( $J$ in Hz)
1	77.4 d	3.53 dd (6.3,3.5)	77.3 s	3.48 t (5.8)	76.4 d	3.39 t (6.4)
2 $\alpha$	39.3 d	2.49 dd (14.5,3.5)	39.6 t	2.60 dd (14.3,5.2)	39.9 t	2.60 dd (13.8,5.8)
$\beta$		2.91 dd (14.5,6.3)		2.81 dd (14.3,6.5)		2.74 dd (13.8,7.0)
3	212.7 s		213.0 s		213.0 s	
4	48.1 s		47.8 s		47.9 s	
5	43.0 d	2.84 br d (10.1)	42.8 d	2.92 d (10.3)	42.7 d	2.86 br d
6a	32.6 t	2.63 dd (16.5,10.1)	32.9 t	2.57 dd (16.0,7.7)	32.8 t	2.53 dd (15.9,9.9)
b		2.24 <sup>a</sup>		2.25 dd (16.0,5.3)		2.28 br d (15.9)
7	174.0 s		173.8 s		173.6 s	
8	144.8 s		145.6 s		145.3 s	
9	49.6 d	2.24 <sup>a</sup>	49.4 d	2.18 d (4.9)	49.2 d	2.11 br d (5.1)
10	43.9 s		44.0 s		44.3 s	
11 $\alpha$	23.8 t	1.66 m	23.4 t	2.25 o	23.5 t	1.63 m
$\beta$		2.24 o		1.60 m		2.17 br dd (15.8,5.3)
12 $\alpha$	29.3 t	1.31 m	28.8 t	1.07 o	27.6 t	2.01 br dd (13.1,5.3)
$\beta$		2.06 m		2.25 o		1.95 ddd (19.7, 13.1, 5.3)
13	41.9 s		41.8 s		41.6 s	
14	80.0 s		79.5 s		80.3 s	
15 $\alpha$	33.5 t	2.88 d (18.1)	33.6 t	2.89 d (18.2)	33.3 t	2.80 d (18.0)
$\beta$		2.60 d (18.1)		2.58 d (18.2)		2.50 d (18.0)
16	169.3 s		169.5 s		169.9 s	
17	79.9 d	5.62 s	77.6 d	5.71 s	83.8 d	5.19 s
18	14.2 q	0.93 s	13.3 q	0.90 s	14.4 q	1.09 s
19	21.7 q	0.96 s	21.4 q	0.87 s	21.4 q	0.79 s
20	163.7 s		134.9 s		82.1 q	
21	98.1 d	6.14 br s	102.3 d	5.77 s	109.9 d	4.92 s
22	121.7 d	6.24 br s	147.6 d	7.18 s	76.1 d	4.20 d (3.2)
23	169.3 s		168.6 s		112.6 d	4.99 d (3.2)
28	25.8 q	1.00 s	26.7 q	1.09 s	27.4 q	1.10 s
29	21.4 q	1.19 s	21.1 q	1.18 s	21.1 q	1.17 s
30a	112.3 t	5.20 br s	117.9 d	5.17 s	112.2 t	5.14,s
b		4.92 br s		4.99 s		4.85 s
OMe-7	52.3 q	3.72 s	51.9 q	3.71 s	52.0 q	3.71 s
OMe-21			57.4 q	3.59 s	56.5 q	3.51 s
OMe-23					55.5 q	3.45 s

<sup>a</sup>Signals were overlapped.

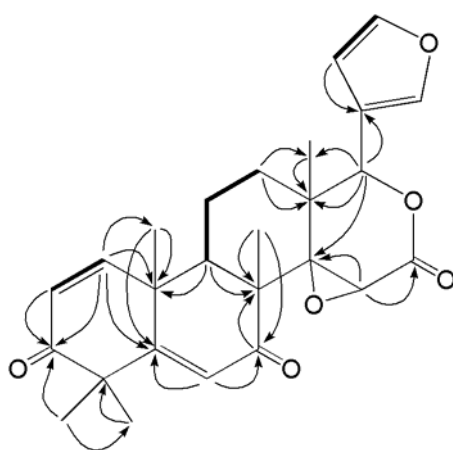


**Figure 8.** COSY and selected HMBC correlations in **8**

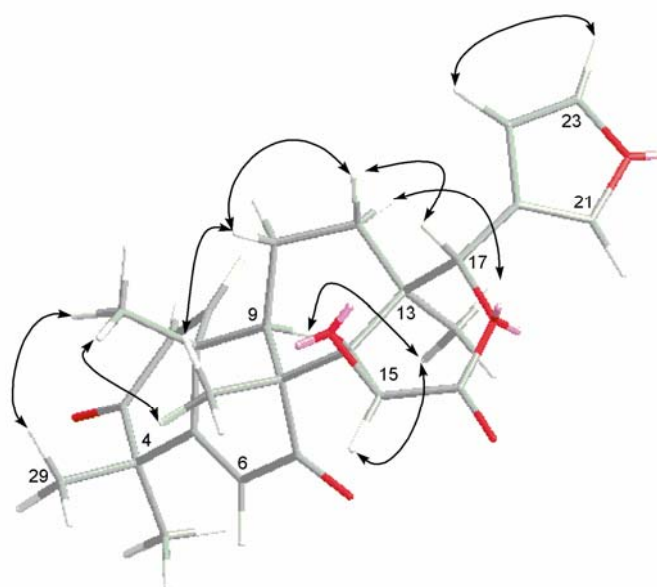


**Figure 9.** Computer-generated energy minimized model of **8** with key NOE correlations observed

Compound **14** was isolated as a white amorphous solid. Its HRFAB-MS spectrum displayed a pseudo-molecular ion at  $m/z$  455.2992,  $[M+H]^+$ ;  $\Delta$  - 0.3 mmu. Combined with  $^{13}C$  NMR data, the molecular formula of this compound was established as  $C_{26}H_{30}O_7$  (11 degrees of unsaturation). The UV absorption observed at 215 nm indicated the presence of a conjugated system as in compound **8**. The following characteristic absorptions observed in IR spectrum 3420, 1720-1736, 1649 and  $875\text{ cm}^{-1}$  corresponded to the presence of hydroxyl group, carbonyl or/and  $\alpha,\beta$ -unsaturated six membered lactone, carbon – carbon double, and furan ring, respectively.

The NMR spectroscopic data of compound **14** (Table 4) showed very close similarities with those of **8**, besides the lack of resonances of tri-substituted double bond. The methylene protons at  $\delta_H$  2.33 (d,  $J = 13.2$  Hz) and 3.41 (d,  $J = 13.2$  Hz) were assigned as  $H_2-6$ , due to the HMBC cross-peak with carbon signal at  $\delta_C$  209.2 (C-7) and 62.9 (C-5). The carbon C-5 showed HMBC correlations with hydroxyl proton ( $\delta_H$  1.67) suggesting its location at this position.

The relative stereochemistry of **14** was determined by NOE considerations (Figure 11). The  $\beta$ -OH orientation at C-5 was determined by the strong NOE correlations observed between the OH proton and two methyl protons (Me-19 and Me-29). Thus, **14** was assigned as 5-hydroxy-7-oxogedunin.

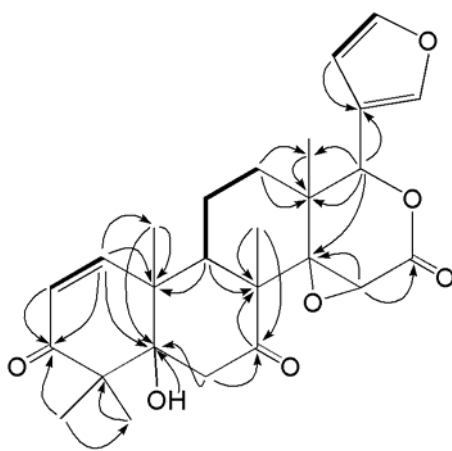


**Figure 10.** COSY and selected HMBC correlations in **14**

### IV.3.3. Mexicanolide derivatives

Angolensin A (**2**) was isolated as amorphous powder and it was shown to have the molecular formula  $C_{32}H_{40}O_8$  by a pseudomolecular ion  $[M + H]^+$  at  $m/z$  553.2794 ( $\Delta - 0.8$  mmu) in the HRFAB-MS and from the analysis of  $^{13}C$  NMR spectroscopic data. The IR spectrum revealed a complex absorption band at 1740-1710  $cm^{-1}$  for many carbonyls. The UV spectrum indicated the presence of conjugated system at 213 nm. From  $^1H$  and  $^{13}C$  NMR spectra, it was clear that eight of the thirteen elements of unsaturation were present as double bonds: four carbon-carbon (one furan ring) and four carbon-oxygen (one ketone and three esters). Therefore, the molecule is pentacyclic. The NMR spectroscopic data (Table 5) also revealed that compound **2** contained seven methyls (five tertiary, one secondary and one methoxy), four methylenes, eleven methynes (five olefinic), and ten quaternary carbons (three olefinic). From the NMR data, the presence of  $\beta$ -furanyl ( $\delta_H$  6.43, 7.24 and 7.49; each 1H) and tigloyl moiety ( $\delta_H$  1.85: d and 1.90: br s; each 3H, and  $\delta_H$  6.96: br q; 1H) was also recognized.

All the protons directly bonded to carbon atoms were assigned by analysis of the HMBQC spectrum. The data from the subsequent 2D NMR studies using  $^1H$ - $^1H$  COSY, HMBC, and NOESY spectra, strongly suggested that **2** was a mexicanolide-type limonoid<sup>116,117</sup>. Thus, the 6-methylene protons at  $\delta_H$  2.41 (dd,  $J = 8.9$  and 17.2 Hz) and 2.50 (br d,  $J = 17.2$  Hz) attached to a carbon at  $\delta_C$  33.6 adjacent to an ester carbonyl ( $\delta_C$  174.4), were coupled with the H-5 broad doublet proton at  $\delta_H$  3.37, and the presence of this moiety and a characteristic low-field H-17 at  $\delta_H$  5.01 showing significant HMBC correlations with the furanyl carbons at  $\delta_C$  109.9 (C-23), 120.0 (C-20) and 141.2 (C-21), revealed that **2** was a rings B,D-seco limonoid. In addition to this knowledge, the absence of signal due to one tertiary methyl at  $\delta_C$  8 $\beta$  (C-30) in the basic skeleton and olefinic signals to be assigned to exo-methylene protons suggested that **2** was a mexicanolide-type compound having the bicyclo[3,3,1]-ring system, instead of angolensate derivatives.

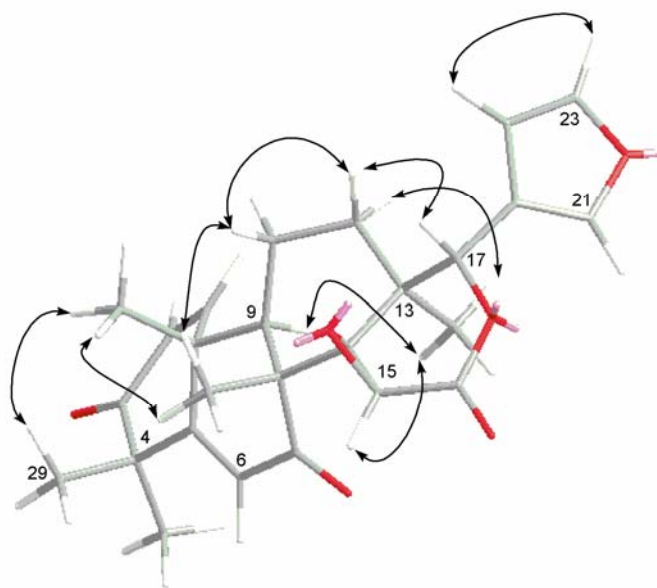


**Figure 11.** Computer-generated energy minimized model of **14** with key NOE correlations observed.

In the HMBC spectrum of **2**, the observed long-range C-H correlations of H-5 signal with the  $^{13}\text{C}$  signals at  $\delta_{\text{C}}$  17.8 (q), 20.3 (q), 24.1 (q), 38.2 (s), 48.7 (d), 51.3 (s), and 78.4 (d) led to their assignments as C-19, C-28, C-4, C-9, C-10 and C-3, respectively. A complex signal due to one methylene proton at  $\delta_{\text{H}}$  2.25 assigned to H-30 $\beta$  showed significant HMBC correlations with a carbonyl carbon at  $\delta_{\text{C}}$  218.6 (C-1), two methine carbons at  $\delta_{\text{C}}$  34.4 and 46.6 to be assigned to C-8 and C-2, and the methine carbons of C-3 and C-9. The presence of tigloyl group at C-3 was also confirmed by the correlations of H-3 doublet at  $\delta_{\text{H}}$  5.71 attached to C-3 with tigloyl carbonyl carbon at  $\delta_{\text{C}}$  167.1. These findings clearly characterized the first molecular fragment, the left-hand bicyclo[3,3,1]nonane ring system.

An olefinic proton at  $\delta_{\text{H}}$  5.71 (s, H-15) attached to a carbon at  $\delta_{\text{C}}$  112.7 adjacent to a lactone carbonyl carbon at  $\delta_{\text{C}}$  164.5 (C-16), showed correlations with another olefinic carbon at  $\delta_{\text{C}}$  170.4 (C-14), a quaternary carbon at  $\delta_{\text{C}}$  38.3 (C-13), and the 8-methine carbon. The carbon signal due to C-13 was correlated to the signals of the 17-methine proton, the methylene protons at  $\delta_{\text{H}}$  1.71-1.77 and  $\delta_{\text{H}}$  1.44 and 1.62 assigned to H<sub>2</sub>-11 and H<sub>2</sub>-12, and the methyl protons at  $\delta_{\text{H}}$  1.03 (Me-18). Finally, the 11-methylene signals attached to the carbon at  $\delta_{\text{C}}$  18.8 showed correlations with C-8—C-10 and C-12 signals together with C-13 signal. These correlations characterized the second fragment of the molecule, C-8, C-9 and C-11—C-17 of the C and D rings, including 13-Me (Me-18) and a furan ring.



**Table 4.**  $^1\text{H}$  and  $^{13}\text{C}$  NMR spectroscopic data of compounds **8-14**.

Position	5,6-dehydro-7-oxogedunin ( <b>8</b> )		5-hydroxy-7-oxogedunin ( <b>14</b> )	
	$\delta_{\text{C}}$ mult.	$\delta_{\text{H}}$ ( $J$ in Hz)	$\delta_{\text{C}}$ mult.	$\delta_{\text{H}}$ ( $J$ in Hz)
1	152.2 d	6.89 d (10.0)	160.9 d	7.13 d (6.2)
2	125.7 d	6.00 d (10.0)	132.9 d	6.29 d (6.2)
3	200.8 s		211.6 s	
4	49.4 s		53.3 s	
5	166.2 s		62.9 s	
6 $\alpha$	123.5 d	6.03 s	123.5 d	2.33 d (13.2)
$\beta$				3.41 d (13.2)
7	198.6 s		209.2 s	
8	48.5 s		52.1 s	
9	44.5 d	2.40 br d	46.7 d	2.16 dd (11.8,3.8)
10	41.4 s		48.2 s	
11 $\alpha$	18.9 t	1.97 dd (13.5,8.0)	16.4 t	1.88 m
$\beta$		1.81 m		1.94 m
12 $\alpha$	32.8 t	1.45 o	29.4 t	1.47 ddd (9.4,7.0,2.5)
$\beta$		1.92 dd (13.9,7.3)		1.80 ddd (18.1,9.4,4.4)
13	37.4 s		38.0 s	
14	64.9 s		66.6 s	
15	52.2 d	3.95 s	55.3 d	4.29 s
16	166.7 s		167.2 s	
17	77.7 d	5.44 s	77.9 d	5.54 s
18	20.6 q	1.03 s	19.8 q	1.15 s
19	22.6 q	1.50 s	26.4 q	1.06 s
20	120.1 s		120.3 s	
21	141.0 d	7.42 s	141.1 d	7.42 s
22	109.8 d	6.38 br s	109.8 d	6.35 br s
23	143.1 d	7.39 t (1.4)	143.1 d	7.39 br s
28	25.5 q	1.40 s	28.5 q	1.01 s
29	28.2 q	1.45 s	21.0 q	1.40 s
30	17.2 q	1.08 s	17.8 q	1.52 s
OH-10				1.67 s

The structure of **2**, including the stereochemistry, was fully explained from the NMR data by consideration of the NOE correlations shown in Figure 13. Strong cross-peak of the broad signal at  $\delta_{\text{H}}$  3.30 (H-8) with the signals at  $\delta_{\text{H}}$  1.62 (H-12 $\beta$ ) and 2.25 (H-30 $\beta$ ) and the H-5 signal, and of the H-12 $\beta$  signal with the H-17 signal indicated the  $\beta$  orientation of these protons. On the other hand, the large coupling of  $J = 10$  Hz and strong NOE correlation between the H-3 signal at  $\delta_{\text{H}}$  5.10 and H-2 signal at  $\delta_{\text{H}}$  3.14, revealed the orientation of H-3. Finally, NOE correlations observed between the H-9 signal at  $\delta_{\text{H}}$  1.74 and the Me-18 and Me-19 proton signals at  $\delta_{\text{H}}$  1.03 and 1.10 established the structure of **2** with certainty.

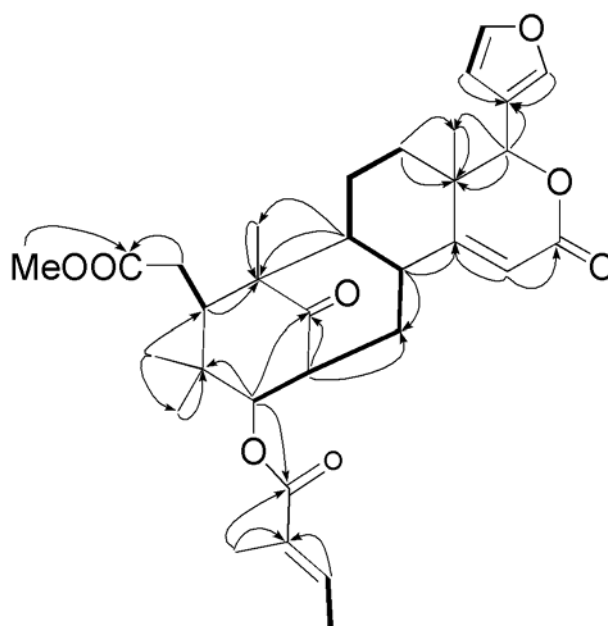


**Figure 12.** COSY and selected HMBC correlations in **2**

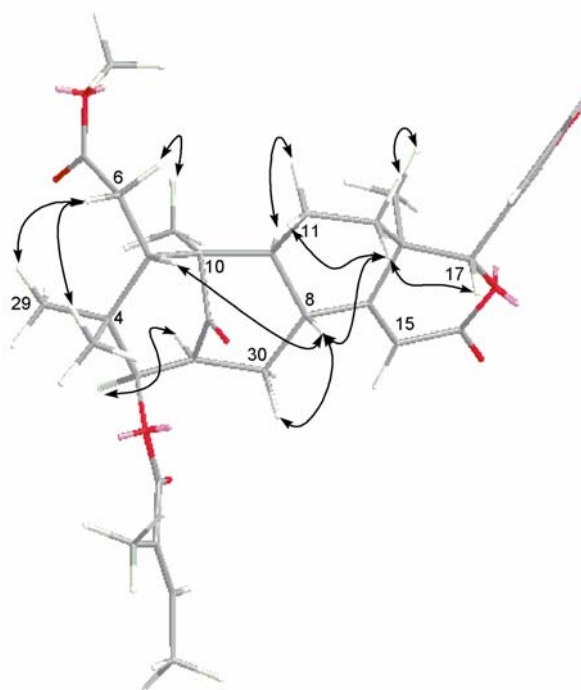


**Figure 13.** Computer-generated energy minimized model of **2** with key NOE correlations observed.

Angolensin B (**16**) was obtained as a white amorphous powder. The molecular formula ( $C_{38}H_{48}O_{14}$ , 15 unsaturations) was determined by HRFAB-MS ( $m/z$ : 729.3102  $[M + H]^+$ ,  $\Delta +0.2$  mmu) and NMR spectra. The IR spectrum showed different absorptions for hydroxyl ( $3600-3200\text{ cm}^{-1}$ ) and carbonyl ( $1736-1720\text{ cm}^{-1}$ ) groups as broad bands and UV spectrum indicated the presence of a similar conjugated system at 216 nm as in **2**. Compare to **2**, the NMR spectrum showed the change of several functional groups in **16**, which included the presence of additional hydroxyl, acetyl and 2-methylpropanoyl groups. The most significant difference was the absence of the keto carbonyl group observed in **2**, and the presence of an acetal carbon at  $\delta_C$  108.1 (s) in **16**.

Since an acetal linkage between C-1 and C-8 has been observed in some mexicanolides,<sup>116,117</sup> the presence of a similar partial structure in **16** was predicted and it was supported by the HMBC correlations of the 1-OH signal at  $\delta_H$  4.52 with three quaternary carbons at  $\delta_C$  108.1 (C-1), 81.1 (C-2) and 43.1 (C-10). The fact that **16** possesses a mexicanolide-type structure having the C-1—C-8 acetal linkage and the C-14—C-15 double bond, was confirmed by the  $^1H$  and  $^{13}C$  NMR data as presented in Table 5 and by NOE correlations (Figure 15).

The location of three ester groups was elucidated by the HMBC correlations of the methine protons at  $\delta_H$  4.67 (H-3), 5.25 (H-6), and 5.46 (H-30) with tiglyol, acetyl, and 2-methylpropanoyl carbonyl carbons at  $\delta_C$  168.2, 169.7 and 175.4, respectively. The configuration of H-30, not coupling with any proton, was assigned to be  $\beta$  from NOE observation with the H-5 $\beta$  signal at  $\delta_H$  2.97, which also showed NOE correlations with H-6, H-11 $\beta$  ( $\delta_H$  2.43) and H-30 signals and the 4 $\beta$ -Me (28) proton signal at  $\delta_H$  0.94 to identify the stereochemistry of the bicyclo[3.3.1]nonane ring. On the other hand, the significant NOE observations between the H-12 $\beta$  ( $\delta_H$  2.05) and H-17 ( $\delta_H$  4.85) signals and the H-12 $\beta$  and H-30 signals clarified the stereochemistry at C-8, C-9 and C-13. From the NOE correlations with 4 $\alpha$ -Me (29) and 1-OH proton signals at  $\delta_H$  1.61 and 4.52, the configuration of H-3 was assigned to be  $\alpha$ . Finally, the *R* configuration at C-6 inferred from that of some known mexicanolides<sup>118,119</sup> was also supported by the very small coupling between the H-5 and H-6 signals referring to the dihedral angle of H5/H6 to be ca 90° and the NOE correlations observed between the H-6 signal and the H-5, H<sub>2</sub>-11 and Me-19 resonances, and the 7-carboxymethyl signal and the 5-H, 4 $\beta$ -Me and tiglyl 2'- and 3'-Me resonances.

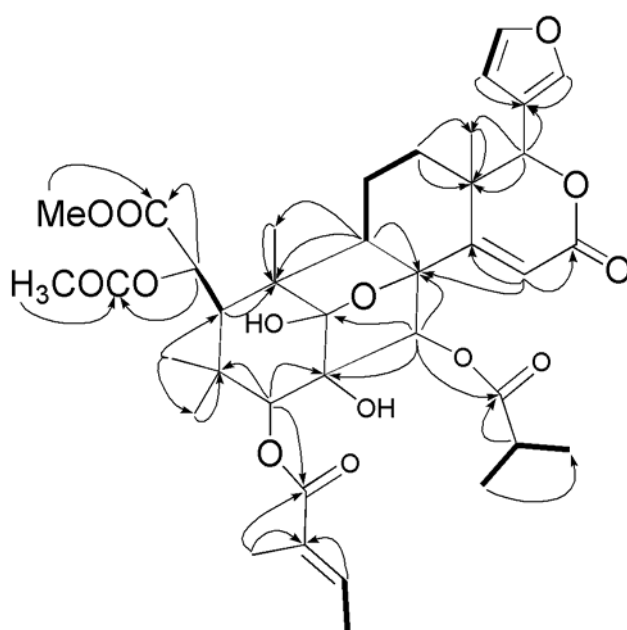


**Figure 14.** COSY and selected HMBC correlations in **16**

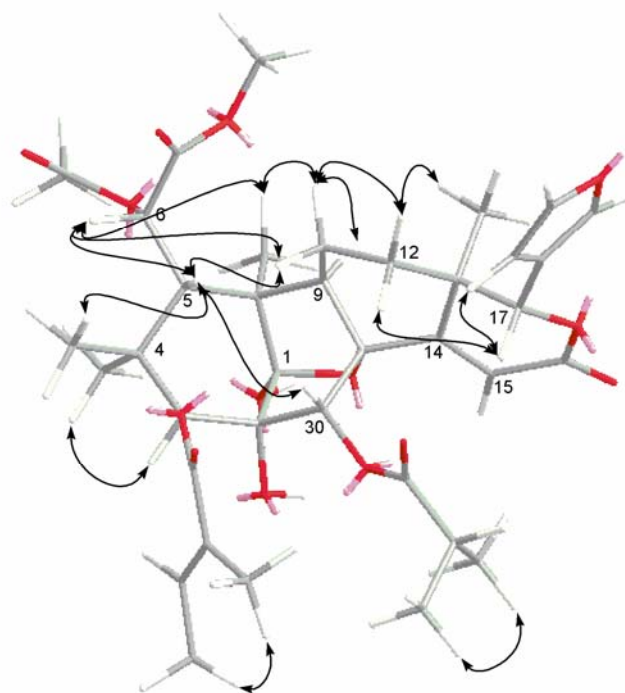


**Figure 15.** Computer-generated energy minimized model of **16** with key NOE correlations observed.

The molecular formula of angolensin C (**18**) was determined as  $C_{29}H_{34}O_{10}$  by HRFAB-MS ( $m/z$ : 543.2223  $[M+H]^+$ ,  $\Delta$  -0.7 mmu). Compound **4** was also predicted by the NMR spectra to be mexicanolide from the presence of the signals due to four quaternary methyls and the 6- $CO_2Me$  group. This compound, having the signals due to 14—15 double bond at  $\delta_C$  165.4 and 116.6 and one acetyl methyl signal at  $\delta_H$  2.18, however, was significantly different from **2** and **16** in the presence of two keto carbonyl groups at  $\delta_C$  208.4 and 212.2 and one hydroxyl group at  $\delta_H$  1.93, and lacked tigloyl group.

These ketone groups were located at C-1 and C-3, because both carbonyl carbons were correlated in the HMBC spectrum to the 30-methylene protons at  $\delta_H$  2.57 and 3.17 attached to a carbon at  $\delta_C$  41.9 (C-30), also each carbonyl carbon to the methyl protons at  $\delta_H$  1.28 (Me-19) and to another two methyl protons at  $\delta_H$  1.08 (Me-28) and 1.13 (Me-29), respectively. The proton signal due to the 2-methine group lying between two carbonyl groups, consequently, was observed at the low field  $\delta_H$  3.36.

The structure of **18**, including its stereochemistry, was fully explained from the NMR data by the consideration of NOE correlations (Figure 17). Strong cross-peaks of the H-5 broad singlet at  $\delta_H$  3.14 with a signal at  $\delta_H$  1.94 (H-12 $\beta$ ) and the characteristic H-17 signal at  $\delta_H$  5.57 indicated the same  $\beta$  orientation of these protons and the folded conformation of **18** as shown in Figure 3. The latter also accounted for the stereochemistry at C-8. An NOE correlation observed between the H-30 $\beta$  and H-15 resonances also accounted well for the stereochemistry of the ring system of **18**. Finally, the configuration at C-6 was assumed to be the same *R* as that of **16** in a similar manner.

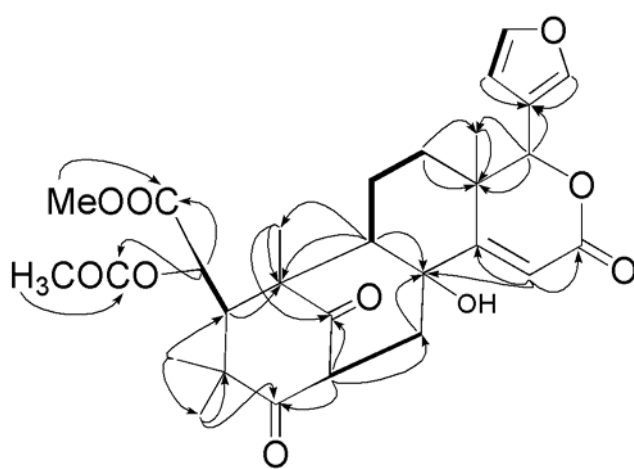


**Figure 16.** COSY and selected HMBC correlations in **18**

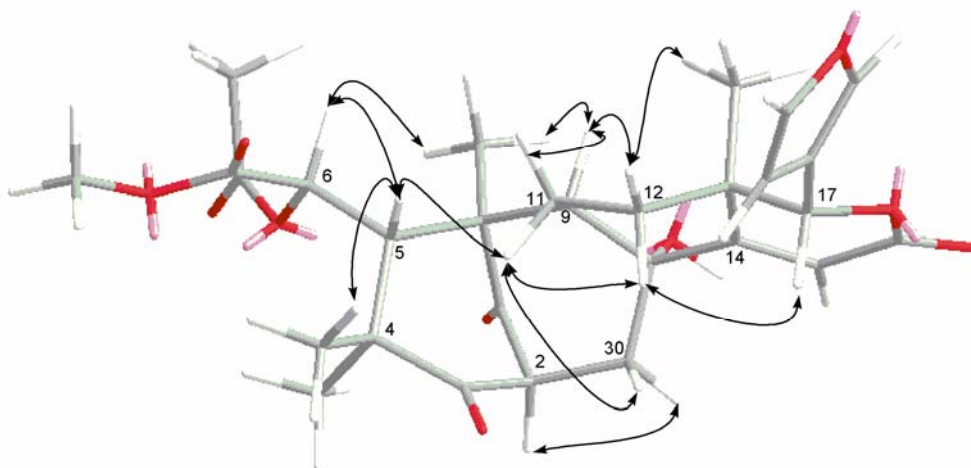


**Figure 17.** Computer-generated energy minimized model of **18** with key NOE correlations observed.

**Table 5.**  $^1\text{H}$  and  $^{13}\text{C}$  NMR spectroscopic data of angolensins A (**2**), B (**16**) and C (**18**)

Position	Angolensin A ( <b>2</b> )		Angolensin B ( <b>16</b> )		Angolensin C ( <b>18</b> )	
	$\delta_{\text{C}}$ mult.	$\delta_{\text{H}}$ ( $J$ in Hz)	$\delta_{\text{C}}$ mult.	$\delta_{\text{H}}$ ( $J$ in Hz)	$\delta_{\text{C}}$ mult.	$\delta_{\text{H}}$ ( $J$ in Hz)
1	218.6 s		108.1 s		212.2 s	
2	46.6 d	3.14 ddd (10.0,3.5,2.5)	81.1 s		56.3 d	3.36 dd (8.4,3.6)
3	78.4 d	5.10 d	85.2 d	4.67 s	208.4 s	
4	38.2 s		39.2 s		50.0 s	
5	40.5 d	3.37 dd (8.9,1.4)	43.8 d	2.97 br s	42.6 d	3.14 br s
6a	33.6 t	2.50 br d (17.2)	71.6 d	5.25 br s	72.5 d	5.59 br s
b		2.41 dd (17.2,8.9)				
7	174.4 s		171.0 s		170.5 s	
8	34.4 d	3.30 br m	80.0 s		72.2 s	
9	48.7 d	1.74 m	51.5 d	2.30 dd (11.3,9.6)	60.2 d	2.18 m
10	51.3 s		43.1 s		50.7 s	
11 $\alpha$	18.8 t	1.71-1.77	15.3 t	2.09 mo	19.3 t	2.09 m
$\beta$				2.43 m		1.71 m
12 $\alpha$	26.9 t	1.44 dd (13.3,6.9)	25.0 t	1.42 dd (13.5,8.8)	29.7 t	1.50 ddd (15.4,9.6,4.1)
$\beta$		1.62 m		2.05 m		1.94 ddd (15.4,9.5,4.5)
13	38.3 s		38.8 s		39.0 s	
14	170.4 s		158.2 s		165.4 s	
15	112.7 d	5.71 d (1.8)	118.4 d	6.03 s	116.6 d	6.05 s
16	164.5 s		163.0 s		164.5 s	
17	81.4 d	5.01 s	81.3 d	4.85 s	79.7 d	5.57 s
18	18.0 q	1.03 s	19.7 q	1.22 s	21.4 q	1.29 s
19	17.8 q	1.10 s	20.5 q	1.19 s	18.7 q	1.28 s
20	120.0 s		119.9 s		119.7 s	
21	141.2 d	7.49 br s	141.2 d	7.49 br s	141.9 d	7.56 br s
22	109.9 d	6.43 br s	109.9 d	6.42 br s	110.4 d	6.50 br s
23	143.0 d	7.42 br s	143.0 d	7.42 br s	143.0 d	7.44 br s
28	20.3 q	0.83 s	24.2 q	0.94 s	21.9 q	1.09 s
29	24.1 q	0.84 s	24.6 q	1.61 s	21.9 q	1.13 s
30 $\alpha$	34.8 t	1.59 m	74.8 d	5.46 s	41.9 t	2.57 dd (15.1,8.4)
$\beta$		2.25 ddd (13.7,4.3,3.2)		4.99, s		3.17 dd (15.1,3.6)
OMe		3.72 s	52.9 q	3.77 s	53.3 q	3.75 s
OH				4.52 br s (1-OH)		1.93 br s
				4.30 br s (2-OH)		
OAc (Me)			21.0 q	2.18 s	20.9	2.18 s
(CO)			169.7 s		169.5	
Tigloyl						
1'	167.1 s		168.2 s			
2'	127.7 s		127.5 s			
3'	139.0 d	6.96 br q (7.1)	139.8 d	6.86 br q		
4'	14.7 q	1.85 d (7.1)	14.6 q	1.86 br d		
4'-Me	12.2 q	1.90 br s	11.9 q	1.81 br s		
2-methylpropanoyl						
1''			175.4 s			
2''			34.1 d	2.48 hept (6.9)		
3''			6.9 q	1.05 d (6.9)		
2''-Me			6.9 q	1.06 d (6.9)		

#### IV.3.4. Phragmalin derivatives

##### IV.3.4.1. Phragmalin bearing orthoacetate bridge

Angolensin D (**9**) possessed the molecular formula  $C_{38}H_{48}O_{13}$  as determined from a pseudomolecular ion  $[M-H]^-$  at  $m/z$ : 711.3010 ( $\Delta$  -0.7 mmu) in the negative HRFAB-MS and from the analysis of  $^{13}C$  NMR spectroscopic data. The IR spectrum revealed absorption bands for hydroxyl ( $3410\text{ cm}^{-1}$ ) and saturated ( $1735\text{ cm}^{-1}$ ) and unsaturated carbonyl ( $1705\text{ cm}^{-1}$ ). The UV spectrum indicated the presence of conjugated system at 225 nm. From the  $^1H$  and  $^{13}C$  NMR spectra, it was clear that seven of the fifteen elements of unsaturation were present as double bonds: three carbon-carbon (one furan ring) and four carbon-oxygen (as esters). Therefore the molecule is octacyclic. The NMR spectroscopic data (Table 6) also revealed that compound **9** contained nine methyls (five tertiary, three secondary and one methoxy), five methylenes, ten methine (four olefinic), fourteen quaternary carbons (two olefinic). From the  $^1H$  and  $^{13}C$  NMR data, the presence of each one  $\beta$ -furyl ( $\delta_H$  6.47, 7.41 and 7.50; each 1H), tigloyl ( $\delta_H$  1.83, d and 1.93, br s: each 3H), and 3-methylpropanoyl moieties ( $\delta_H$  1.04 and 1.17, each d: 3H, and 2.52, hept: 1H) was recognized. The presence of one orthoacetate groups was also assumed from the characteristic signals due to an orthoester carbon at  $\delta_H$  119.0 (s) and acetate methyl protons at  $\delta_H$  1.678 (s). Each one of methoxy ( $\delta_H$  3.69) and hydroxyl ( $\delta_H$  2.69) groups was also observed.

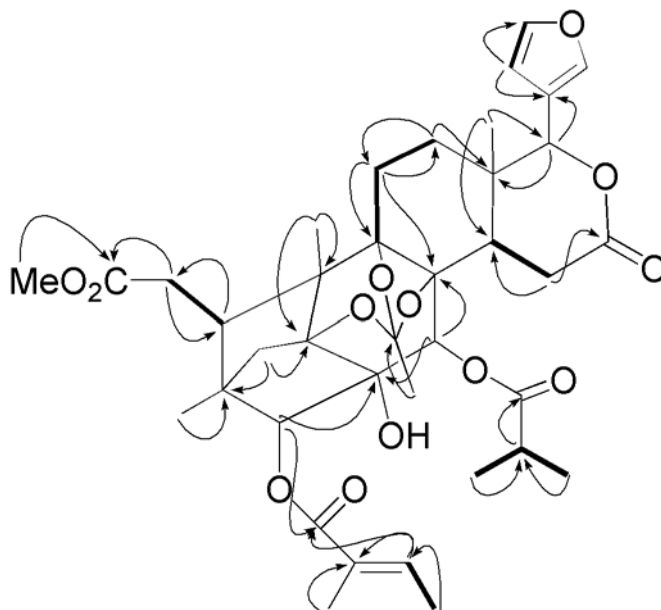


**Figure 18.** COSY and selected HMBC correlations in **9**

All of the protons directly bonded to carbon atoms were assigned by analysis of the HMQC spectrum. The data from decouplings and the subsequent 2D NMR studies strongly suggested that **9** was a phragmalin-type limonoid (Table 1).<sup>116,120</sup> Thus, a characteristic low-field singlet at  $\delta_H$  5.54 due to H-17 was observed and the 6-methylene protons at  $\delta_H$  2.28 (dd,  $J = 2.5$  and 15.9) and 2.47 (dd,  $J = 9.1$  and 15.9 Hz) attached to a carbon at  $\delta_C$  33.7 (t) adjacent to an ester carbonyl ( $\delta_H$  173.1), were coupled with the H-5 double doublet proton at  $\delta_H$  3.01 (dd,

$J = 2.5$  and  $9.1$  Hz). These observations strongly suggested that **4** was a rings B,D-seco limonoid. In addition to this knowledge, the absence of two tertiary methyl signals due to  $4\beta$ - and  $8\beta$ -Me (Me-29 and 30) in the basic limonoid skeleton and the presence of isolated geminal proton signals at  $\delta_{\text{H}}$  1.77 and 1.90 (each 1H, d,  $J = 10.7$  Hz) assigned to 29-methylene group, strongly supported that **9** was a phragmalin having the tricyclo[3.3.1<sup>2,10</sup>.1<sup>1,4</sup>]decane ring system.

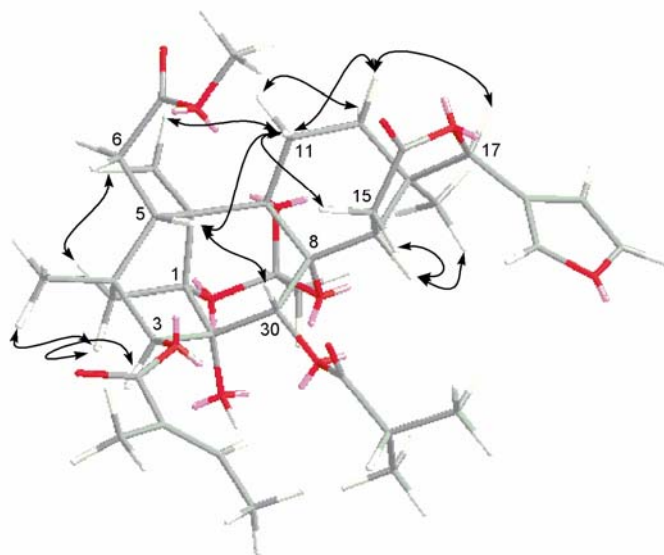


**Figure 19.** Computer-generated energy minimized model of **9** with key NOE correlations observed.

The presence of an orthoester group in **9** was also presumed from the characteristic orthocarbon resonance at  $\delta_{\text{H}}$  119.0. Many of the phragmalins isolated so far have been reported to be 1,8,9- or 8,9,14- orthoacetates except for some exceptions,<sup>116,121</sup> and their orthocarbon signals have been observed around 119.<sup>7</sup> The  $^1\text{H}$  and  $^{13}\text{C}$  NMR data due to the tricyclodecane ring of **9** were very similar to those of swietenialide D<sup>122</sup> isolated from the stem bark of *S. mahogany*, having six oxygenated  $\text{sp}^3$  carbon attributable to C-1, C-2, C-3, C-8, C-9 and C-30.

In the HMBC spectrum of **9** (Figure 18), the observed long-range C-H correlations of the H-5 signal with the  $^{13}\text{C}$  signals at  $\delta_{\text{H}}$  16.4 (q), 39.5 (t), 45.5 (s), 83.7 (d) and 87.2 (s) led to their assignments as C-19, C-29, C-10, C-3 and C-9, respectively. A down-field shifted methine proton singlet at  $\delta_{\text{H}}$  5.90 assigned to H-30 showed significant HMBC correlations with the three quaternary carbon signals at  $\delta_{\text{C}}$  79.9, 85.6 and 86.4 to be assigned to C-2, C-1 and C-8, and with the C-3 signal. The presence of two acetyloxy groups at C-3 and C-30 was confirmed from the correlations of H-3 and H-30 singlets at  $\delta_{\text{H}}$  4.73 and 5.90 attached to C-3 and C-30 at  $\delta_{\text{C}}$  70.5 with tigloyl and 2-methylpropanoyl ester carbonyl carbon signals at  $\delta_{\text{H}}$  167.3 and 174.6 in the HMBC spectrum. The presence of 2-OH group was also elucidated by the correlation of the OH signal at  $\delta_{\text{H}}$  2.69 with the C-2 signal, which located the orthoacetate group at position 1,8 and 9. Further, the methylene 29-methylene protons showed HMBC correlations with C-1, C-5, C-10 and C-28 (4-Me) at  $\delta_{\text{C}}$  14.5. These findings clearly characterized the first molecular fragment, the left-hand tricyclo[3.3.1.1]decane ring system.

A methine proton at  $\delta_{\text{H}}$  2.04 assigned to H-14 coupling with 15-methylene protons at  $\delta_{\text{H}}$  2.68 and 3.24 attached to a carbon at  $\delta_{\text{C}}$  26.6 (t) adjacent to a lactone carbonyl group at  $\delta_{\text{C}}$  170.4 (C-16), showed HMBC correlations



with three quaternary carbons C-8, C-9 and C-13 at  $\delta_C$  34.7, two methine carbons C-30 and C-17 at  $\delta_C$  78.2, and a Me-13 (Me-18) carbon at  $\delta_C$  19.6. Finally, the 11-methylene proton signals at  $\delta_H$  1.65 and 2.17 attached to the carbon at  $\delta_C$  25.4 showed correlations C-8-C-10, C-12 at  $\delta_H$  20.0 and C-13 signals. These correlations characterized the second fragment of the molecule, C-8, C-9 and C-11-C-17 of the C and D rings, including Me-13 and the furan ring.

The structure of **9**, including its stereochemistry, was fully explained from the NMR data by consideration of NOE correlations (Figure 19). Strong cross-peaks of the H-5 signal with one of the H<sub>2</sub>-11 at  $\delta_H$  1.65 and the H-30 signals, the H-11 signal with H-17 and H-30 signals, and H-17 signal with H-30 signal indicated the  $\beta$  orientation for these protons and the chair conformation of the ring C. On the other hand, the 29-methylene protons at  $\delta_H$  1.90 (d,  $J = 10.7$  Hz, *pro-S*) and 1.77 (d,  $J = 10.7$  Hz, *pro-R*) showed NOE correlations with H-3 and Me-10 (Me-19) protons at  $\delta_H$  1.15, respectively. These NOE correlations clarified the relative stereochemistry of these protons in the tricyclodecane ring system. Finally, a NOE correlation between H-14 and the Me-18 protons clarified the *cis*-fusion of the rings C/D.

Angolensin E (**15**) was obtained as a white amorphous powder. The molecular formula (C<sub>36</sub>H<sub>42</sub>O<sub>15</sub>, 16 unsaturations) was determined by analysis of its HRFAB-MS ( $m/z$ : 715.2600 [M+1]<sup>+</sup>,  $\Delta$  -0.2 mmu) and NMR data. The UV and IR spectra showed similar absorptions to those of **9** at 225 nm and at 3600-3250 and 1745-1739 cm<sup>-1</sup> as broad bands, and the NMR spectra suggested **15** to be a phragmalin derivative having an orthoacetate group ( $\delta_H$  1.54, 3H, s;  $\delta_C$  21.0 q and 118.0 s). However, the NMR spectra showed some difference with **9** by the presence of an additional oxygenated sp<sup>3</sup> carbon, chemical shift change of few protons and carbon signals, and the variation of ester groups, the latter of which included the absence of the tigloyl and 2-methylpropanoyl ester groups observed in **9**, and the presence of one propanoyl ester ( $\delta_H$  1.14, 3H, t,  $J = 7.6$  Hz and 2.29, 2H, q,  $J = 7.6$  Hz;  $\delta_C$  9.14 d, 27.0 d and 171.7 s) and two acetoxy groups ( $\delta_H$  2.33, 6H, s;  $\delta_C$  171.7 s and 172.7 s) in **15**. The most significant difference was the presence of a trisubstituted double bond ( $\delta_C$  116.9 d and 162.8 s) in the ring D.

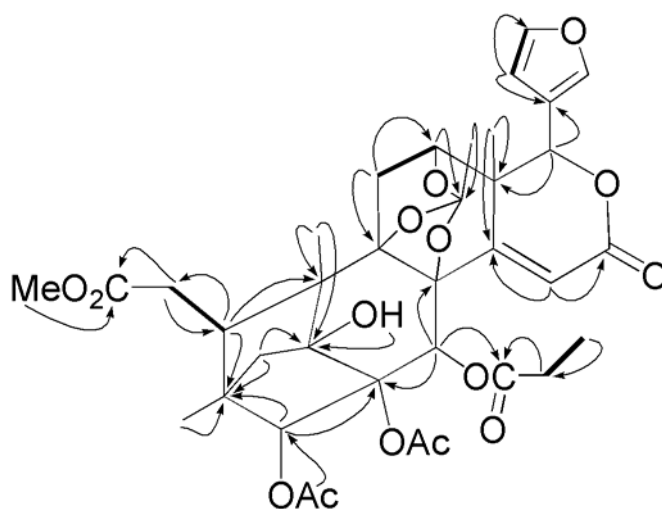


**Figure 20.** COSY and selected HMBC correlations in **15**

An olefinic proton singlet at  $\delta_{\text{H}}$  7.08 attached to a carbon at  $\delta_{\text{C}}$  116.9 adjacent to a lactone carbonyl carbon at  $\delta_{\text{C}}$  163.7 (C-16) was assigned to H-15, which showed HMBC correlations with another olefinic carbon at  $\delta_{\text{C}}$  162.8 (s, C-14) and two quaternary carbons at  $\delta_{\text{C}}$  80.0 and 45.4 assigned to C-8 and C-13. The carbon signal due to C-13 was further correlated to two methine signals at  $\delta_{\text{H}}$  3.91 and 5.21 assigned to H-12 and H-17, methylene signals at  $\delta_{\text{H}}$  1.63 and 2.42 assigned to H<sub>2</sub>-11, and methyl signals at  $\delta_{\text{H}}$  1.51 (Me-18). The 11-methylene protons showed correlations with three singlet carbons at  $\delta_{\text{C}}$  80.0, 85.8 and 47.1 assigned to C-8, C-9 and C-10 together with C-12 at  $\delta_{\text{C}}$  71.7 and C-13. On the other hand, the H-12 signal showed a strong correlation with the characteristic orthocarbon resonance at  $\delta_{\text{C}}$  118.0. These findings characterized the right-hand C and D rings of the molecule. Further, the configuration of H-12 coupling with only one of the methylene-11 protons at  $\delta_{\text{H}}$  2.42 (dd,  $J = 4.7$  and 13.0 Hz) was assigned to be  $\beta$  from a remarkable NOE correlation with H-17.

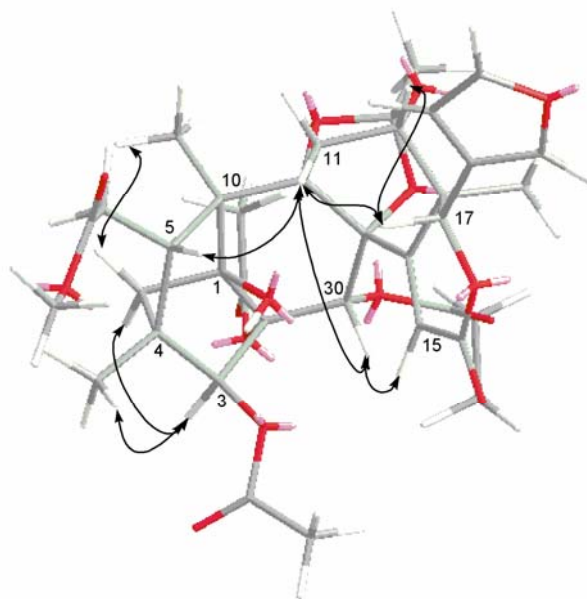


**Figure 21.** Computer-generated energy minimized model of **15** with key NOE correlations observed.

The structure of the remaining tricyclodecane ring system and the location of the orthoester group were elucidated by HMBC correlations. One of the two acetoxy and the propanoyloxy group were located to C-3 and C-30 by correlation of two methine protons at  $\delta_{\text{H}}$  5.22 and 6.28 assigned to H-3 and H-30 to C-3 and C-30 by correlation with the acetyl and propanoyl ester carbonyls at  $\delta_{\text{C}}$  169.4 and 171.7. On the other hand, the hydroxyl group observed at  $\delta_{\text{H}}$  2.55 was elucidated to be present at C-1 by the correlations of the OH signal with signals of C-1, C-10 and C-29 at  $\delta_{\text{H}}$  81.4, 47.1 and 41.4. The presence of 1-OH group located the orthoacetate group at positions 8, 9 and 12. Finally, the remaining second acetoxy group was assigned to C-2.

The stereochemistry of **15** was elucidated by NOE correlation using molecular model and indicated that all of the asymmetric carbons except for C-12 had the configurations as in **9**. However, the H-30 signal showed a significant low-field shift to  $\delta_{\text{H}}$  6.28 together with a new NOE correlation with the H-15 signal, not with the H-5, 11 $\beta$ -H and H-17 signals observed in **9**. These findings suggested strongly that the ring system of **15** was in a different conformation from that of **4**. The conformational change could be well accounted by the alteration of the ring C to twist-boat form, from the chair conformation in **9**, which derived from the formation of 8,9,12-

orthoester linkages. Taking into account this boat conformation, the low-field shift of H-30 could be explained by an effect of the C-14/C-15 double bond. Many phragmalin limonoids possessing an orthoester group have been reported, but this is the first isolation of the 8,9,12-orthoester derivative.

Angolensin F (**7**) was obtained as a white amorphous powder. The molecular formula,  $C_{41}H_{54}O_{15}$ , was determined by analysis of its HRFAB-MS ( $m/z$ : 787.3543  $[M+H]^+$ ,  $\Delta +0.2$  mmu) and NMR spectra. Compound **7** showed similar UV and IR absorption bands with those of **9** and **15** at 215 nm and at 3600-3300 and 1745-1720  $cm^{-1}$ . The  $^1H$  and  $^{13}C$  NMR spectra suggested that **7** had similar structure to **9**, having each one of orthoacetate, tiglate, 2-methylpropanate and hydroxyl groups, except for the presence of additional acetyl ( $\delta_H$  1.94) and carbomethoxy ( $\delta_H$  3.67) groups in **7**. The chemical shifts of some signals due to the limonoid skeleton in **7** were somehow different from those of **9**, but the HMQC assignment of all the proton and carbon signals indicated **7** to be a phragmalin limonoid having the same tricyclo[3.3.1. $^{2,10}1^{1,4}$ ]decane ring system as **9**. Thus, the  $^{13}C$  NMR spectrum exhibited six oxygenated  $sp^3$  carbon signals attributable to C-1, C-2, C-3, C-8, C-9 and C-30 at  $\delta_C$  85.7 (s), 80.5 (s), 84.0 (d), 87.3 (s), 87.2 (s) and 70.4 (d). On the other hand, it was also evident that **7** was pentacyclic different from **9** and **15**, and its eight elements of unsaturations were present as double bonds: three carbon-carbon (one furan) and five CO (as esters).

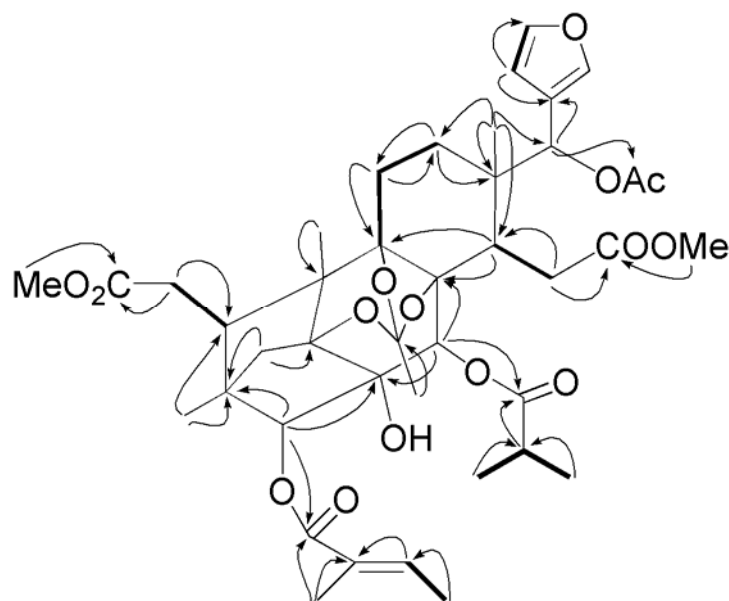


**Figure 22.** COSY and selected HMBC correlations in **7**

Significant information regarding the rest of the molecule was provided by the HMBC spectrum. Long-range  $^1H$ - $^{13}C$  correlations of the characteristic H-17 singlet at  $\delta_H$  5.73 with an acetoxy carbonyl carbon signal at  $\delta_C$  169.0 and one methoxy signal of the two carbomethoxy groups at  $\delta_H$  3.67 with the 16-ester carbonyl signal at  $\delta_C$  174.6 clarified that **7** was a ring D opened phragmalin limonoid like procerin<sup>116</sup> and swietenialides<sup>122</sup> from *Carapa procera* and *Swietenia mahogani*. Although the location of the orthoacetate group at positions 1,8,9 was assumed by a weak HMBC correlation of the acetate methyl signal at  $\delta_H$  1.61 with the C-1 signal at  $\delta_C$  85.7. The

location of the remaining hydroxyl group was determined to be at C-2 by the correlation of its signal at  $\delta_{\text{H}}$  2.66 with the C-2 and C-3 signals at  $\delta_{\text{C}}$  80.5 and 84.0. As in **9**, the same locations of the tiglate and methylpropanoate groups were elucidated by HMBC correlations of the H-3 and H-30 signals at  $\delta_{\text{H}}$  4.67 and 5.76 with the carbonyl carbon signals at  $\delta_{\text{C}}$  167 and 174.0. The configuration of these protons were also assigned as  $\alpha$  and  $\beta$  on the basis of the NOE correlations (Figure 23), in which the H-30 signal showed similar correlations to those of **9**, but H-30 signal exhibited a new correlation with 12 $\beta$ -H, not with the 11 $\beta$ -H signal, together with H-5 signal. The H-5 signal also showed a new NOE correlation with 12 $\beta$ -H signal. On the other hand, the H-8, 11 $\alpha$ -H and Me-13 signals showed remarkable NOE correlations to each other. These findings suggested strongly a conformation change of the ring C to a boat form, and this alteration accounted nicely for the chemical shift deviation of many NMR signals in **7** from those of **9**.

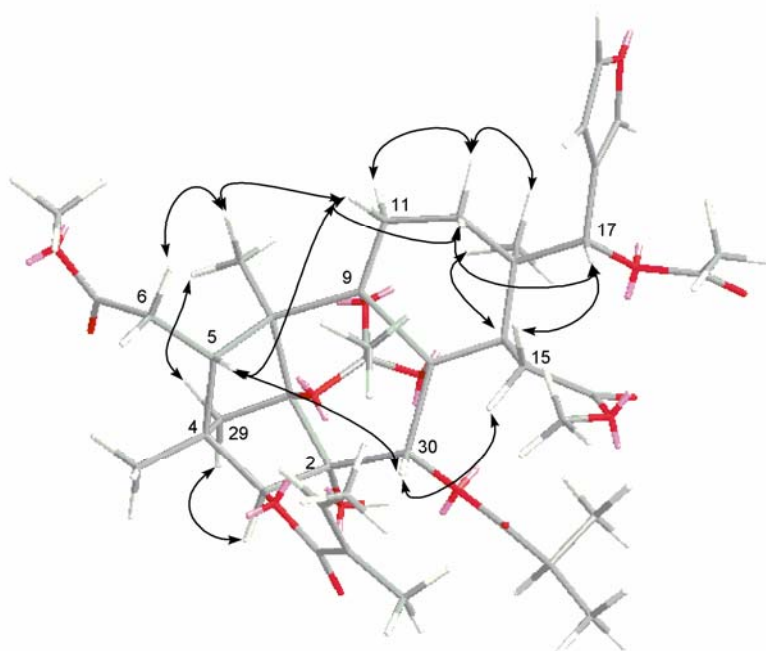


**Figure 23.** Computer-generated energy minimized model of **7** with key NOE correlations observed.

#### IV.3.4.2. Phragmalin with newly formed lactone ring fused to the C-ring of basic skeleton

Compound **6** was isolated as amorphous powder and was found to have the molecular formula  $\text{C}_{40}\text{H}_{50}\text{O}_{14}$  (degree of unsaturations: 16) by accurate mass measurement (HRFAB-MS:  $m/z$  755.3257  $[\text{M}+\text{H}]^+$ ) and  $^{13}\text{C}$  NMR data. The UV maximum at 225 nm and the IR absorption at 3434-3248, and 1740-1715  $\text{cm}^{-1}$  showed the presence conjugated double bond, hydroxyl and several carbonyl groups. From the  $^1\text{H}$  and  $^{13}\text{C}$  NMR data, it was evident that eight of the elements of unsaturation were present as double bonds: four carbon-carbon (one furan ring) and four CO (as esters). Thus, the molecule is octacyclic. The NMR data also revealed that compound **6** had eight tertiary methyls (one acetyl and one methoxy), two secondary methyls, four methylenes, ten methines (four olefinic), fifteen carbons (four olefinic and four ester carbonyls) not bonded to hydrogen. From the NMR data, the presence of each one of  $\beta$ -furyl moiety ( $\delta_{\text{H}}$  6.42, 7.33 and 7.43, each 1H), 1-methylpropyl ( $\delta_{\text{H}}$  1.13 and

1.229 each d: 3H, and 2.96, hept: 1H) and acetyl group ( $\delta_{\text{H}}$  1.96) was recognized. The presence of one tigloyl and one orthoester groups was also assumed from the characteristic signals of 2' and 3'-Me and 3'-H in tigloyl at  $\delta_{\text{H}}$  1.78 and 1.99 (3H, d,  $J = 7.0$  Hz and br s, respectively) and 7.09 (1H, qq,  $J = 7.0, 1.3$  Hz) and of an orthoester carbon at  $\delta_{\text{C}}$  116.8 s. One carboxylate methyl ( $\delta_{\text{H}}$  3.67) and one hydroxyl group ( $\delta_{\text{H}}$  2.83) were also observed.

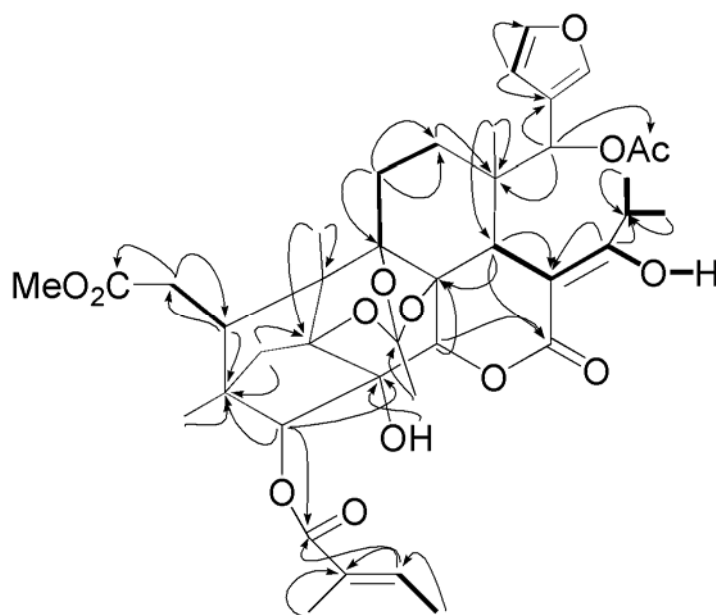
All protons directly bonded with carbon atoms were assigned by the HMQC spectrum. From decouplings and the subsequent 2D NMR studies using the  $^1\text{H}$ - $^1\text{H}$  COSY, HMBC and NOE spectra, it was strongly suggested that **6** was a ring D opened phragmalin-type compound.

**Table 6.**  $^1\text{H}$  and  $^{13}\text{C}$  NMR spectroscopic data angolensins D (**9**), E (**15**) and F (**7**)

Position	Angolensin D ( <b>9</b> )		Angolensin E ( <b>15</b> )		Angolensin F ( <b>7</b> )	
	$\delta_{\text{C}}$ mult.	$\delta_{\text{H}}$ ( $J$ in Hz)	$\delta_{\text{C}}$ mult.	$\delta_{\text{H}}$ ( $J$ in Hz)	$\delta_{\text{C}}$ mult.	$\delta_{\text{H}}$ ( $J$ in Hz)
1	85.6 s		81.4 s		85.7 s	
2	79.9 s		83.1 s		80.5 d	3.36 dd (8.4,3.6)
3	83.7 d	4.73 s	85.5 d	5.22 s	84.0 s	4.67 s
4	45.2 s		44.4 s		45.1 s	
5	37.1 d	3.01 dd (9.1,2.5)	37.9 d	2.33 br d (7.2)	37.2 d	2.88 dd (9.0,3.1)
6a ( <i>pro-R</i> )	33.7 t	2.47 dd (15.9,9.1)	33.3 t	2.37 dd (13.7,7.2)	34.3 t	2.39 dd (15.3,9.0)
b ( <i>pro-S</i> )		2.28 dd (15.9,2.5)		2.27 br d (13.7)		2.24 dd (15.3,3.1)
7	173.1 s		172.7 s		172.7 s	
8	86.4 s		80.0 s		87.3 s	
9	87.2 s		85.8 s		87.2 s	
10	45.5 s		47.1 s		45.7 s	
11 $\alpha$	25.4 t	2.17 m	28.3 t	2.42 dd (13.0,4.7)	25.5 t	1.70 dt
$\beta$		1.65 m		1.63 d (13.0)		1.93 m
12 $\alpha$	20.0 t	1.25 -1.29	71.7 d		31.5 t	0.94 ddd (14.8,4.2,2.0)
$\beta$		1.25-1.29		3.91 d (4.7)		1.36 br t (14.8)
13	34.7 s		45.4 s		39.0 s	
14	42.8 d	2.04 dd (10.7,1.2)	162.8 s		47.4 d	2.34 dd (7.7,5.4)
15 $\alpha$	26.6 t	2.68 dd (20.0,10.7)	116.9 d	7.08 s	30.5 t	2.82 dd (15.5,5.3)
$\beta$		3.24 dd (20.0,1.2)				2.28 dd (15.5,7.8)
16	170.4 s		163.7 s		174.6 s	
17	78.2 d	5.54 s	78.3 d	5.21 s	70.4 d	5.73 s
18	19.6 q	1.04 s	17.9 q	1.43 s	21.1 q	1.18 s
19	16.4 q	1.15 s	14.3 q	1.36 s	16.3 q	1.11 s
20	121.2 s		119.5 s		122.5 s	
21	142.8 d	7.50 br s	143.5 d	7.44 br s	142.6 d	7.63 br s
22	109.7 d	6.47 br d (0.8)	110.1 d	6.45 br s	109.4 d	6.40 br s
23	142.8 d	7.41 t (1.5)	143.5 d	7.44 t (1.6)	142.6 d	7.33 br s
28	14.5 q	0.91 s	14.7 q	0.78 s	14.4 q	0.90 s
29( <i>pro-R</i> )	39.5 t	1.77 d (10.7)	41.4 t	2.08 d (11.5)	39.4 t	1.86 d (10.8)
( <i>pro-S</i> )		1.90 d (10.7)		1.79 d (11.5)		1.70 d (10.8)
30	70.5 d	5.90 s	63.8 d	6.28 s	70.4 d	5.76 s
7-OMe	52.0 q	3.69 s	52.2 q	3.62 s	51.5 q	3.53 s
16-OMe					53.0 q	3.67 s
OH		2.69 s		2.55 s		2.66 s

**Table 6** (continued).  $^1\text{H}$  and  $^{13}\text{C}$  NMR spectroscopic data angolensins D (**9**), E (**15**) and F (**7**)

Position	Angolensin D ( <b>9</b> )		Angolensin E ( <b>15</b> )		Angolensin F ( <b>7</b> )	
	$\delta_{\text{C}}$ mult.	$\delta_{\text{H}}$ ( $J$ in Hz)	$\delta_{\text{C}}$ mult.	$\delta_{\text{H}}$ ( $J$ in Hz)	$\delta_{\text{C}}$ mult.	$\delta_{\text{H}}$ ( $J$ in Hz)
OAc (Me)			21.2 q	2.11 s	21.3 q	1.94 s
(CO)			169.4 s		169.0 s	
OAc (Me)						
(CO)						
Orthoacetate						
1	119.0 s		118.0 s		118.9 s	
2	21.2 q	1.67 s	21.0 q	1.54 s	20.8 q	1.61 s
Tigloyl						
1'	167.3 s				167.6 s	
2'	128.9 s				129.4 s	
3'	137.5 d	7.01 qq (7.1)			136.7 d	7.02 qq (7.1,1.2)
4'	14.4 q	1.83 br d (7.1)			14.4 q	1.91 dq (7.1,0.7)
4'-Me	12.1 q	1.93 br s			12.4 q	1.95 br s
O-Acyl groups(Propanoyl, 2-methylpropanoyl)						
1''	174.6 s		171.7 s		174.0 s	
2''	34.5 d	2.52 hept (7.0)	27.0 d	2.29 q (7.6)	34.6 d	2.63 hept (6.9)
3'' (Me)	18.1 q	1.05 d (7.0)	9.1 q	1.14 t (7.6)	18.2 q	1.22 d (6.8)
2''-Me	19.1 q	1.17 d (7.0)			18.8 q	1.24 d (6.9)

**Figure 24.** COSY and selected HMBC correlations in **6**

Thus, H<sub>2</sub>-6 methylene protons at  $\delta_{\text{H}}$  2.23 (dd,  $J = 16.4, 2.1$  Hz) and 2.50 (dd,  $J = 16.4, 10.2$  Hz) attached to a carbon adjacent to an ester carbonyl at  $\delta_{\text{C}}$  33.8 (C-6) were coupled with the H-5 doublet doublet proton at  $\delta_{\text{H}}$  3.09 (dd,  $J = 10.2, 2.0$  Hz) and the presence of this moiety and a characteristic low-field singlet H-17 proton at  $\delta_{\text{H}}$  5.64 strongly suggested that **6** was a rings B,D-seco limonoid. In addition to this knowledge, the absence of one tertiary methyl signal at  $8\beta$  (Me-30) in the basic limonoid skeleton and the presence of 29-methylene signals

( $\delta_{\text{H}}$  1.93 and 1.86, each 1H, d,  $J = 10.9$  Hz) supported that **6** was a phragmalin-type limonoid having the tricyclo[3.3.1.2,1011,4]decane ring system.

In the HMBC spectrum of **6**, long range  $^1\text{H}$ - $^{13}\text{C}$  correlations of the H-17 signal with an acetoxy carbonyl carbon signal at  $\delta_{\text{C}}$  168.9 clarified that **6** was a ring D cleaved phragmalin-limonoid like swietenialide series<sup>122</sup>. The presence of orthoester group in **6** was presumed from the fact that almost all of the phragmalin groups isolated so far contained an orthoester carbon resonance observed at  $\delta_{\text{C}}$  118.6. The presence of the 3-tigloyloxy and 2-hydroxyl groups was also elucidated by the HMBC correlations of the H-3 signal at  $\delta_{\text{H}}$  4.92 with the tigloyl carbonyl carbon signal at  $\delta_{\text{C}}$  167.4 and the OH signal at  $\delta_{\text{H}}$  2.83 with the C-2 carbon signal at  $\delta_{\text{C}}$  77.8. Especially, the presence of 2-OH group located the orthoacetate group at positions 1, 8, and 9, since the group has been observed either at positions 8, 9, 14 or at 1, 8, 9 in phragmalins except some rares compounds.

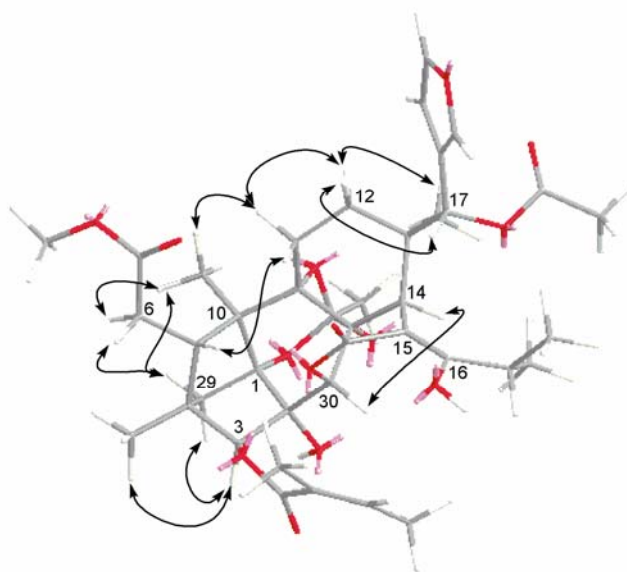


**Figure 25.** Computer-generated energy minimized model of **6** with key NOE correlations observed.

In the HMBC spectrum, the lactonic carbonyl at  $\delta_{\text{H}}$  167.4 (C-16) correlated to the downfield shifted proton at  $\delta_{\text{H}}$  5.37 (H-30) and a methine proton at  $\delta_{\text{H}}$  2.64 (H-14) attached to the carbon resonating at  $\delta_{\text{C}}$  43.6 (C-14) suggesting the presence of  $\delta$ -lactone constituted by C-30, C-8, C-14, C-15 at  $\delta_{\text{C}}$  91.2 and C-16; fused at C-8 and C-30. The resonance of  $\delta_{\text{C}}$  91.2 suggested the presence of an hydroxylmethylidene moiety as observed in some bussein<sup>77</sup> and neobeguin<sup>123</sup> located at C-15. This deduction was confirmed by the coupling of the methylpropyl group methine proton with the hydroxyl proton (OH-1'') which correlated weakly with C-15 and strongly with a quaternary carbon at  $\delta_{\text{C}}$  183.0 (C-1'') and the latter showed also weak cross peak with H-8 and located the 1''-hydroxy-2''-methylpropylidene at C-15. The structure of **6** including the stereochemistry was clearly explained by the NMR data and the NOE spectrum. Significant NOE correlations between the H-30 signal and H-5, H-30 and H-17, and H-17 and H-12 $\beta$  signals, the  $H_{\text{pro-S}}$  signal of the 29-methylene at  $\delta_{\text{H}}$  1.93 and the 10-Me (Me-19) signal at  $\delta_{\text{H}}$  1.16, and the other  $H_{\text{pro-R}}$  signal at  $\delta_{\text{H}}$  1.86 and the H-3 signal clarified relative stereochemistry between these protons in **6**. On the other hand, H-14 showed NOE correlations with H-11 $\alpha$ , Me-18 indicating their  $\alpha$  orientation.

Compound **11** possessed a molecular formula of  $C_{41}H_{54}O_{14}$  (HRFABMS,  $[M-H]^-$   $m/z$  769.3428) and the UV and IR spectra showed some similar absorptions with those of **6** especially the presence of a conjugated system at 212 nm and hydroxyl and carbonyl at 3409-3250, 1740 and 1651  $cm^{-1}$ .

However, the NMR spectrum of **11** showed the presence of an orthoacetate group with the orthoacetate carbon resonance at  $\delta_C$  122.7 s different from the one in compound **6**. From the  $^1H$  and  $^{13}C$  NMR data (Table 7), it was evident that **11** was heptacyclic and its octaunsaturations were present as double bonds: three carbon-carbon (one furan ring) and five CO (as esters). The NMR data also revealed that **11** had eleven methyls (one acetyl, one methoxy and one carboxylate methyl), four methylenes, twelve methines (four olefinic), twelve quaternary carbons (two olefinic) and one hydroxyl groups. A  $\beta$ -furyl moiety ( $\delta_H$  6.26, 7.29 and 7.38, each 1H), one tigloyl moiety ( $\delta_H$  1.80, d and 2.03, br s: each 3H, and 7.01 qq: 1H) and one isopropyl group ( $\delta_H$  1.24 and 1.28 each d: 3H, and 2.99, dq: 1H) were also observed from the NMR data.

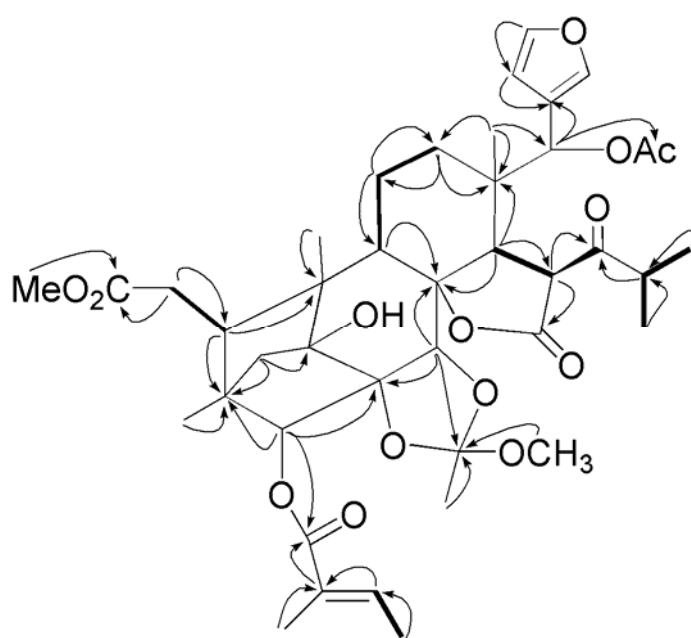


**Figure 26.** COSY and selected HMBC correlations in **11**

Although the chemical shifts of many signals due to the limonoid skeleton in **11** were somehow different from those of **6**, the HMBC assignment of all the proton and carbon signals indicated **11** to be also a ring-D cleaved phragmalin-limonoid. The  $^1H$  NMR spectrum showed the presence of the characteristic H-17 singlet at  $\delta_H$  6.17 s, two 29-methylene doublet at  $\delta_H$  2.04 and 1.75 (each  $J = 11.0$  Hz) and one carbomethoxy group assigned to 7-OME at  $\delta_H$  3.64. The correlation of the methoxy at  $\delta_H$  3.15 with the orthoester carbon at  $\delta_C$  122.7, located it on the orthoacetate group which was located to C-2 and C-30 from singlet signals due to H-3 ( $\delta_H$  5.28) and H-30 ( $\delta_H$  5.05) and the HMBC correlations of the H-30 signal with the orthoacetate carbon signal ( $\delta_C$  122.7).

The proton signal due to 15-methine proton, lying between two carbonyl groups was downfield shifted at  $\delta_H$  4.56, coupled with the proton H-14 at  $\delta_H$  2.96 which showed also HMBC correlations with the lactonic carbonyl group at  $\delta_C$  170.9 (C-16) and an oxygenated carbon at  $\delta_C$  86.4 assigned to C-8. The presence of isopropoxy moiety was also elucidated by HMBC correlation of H-15 signal with the ketonic carbonyl carbon



signal at  $\delta_C$  209.3 which showed also cross-peak with the methine proton of the isopropyl at  $\delta_H$  2.99. These findings suggested the presence in **11** of  $\gamma$ -lactone moiety substituted at  $\alpha$ -position (C-15) by isopropoxy moiety and fused at carbons C-8 and C-14.

The stereochemistry **11** was established by analysis of NOE spectrum. The correlations were observed from H-9, H-12 $\alpha$ , H-14 and Me-18 indicated the  $\alpha$  orientation of these protons.

The NOE correlations from H-3 to H<sub>pro-R</sub>-29 at  $\delta_H$  2.04 helped to establish the  $\beta$  orientation of tigloyl group. Similarly, NOE interactions of H-30/H-5, H-17 and H-11 $\beta$ , H-17 and H-30, indicated that the B/C rings were cis-fused and C-ring adopts chair-like and the newly formed lactone ring was *cis*-fused to C-ring.

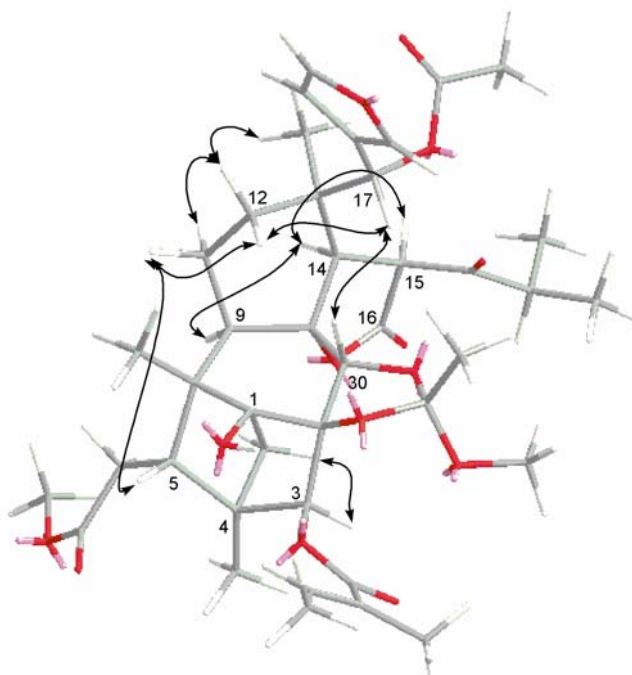


**Figure 27.** Computer-generated energy minimized model of **11** with key NOE correlations observed.

The molecular formula of compound **17**, isolated as an amorphous solid, was established to be  $C_{38}H_{49}O_{13}$  by HRFAB-MS ( $m/z$ : 713.3178). The UV and IR spectrum showed close similarities with those of **11**. The closely relationship was also confirmed by the analysis of  $^1H$  and  $^{13}C$  NMR spectra from which **17** was predicted to be a phragmalin-type compound with the D-ring cleaved. However, **17** was different to **11** by the lack of signals due the orthoacetate group at C-2 and C-30. As, the oxygenated carbons signals number did not change, it was then, deduced that **17** is having two hydroxyl groups at C-2 and C-30.

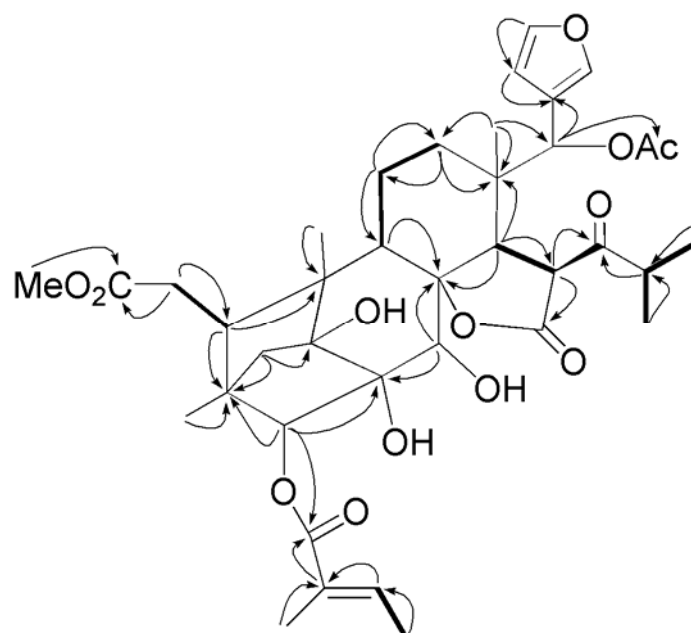


**Figure 28.** COSY and selected HMBC correlations in **17**

The structure of **17** including the stereochemistry appears to be fully explained by the consideration NOE correlations. Significant NOE correlations between the H-30 signal and H-5 and H-17 signals, the H<sub>pro-S</sub> signal of the 29-methylene at  $\delta_{\text{H}}$  2.01 and the 10-Me (Me-19) signal at  $\delta_{\text{H}}$  1.10 and the other H<sub>pro-R</sub> signal at  $\delta_{\text{H}}$  1.69 and the H-3 ( $\delta_{\text{H}}$  4.69) signal clarified relative stereochemistry between these protons in the tricyclo[3.3.1.1]decane ring system. The newly formed lacton ring was found also *cis*-fused as in **11**.

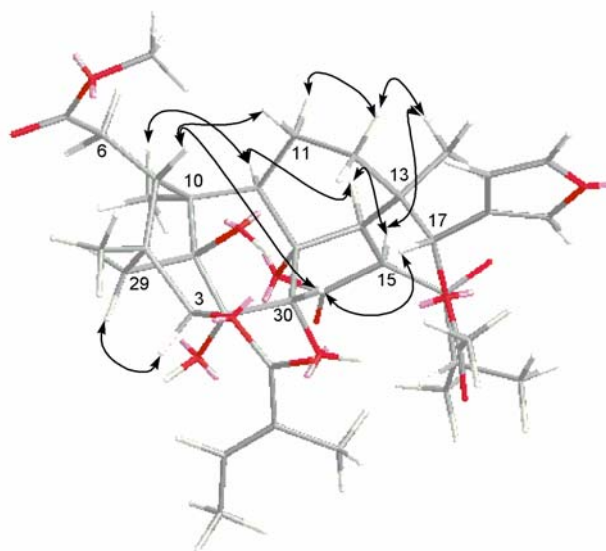


**Figure 29.** Computer-generated energy minimized model of **17** with key NOE correlations observed.

## IV.3.4.3. Other Phragmalin-type compounds

Analysis of the HRFABMS spectrum of **22** showed a pseudomolecular  $[M-H]^-$  ion at  $m/z$  756.3013 corresponding to a molecular formula of  $C_{39}H_{48}O_{15}$ . The UV spectrum displayed an extra absorption at 341 nm in addition to 214 nm. The IR revealed absorption bands for hydroxyl ( $3350-3000\text{ cm}^{-1}$ ), carbonyl ( $1750-1705\text{ cm}^{-1}$ ). From the examination of the  $^1\text{H}$  and  $^{13}\text{C}$  NMR spectra, it was deduced that **22** has a hexacyclic molecule because ten out of sixteen elements of unsaturation were present as double: four carbon-carbon (one furan ring) and four ester CO. From the  $^1\text{H}$  NMR data, the presence of 2-methylpropanoyl ( $\delta_{\text{H}}$  1.13 and 1.15, each d: 3H and 2.56 hept: 1H), one  $\beta$ -furyl ( $\delta_{\text{H}}$  6.44, 7.46 and 7.53; each 1H), one tigloyl ( $\delta_{\text{H}}$  1.78, br s and 1.81, d: each 3H, and 6.86 qq: 1H) was recognized. One methoxy and one acetyl groups were also observed. All protons bonded directly to carbon atoms were assigned by analysis of the HMQC spectrum. The data from decouplings and the subsequent 2D NMR strongly suggested that **22** was a phragmalin-type limonoid. Thus, a signal at  $\delta_{\text{H}}$  5.56 assigned to H-6 attached to a carbon at  $\delta_{\text{C}}$  71.9 adjacent to an ester carbonyl at  $\delta_{\text{H}}$  169.9 (C-7) and coupled with the H-5 signal observed at  $\delta_{\text{H}}$  2.78 as broad singlet. The presence of this moiety and a characteristic H-17 signal at  $\delta_{\text{H}}$  4.92 strongly suggested that **22** was a rings B,D-seco limonoid. The absence of one tertiary methyl at  $8\beta$  (Me-30) in the basic skeleton and the presence of 29-methylene signals at  $\delta_{\text{H}}$  2.29 and 2.02 (d:  $J = 10.4\text{ Hz}$ , each 1H) supported the suggestion that **22** should be a phragmalin-type limonoid<sup>69</sup>. The  $^1\text{H}$  and  $^{13}\text{C}$  NMR spectra of **22** was very similar to those of tabulalin however the presence of additional tetrasubstituted double and at  $\delta_{\text{C}}$  157.0 s and 120.1 s and an acetal carbon signal at  $\delta_{\text{C}}$  109.8 d.

**Table 7.**  $^1\text{H}$  and  $^{13}\text{C}$  NMR spectroscopic data of compounds **6**, **11** and **17**

Position	Compound <b>6</b>		Compound <b>11</b>		Compound <b>17</b>	
	$\delta_{\text{C}}$ mult.	$\delta_{\text{H}}$ ( $J$ in Hz)	$\delta_{\text{C}}$ mult.	$\delta_{\text{H}}$ ( $J$ in Hz)	$\delta_{\text{C}}$ mult.	$\delta_{\text{H}}$ ( $J$ in Hz)
1	85.1 s		81.6 s		82.8 s	
2	77.8 s		87.2 s		76.5 s	
3	83.9 d	4.92 s	85.6 d	5.28 s	87.3 d	4.67 s
4			43.8 s		43.1 s	
5	37.1 d	3.09 dd (10.2,2.0)	38.7 d	2.94 <sup>a</sup>	39.1 d	3.03 br d (11.9)
6a	33.8 t	2.50 dd (16.4,10.2)	33.7t	2.28 dd (16.7,10.3)	33.6 t	2.33 dd (15.9,11.2)
b		2.23 dd (10.2,2.0)		2.24 dd (16.7,4.2)		2.23 dd (15.9,0.3)
7	172.7 s		173.4 s		173.3 s	
8	80.9 s		86.4 s		89.0 s	
9	84.4 s		51.0 d	1.97 <sup>a</sup>	49.4 d	1.89 <sup>a</sup>
10	45.9 s		46.3 s		45.1 s	
11 $\alpha$	24.9 t	1.70 m	23.0 t	1.89 m	1.84 m	
$\beta$		2.06 m		1.97 <sup>a</sup>	1.89 <sup>a</sup>	
12 $\alpha$	30.7 t	1.58 m	36.5 t	1.75 <sup>a</sup>	1.22 m	
$\beta$		1.06 m		1.28	1.69 <sup>a</sup>	
13	40.0 s		39.3 s		39.1 s	
14	43.6 d	2.64 s	58.3 d	2.96 d (13.7)	57.4 d	2.89 d (13.4)
15	91.2 s		52.5 d	4.56 d (13.7)	52.9 d	4.78 d (13.4)

**Table 7** (continued).  $^1\text{H}$  and  $^{13}\text{C}$  NMR spectroscopic data of compounds **6**, **11** and **17**

Position	Compound <b>6</b>		Compound <b>11</b>		Compound <b>17</b>	
	$\delta_{\text{C}}$ mult.	$\delta_{\text{H}}$ ( $J$ in Hz)	$\delta_{\text{C}}$ mult.	$\delta_{\text{H}}$ ( $J$ in Hz)	$\delta_{\text{C}}$ mult.	$\delta_{\text{H}}$ ( $J$ in Hz)
16	170.7 s		170.9 s		171.1 s	
17	71.3 d	5.64 s	72.0 d	6.17 s	71.9 d	6.03 s
18	21.9 q	1.27 s	23.8 q	0.81 s	22.3 q	0.87 s
19	15.6 q	1.16 s	21.9 q	1.12 s	20.9 q	1.10 s
20	112.6 s		122.4 s		122.8 s	
21	140.8 d	7.43 br s	142.9 d	7.38 s	142.9 d	7.35 br s
22	110.1 d	6.42 d (0.9)	109.8 d	6.26 br s	110.0 d	6.27 br s
23	142.5 d	7.33 t (0.9)	140.1 d	7.29 br s	140.5 d	7.29 br s
28	14.8 q	0.97 s	14.8 q	0.80 s	14.5 q	0.87 s
29( <i>pro-R</i> )	39.8 t	1.93 d (10.9)	41.6 t	2.04 d (11.0)	41.1 t	2.01 d (11.1)
( <i>pro-S</i> )		1.86 d (10.9)		1.75 (11.0)		1.69 d (11.1)
30	74.8 d	5.37 s	75.1 d	5.05 s	67.8 d	4.45 s
7-OMe	52.0 q	3.67 s	51.8 q	3.64 s	51.8 q	3.70 s
1-OH				4.03 s		
2-OH		2.83 s				
30-OH						3.51 s
17-OAc (Me)	20.7 q	1.96 s	21.2 q	2.10 s	21.1 q	2.04 s
(CO)		168.9 s	168.4 s		168.7	
Orthoacetate						
	118.6 s		122.7 s			
Me	21.1 q	18.6 q	1.55 s			
OMe		51.1 q	3.15 s			
Tigloyl						
1'	167.4 s				167.8 s	
2'	128.1 s				128.8 s	
3'	138.8 d	7.09 qq (7.0,1.3)			138.6 d	7.15 qq (7.0,1.3)
4'	14.6 q	1.78 br d (7.1)			14.5 q	1.82 br d (7.0)
2'-Me	12.4 q	1.99 br s			11.9 q	1.97 br s
1''-hydroxy-2''-methylpropylidene						
1''	183.0 s					
2''	30.0 d	2.96 br hept (6.0)				
2''a-Me	18.5 q	1.29 (6.6)				
2''b-Me	30.4 q	1.13 (6.6)				
1''-OH		14.0 d (1.1)				
isopropoxyloxo						
1'''			209.3 s		210.4 s	
2'''			43.0 d	2.99 hept (6.6)	43.0 d	2.99 hept (7.0)
2'''a-Me			17.3 q	1.24 d (5.4)	17.2 q	1.22 d (6.8)
2'''b-Me			17.4 q	1.28 d (7.9)	17.2 q	1.27 d (7.0)

In the HMBC spectrum of **22**, the observed long-range correlations of H-5 signal with the carbon signals at  $\delta_{\text{C}}$  15.3, 41.3, 49.4, 153.2 and 86.1 led to their assignments as C-19, C-29, C-10, C-9 and C-3 respectively. A downfield shifted singlet methine proton at  $\delta_{\text{H}}$  5.55 assigned to H-30 showed significant HMBC correlations with the carbon signal of C-9 and also with three quaternary carbon signals at  $\delta_{\text{C}}$  75.4, 120.1, and 80.7 to be

assigned to C-2, C-8, and C-1 respectively. The presence of three acetoxy groups at C-3, C-6 and C-30 was confirmed from the correlations of their attached protons 3-H, 6-H, 30-H signals observed at  $\delta_{\text{H}}$  5.00, 5.56, and 5.55 with tigloyl, acetoxy and 2-methylpropanoyl ester carbonyl signals at 167.0, 169.0 and 178.6. The 29-methylene protons showed HMBC correlations with C-1-C-5, C-9 and C-10. These observations characterized the left-hand tricyclo[3.3.1.1]decane ring system.

The proton signal of H-17 attached to the carbon at  $\delta_{\text{C}}$  80.6 showed correlations with an olefinic carbon at  $\delta_{\text{C}}$  157.0 (C-14), two quaternary carbons at 36.8 (C-13) and 119.8 (C-20, furan ring carbon), a methyl carbon at 15.6 (Me-18) and a methylene carbon at 30.5 (C-12). The methylene protons assigned to H<sub>2</sub>-11 attached to the carbon at  $\delta_{\text{C}}$  24.1 showed correlations with two olefinic carbons at  $\delta_{\text{C}}$  120.1 (C-8) and C-9, also with C-10, C-12 and C-13 carbon signals. Finally, the presence of dihydroxymethine group was elucidated by the correlation of the methine proton at  $\delta_{\text{H}}$  5.59 attached to an acetal carbon at  $\delta_{\text{C}}$  109.8 with the C-15 located the cited group also at this position. This proton correlated also with a lactone carbonyl carbon at  $\delta_{\text{C}}$  164.9 (C-16), and the olefinic carbons at C-14. These correlations fully characterized the second fragment of the molecule, C-8, C-9 and C-11-C-17 of the C and D rings, including Me-18 and furan ring.

The structure of **22**, including its stereochemistry was fully explained from the NMR data and by consideration of NOE correlations. The strong cross-peaks of H-5 signal and H-11 $\beta$ , H-17 and H-12 $\beta$ , and H-17 and H-30 indicated the  $\beta$  orientation for these protons and the folded conformation of **22**. The 29-methylene protons signals at  $\delta_{\text{H}}$  2.29 (pro-*S*) and 2.02 (pro-*R*) showed NOE correlations with H-3 and Me-19 protons signals respectively. Finally the configuration of at C-6 was assumed to be *R* as it was determined for angolensin B and C combined with the fact that they are isolated from the same source.

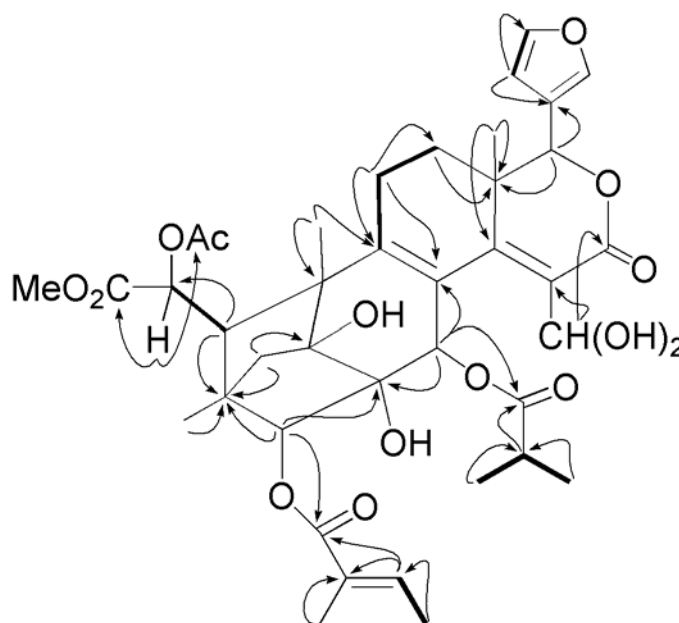


**Figure 30.** COSY and selected HMBC correlations in **22**

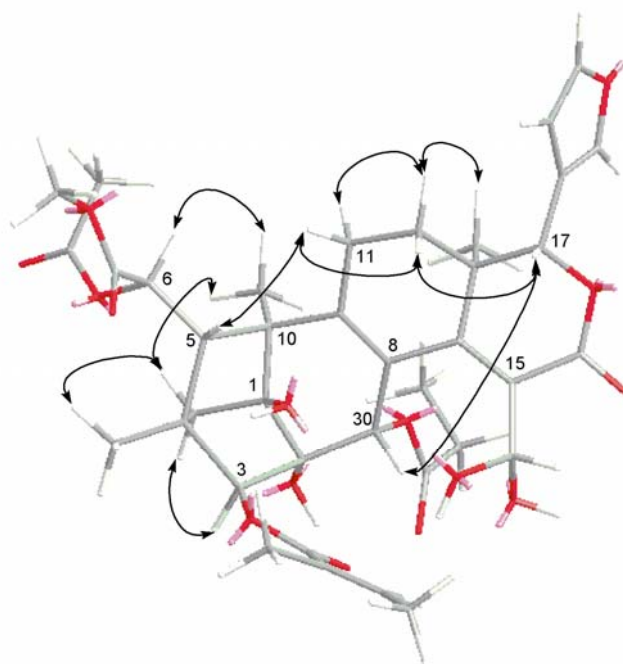


**Figure 31.** Computer-generated energy minimized model of **22** with key NOE correlations observed

Compound **23** was isolated as an amorphous solid. In the HRESIMS spectrum, a pseudomolecular  $[M+Na]^+$  was seen at  $m/z$  799.2578 corresponding to a molecular formula of  $C_{41}H_{44}O_{15}Na$ . Compound **23** showed similar UV and IR absorption bands with those **22** at 214 and 340 nm, and at  $3350-3000\text{ cm}^{-1}$  (hydroxyl) and  $1750-1705\text{ cm}^{-1}$  (several carbonyls). The  $^1\text{H}$  and  $^{13}\text{C}$  NMR spectra suggested that **23** had a similar structure to **22**. However, the presence of additional signals corresponding to two ethanoate groups and the absence of 2-methyl propanate were observed. Carefully examination of the chemical shifts of some signals indicated that **23** is a phragmalin limonoid having the same basic skeleton system than **22** and also the molecule is hexacyclic. Thus, the number of oxygenated carbons, being the same, significant information regarding the molecule was obtained from the HMBC spectrum. Thus, one ethanoyl groups were place at C-30 by the correlation of H-30 observed at  $\delta_{\text{H}}$  5.58 with this acyl group carbonyl at  $\delta_{\text{C}}$  178.1. As, in **22**, tigloyl and acetoxy were placed at C-3 and C-6 by the HMBC correlations their carbonyl carbon signal at  $\delta_{\text{H}}$  167.0 and 169.7 with the protons assigned to H-3 at  $\delta_{\text{H}}$  5.00 and H-6 at  $\delta_{\text{H}}$  5.56. The remaining ethanoyl was placed evidently at C-2. The stereochemistry of **23** was also explained by NOE correlations and NMR data and was exactly as the one observed in **22**.

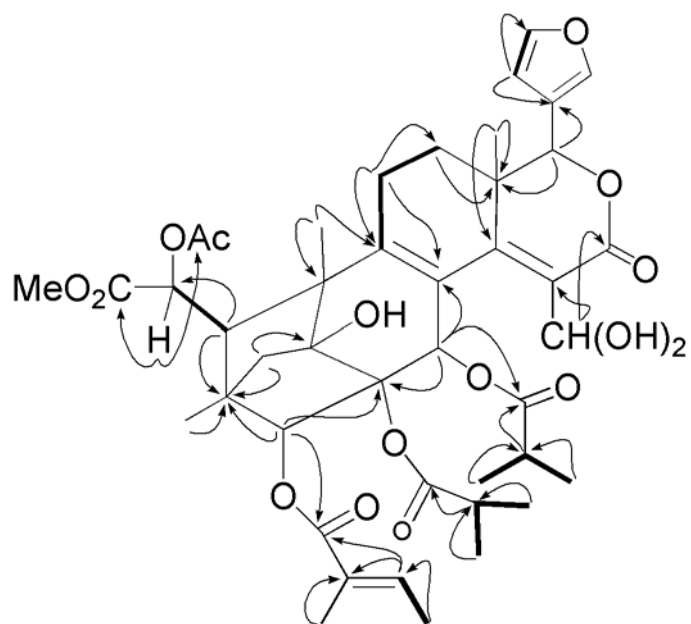


**Figure 32.** COSY and selected HMBC correlations in **23**

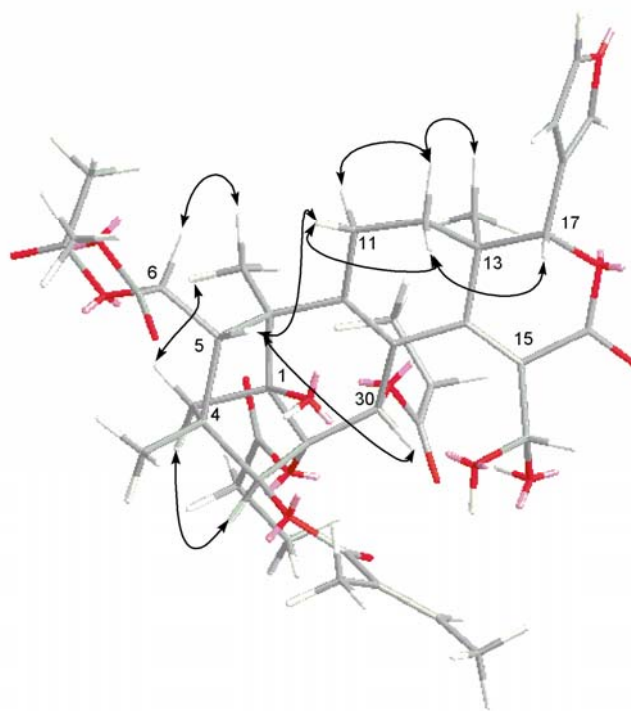


**Figure 33.** Computer-generated energy minimized model of **23** with key NOE correlations observed

**Table 8.**  $^1\text{H}$  and  $^{13}\text{C}$  NMR spectroscopic data of compounds **22** and **23**

Position	Compound <b>22</b>		Compound <b>23</b>	
	$\delta_{\text{C}}$ mult.	$\delta_{\text{H}}$ ( $J$ in Hz)	$\delta_{\text{C}}$ mult.	$\delta_{\text{H}}$ ( $J$ in Hz)
1	80.7 s		80.7 s	
2	75.4 s		75.4 s	
3	86.1 s	5.00 s	86.2 d	5.00 s
4	44.2 s		44.2 s	
5	48.3 d	2.78 br s	48.3 d	2.77 br s
6	71.9 d	5.56 d (2.0)	71.9 d	5.56 br s
7	169.9 s		169.9 s	
8	120.1 s		120.1 s	
9	153.2 s		153.1 s	
10	49.4 s		49.5 s	
11 $\alpha$	24.1 t	2.45 ddd (18.7,12.6,6.1)	24.1 t	2.43 ddd (17.7,12.5,5.3)
$\beta$		2.30 m		2.30 <i>o</i>
12 $\alpha$	30.5 t	1.68 m	30.5 t	1.68 m
$\beta$		1.35 ddd (17.7,12.6,5.2)		1.34 ddd (17.6,12.5,5.2)
13	36.8 s		36.8 s	
14	157.0 s		156.9 s	
15	120.1 s		120.1 s	
16	164.9 s		164.9 s	
17	80.6 d	4.92 s	80.6 d	4.92 s
18	15.6 q	1.03 s	15.6 q	1.03 s
19	15.3 q	1.25 s	15.3 q	1.25 s
20	119.8 s		119.9 s	
21	141.1 d	7.53 br s	141.1 d	7.49 br s
22	109.9 d	6.44 d (2.0)	109.9 d	6.44 br s
23	143.2 d	7.46 t (1.6)	143.2 d	7.45 (2.0)
28	16.5 q	1.03 s	16.5 q	1.03 s
29( <i>pro-R</i> )	41.3 t	2.02 d (10.4)	41.3 t	2.02 br d (10.2)
( <i>pro-S</i> )		2.29 d (10.4)		2.30 br d (10.2)
30	64.3 d	5.55 s	64.3 d	5.55 s



**Table 8** (continued).  $^1\text{H}$  and  $^{13}\text{C}$  NMR spectroscopic data of compounds **22** and **23**

Position	Compound <b>22</b>		Compound <b>23</b>	
	$\delta_{\text{C}}$ mult.	$\delta_{\text{H}}$ ( <i>J</i> in Hz)	$\delta_{\text{C}}$ mult.	$\delta_{\text{H}}$ ( <i>J</i> in Hz)
7-OMe	52.8 q	3.53 s	52.8 q	3.69 s
15-CH(OH) <sub>2</sub>	109.8 d	5.59 s	109.8 d	5.67 s
OAc (Me)	21.0 q	2.23 s	21.0 q	2.23 s
(CO)	169.7 s		169.7 s	
Tigloyl				
1'	167.0 s		167.0 s	
2'	127.4 s		127.4 s	
3'	139.2 d	6.86 qq (7.1,1.3)	139.2 d	6.86 qq (7.0,1.2)
4'	14.7 q	1.81 br d (7.1)	14.6 q	1.81 d (7.0)
4'-Me	12.0 q	1.95 br s	11.7 q	1.78 br s
2-propanoyl				
1"			178.3 s	
2"a			41.3 t	2.38 q (6.2)
2"b				2.38 q (6.2)
3"-Me			17.0 q	1.12 t (6.2)
(30-Propanoyl, 2-methylpropanoyl)				
1"	178.6 s		178.1 s	
2"	34.1 d	2.56 hept (6.9)	26.5 t	1.43 m
3" (Me)	18.7 q	1.15 d (7.0)		1.67 m
2"-Me	19.1 q	1.13 d (7.0)	11.6 q	0.84 dt (7.4,3.3)

## Chapter V. Summary

Limonoids are tetranortriterpenoids derived from tirucallane (H-20 $\alpha$ ) or euphane (H-20 $\beta$ ) triterpenoids with 4,4,8-trimethyl-17-furanylsteroidal skeleton. They are mainly found in Meliaceae and Rutaceae plants. Limonoids have attracted considerable interest because of their fascinating structural diversity and their wide range of biological activities, including insect anti-feedant and growth regulating properties, anti-bacterial, anti-fungal and anti-viral activities, anti-protozoal, and anti-sickling properties.

In a search of antifeedant limonoids, the extract of *Entandrophragma angolense*, a Meliaceae plant used in Africa folk medicine against malaria, displayed considerable activity against *Spodoptera* insects. The limonoids components of its extracts have been investigated. Past phytochemical studies of this plant reported the isolation of triterpenoids, sterol, protolimonoid and limonoids. The limonoids found so far from this plant are D-*seco* compound gedunin, ring B,D-*seco* compound of andirobin type, methyl angolensate and recently A,D-*seco* limonoids of nomilin type, 7 $\alpha$ -acetoxydihydronomilin, and obacunol type 7 $\alpha$ -obacunylacetate have been reported.

The fractionation of the hexane, ether and methanol extracts of *E. angolense* by chromatographic techniques led to the isolation of 23 limonoid and two non-limonoid compounds. The structures of these compounds were elucidated on the basis of spectroscopic means, and could be classified as protolimonoids (**3**, **4** and **12**), gedunin (**8** and **14**), andirobin (**1**, **5** and **13**), mexicanolide (**2**, **16**, **18-20**) and phragmalin (**6-7**, **9**, **11**, **15**, **17**, **22-23**) derivatives. A search, in the literature permitted to established that compounds **1**, **5**, **13**, **19** and **20** are known and have been identified as methyl angolensate, secomahoganin, methyl 6-acetoxyangolensate, 3 $\beta$ -hydroxy-3-deoxycarapin, and xylocensin K respectively. Phragmalin limonoids have very complex structure feature with an orthoester bridge and have been classified according to the position of the orthoacetate groups at 1,8,9-; 8,9,14-; and 8,9,30-. Compound **15** is the first limonoid to be reported with the orthoester group located at 8,9,12-. Compounds **6** and **11** have the D-ring cleaved and new ring has been formed as lactone attached to the C-ring of the basic skeleton. These features are very rare in limonoid compounds in general, and only two limonoids with these features have been reported recently from *Switenia mahogani*.

Among the isolated compounds, methyl angolensate has been reported for its spasmolytic and moderate antimalarial activities while gedunin is known for its anti-malarial activity and has been expected as a possible lead compound for new drug. Thus, compounds **8** and **14** can be used as analogues for a better understanding of structure-activity relationship. The protolimonoids also are expected to play the same role as a compound having the same basic skeleton, domesticule D, has been reported for its antimalarial activity. Mexicanolide and phragmalin compounds have been reported for their antifeedant activity which, in general, is much weaker than that of well-known C-*seco* antifeedants azadirachtins and meliacarpinins.

## **Introduction**

In the discovery of drugs, several approaches have been used. In the past, most drugs have been discovered by identifying the active compound from traditional remedies. A new approach has been to understand how disease and infection are controlled at the molecular and physiological level and to target specific entities based on this knowledge. Using, this approach, several drugs have reached the market such as olanzapine, alosetron, leflunomide...

The process of drug discovery involves the identification of candidates, synthesis, characterization, screening and assays for the therapeutic efficacy. The synthesis research part of a drug candidate is a very challenging step since the complete process should comprise short, efficient, ecological, economical and technically feasible chemical synthesis and ready for technical development towards large scale industrial production.

Influenza, commonly known as flu, is an infectious disease of birds and mammals caused by RNA viruses of the family Orthomyxoviridae. There are three types of influenza virus: Influenza virus A, Influenza virus B, and Influenza virus C. Influenza A and C infect multiple species, while influenza B almost exclusively infects humans. The type A viruses are the most virulent human pathogens among the three influenza types and cause the most severe disease.

Influenza infection has been the cause of some of the worst epidemics in human history and continues to be a major health concern. Yearly, human influenza virus infections are associated with significant morbidity and mortality worldwide. This fact makes the research of effective and safe anti-influenza therapeutics a high-priority and attractive area for drug discovery.

Of course, vaccination constitutes the primary option for the control of influenza epidemics. However, vaccines are least effective in high-risks groups, young children and elderly, and constant antigenic drift related error-prone RNA replication demands ongoing development of updated vaccines for each season<sup>124</sup>. Anti-viral drugs might be a much better way to control flu epidemics.

In recent years, virology studies of influenza virus have resulted in an improved understanding of the replication mechanism of the virus. Several molecular targets have been identified for drug intervention, including haemagglutinin (H), neuraminidase (NA), M2 protein and endonuclease<sup>125</sup>.

Inhibitors of the M2 proton pump have been known for decades, but the widespread use of amantadine and rimantadine, the two marketed, clinically effective inhibitors, has been thwarted by the emergence of drug resistance and by toxic side effects. In addition, applicability to influenza A only is a serious limitation<sup>126</sup>.

In contrast, NA is one of the two major surface proteins expressed by both all three classes of viruses. NA catalyzes the cleavage of sialic acid residues from glycoproteins, glycolipids and oligosaccharides. This catalytic activity is essential for influenza virus replication and infectivity since it liberates viruses from infected cells and prevents virus entrapment by respiratory secretions and virus self-aggregation<sup>125</sup>.

NA is a tetramer made up of identical subunits, and its X-ray crystal structure has been solved, as has the structure of its complex with sialic acid. The active site is highly conserved across all influenza A and B virus strains, thus suggesting NA as a target for the development of broad-spectrum influenza antibiotics. Structural data have allowed the rational design of potent inhibitors. Two of these have reached the market, namely zanamivir (GSK's Relenza) in July 1999, and oseltamivir phosphate (Gilead Tamiflu, marketed by Roche) in October 1999<sup>127</sup>.

Zanamivir has low bioavailability and is administered by inhalation, which can cause problems in patients with underlying respiratory disease. Oseltamivir phosphate is administered as capsules and has very high bioavailability. Its ester function is cleaved *in vivo*, and oseltamivir phosphate must therefore be considered as prodrug. Both inhibitors are active *in vitro* against all known influenza strains, including the H5N1 avian strain. Because the amino acid residues at the enzyme active site are highly conserved, there is hope that these inhibitors may be active against an influenza pandemic regardless of the particular viral strain<sup>127</sup>.

Notably, oseltamivir phosphate has been shown to be effective in the prevention of influenza infection. Its drawback, shared with zanamivir, is that it must be administered to influenza patients no later than 36-48 h after the manifestation of the symptoms in order to be effective. This has led to public demand for stockpiles of Tamiflu, both as a reasonable frontline therapy against a possible flu pandemic and as a preventive agent<sup>128</sup>.

However, the scarcity of the synthetic precursors (shikimic acid and quinic acid) which are extracted from plants and the use of hazardous azide-based reagents are factors limiting the large-scale production of the oseltamivir. Thus, more efficient process using easily available starting materials and safer reactions is still required attention for the stockpile of drug in preparation for a possible flu pandemic. To address these problems, further synthetic investigations have been carried out either by chemists in the industry or chemists in the academia.

Our research group found a unique base-catalyzed Diels-Alder (DA) reaction of 3-hydroxy-2-pyridone derivatives that gave sterically controlled and highly functionalized bicyclic lactams as products. These compounds seemed to be good building blocks for aminocyclitols having C7N structures as basic skeleton, and indeed, (±)-validamine and its epimers were synthesized from the DA adduct in short steps<sup>129</sup>. Since Tamiflu is also structurally related to aminocyclitols, we planned its short and efficient synthesis.

Considering the known synthetic pathways, Corey's synthesis is an elegant approach being concise and the one affording the highest overall yield. This approach eliminated the use of shikimic and quinic acids as raw

materials and no hard-to-deal azide reagent were needed. If the steps could be reduced again, the process would become much more attractive as a practical production method.

In the Corey's synthesis, the 5-boc-amino-cyclohexa-1,3-dienecarboxylic acid ethyl ester is one of the key intermediate which has a simple C<sub>7</sub>N structure, and from this intermediate 5 steps are needed to complete the Tamiflu synthesis. Thus we chose it as a primary target of our synthesis using the DA adduct as a starting material. Here, we report a short and efficient synthesis of 5-nosyl-amino-cyclohexa-1,3-dienecarboxylic acid ethyl ester and its equivalent 5-boc-amino-cyclohexa-1,3-dienecarboxylic acid ethyl ester.

## Chapter I. Tamiflu design and total synthesis

### I.1. Introduction

Influenza infection has been the cause of the worst epidemics in human history and continues to be a major health concern. Effective and safe anti-influenza therapeutics are lacking, making anti-influenza therapy a high priority and attractive area of drug discovery. In recent years, virology studies of influenza virus have resulted in an improved understanding of the replication mechanism of the virus. Several molecular targets have been identified for drug intervention including haemagglutinin, neuraminidase (sialidase), M2 protein and endonuclease. Amantadine and rimantadine are two relatively old anti-influenza drugs that act through the blockade of M2 channel. However, both compounds are only active against influenza A and lack activity against influenza B, which does not express the M2 protein. In addition both compounds suffer from significant central nervous system side effects and relatively rapid onset of drug resistance. Thus, discovery of anti-influenza drugs with different mechanism of action, active against both influenza A and B and diminished onset of drug resistance remains a significant challenge as well as an attractive opportunity of drug discovery and development<sup>125</sup>.

Neuraminidase is one of the two major surface proteins expressed by both type A and type B influenza virus, along with haemagglutinin. The influenza neuraminidase (NA) molecule is a tetramer of four identical subunits, each of which is independently inactive. Structurally, each subunit has a large catalytic domain and a long stem that is anchored onto the lipid bilayer envelope of the virus particle. Neuraminidase catalyses the cleavage of sialic acid (*N*-acetyl-neuraminidase acid) residues from glycoproteins, glycolipids and oligosaccharides via the oxocarbenium intermediate. This catalytic activity is essential for influenza virus replication and infectivity since it liberates viruses from infected cells and prevents virus entrapment by respiratory secretions and self-aggregation. The cleavage of sialic acid by neuraminidase is required for elution of newly synthesized virions from infected cells, whereas binding of haemagglutinin to sialic acid-containing receptors on the surface of host cells. In addition, neuraminidase also facilitates the movement of the virus through the mucus of the respiratory tract<sup>125</sup>.

The X-ray crystal structure of influenza neuraminidase was first solved in early in the 1980s and the high-resolution X-ray structures of NA A and NA B, complexed with sialic acid were reported in 1992. Since then, structures of NA complexed with a variety of inhibitors have been reported. These structural studies provided a detailed understanding of the molecular interactions involved in the binding of various inhibitors to NA and formed the foundation for several successful rational drug design programs, which lead to a variety of highly potent NA inhibitors. Overall, the active site of NA contains a larger number of polar and charged amino acid residues, suggesting that electrostatic interactions play a critical role in substrate binding and should be an important consideration in inhibitor designing. Furthermore, the active site of NA was found to be highly conserved across all influenza A and B virus strains, rendering broad spectrum anti-influenza agents possible<sup>126</sup>.

Several representative NA inhibitors were developed based on the structure of NA active site, all these compounds contain a carboxylate and an acetyl (or trifluoroacetyl) group that are separated by seven single bond, consistent with the model postulated. Two of these inhibitors reached the market namely zanamivir and oseltamivir.

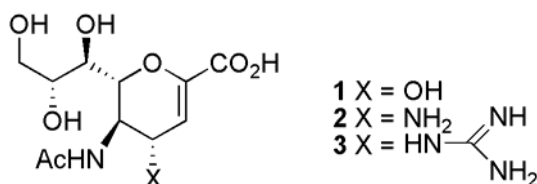
Oseltamivir is now the most used drug against influenza and it can be used also in the prevention of the disease. There is a mounting fear that a major flu pandemic will eventually strike again. This led to public demand for stockpiles of oseltamivir both as reasonable frontline therapy against a possible flu pandemic and as a preventive agent.

In this chapter, reported routes are described starting by the Gilead drug discovery synthesis.

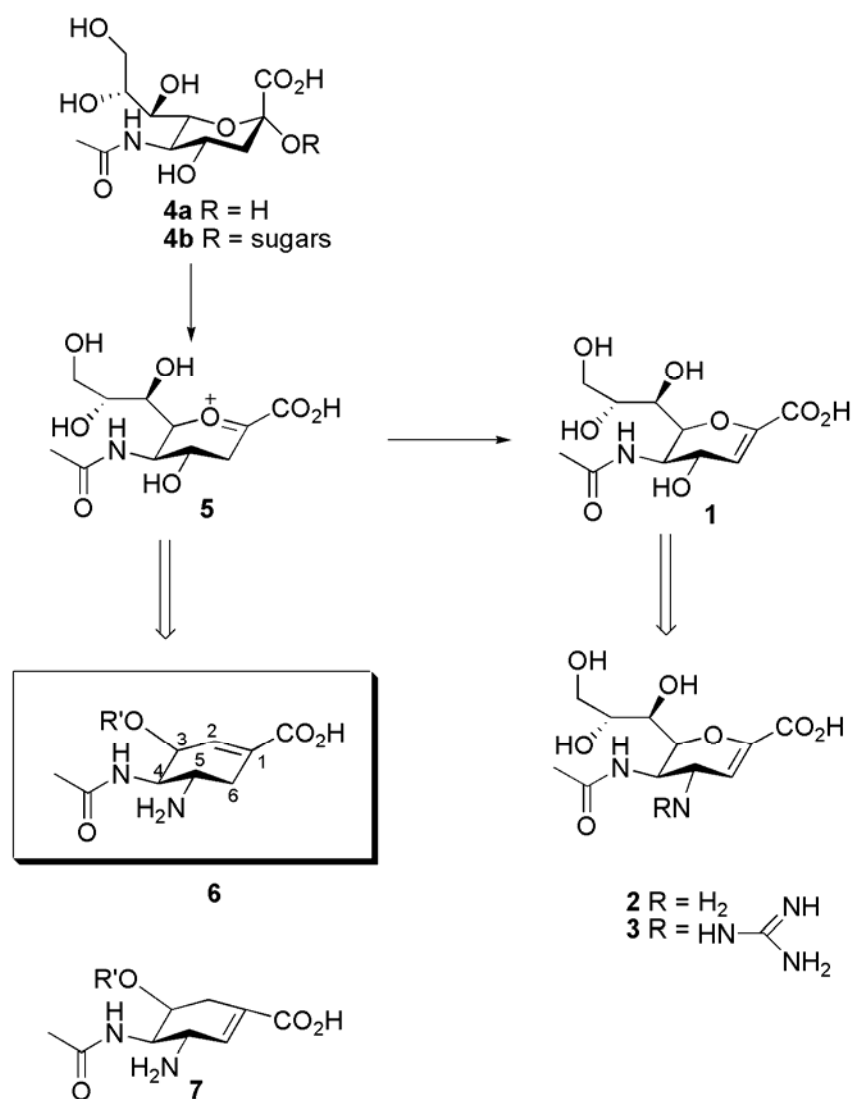
## I.1. Gilead drug design and synthesis.

### I.1.1. Drug design

Scientists at Gilead Science Inc. based their design on the earlier studies on 2,3-didehydro-2-deoxy-*N*-acetylneuraminic acid which was found to be an influenza NA inhibitor. Biochemical studies indicated that 2,3-didehydro-2-deoxy-*N*-acetylneuraminic acid (**1**) is considered as transition state-like analogue binding to the active site of NA. On the basis of structural information generated from the X-ray crystallographic study of 2,3-didehydro-2-deoxy-*N*-acetylneuraminic acid complexed NA, von Itztein and co-workers rationally designed NA inhibitors (**2** and **3**) more potent than **1**<sup>130</sup>.



Compound **3** exhibited potent antiviral activity against a variety of influenza A and B strains in the cell culture assay and was being evaluated in human clinical trials, however, poor oral bioavailability and rapid excretion precluded **3** as a potential oral agent against influenza infection and **3** has to be administered by either intranasal or inhaled routes in clinical trials.



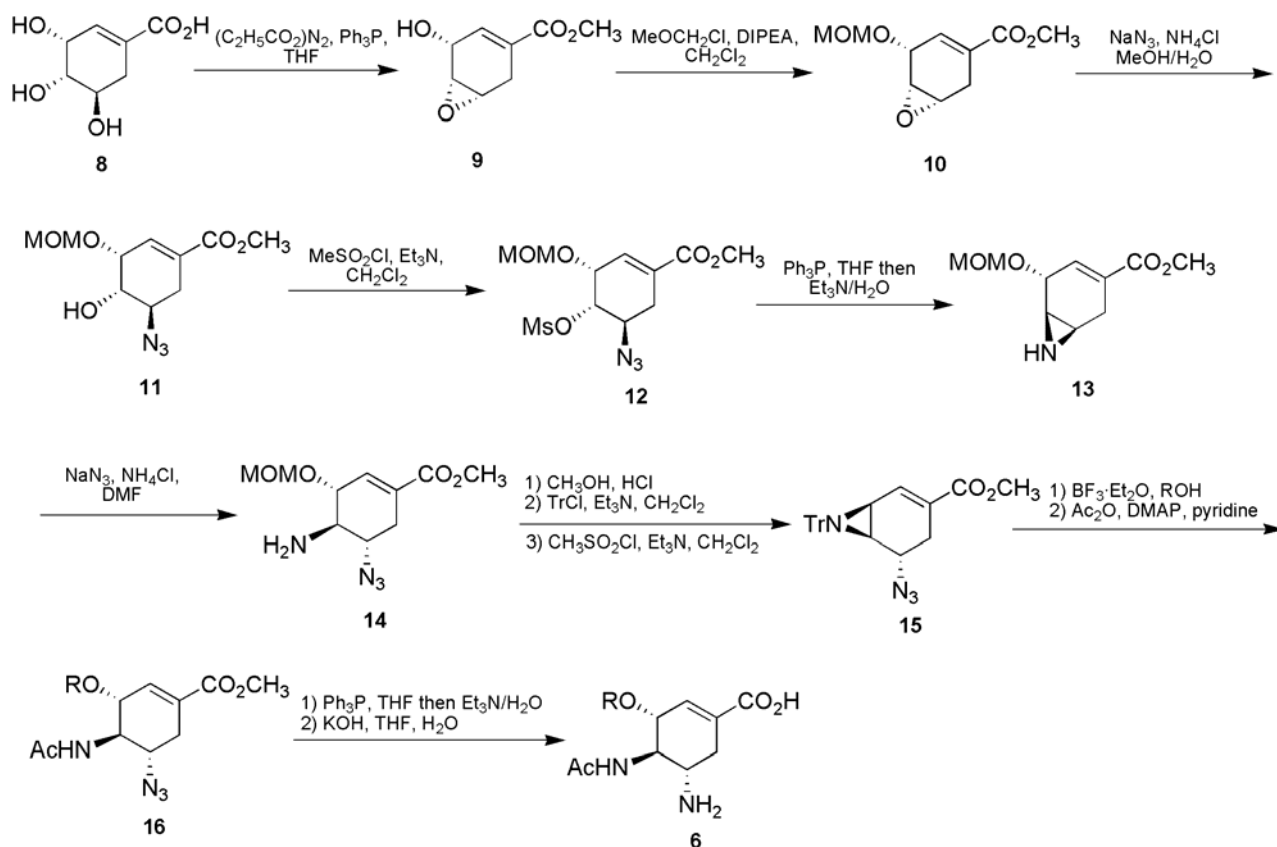
**Scheme 9.** Rational design of carbocyclic Transition-State Analogues

Kim and co-workers thought that in the case of an influenza epidemic, oral administration may be more convenient and economical method for the treatment and prophylaxis. Thus, they carried out investigation on the development of a new class of orally active NA inhibitors, having carbocyclic templates in the place of the dihydropyran ring. It was expected that the carbocyclic ring would be chemically more stable than the dihydropyran ring and easier to modify for optimization of antiviral and pharmacological properties. The validity of this approach was verified by the discovery of very potent NA inhibitors in this new carbocyclic series. New lipophilic side chains at C<sub>3</sub> position of the carbocyclic system imparted potent NA inhibitor activity. X-ray crystallographic analysis of the carbocyclic analogue bound to NA confirmed that there was in fact hydrophobic space in the glycerol-binding subsite to accommodate bulky lipophilic group. The discovery of this hydrophobic pocket in the active site of NA was exploited to increase the lipophilicity of inhibitors to optimize pharmacologic properties for potential oral bioavailability while maintaining potent antiviral activity<sup>131</sup>.



Kim and co-workers synthesized a series analogues of the carbocyclic compound **6** in a general and efficient way to introduce various alkyl ethers at C<sub>3</sub> position (Scheme 9). And their NA inhibitory activities were evaluated.

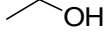
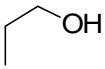
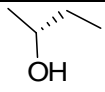
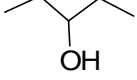
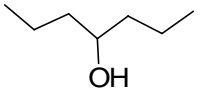
The synthesis of these carbocyclic analogues, as outlined in Scheme 10, started with shikimic acid (**8**). The conversion of shikimic acid to epoxide **9** has been done by treatment of diethyl azodicarboxylate in presence of triphenylphosphine in THF and then the hydroxyl group was protected by MOMCl in presence of DIPEA to afford **10**. Nucleophilic ring opening of epoxide **10** with sodium azide in presence of ammonium chloride generated the azido alcohol **11**. The ring opening of epoxide was both regio- and stereospecific and this could be attributed to the steric and electronegative inductive influence of the MOM group in **10**. Conversion of the azide **11** to aziridine was efficiently accomplished via two-step sequence mesylation of the hydroxyl group and reduction of the azide functionality in presence of triethylamine and water. The aziridine opening by nucleophilic attack of the azide ion, gave exclusively compound **14**. The aziridine **15** was derived from the trans amino alcohol by acid MOM deprotection in methanol and selective protection of the amino functionality with tritylchloride and mesylation of the hydroxyl in the presence of triethyl amine and under these conditions, the mesylate intermediate was converted to the desired aziridine. Treatment with various alcohol in the presence of Lewis acid BF<sub>3</sub>•Et<sub>2</sub>O followed by acetylation provide the ether **16** and no other products was observed. Finally reduction of the azide functionality and saponification of the ester group gave **6** and its analogues.



Scheme 10. Synthetic pathway of NA carbocyclic inhibitors

This study developed a new series of potent carbocyclic analogues NA inhibitors in which the clear structure-activity relationship was observed among analogues with various alkyl chains (Table 9). Finally, the ethyl ester of **6** exhibited good oral bioavailability in several animals (mice, rats and dogs) and demonstrated oral efficacy in the mouse and ferret influenza model. On the basis of potent *in vitro/in vivo* activity and very favorable pharmacological properties, compound **6** has been selected as a clinical candidate for the oral treatment and prophylaxis of influenza infection.

**Table 9.** Structure-activity relationship among analogue with various alkyl chains

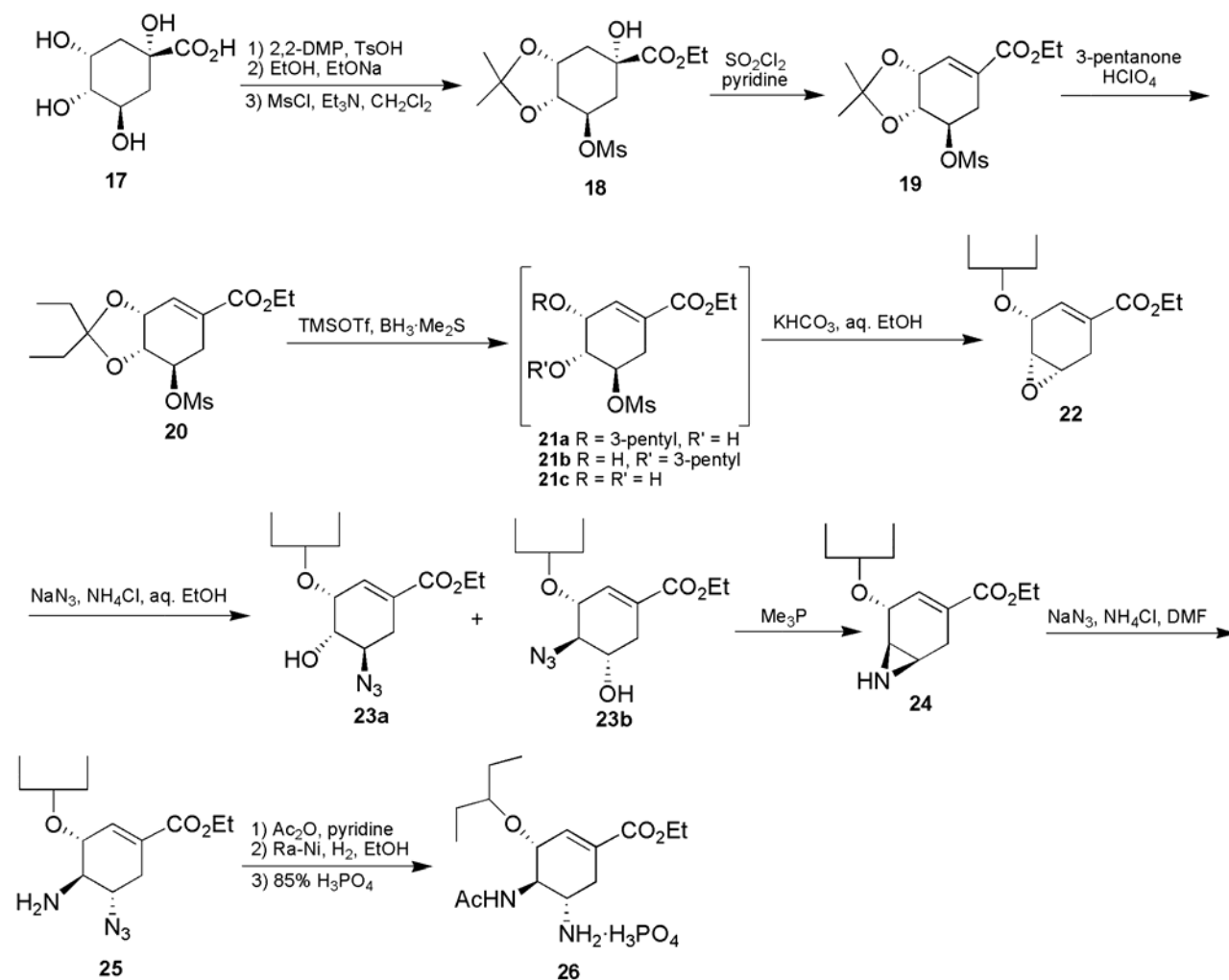
ROH	IC <sub>50</sub> (nM)
<b>6a</b> CH <sub>3</sub> OH	3700
<b>6b</b> 	2000
<b>6c</b> 	180
<b>6d</b> 	10
<b>6e</b> 	1
<b>6f</b> 	16

However, for the production of compound **6e** in large quantities for clinical and toxicological studies, this route shown in Scheme 10 was impractical. To supply a large amount of the product, a practical kilogram-scale preparation was needed. Scientists at Gilead Science Inc investigated a novel approach to the synthesis of compound **6e** and developed a new 12-step synthesis utilizing a novel and efficient reductive ketal opening to construct the 3-pentyl ether. This new process was highly amenable to kilogram-scale synthesis.

### **I.1.2. Large scale production of compounds 6a-6f**

In their first attempt, they utilized (-) shikimic acid as starting material to prepare the key intermediate ketal compound **20**. Due to the limited commercial availability of this ingredient, they utilized the ready available (-) quinic acid.

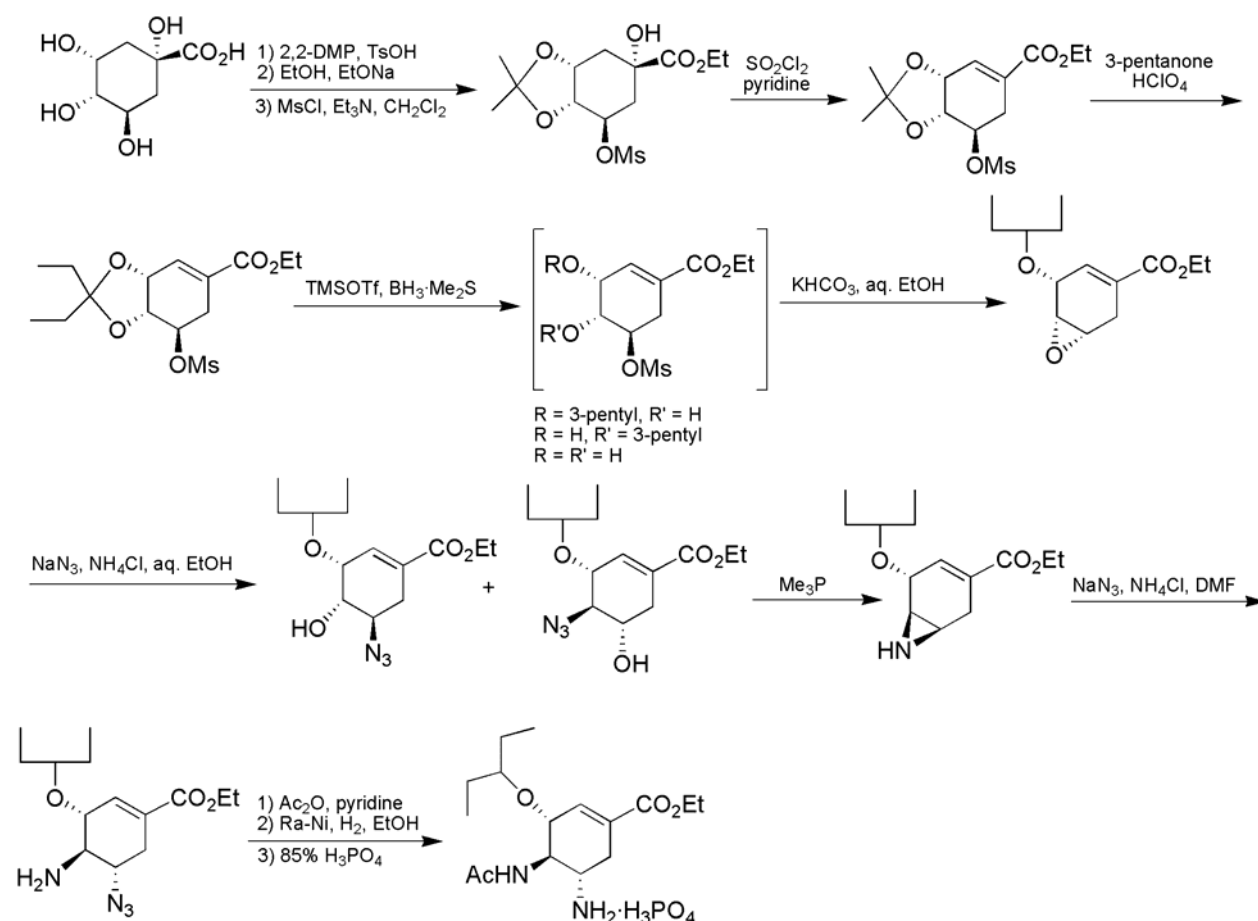
Quinic acid was treated with 2,2-DMP in TsOH to afford a quinic lactone acetonide (not shown in Scheme 11) that was converted to hydroxy ester in dry ethanol in presence of catalytic amount of sodium ethoxide. The crude mixture of the hydroxyl ester was treated with methanesulfonyl chloride in presence of triethylamine in methylene chloride to afford the monomesylate **18**. Filtration and evaporation of solvent gave an oil mesylate hydroxy ester which dehydration with sulfuryl chloride and pyridine in methylene chloride provided the shikimic ring system compound **19**. This compound was purified upon treatment with pyrrolidine and catalytic tetrakis(triphenylphosphine)-palladium (0) in ethyl acetate and the undesirable products were removed by aqueous sulfuric acid extraction. The quinic acid-derived acetonide **14** was transketalized using catalytic perchloric acid in pentanone. The oily 3,4-pentylidene ketal **20** was treated with trimethylsilyl trifluoromethanesulfonate and borane methyl sulfide complex in methylene chloride and the resulting mixture heated in aqueous ethanol in the presence of potassium bicarbonate to afford selectively epoxide **22**. The epoxide was heated with sodium azide and ammonium chloride to afford isomeric azido alcohols **23a** and **23b**. Intramolecular reductive cyclization of the crude mixture with trimethylphosphine in anhydrous acetonitrile cleanly afforded a single aziridine **24**. Aziridine opening proceeded smoothly with sodium azide and ammonium chloride in dimethylformamide affording azidoamine (ethyl ester) which was acetylated with acetic anhydride. The azide group of resulting azidoacetamide was reduced using catalytic hydrogenation with Raney nickel in ethanol. After filtration, the addition 85% phosphoric acid gave a feathery needle crystals, oseltamivir phosphate (**26**)<sup>132</sup>.



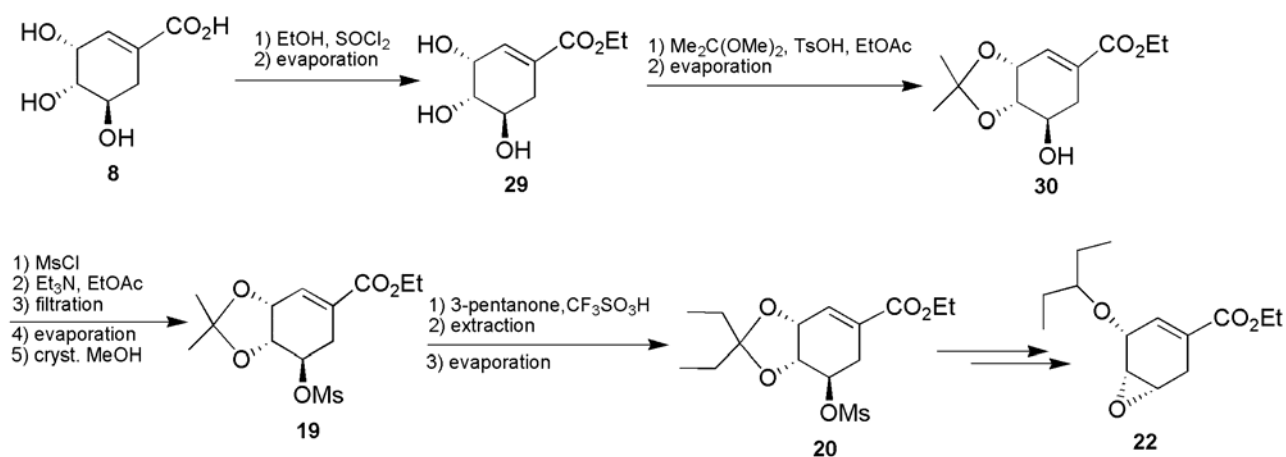
Scheme 11. Large-scale production of oseltamivir phosphate for clinical studies

### I.1.3. Current industrial synthesis of oseltamivir phosphate

For the industrial production of oseltamivir phosphate, scientists at Hoffman-Laroche, developed an industrial route for the production of epoxide **22** which is the key intermediate in oseltamivir production. Starting from (-)-quinic acid, **22** was synthesized in seven chemical steps and an overall yield of 35-38%. The route of the improved Gilead synthesis was not changed. However, significant improvements in each step led to a doubled overall yield, a 30% reduction in the number of unit operations, and an excellent quality ( $\geq 99\%$ ) of the resulting epoxide. A highly regioselective method for the dehydration of a quinic acid to a shikimic acid derivative and for the reduction of a cyclic ketal was found. Alternatively, **22** was synthesized in six chemical steps and 63-65% yield from commercially available (-)-shikimic acid. Compared to the optimized quinic acid route, the production time was reduced by about 50%. The quality of epoxide produced from either natural product was equivalent. Therefore (-)-shikimic acid is the preferred raw material. The absolute configuration of the epoxide was determined by X-ray single crystal structure analysis and it was demonstrated that the epoxide **22** was stereoisomerically pure<sup>133</sup>.



Scheme 12. Quinic acid route to industrial production of epoxide **22**.



Scheme 13. Shikimic acid route to industrial production of epoxide **22**

Thus, the industrial production of oseltamivir phosphate was established. The process is using two starting material which are convenient because of easy conversion to the key epoxy intermediate **22**. However, the preferred raw material, shikimic acid, is highly expensive and its availability is low. Furthermore, transformation on the epoxy calls use of the azide chemistry. Azide is a hazardous reagent and can explode if

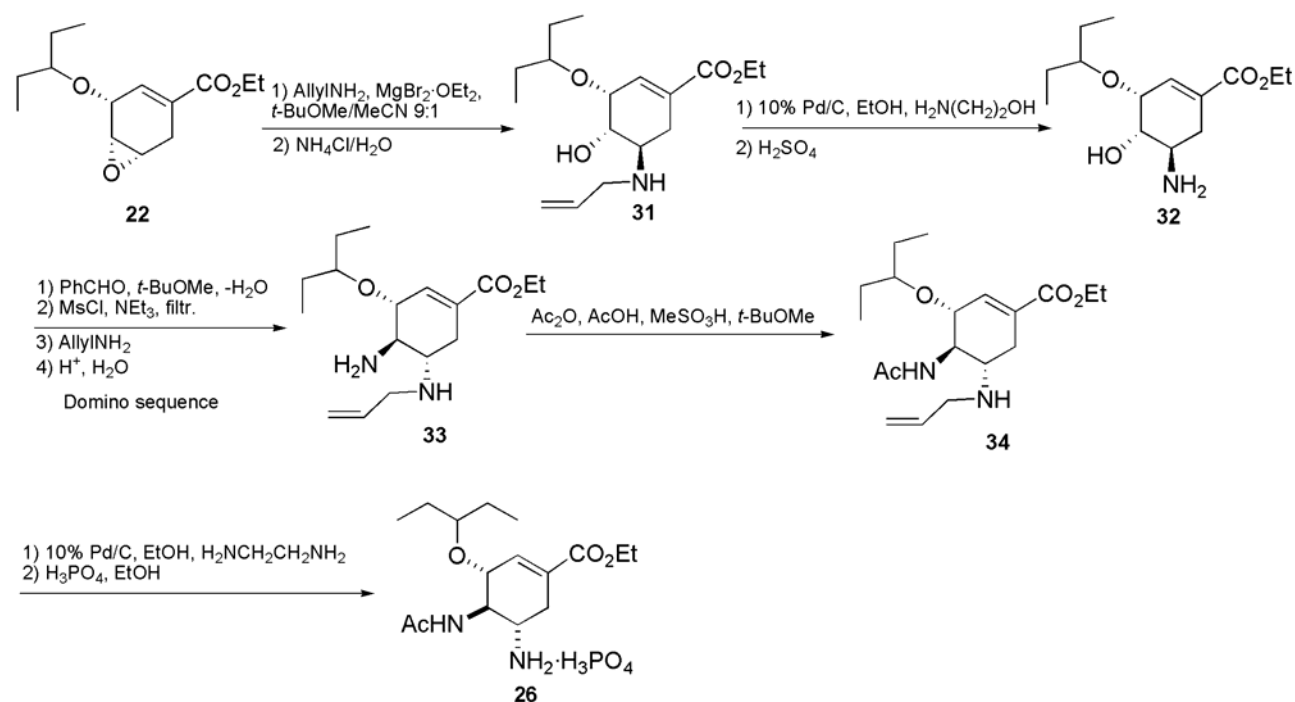
it is not handled with a lot of care. Intensive investigations have been made by scientists for the establishment of new routes which use cheap starting materials and much safer and economical chemical reactions.

Thus, scientists at Roche evaluated an azide-free transformation of the key precursor epoxide in order to establish an independent and efficient alternative route for large-scale production of oseltamivir phosphate.

#### I.4.1 Azide-free transformations

##### 1. Allylamine route

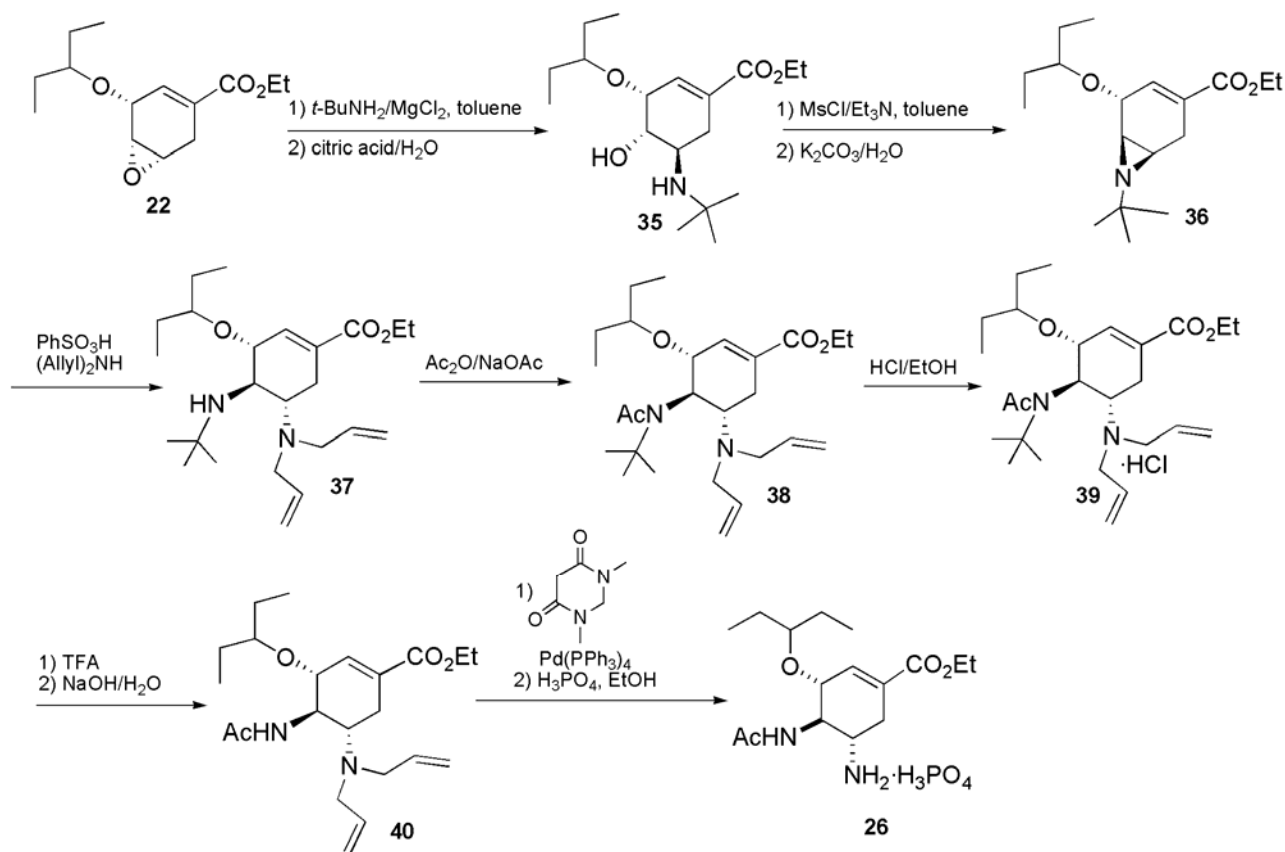
Treatment of the epoxide **22** with allylamine in presence of  $\text{MgBr}_2 \cdot \text{OEt}_2$  as catalyst afford compound **31**. The deallylation of **31**, was achieved with Pd/C in EtOH in the presence of ethanolamine. The conversion of **32** to **34** with concomitant introduction of the second amino function was performed without isolation of the intermediates. Selective acetylation of the 4-amino group of **34** was achieved with acetic anhydride in presence of  $\text{MeSO}_3\text{H}$  and an excess of acetic acid in ethyl acetate. Deallylation of **34** over 10% Pd/C in refluxing EtOH and ethanolamine followed by filtration of the catalyst, acidic hydrolysis and extraction provided the free base of the drug substance which was converted into the phosphate salt **26**<sup>134</sup>.



Scheme 14. Azide-free allylamine route to oseltamivir phosphate

2. *t*-Butylamine-Diallylamine route, second-generation process

In this route, the epoxyde ring opening is induced by the catalytic action of a magnesium chloride-amine complex with *t*-butylamine to afford compound **35** followed by *O*-sulfonylation without requiring N-protection. The subsequent aziridine ring closure to compound **36** was followed by the selective benzenesulfonic acid-induced opening of the aziridine ring using diallylamine led to compound **37**. N-acetylation using acetic anhydride and sodium acetate followed by chlorhydric acid treatment in ethanol provided **39**, the hypochloride of **38**. The cleavage of the *t*-butyl group was then accomplished using neat trifluoroacetic acid. The removal of both allyl groups in **40** was accomplished by Pd(0)-catalyzed allyl transfer to *N,N*-dimethylbarbituric acid leading after work-up and treatment with phosphoric acid to oseltamivir phosphate of high purity<sup>135</sup>.



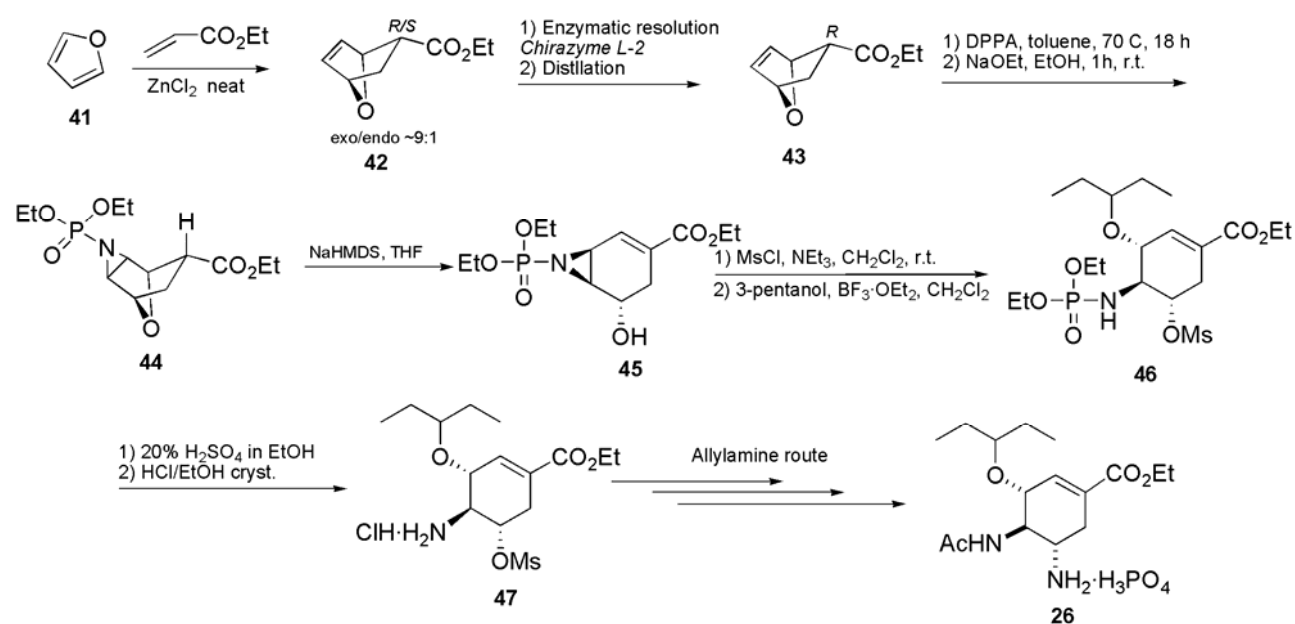
**Scheme 15.** Azide-free *t*-butylamine-diallylamine route to oseltamivir phosphate

## I.1.5. Shikimic and quinic acids-independent routes

The elimination of shikimic or quinic acids as starting materials has proved to be more challenging, and several attempts have been described.

## 1. Diels-Alder concept

This concept was based on the exo-directed Zn-catalyzed Diels-Alder reaction of furan and acrylates. The reaction provided a racemate exo/endo in 9:1 ratio. An enzymatic process was used for optical resolution of rac-**42** and the enzyme named Chirazyme L-2 was found to be the best for this purpose. Phosphoryl azide allowed the functionalization the double bond to form the exo-triazoles which was thermally decomposed to afford the *endo*-aziridine **44**. This *endo*-aziridine underwent elimination ring opening to form **45** followed by direct *O*-mesylation and regio- and stereoselective introduction of 3-pentyl-ether side chain which efficiently afforded compound **46**. Acidic condition allowed the cleavage of P,N-bond and crystallisation occurred in presence of chlorhydric acid in ethanol to afford **47**. Using allylamine protocole described above, **47** was transformed to oseltamivir phosphate<sup>136</sup>.



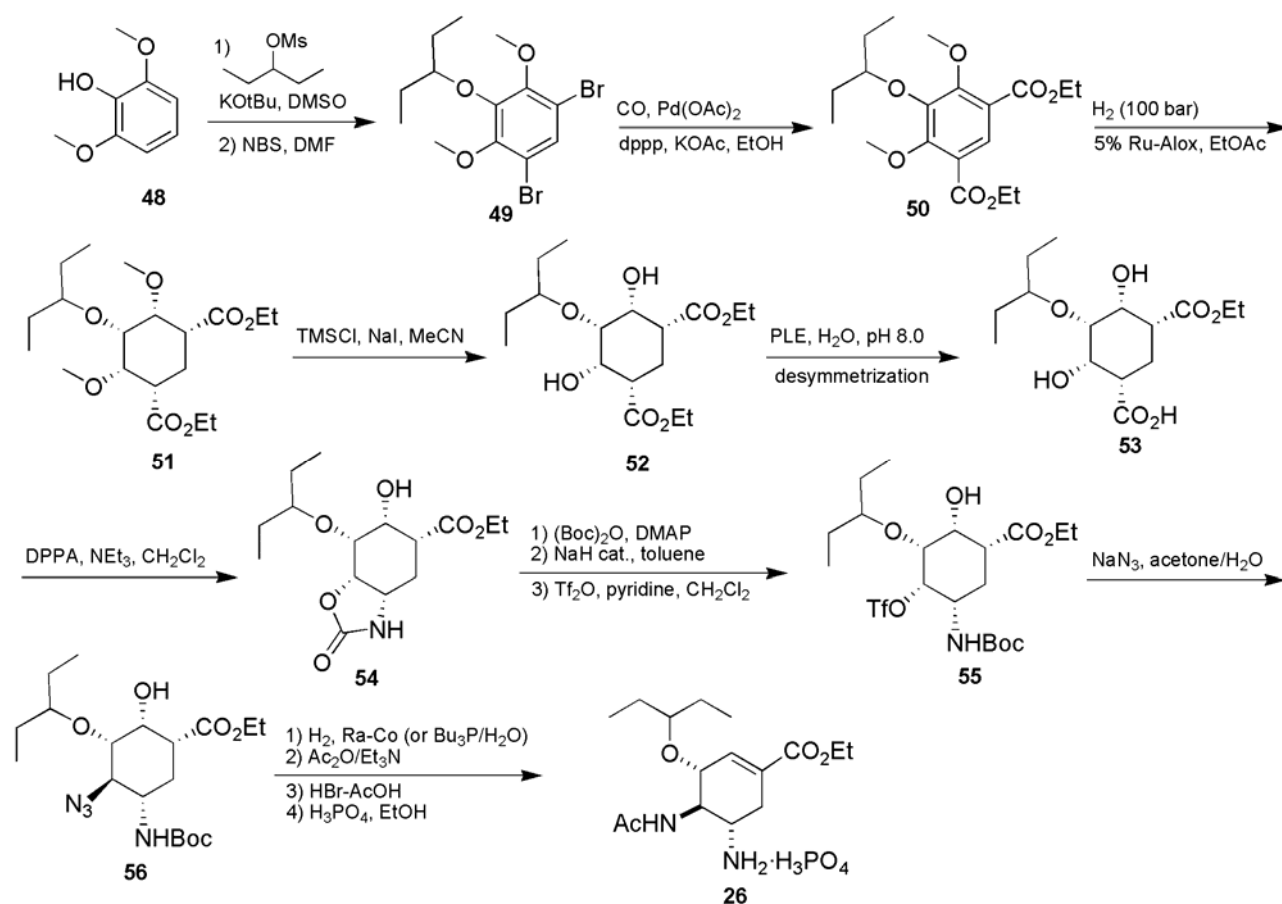
**Scheme 16.** Diels-Alder concept in the synthesis of oseltamivir.

Although the process eliminated the use of shikimic and quinic acids, it suffered from several impractical steps that required high dilution, which in turn can seriously affect the production output. In addition, the yield of the enzymatic resolution step is quite low<sup>127</sup>.



## 2. Aromatic Ring transformations: the desymmetrization concept.

This process started with the inexpensive 1,6-dimethoxy phenol (**48**) which was transformed to 3-pentyl ether by the action of 3-pentyl mesylate in presence of a base, potassium *t*-butanolate. Treatment of the obtained compound with *N*-bromosuccinimide gave a dibromide product **49**. From this product, isophthalic diester **50** was prepared by Pd-catalyzed double carbonylation. Hydrogenation of the diester over Ru-Alox led to the all-*cis* meso-diester **51**. Selectively, methyl ether groups were cleaved using the *in situ* generated TMS-iodide to provide the meso-dihydroxy intermediate **52**. The enzymatic hydrolytic desymmetrization of **52** using pig liver esterase afforded **53** the desired (*S*)-(+)-mono-acid in high yield and 96-98% *ee*. This hydroxy-acid was degraded using Yamada-Curtius reaction to generate the oxazolidinone **54**. Treatment with (Boc)<sub>2</sub>O in presence of DMAP led to the N-Boc-protected oxazolidinone which treatment upon a catalytic amount of sodium hydride allowed selective formation of double bond and at the same time the cleavage of the oxazolidinone ring system. This was followed by introduction of a good leaving group to provide the triflate **55**. S<sub>N</sub>2 substitution of the triflate using sodium azide introduced the azide at C-4 (compound **56**). Azide reduction, N-acetylation, Boc-deprotection and phosphate salt formation gave the final product in an overall yield 30% starting from 1,6-dimethoxyphenol<sup>136</sup>.



Scheme 17. Aromatic ring transformation route to oseltamivir phosphate

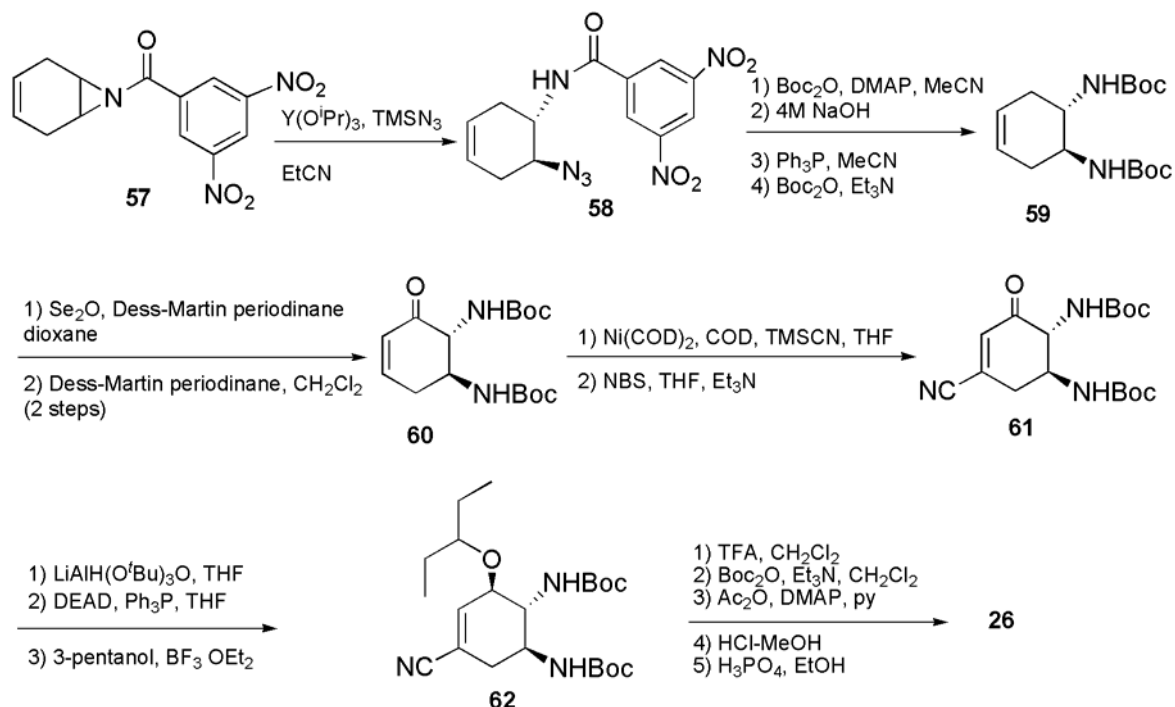
This route eliminated the use of shikimic and quinic acids but still use sodium azide which is undesirable from a reaction safety standpoint. Recently, the supply problem of Tamiflu gained the attention of academic chemists resulting in the development of some new approaches.

### I.1.6. Academic chemists approaches on Tamiflu synthesis

#### 1. Shibasaki's routes

##### Route 1

Shibasaki and co-workers reported an enantioselective approach to oseltamivir by using another cheap and widely available raw material, 1,4-cyclohexadiene. One of the double bonds of the starting material is converted to acylaziridine **57**. Thus, opening of the acylaziridine with trimethylsilyl azide under the catalysis of yttrium complex and further functional manipulations gave the diamine **59** which is oxidized in two steps using selenium dioxide and Dess-Martin periodinane to give the enone **60**. The Ni-catalyzed cyanation of the enone yielded a cyano derivative which was stereoselectively transformed to an alcohol. The crucial ether bond was formed by Mitsunobu reaction, and then standards manipulations yielded oseltamivir in 17 steps and overall yield of 1%<sup>137</sup>.



Scheme 18. Shibasaki route 1 to oseltamivir phosphate

### Route 2

Shibasaki and co-workers reported an alternative route that significantly improves their initial synthesis. The route utilizes the catalytic enantioselective desymmetrization of *meso*-aziridine **63** with TMSN<sub>3</sub> in the presence of chiral yttrium catalyst derived from ligand **64**. After boc-protection, the azido protected product **66** was treated with I<sub>2</sub> in presence of potassium carbonate, followed by subjection of the resulting cyclic carbamate to an elimination reaction of HI with DBU produced **67**. Protection of the carbamate nitrogen atom with Boc group and reductive acetylation of the azide with AcSH produced **68** which was selectively hydrolyzed and oxidized with Dess-Martin periodinane to produce enone **69**. Cyanophosphorylation of this enone proceeded with DEPC in the presence of LiCN, and cyanophosphate **70** was obtained as a single detectable isomer. Heating of **70** in toluene followed by treatment with a saturated solution of NH<sub>4</sub>Cl afforded the desired allyl alcohol **71** which was inverted using Mitsunobu reaction with *p*-nitrobenzoic acid followed by hydrolysis of the nitrobenzoate to afford β-allylic alcohol **72**. This alcohol was converted to aziridine through Mitsunobu conditions, producing **73** which was presented to 3-pentanol in presence of a Lewis acid to enhance the opening of the aziridine to produce **74**. Ethanolysis of the cyanide and cleavage of the Boc group under acidic ethanol conditions, followed by basification and H<sub>3</sub>PO<sub>4</sub> treatment, produced oseltamivir phosphate<sup>138</sup>.

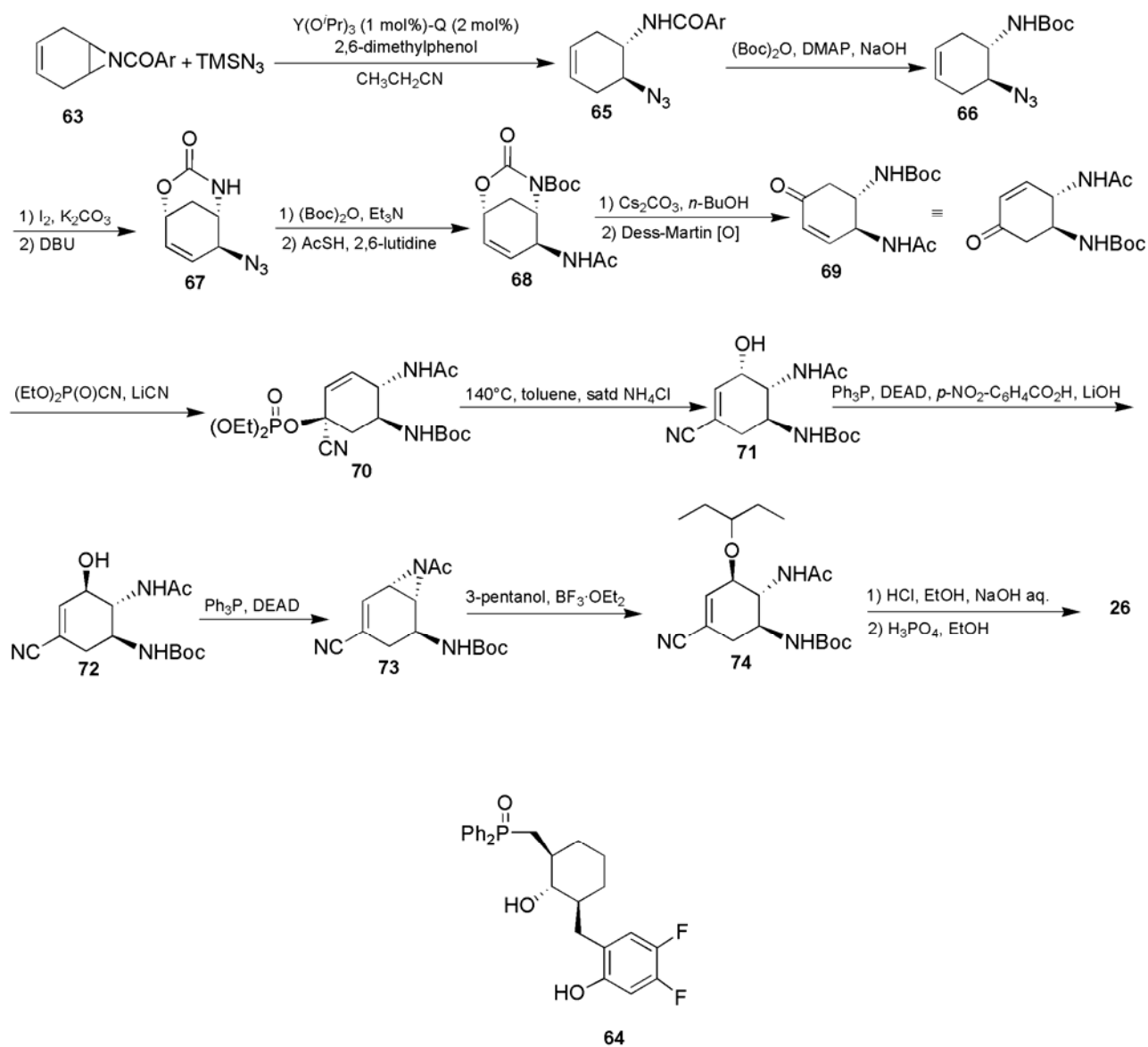
This route solves the two main problems encountered in the previously reported synthetic route: allylic oxidation (using the toxic selenium reagent) and protection group shuffling. In addition the synthetic scheme is shorter than that of the previously reported synthesis.

Finally, Shibasaki and co-workers reported another tamiflu synthesis using Diels-Alder reaction and Curtius rearrangements as key steps.

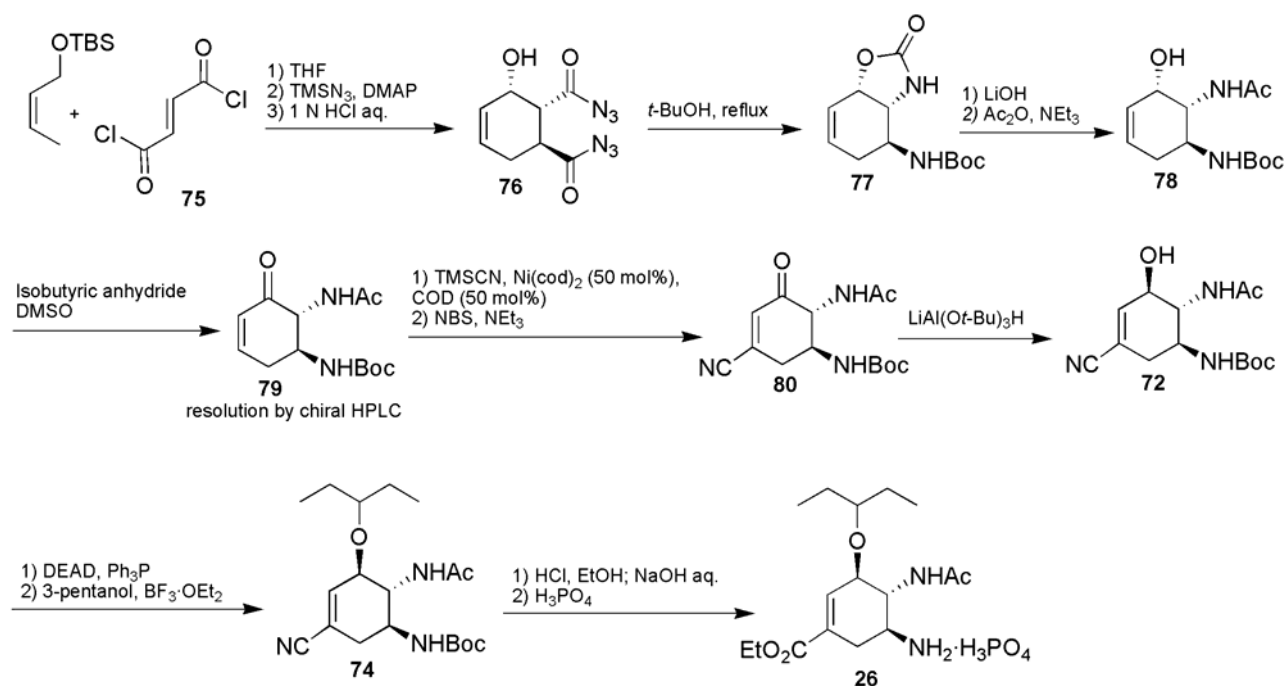
### Route 3

This route started with the preparation of diacid chloride by Diels-Alder reaction between 1-(*tert*-butyldimethylsiloxy)-1,3-butadiene and fumaryl chloride (**75**). The crude extract from this reaction was treated with TMSN<sub>3</sub> in the presence of DMAP, and the action of HCl induced the cleavage of trimethylsilyl ether. Curtius rearrangement of **76** proceeded cleanly in *t*-BuOH and oxazolidin-2-one **77** was produced. The basic hydrolysis of the cyclic carbamate moiety of oxazolidin-2-one, followed by N-acetylation afforded the alcohol **78**. The oxidation of **78** in DMSO by the action of isobutyric anhydride furnished the enone **79** which was obtained after resolution by chiral HPLC. From this enone, β-cyanoenone **80** was produced by the addition of TMSCN in the presence of Ni(cod)<sub>2</sub> and 1,5-cyclooctadiene (50 mol%) followed by the conversion of the obtained enol silyl ether by α-bromination and subsequent elimination of HBr with triethylamine. The ketone function of β-cyanoenone **80** was reduced stereoselectively with LiAl(O-*t*-Bu)<sub>3</sub>. Aziridine formation under Mitsunobu conditions, followed by the ring-opening reaction of the resulting aziridine with 3-pentanol, afforded **74**. Ethanolysis of the cyanide and cleavage of the Boc group

proceeded well and the free amine was obtained after basic treatment using NaOH. Treatment of the free amine with  $\text{H}_3\text{PO}_4$  produced the desired oseltamivir phosphate<sup>139</sup>.



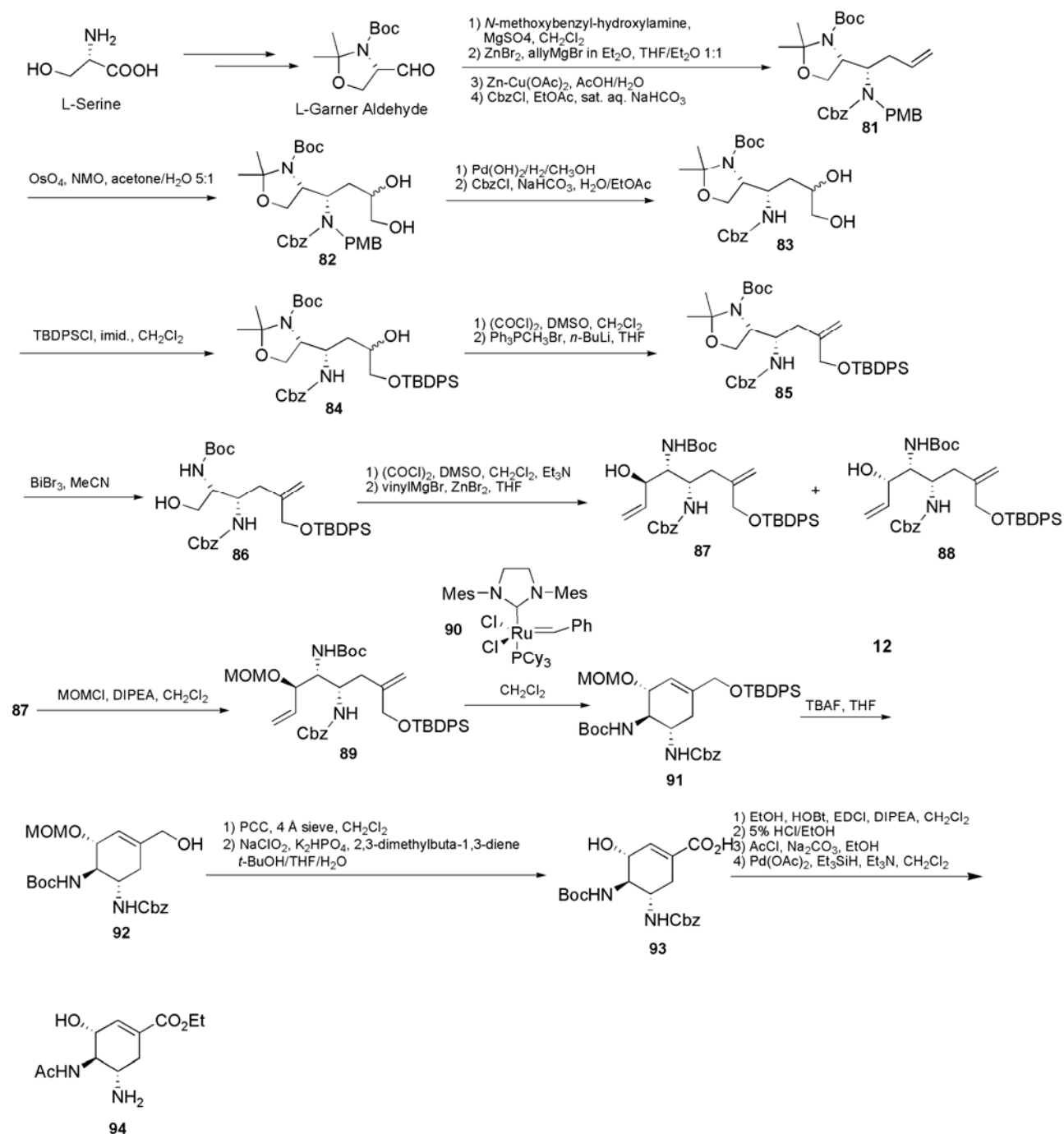
Scheme 19. Shibasaki route 2 to oseltamivir phosphate



**Scheme 20.** Shibasaki route 3 to oseltamivir phosphate

## 2. Cong route

Cong and co-worker reported a synthesis of the active pharmaceutical ingredient by using a cheap and widely available chiral starting material, L-serine. The synthesis is based on ring-closing metathesis reaction, catalyzed by second-generation Ru carbene species to form the key cyclohexene core. Unfortunately, formation of the diene is poorly diastereoselective (3:1) and this may be a serious drawback from the viewpoint of efficiency. Finally, standard manipulations completed the synthesis of tamiflu in a total of 18 steps and 16.5% overall yield<sup>140</sup>.

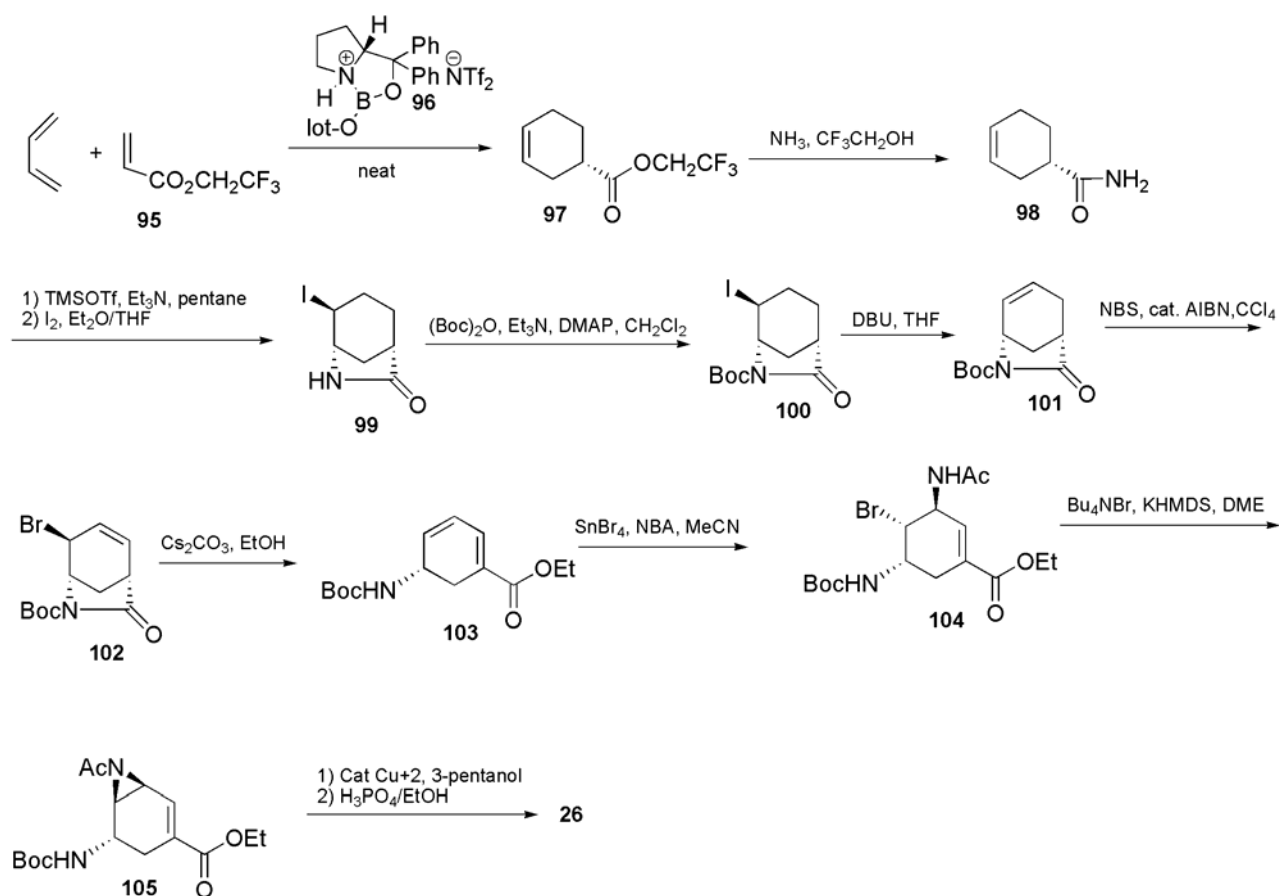


**Scheme 21.** Cong route to oseltamivir phosphate active ingredient

### 3. Corey route

Corey's group reported an interesting approach employing 1,3-butadiene and trifluoroethyl acrylate (**95**) as raw material. The approach features a highly enantioselective and high-yielding cycloaddition promoted by a catalytic amount of oxazaborolidine. The cycloaddition was followed by amidation, iodo-lactamization, and protection to yield Boc-protected iodo-lactam **100**. Dehydrohalogenation of which followed by allylic bromination yielded boc protected bromo-lactam **102**. Base promoted dehydrohalogenation gave a diene **103**, and regio and stereoselective bromo-amidation of the diene yielded the bromo diamino ester **104**. Sequential

dehydrohalogenation of this, gave an intermediate aziridine **105**, which was regioselectively opened with 2-pentanol and the resulting product was deprotected to furnish oseltamivir in 11 chemical steps and about 30% overall yield<sup>141</sup>.

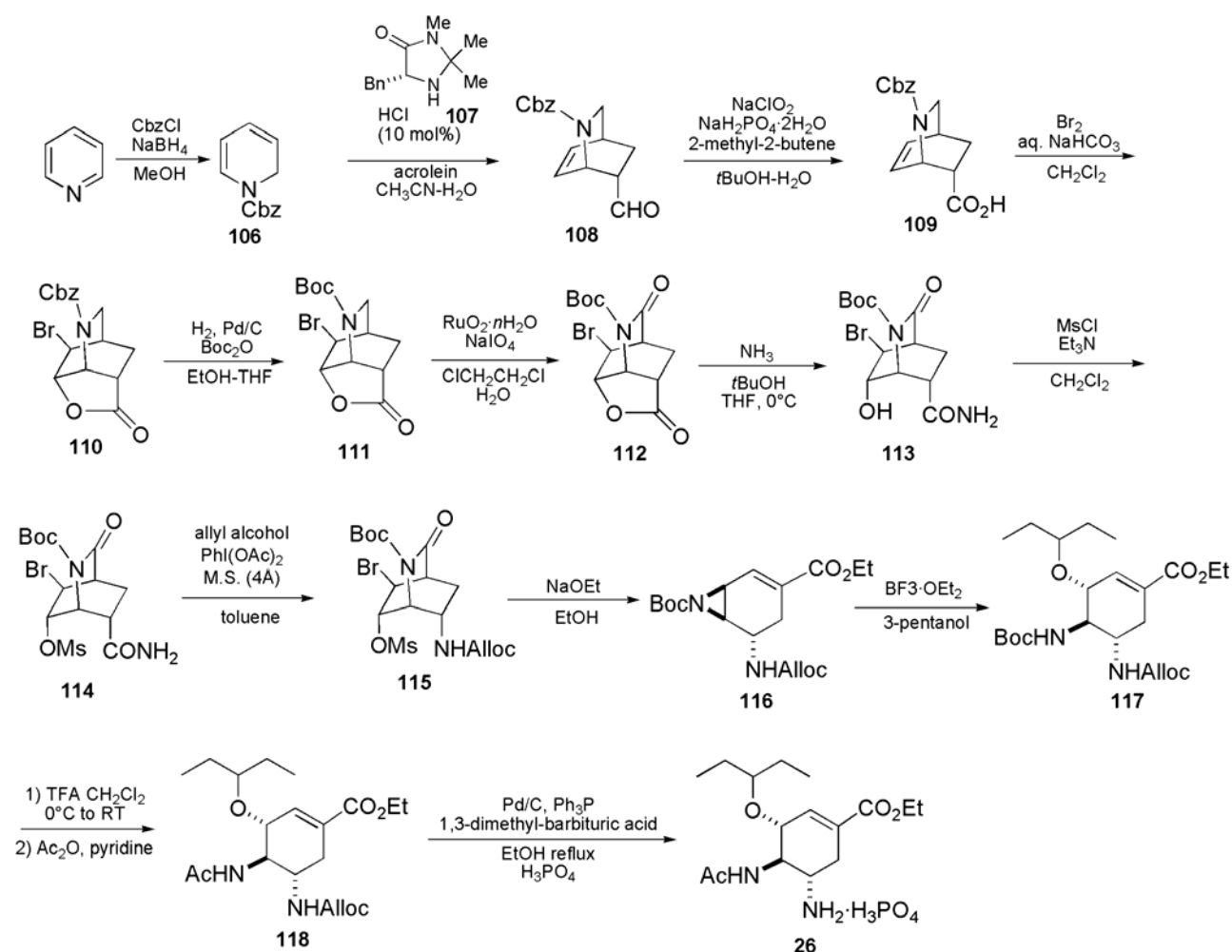


**Scheme 22.** Corey synthesis of oseltamivir phosphate

#### 4. Fukuyama route

Fukuyama and co-workers reported also another approach in the synthesis of oseltamivir phosphate. This approach started with the reduction of pyridine with benzyl chloroformate to afford dihydropyridine **106**, the diene, which goes through a catalyzed Diels-Alder reaction. The obtained Diels-Alder adduct **108** was transformed to a bromolactone using standard transformations and the latter underwent a series of transformations including a Hofmann rearrangement to provide the allyl carbamate **115**. This allyl carbamate was converted to cyclohexene derivative **116** by ethanolysis, dehydrobromination, and aziridine formation. Then, the regioselective cleavage of the aziridine ring, followed by the removal of Boc-protective group, acetylation, deprotection of the alloc-substituted amine and addition of phosphoric acid furnished oseltamivir phosphate (**26**) in 13 chemical steps and about 5.6% overall yield.

This approach used inexpensive and commonly used reagents, and the relatively expensive catalyst  $\text{RuO}_2 \cdot n\text{H}_2\text{O}$  can be recovered and reused. Unfortunately, the production of lactone **110** is occurring with low yield and this can be a drawback in the efficiency of the process<sup>142</sup>.



**Scheme 23.** Fukuyuma synthesis of oseltamivir phosphate

### 5. Bromfield route

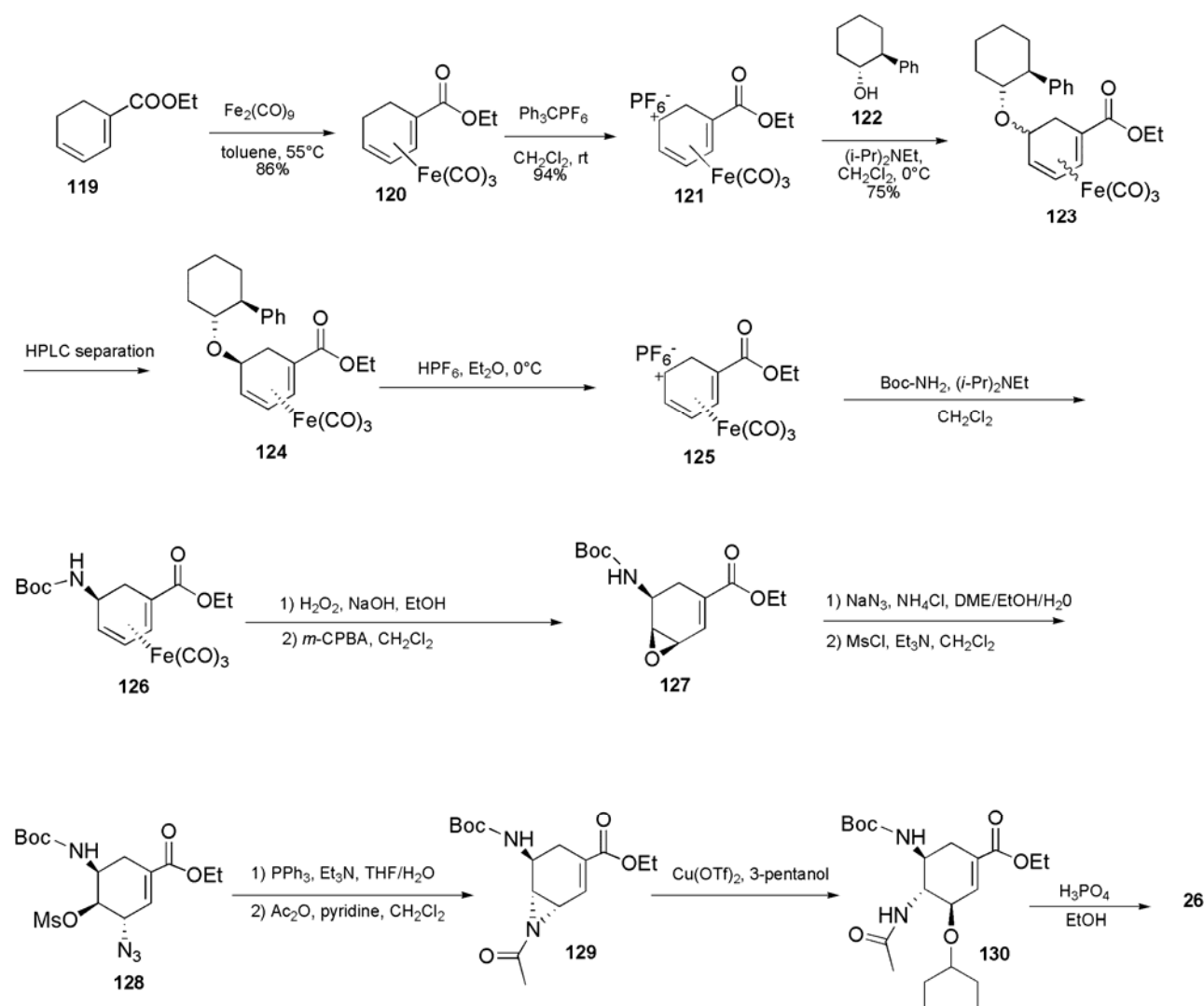
Bromfield and co-worker based their strategy on oseltamivir phosphate synthesis on the production of cationic iron carbonyl complex of cyclohexadiene. Transformation of the diene moiety liberated after oxidative decomplexation using standard reactions lead to oseltamivir phosphate.

The synthetic route started by the formation of the iron complex by the reaction in toluene of diiron nonacarbonyl with cyclohexanedieneoic acid ethyl ester **119**, this ester was prepared in early stage in a tandem Michael/Wittig reaction of acrolein and the phosphonium salt of 4-bromobut-2-enoic acid ethyl ester. Attempt to separated the racemic cationic iron complex produced was done by hydride abstraction and then reaction with (-)-(1*R*,2*S*)-*trans*-2-phenylcyclohexanol (**122**) which gave a HPLC separable diastereomers. After removal of phenylcyclohexanolate group to the appropriate enantiomer, Boc-NH group was introduced and then



decomplexation was conducted using hydrogen peroxide in aqueous sodium hydroxide to afford the cyclohexadiene derivative. The selective epoxidation of the more electron-rich alkene resulted in the desired *cis*-isomer epoxy **127**. The epoxide ring was replaced by the aziridine via azido alcohol by using sodium azide, mesylation and treatment with triphenylphosphine; and the resulting azidirine was acetylated *in situ* to afford **129**. The azidine ring is opened by nucleophilic attack of 3-pentanol in presence of  $\text{Cu}(\text{Otf})_2$ . Treatment of the amine obtained after Boc-deprotection, with  $\text{H}_3\text{PO}_4$  gave oseltamivir. This route employing iron carbonyl chemistry allows the synthesis of oseltamivir phosphate in a total of 12 steps from the cyclohexadienoic acid ethyl ester in 15 % overall yield<sup>143</sup>.

This approach avoids the use natural products as starting material. However, it is still used sodium azide in later stage and *m*-CPBA another reagent known as explosive and then difficult to handle at large scale. Also, the production the enantiopure compound **124** is occurring with low yield and its purification by HPLC makes the process difficult to be carried out at industrial level.



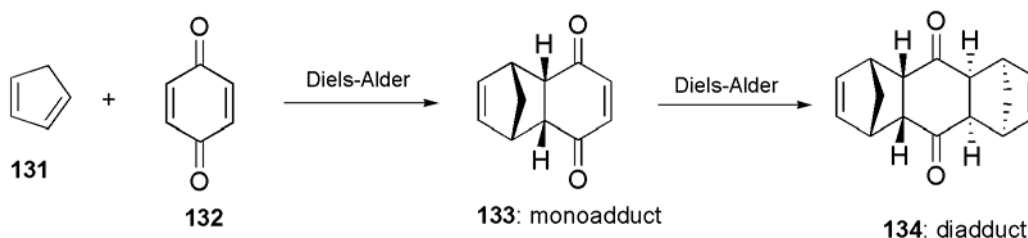
Scheme 24. Bromfield approach to oseltamivir synthesis

## Chapter II. Base-catalyzed Diels-Alder approach to oseltamivir intermediate

### II.1. Introduction

The Diels-Alder reaction is an organic chemical transformation (specifically, a cycloaddition) between a conjugated diene and a substituted alkene, commonly termed the dienophile, to form a substituted cyclohexene system.

This reaction was discovered by Professor Otto Diels and his student, Kurt Alder in identifying the products (**133** and **134**, Scheme 26) arising from the reaction of cyclopentadiene (**131**) with quinone (**132**). This denotes a historic event in the field of chemistry for which these two individuals were awarded with a reaction that would henceforth bear their names<sup>144</sup>.



**Scheme 25.** Discovery of Diels-Alder reaction.

Thus, the original version of the Diels-Alder reaction joins together a wide variety of conjugated dienes and alkenes with electron withdrawing group dienophiles, to produce a cyclohexene ring in which practically all six carbon atoms can be substituted as desired. The reaction may be executed under relatively simple reaction conditions by heating together the two components, diene and dienophile, in non-polar solvents, followed by evaporation which leads usually to high yields of the product(s)<sup>145</sup>.

The reaction is disciplined by the Woodward-Hoffmann rules 4-6 as a cycloaddition occurring in a concerted but probably not symmetrically synchronous fashion, thus leading to highly predictable product structures in which two new carbon-carbon sigma bonds are formed in a stereospecific manner with the creation of up to four new stereogenic centres. The classical empirical rules have now found strong theoretical basis in the Woodward-Hoffmann rules, with regards to regiochemistry (“ortho” and “para” orientations) and stereochemistry (endo transition state kinetically favoured over the exo transition state in most of the reactions)<sup>145</sup>.

Many different versions of the Diels-Alder reaction were elaborated, including Lewis acid-catalyzed Diels-Alder, intramolecular and [4+2] cycloadditions, transannular Diels-Alder reactions, hetero Diels-Alder reactions, pressure-accelerated Diels-Alder reactions. According to E. J. Corey, if one chemical reaction had to be selected from all those in the repertoire of synthetic organic chemists as the most useful and powerful synthetic construction, it was clear by 1970 that the Diels-Alder reaction would be the logical choice. Its application not only leads to a strong increase in molecular complexity (molecular size, topology, stereochemistry, functionality, and appendages), but also can result in structures that lend themselves to additional amplification of complexity by the use of other powerful synthetic reactions. Yet, further advances in scope and utility of this Grand Old Reaction of synthesis were to come<sup>146</sup>. While Nicolaou and co-workers stated that the Diels-Alder reaction has both enabled and shaped the art and science of total synthesis over the last few decades to an extent which, arguably, has yet to be eclipsed by any other transformation in the current synthetic repertoire. With myriad applications of this magnificent pericyclic reaction, often as a crucial element in elegant and programmed cascade sequences facilitating complex molecule construction, the Diels-Alder cycloaddition has afforded numerous and unparalleled solutions to a diverse range of organic synthetic<sup>144a</sup>.

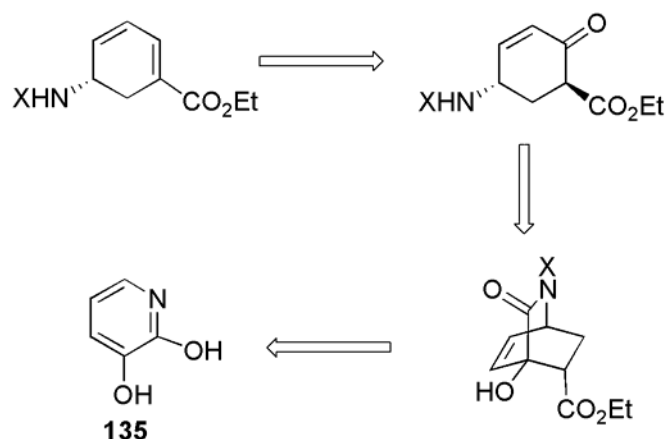
## **II.2. Base catalyzed Diels-Alder reaction in our laboratory**

As stated above, several methods have been found for the promotion of Diels-Alder reaction. A rapid look on the different reported processes, showed that mostly Lewis acids have been developed to facilitate the reaction. The Lewis acid is known to lower the LUMO level of the dienophile.

Our laboratory has developed a base-catalyzed Diels-Alder reaction of 3-hydroxy-2-pyridone derivatives and electron deficient dienophiles. The resulting product of this reaction is a highly functionalized bicyclic lactam and thus it can be a useful building block to synthesize small biologically active compounds. Indeed, using this concept, validamine and its epimer have been synthesized via a common intermediate obtained from the bicyclic lactam in short steps<sup>147, 148</sup>.

## **II.3. Retrosynthesis of Tamiflu Intermediate**

Our synthesis strategy of Tamiflu intermediate is based on the use of the highly functionalized bicyclic lactam obtained by Diels-Alder reaction. This compound is converted using standard manipulations: reduction and oxidation. The retrosynthesis is outlined in Scheme 26.



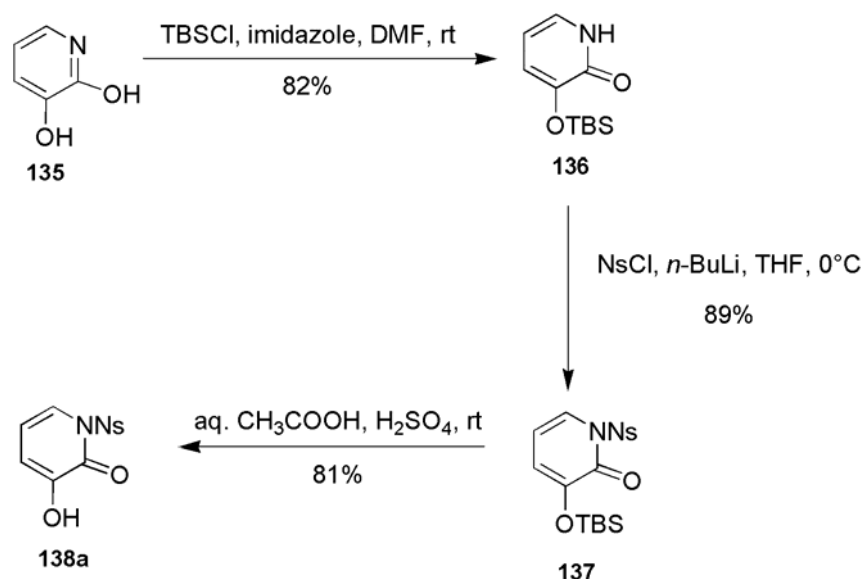
**Scheme 26.** Retrosynthesis of Corey's Intermediate

We propose that the *N*-protected enone ester can be obtained by the oxidative cleavage of the product yielded by chemoselective reduction of the bicyclic lactam. This bicyclic system could be constructed by the Diels-Alder reaction where *N*-protected-3-hydroxy-2-pyridone is playing the role of diene and it would be synthesized from the commercially available 2,3-pyridinediol (**135**).

## II.4. Synthesis of the Intermediate

### II.4.1. Preparation of the diene

The synthesis commenced with the protection of 2,3-pyridinediol according to a modified protocol reported by Posner<sup>149</sup>. Pyridine-2,3-diol was treated with *tert*-butyldimethylsilyl chloride in the presence of imidazole in dry dimethylformamide at room temperature to give 3-(*tert*-butyldimethylsilyloxy)-2-pyridone (**136**). The *N*-atom of **136** was protected by the action of nosyl chloride in presence of *n*-BuLi in dry tetrahydrofuran. The reaction was carried out under nitrogen atmosphere at 0°C, resulting to nosyl-protected product **137** whose TBS-protective group was removed by treatment with acetic acid in presence of sulfuric acid to afford *N*-nosyl-3-hydroxy-2-pyridone **138** (Scheme 27).



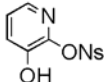
Scheme 27. Production of the diene 138

#### II.4.2. Diels-Alder reaction of *N*-nosyl-3-hydroxy-2-pyridone

To look for an optimal condition of the Diels-Alder reaction of *N*-nosyl-3-hydroxy-2-pyridone, several reaction conditions were examined. First of all, the tosyl-protected underwent a Diels-Alder with methyl acrylate using  $\text{Et}_3\text{N}$  as base in  $\text{CH}_2\text{Cl}_2$  at room temperature as reported in the synthesis of Validamine. We assumed that the same conditions may be applied to the reaction of *N*-nosyl-3-hydroxy-2-pyridone with ethyl acrylate as the diene and dienophile are similar with the reported one. Surprisingly, no Diels-Alder adduct was observed. The reaction afforded a product 3-hydroxy-2-(2'-nitrobenzenesulfonyloxy)-pyridine resulting to migration of nosyl (see Table 9).

Table 9. Base-catalyzed Diels-Alder reaction of 3-hydroxy-2-pyridone derivatives\*

entry	dienophile	condition	yield (%)
1	R = Me, 1.1 eq.	$\text{Et}_3\text{N}$ , $\text{CH}_2\text{Cl}_2$ , RT, 24 h	66 <sup>a</sup>
2	R = Et, 1.1 eq.	$\text{Et}_3\text{N}$ , $\text{CH}_2\text{Cl}_2$ , RT, 24 h	0 <sup>b</sup>
3	R = Et, excess	$\text{NaOH}$ , $\text{H}_2\text{O}$ , RT, 24 h in suspension	83

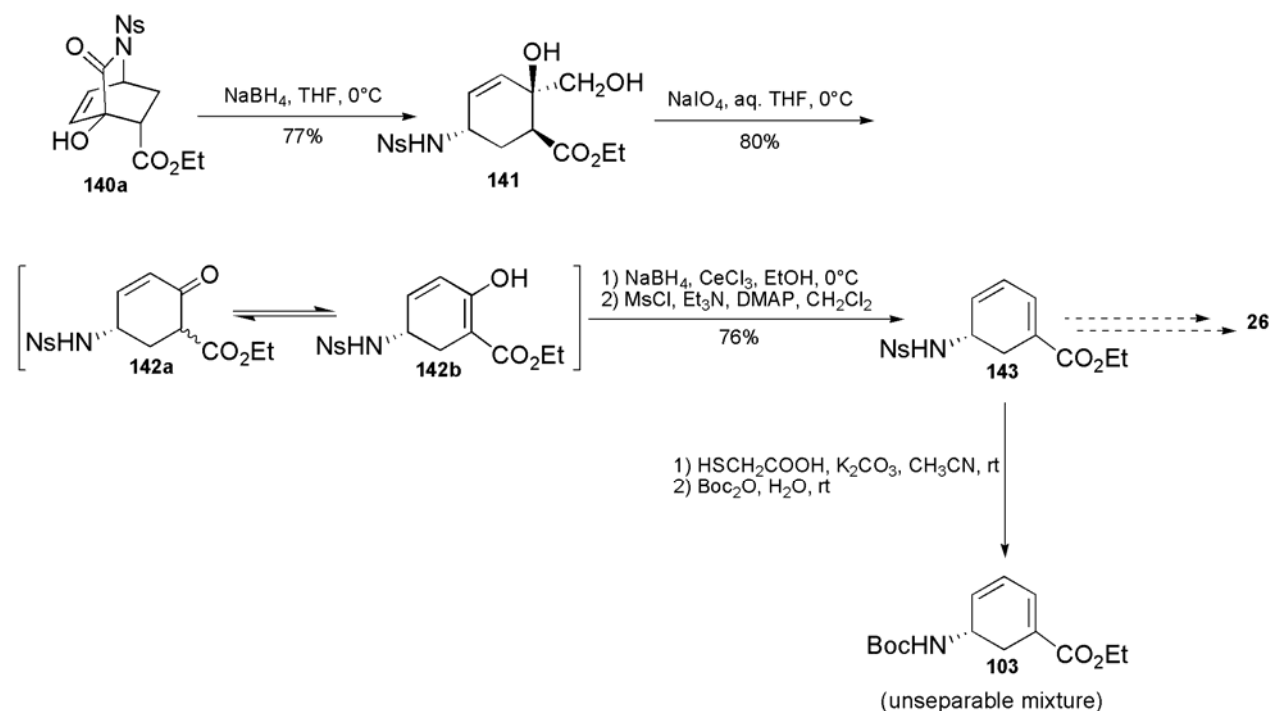
a) ref. 148. b)  was formed in 30 %.

\* Conditions developed in our laboratory by Kengo Kina

After several attempts, to prevent the Ns migration, it was found that a heterogeneous reaction of aqueous alkaline solution of *N*-nosyl-3-hydroxy-2-pyridone **138a** and excess of ethyl acrylate is appropriate condition to provide the corresponding Diels-Alder adduct as a single isomer **140a** in good yield (83%) without migration (entry 3).

#### II.4.3. Synthesis of the targeted compound

Having Diels-Alder adduct in the hand, the synthesis of the targeted compound could start. Next, we conducted the chemoselective reduction of **140a** using NaBH<sub>4</sub>. Several conditions were using, and THF was found to be a suitable solvent while no reaction occurred in methanol and ethanol. Thus, **140a** was chemoselectively reduced using NaBH<sub>4</sub> in THF at 0°C for 2 hours and a diol compound **141** was obtained. Oxidative cleavage of the 1,2-diol moiety produced an unexpected mixture. By a careful examination of the proton NMR charts of the mixture, it was found out that the expected ketone was obtained in the mixture as a relatively unstable mixture of two diastereomers **142a** and one enol tautomer **142b**. Reduction of the mixture using NaBH<sub>4</sub> in accord with the Luche protocol<sup>150</sup> in ethanol followed by elimination of the resulting alcohol by mesylation afforded the diene **143** which is the equivalent of the Corey's Tamiflu intermediate (Scheme 28). To confirm the structure, a trial of converting the product into the intermediate itself was made. Deprotection of Ns group using standard PhSH-Cs<sub>2</sub>CO<sub>3</sub> condition was unsuccessful and gave complex mixture because of conjugated addition of nucleophilic thiolate to the dienoic ester system. Much milder conditions using the combination of thioglycolic acid and K<sub>2</sub>CO<sub>3</sub><sup>151</sup> followed by Boc-protection in aqueous solution<sup>152</sup> proceeded quite well and the formation of **103** could be established by careful analysis of <sup>1</sup>H NMR. Unfortunately, purification of **103** was difficult due to the contamination of by-products of deprotection.

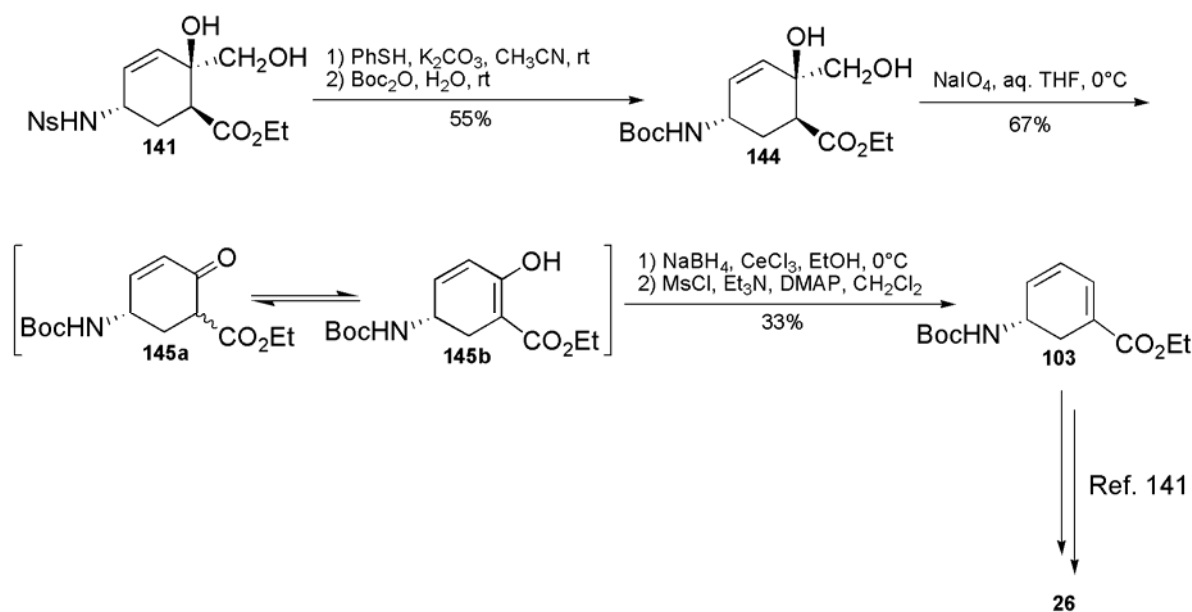


**Scheme 28.** Preparation of Corey's intermediate equivalent **143**

#### II.4.4. Alternative route to the Corey's Tamiflu Intermediate

As, the purification process for the isolation of Corey's Tamiflu Intermediate **103** failed, investigation has been carried out to find an alternative synthetic pathway. As, the most stable compound in the process was the diol **141**, the order on conversion of functional was changed. Thus, Boc-group was introduced in an earlier step of the synthesis.

Thus, the diol **141** was deprotected using the standard combination of PhSH and  $\text{K}_2\text{CO}_3$  in distilled acetonitrile. Addition of water was followed by extraction with EtOAc. The aqueous layer, containing the very polar aminodiol intermediate, was treated with  $\text{Boc}_2\text{O}$  at room temperature for 24 h to afford the Boc-protected diol **144**. Oxidative cleavage and subsequent reduction and elimination were again successfully accomplished in according the same manner as described above, and the Corey's intermediate **103** could be prepared (Scheme 29).

Scheme 29. Alternative route to the Corey's intermediate **103**

## II.5. Conclusion

A bicyclic lactam produced by a base-catalyzed reaction of *N*-nosyl-hydroxy-2-pyridone with methyl acrylate, has been used successfully as a building block for the production of an intermediate which can be converted to Tamiflu. The characteristic features of this synthesis are the shortness of the steps and ease of production. As shown in Scheme 30, only four chemical conversions and three purification steps were needed from the DA product **140a** to **143**, an equivalent of Corey's intermediate, and the overall yield was satisfactory (47%). Also for the Corey's intermediate **103** itself, only four purification steps were needed, although the overall yield was not high enough because the steps were not optimized.

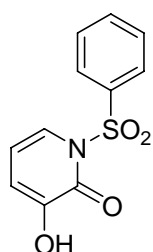
The key building block **140a** was available from the green DA reaction in an aqueous reaction medium with over ten grams scale and the following transformations required only regular chemical conversions using inexpensive reagents were also beneficial for easy production. Although the resulting products in the process were all racemate, the potential usefulness of the bicyclic lactam (key building block) and the advantage of this methodology for the synthesis of oseltamivir can be demonstrated.



### Chapter III. Experimental Section

**General methods.** Except the nosyl protection of pyridone derivatives **136** which has been carried out under N<sub>2</sub> atmosphere, all reactions were performed directly in air atmosphere. Commercial reagents were used as received. Thin-layer chromatography (TLC) was performed using E. Merck silica gel 60 F<sub>254</sub> precoated plates (0.25 mm). Column chromatography was performed using silica gel 60 (Wako gel, 70-230 mesh). NMR spectra were recorded on JEOL FX-400 instrument in CDCl<sub>3</sub> or DMSO using TMS as an internal reference. IR spectra were recorded on JASCO FT/IR 5300. ESI-TOFMS measurements were performed on a Bruker Daltonics.

#### Typical procedure:

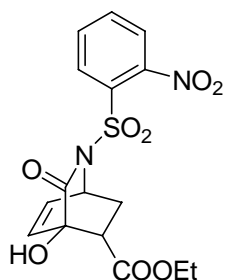


*N*-nosyl-3-hydroxy-2-pyridone (**138a**)

Chemicals used: 3-*O*-TBS-2-pyridone (318 mg, 1.41 mmol), 2-nitrobenzenesulfonyl chloride (NsCl, 315 mg, 1.41 mmol), *n*-butyllithium (0.90 mL, 1.44 mmol), THF (distilled from Na-benzophenone, 16 mL), distilled water, Magnesium sulfate, acetic acid, conc. sulfuric acid.

Procedure: (a) nosyl protection: A solution of 318 mg in dry THF was prepared under N<sub>2</sub> atmosphere at 0°C by stirring. 0.90 mL of *n*-BuLi was added drop-wise carefully and the stirring was pursued for twenty minutes. While stirring, 315 mg of NsCl was added and the temperature maintained at 0°C. After 24 hours, the solution was warmed to room temperature and distilled water (15 mL) was added. The mixture was extracted with EtOAc (3 x 10 mL) and the organic layer was dried over MgSO<sub>4</sub>. The solvent was removed under *vacuo* and the residue was purified by silica gel column chromatography using hexane-EtOAc (4:1) as eluent to give a light yellow powder 3-*tert*-butyldimethylsilyloxy-1-(2'-nitrobenzenesulfonyl)-2-pyridone (515 mg, 89%). (b) TBS deprotection: to the resulting product (526 mg, 1.3 mmol) in aqueous CH<sub>3</sub>COOH (1:1 mixture, 10.5 mL), two drops of conc. H<sub>2</sub>SO<sub>4</sub> were added and the obtained mixture was stirred for 30 hours at room temperature. The reaction is quenched by addition of 1 mL of distilled water and the yellow solid produced was filtered properly and then dried. This yellow product was pure **138** (307 mg, 81%). Elemental Anal.: calcd for C<sub>11</sub>H<sub>8</sub>N<sub>2</sub>O<sub>6</sub>S: C, 44.60; N, 9.46; H, 2.72% found: C, 44.54; N, 9.27; H, 2.86%; ESI-TOFMS *m/z* [M-H]<sup>-</sup> calcd for C<sub>11</sub>H<sub>9</sub>N<sub>2</sub>O<sub>6</sub>S: 295.0019, found 295.0307; IR (KBr): 3322, 3125, 2363, 1658, 1624, 1534, 1390, 1350, 904, 858, 743, 652; <sup>1</sup>H NMR (400 MHz, DMSO) δ 9.93 (1H, s), 8.44 (1H, dd, *J* = 7.6, 2.1 Hz), 8.09 (1H, dd, *J* = 8.1, 1.6), 8.05-7.97 (2H, m), 7.40 (1H, dd, *J* = 7.8, 1.4), 6.79 (1H, dd, *J* = 7.3, 1.8 Hz), 6.36 (1H, t, *J* = 7.3); <sup>13</sup>C NMR (100 MHz, DMSO) δ 156.3, 147.6, 147.5, 137.1, 135.0, 132.8, 128.7, 125.4, 121.3, 116.8, 107.1.

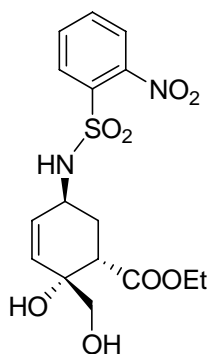
Diels Alder reaction of *N*-nosyl-3-hydroxy-2-pyridone and ethyl acrylate (**138a**)



Chemicals used: *N*-nosyl-3-hydroxy-2-pyridone (325 mg, 1.09 mmol), ethyl acrylate (4.5 mL, 42.3 mmol), distilled water (12 mL), 2N NaOH in water (1.1 mL).

Procedure: to 325 mg of *N*-nosyl-3-hydroxy-2-pyridone, 12 mL of water, 1.1 mL 2N NaOH solution and 4.5 mL of ethyl acrylate were successively added. The resulting mixture was stirred vigorously at room temperature. After twenty four hours, the reaction mixture was extracted by CH<sub>2</sub>Cl<sub>2</sub> (3 x 10 mL). The combined organic layer was dried over MgSO<sub>4</sub> and concentrated under vacuum. The residue was re-dissolved in 20 mL ether and left at room temperature until appearance of crystal. Re-crystallization provided pure compound **140a** as a single isomer (361 mg, 83% yield). Elemental Anal.: calcd for C<sub>16</sub>H<sub>16</sub>N<sub>2</sub>O<sub>8</sub>S: C, 48.48; N, 7.07; H, 4.07% found: C, 48.49; N, 7.05; H, 4.14%; ESI-TOFMS m/z [M-H]<sup>-</sup> calcd for C<sub>16</sub>H<sub>16</sub>N<sub>2</sub>O<sub>8</sub>S: 395.0544, found 395.0660; IR (KBr): 3315, 3102, 2899, 1746, 1717, 1591, 1365, 1304, 960, 881; <sup>1</sup>H NMR (400 MHz, CDCl<sub>3</sub>) δ 8.50 (1H, m), 7.79-7.82 (3H, m), 6.70 (1H, t, *J* = 6.6 Hz), 6.26 (1H, dd, *J* = 8.0, 1.1 Hz), 5.53 (1H, m), 4.19 (2H, q, *J* = 7.3 Hz), 3.90 (1H, s), 2.93 (1H, dd, *J* = 9.6, 5.0 Hz), 2.69 (1H, m), 1.99 (1H, dd, *J* = 13.3, 5.0 Hz), 1.71 (1H, s), 1.25 (3H, t, *J* = 7.3 Hz); <sup>13</sup>C NMR (100 MHz, CDCl<sub>3</sub>) δ 171.4, 171.3, 147.8, 135.3, 134.2, 134.0, 132.4, 131.6, 131.4, 124.6, 77.9, 61.6, 53.6, 43.2, 33.4, 14.1

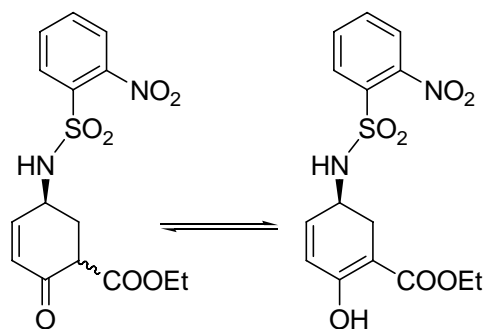
Ethyl 2-hydroxy-2-hydroxymehtyl-5-(2'-nitrobenzenesulfonamido)-3-ene carboxylate (**141**)



Chemicals used: Diels Alder adduct (294 mg, 0.74 mmol) sodium borohydride (42 mg, 1.1 mmol) THF (distilled from Na-benzophenone, 8.0 mL), 5% H<sub>3</sub>PO<sub>4</sub>.

Procedure: 42 mg of NaBH<sub>4</sub> were added to a solution of Diels Alder adduct 294 mg in 8.0 mL of THF at 0°C. The mixture was stirred at this temperature for two hours and half. And then a solution of 5% H<sub>3</sub>PO<sub>4</sub> was added drop wise until bubbling ceased. The mixture was extracted with EtOAc (3 x 5 mL) and the resulting organic layer washed with brine and dried over MgSO<sub>4</sub>. The solvent was removed in *vacuo* and the pale yellow oil obtained was chromatographed with MeOH-CH<sub>2</sub>Cl<sub>2</sub> (1:50) to afford 229 mg of the diol **141** as a pale yellow oil, 77% yield. ESI-TOFMS: m/z [M-H]<sup>-</sup> calcd for C<sub>16</sub>H<sub>20</sub>N<sub>2</sub>O<sub>8</sub>S 399.0857, found 399.0865; IR (film): 3466, 2982, 2361, 1715, 1593, 1539, 1343, 855; <sup>1</sup>H NMR (400 MHz, CDCl<sub>3</sub>) δ 8.17 (1H, m), 7.89 (1H, dd, *J* = 6.0, 3.2 Hz), 7.79-7.76 (2H, m), 5.79 (1H, dd, *J* = 10.1, 1.4 Hz), 5.65 (1H, dd, *J* = 10.1, 4.6 Hz), 5.54 (1H, d, *J* = 7.8 Hz), 4.38 (1H, s), 4.20-4.11 (3H, m), 3.59-3.53 (2H, m), 2.96 (1H, dd, *J* = 10.3, 3.4 Hz), 2.36 (1H, br s), 2.29 (1H, m), 1.99 (1H, dt, *J* = 14.2, 4.1 Hz), 1.74 (2H, s), 1.25 (3H, t, *J* = 7.1 Hz); <sup>13</sup>C NMR (100 MHz, CDCl<sub>3</sub>) δ 174.8, 147.8, 134.6, 133.7, 133.7, 133.0, 130.8, 128.5, 125.5, 70.3, 68.0, 61.4, 48.4, 41.2, 29.7, 14.1.

Ethyl 5-(2'-nitrobenzenesulfonyl)-2-oxocyclohex-3-enylcarboxylate and its enol tautomer (**142a** and **142b**)

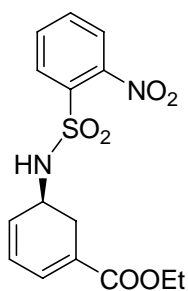


Chemicals used: diol (205 mg, 0.51 mmol), sodium periodate (164 mg, 0.77 mmol), THF:H<sub>2</sub>O (1:1, 8.0 mL), distilled water (5.0 mL).

Procedure: To a solution of the above diol 205 mg in 8 ml of THF:H<sub>2</sub>O (1:1, 8.0 mL) was added NaIO<sub>4</sub> (163.6 mg) at 0°C.

The solution was stirred for three hours at this temperature, warmed to room temperature and then diluted by addition of 5 mL of distilled water. To the clear solution obtained, ethyl acetate (5 mL) was added and the organic layer was separated. The aqueous layer was washed two times with 10 mL of ethyl acetate. The combined organic layer was washed with brine and dried over MgSO<sub>4</sub>, then filtered and concentrated. The residue was purified by silica gel column chromatography with Hexane:EtOAc (7:3) to afford the desired product as nearly 1:1 mixture of the enone esters **142a** and its enol tautomer **142b**, 151 mg in 80% yield. Since the resulting mixture was relatively unstable, it was used for next step without detailed spectral examinations.

The equivalent of Corey's intermediate (**143**)



- Chemicals used: enone (160.3 mg, 0.44 mmol), sodium borohydride (powdered, 26.5 mg, 0.70 mmol), Cerium trichloride (147.9 mg, 0.60 mmol), distilled methanol (4 mL), saturated ammonium chloride solution (1 mL).

Procedure: The enone and cerium trichloride were stirred in methanol at 0°C and the NaBH<sub>4</sub> was added. The stirring was maintained at this temperature for 2 hours, and then the reaction was quenched by adding saturated aqueous ammonium chloride solution (ca 1 mL).

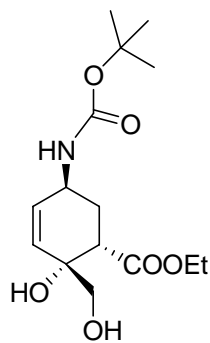
The methanol was removed under vacuum and the residue re-dissolved in water and extracted 3 times with ethyl acetate. The organic layer was washed with brine and dried over MgSO<sub>4</sub>, filtered through celite, concentrated and the resulting syrup containing the corresponding alcohol was used for next step.

- Chemicals used: primary alcohol, tetrahydrofuran (distilled from sodium-benzophenone, 9 mL), dried triethylamine (290 μL), 4-dimethylaminopyridine (DMAP) (80.3 mg, 1.5 equiv), methanesulfonyl chloride (112.4 mg, 76.2 μL, 0.98 mmol), water (5 mL), ethyl acetate (30 mL).

Procedure: To the syrup containing the alcohol in THF (9.0 mL) was added triethylamine (290 μL) and DMAP (80 mg, 0.7 mmol) at 0 °C and the resulting mixture was stirred for 30 minutes before drop wise addition of MsCl (112 mg). The resulting white suspension was left to slowly warm to room temperature while stirring for 4 hours. Quenching of the light brown suspension with water (5 mL) was followed by extraction with AcOEt (3 x 10 mL). The combined organic fractions were dried over MgSO<sub>4</sub>, filtered and the solvent removed. The resulting crude product was purified by silica gel column chromatography with hexane:AcOEt (7:3) to yield the desired product **143** as a pale yellow oil 87.4 mg in 76% yield over two steps. ESI-TOFMS: m/z [M-H]<sup>-</sup> calcd for C<sub>15</sub>H<sub>16</sub>N<sub>2</sub>O<sub>6</sub>S: 351.0645, found 351.0743; IR (film): 3297, 3098, 2984, 1701, 1642, 1578, 1537, 1346, 1165,

1100, 854;  $^1\text{H}$  NMR (400 MHz)  $\delta$  8.20 (1H, m), 7.89 (1H, m), 7.81-7.74 (2H, m), 6.21 (1H, dd,  $J = 9.4, 5.7$ ), 6.00 (1H, dd,  $J = 9.6, 5.0$ ), 5.53 (1H, d,  $J = 9.2$ ), 4.31 (1H, m), 4.16 (2H, q,  $J = 6.9$  Hz), 2.75 (1H, dd,  $J = 18.1, 5.8$ ), 2.51 (1H, ddd,  $J = 18.1, 8.0, 2.5$ ), 1.26 (3H, t,  $J = 7.1$ );  $^{13}\text{C}$  NMR (100 MHz)  $\delta$  166.1, 147.7, 135.2, 133.7, 133.2, 131.5, 130.6, 130.3, 126.7, 126.3, 125.6, 125.5, 60.7, 47.5, 28.6, 14.2.

Ethyl 5-(*tert*-butoxycarbonyl)-2-hydroxy-2-(hydroxymethyl)cyclohex-3-enecarboxylate (**144**)

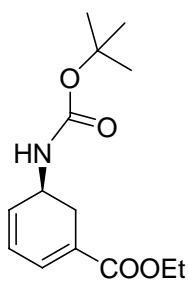


Chemicals used: diol (338 mg, 0.85 mmol), thiophenol (130  $\mu\text{L}$ , 1.3 mmol), potassium carbonate (152.0 mg, 1.1 mmol), anhydrous acetonitrile (10 mL), ethyl acetate, Di-*tert*-butyl dicarbonate (204 mg, 0.93 mmol), water

Procedure: a solution of the diol (338 mg) in anhydrous MeCN (4.0 mL) was treated with  $\text{K}_2\text{CO}_3$  (152 mg) in the presence of PhSH (130  $\mu\text{L}$ ) and the resulting reaction mixture was stirred for 3 hours at room temperature. The solution was diluted with water (10 mL) and extracted 2 x with AcOEt. To the aqueous layer,  $\text{Boc}_2\text{O}$  (204 mg) was added. The mixture was stirred for 24 hours and extracted with AcOEt ( $3 \times 8$  mL).

The combined organic extracts were dried over  $\text{MgSO}_4$  and concentrated in *vacuo*. The residue was purified by silica gel column chromatography with EtOAc:hexane (1:4) to give **144** as colorless oil (124 mg, 55% yield). IR (film): 3362, 2978, 2936, 1689, 1522, 1456, 1393, 1248, 1171, 995, 779;  $^1\text{H}$  NMR (400 MHz)  $\delta$  5.84 (1H, dd,  $J = 10.1, 3.7$  Hz), 5.76 (1H, dd,  $J = 10.1, 1.4$  Hz), 4.57 (1H, br s), 4.46 (1H, s), 4.26 (1H, br s), 4.21 (2H, q,  $J = 7.3$  Hz), 3.59-3.51 (2H, m), 2.91 (1H, dd,  $J = 9.6, 2.7$  Hz), 2.38-2.31 (2H, m), 1.91 (1H, dt,  $J = 13.3, 4.1$  Hz), 1.70 (2H, s), 1.45 (9H, s), 1.30 (3H, t,  $J = 7.1$  Hz);  $^{13}\text{C}$  NMR (100 MHz)  $\delta$  175.3, 155.0, 132.2, 130.5, 108.7, 70.5, 68.2, 61.4, 41.7, 29.4, 28.4(?), 14.1

Corey's intermediate (**103**)



The experimental procedures for the conversions from **144** to **103** were essentially same with the above mentioned method. The spectra data of **103** showed good agreements with the reported one. ESI-TOFMS:  $m/z$   $[\text{M} + \text{Na}]^+$  calcd for  $\text{C}_{14}\text{H}_{21}\text{NO}_4\text{Na}$ : 290.1363, found 290.1340; IR (film): 3353, 2978, 2361, 1707, 1512, 1368, 1254, 1167, 1098, 478, 444;  $^1\text{H}$  (400 MHz,  $\text{CDCl}_3$ ):  $\delta$  7.06 (1H, d,  $J = 4.1$  Hz), 6.18-6.08 (2H, m), 4.64 (1H, br s), 4.44 (1H, br s), 4.22 (2H, q,  $J = 7.1$ ), 2.77-2.63 (2H, m), 1.40 (9H, s), 1.31 (3H, t,  $J = 7.1$  Hz);  $^{13}\text{C}$  (100 MHz,  $\text{CDCl}_3$ ): 166.9, 154.9, 132.5, 131.8, 128.9, 127.0, 124.8, 60.6, 53.4, 28.9, 28.4, 14.3.

## Chapter IV. Summary

Diels-Alder reaction is one of the powerful tools used in organic chemistry. In this reaction, a six-membered ring is formed through fusion of a four  $\pi$ -component, usually a diene and a two  $\pi$  component, which is commonly referred to as the dienophile. The Diels-Alder reaction has proven to be of great synthetic value, forming a key-step in the construction of compounds containing six-membered rings. Many different versions of the Diels-Alder reaction were elaborated, including intramolecular [4+2] cycloadditions, catalyzed hetero Diels-Alder reactions, pressure-accelerated Diels-Alder reactions, and catalyzed carbons accelerated Diels-Alder reactions.

Among catalysts used to facilitate the carbons Diels-Alder reaction, almost developed catalysts are Lewis acids. Our lab developed unique base-catalyzed diastereoselective Diels-Alder reaction of pyridone derivative as diene and electron deficient dienophiles. On the basis of this concept, a poly-functionalized bicyclic lactam was obtained by DA reaction of pyridone derivatives and acrylate derivatives. This unique bicyclic lactam can be used as key intermediate for the synthesis of biologically active compounds having C7N as basic skeleton. Thus, Validamine and its epimers have been synthesized successfully using this bicycle system as key building block.

Tamiflu is biologically active compound which has been developed as an inhibitor of the influenza viral neuraminidase. Because it can inhibit both the influenza virus A and B, it is widely used for the treatment and prophylaxis of influenza. With the emergence of bird flu, an eventual influenza pandemic can occur and, to get prepared for this, several countries are planning to stockpile Tamiflu. However, the insufficiency of the starting material and the complexity of the synthesis make this difficult to achieve.

Therefore, several groups developed novel synthetic methods. Among these new routes, Corey's group reported an elegant method for the synthesis of Tamiflu. One intermediate involved in Corey's route is 5-*tert*-butoxycarbonylamino-cyclohexa-1,3-dienecarboxylic acid ethyl Ester, which has been targeted for synthesis.

Using our base-catalyzed DA reaction concept, a compound equivalent to this Corey's Tamiflu intermediate has been synthesized from the bicyclic lactam obtained by DA reaction of *N*-nosyl-3-hydroxy-2-pyridone and ethyl acrylate in a satisfactory overall yield (47%). Four chemical transformation of the DA adduct and two purifications led to the targeted compound which could also be converted to Tamiflu according to Corey's route. The characteristic features of this synthesis are shortness of the steps and easy production. Although the resulting products in the process are all racemate, potential usefulness of the bicyclic lactam and advantage of this methodology for the synthesis of Tamiflu could be demonstrated.

## References

1. Balandrin, F. M.; Klocke, J. A.; Wurtele, E. S.; Bollinger, W. H. *Sciences* **1995**, 228, 1154-1160.
2. Dewick, P. M. *Medicinal Natural Products. A Biosynthetic Approach*. Second Edition. John Wiley & Sons, West Sussex, **2001**.
3. Da Silva, M. F. G.; Gottlieb, O. R.; Dreyer, L. D. *Biochemical Systematics and Ecology* **1984**, 12, 299-310.
4. Roy, A.; Saraf, S. *Biol. Pharm. Bull.* **2006**, 29, 191-201.
5. Bevan, C. W. L.; Powell, J. W.; Taylor, D. A. H.; Halsall, T. G.; Toft, P.; Welford, M. *J. Chem. Soc. (C)* **1967**, 163-170.
6. Akisanya, A.; Bevan, C. W. L.; Hirst, J.; Halsall, T. G.; Taylor, D. A. H. *J. Chem. Soc.* **1960**, 3827-3829.
7. Taylor, D. A. H. *Progress in the Chemistry of Organic Natural Products* **1984**, 45, 1-93.
8. Okorie, D. A.; Taylor, D. A. H. *Phytochemistry* **1977**, 16, 2029-2030.
9. Orisadipe, A. T.; Adesomoju, A. A.; D'Ambrosio, M.; Guerriero, A., Joseph I. Okogun, I. J. *Phytochemistry* **2005**, 66, 2324-2328.
10. Bickii, J.; Tchouya, G. R. F.; Tchouankeu, J. C.; Tsamo, E. *African Journal of Traditional, Complimentary and Alternative Medicines* **2007**, 4, 135-139.
11. Ran, X.; Fazio, G. C.; Matsuda, S. P. T. *Phytochemistry* **2004**, 65, 261-291.
12. MacGarvey, D. J.; Croteau, R. *The Plant Cell* **1995**, 7, 1015-1026.
13. Champagne, D., E; Koul, O.; Isman, M. B.; Scudder, G. G. E; Towers, G. H. N. *Phytochemistry* **1992**, 31, 377-394.
14. Fraser, L. A.; Mulholland, D. A.; Fraser, D. D. *Phytochemical Analysis* **1997**, 8, 301-311.
15. Mulholland, D. A.; Parel, B.; Coombes, P. H. *Current Organic Chemistry* **2000**, 4, 1011-1054.
16. MacKinnon, S.; Durst, T.; Arnason, J. T.; Angerhofer, C.; Pezzuto, J.; Sanchez-Vindas, P. E.; Poveda, L. J.; Gbeassor, M. *J. Nat. Prod.* **1997**, 60, 336-341.
17. Bickii, J.; Njifutie, N.; Foyere, J. A.; Basco, L. K.; Ringwald, P. *Journal of Ethnopharmacology* **2000**, 69, 27-33.
18. Krief, S., Martin, M.-T.; Grellier, P.; Kasenene, J.; Sevenet, T. *Antimicrobial agents and chemotherapy* **2004**, 48, 3196-3199.
19. Rochanakij, S.; Thebtaranonth, Y.; Yenjai, C.; Yuthvong, Y. *Southeast Asian J. Trop. Med. Public Health* **1985**, 16, 66-72.
20. Battinelli, L.; Mengoni, F.; Lichtner, M.; Mazzanti, G.; Saija, A.; Matroianni, C. M.; Vullo, V. *Planta Medica* **2003**, 69, 910-913.
21. Sunthitikawinsakul, A.; Kongkathip, N.; Kongkathip, B.; Phonnakhu, S.; Daly, J. W.; Spande, T. M.; Nimit, Y.; Napaswat, C.; Kasisit, J.; Yoosook, C. *Phytotherapy Research* **2003**, 17, 1101-1103.
22. Kim, M.; Kim, S. K.; Park, B. N.; Lee, K. H.; Min, G. H.; Seoh, J. Y.; Park, C. G.; Hwang, E. S.; Cha, C. Y.; Kook, Y. H. *Antiviral Research* **1999**, 43, 103-112.

23. Alché, L. E; Ferek, G. A.; Meo, M.; Coto, C. E.; Maier, M. S. *Zeitschrift fur Naturforschung – Section C Journal of Biosciences* **2003**, *58*, 215-219.
24. Musza, L. L.; Killar, M. L.; Speight, P.; McElhiney, S.; Barrow, C. J.; Gillum, M. A.; Cooper, R. *Tetrahedron* **1994**, *50*, 11369-11378.
25. Takeya, K.; Qiao, Z.-S.; Hirobe C.; Itokawa, H. *Phytochemistry* **1996**, *42*, 709-712.
26. Itokawa, H.; Qiao, Z.-S.; Hirobe, C.; Takeya, K. *Chem. Pharm. Bull.* **1995**, *43*, 1171-1175.
27. Polonsky, J.; Varon, Z.; Arnoux, B.; Pascard, C.; Pettit, G. R.; Schmidt, J. H.; Lange, L. M. *J. Am. Chem. Soc* **1978**, *100*, 2575-2576.
28. Polonsky, J.; Varon, Z.; Arnoux, B.; Pascard, C.; Pettit, G. R.; Schmidt, J. M. *J. Am. Chem. Soc* **1978**, *100*, 7731-7733.
29. Ahn, J.-W.; Choi, S.-U.; Lee, C.-O. *Phytochemistry* **1994**, *36*, 1493-1496.
30. Cohen, E.; Quistad, G. B.; Casida, J. E. *Life Sciences* **1996**, *58*, 1075-1081.
31. Berhow, M. A., Fong, C. H.; Hasegawa, S. *Biochemical Systematics and Ecology* **1996**, *24*, 237-242.
32. Guthrie, N.; Morley, K.; Hasegawa, S.; Manners, G. D.; Vandenberg, T.; ACS Symposium Series **2000**, Vol. 758, 164-174.
33. Lam, L. K. T.; Li, Y.; Hasegawa, S. *J. Agric. Food chem.* **1989**, *37*, 878-880.
34. Miller, E. G.; Porter, J. L.; Binnie, W. H.; Guo, I. Y.; Hasegawa, S. *J. Agric. Food Chem.* **2004**, *52*, 4908-4912.
35. Nakatani, M. Limonoids from Meliaceae and their Biological Activities. In *Bioactive Compounds from Natural Sources. Isolation, Characterization and biological properties*; Edited by Corrado Tringali, **2000**, 528-554.
36. Koul, O.; Daniewski, W. M.; Multani, J. S.; Gumulka, M.; Singh, G. *J. Agric. Food Chem.* **2003**, *51*, 7271-7275.
37. Nakatani, M.; Huang, R. C.; Okamura, H.; Iwagawa, T. *Chemistry Letters* **1993**, *12*, 2125-2128.
38. Bohnenstengel F. I.; Wray V.; Witte L.; Srivastava R. P.; Proksh P. *Phytochemistry* **1999**, *50*, 977-982.
39. Nakatani, M.; James. J. C.; Nakanishi, K. *J. Am. Chem. Soc.*, **1981**, *103*, 1228-1230.
40. Bordoloi, M.; Saikia, B.; Mathur, R. K.; Goswami, B. N. *Phytochemistry* **1993**, *34*, 583-584.
41. Govindachari, T. R.; Suresh, G.; Banumathy, B.; Masilamani, S.; Gopalakrishnan, G.; Kumari, G. N. K. *J. Chem. Ecol.* **1999**, *25*, 923-933.
42. Abdelgaleil, S. A. M.; Hashinaga, F.; Nakatani, M. *Pest Manag Sci* **2005**, *61*, 186-190.
43. Madhu, D. C.; Nair, G. R. N. *Indian Drugs* **2001**, *38*, 629-632.
44. Nakatani, M.; Takao, H.; Iwashita, T.; Naoki, H.; Hase, T. *Phytochemistry* **1988**, *27*, 1429-1432.
45. Yu, J.; Wang, L.; Walzem, R. L.; Miller, E. G.; Pike, L. M.; Patil, S. B. *J. Agric. Food Chem.* **2005**, *53*, 2009-2014.
46. Poulose, S. M.; Harris, E. D.; Patil, S. B. *J. Nutr.* **2005**, *135*, 870-877.
47. Madhu, D. C.; Nair, G. R. N. *Indian Drugs* **2001**, *38*, 629-632.
48. Njar, V. C. O.; Adesanwo, J. K.; Rajo, Y. *Planta Medica* **1995**, *61*, 91-92.
49. Cespedes, C. L; Calderon, J. S.; Salazar, J. R.; Hennsen, B. L.; Segura, R. *J. Chem. Ecol.* **2001**, *27*, 137-149.

50. Jayaprakasha, G. K.; Singh, R. P.; Pereira, J.; Sakariah, K. K. *Phytochemistry* **1997**, *44*, 843-846.
51. Cespedes, C. L.; Calderon, J. S.; Lina, L.; Aranda, E. *J. Agric. Food Chem.* **2000**, *48*, 1903-1908.
52. Ndong'u, M.; Hassanali, A.; Hooper, A. M.; Chabra, S.; Miller, T. A.; Paul, L. R.; Torto, B. *Phytochemistry* **2003**, *64*, 817-823.
53. Muellner, A. N.; Samuel, R.; Johnson, S. A.; Cheek, M.; Pennington, T. D.; Chase, M. W. *American Journal of Botany* **2003**, *90*, 419-540.
54. Willis, J. C. A dictionary of Flowering Plants and Ferns, **1966**, 7th ed. (revised by Airshaw, H. K.) Cambridge University Press, Cambridge, p. 709.
55. Styles, B. T.; Pennington, T. D. *Blumea* **1975**, *22*, 419-540.
56. Hutchings, A.; Scott, A. H.; Lewis, G.; Cunningham, A. *Zulu Medicinal Plants – An Inventory*, University of Natal Press, Pietermaritzburg, **1996**.
57. Kerharo, J.; Bouquet, A. *Plantes médicinales et toxiques de la Côte-d'Ivoire Haute-Volta*, Vigot Frères Paris (VIe), Paris, **1950**.
58. Iwu, M. M. *Handbook of African Medicinal Plants*. **1993**, CRC Press Inc., 252–253.
59. Ishibashi, F.; Satasook, C.; Ismant, M. B.; Towers, G. H. N. *Phytochemistry* **1993**, *32*, 307-310.
60. Um, B. H.; Lobstein, A.; Weniger, B.; Spiegel, C.; Yice, F.; Rakotoarison, O.; Andriantsitohaina, R.; Anton, R. *Fitoterapia* **2003**, *74*, 638-642.
61. Tane, P.; Akam, M. T.; Tsopmo, A.; Ndi, C. P.; Sterner, O. *Phytochemistry* **2004**, *65*, 3083-3087.
62. Chowdhury, R.; Hasan, C. M.; Rashid, M. A. *Phytochemistry* **2003**, *62*, 1213-1216.
63. Lago, J. H. G.; Brochini, C. B.; Roque, N. F. *Phytochemistry* **2002**, *60*, 333-338.
64. He, K.; Timmermann, B. N.; Aladesanmi, A. J.; Zeng, L. *Phytochemistry* **1996**, *42*, 1199-1201.
65. Qiu, S.-X.; van Hung, N.; Xuan, L. T.; Gu, J.-Q.; Lobkovsky, E.; Khanh, T. C.; Soejarto, D. D.; Clardy, J.; Pezzuto, J. M.; Dong, Y.; Tri, M. V.; Huong, L. M.; Fong, H. H. S. *Phytochemistry* **2001**, *56*, 775-780.
66. Maclachlan, L. K.; Taylor, D. A. H. *Phytochemistry* **1982**, *21*, 1701-1703.
67. MacFarland, K.; Mulholland, D. A.; Fraser, L.-A. *Phytochemistry* **2004**, *65*, 2031-2037.
68. Randrianarivelojosia, M.; Kotsos, M. P.; Mulholland, D. A. *Phytochemistry* **1999**, *52*, 1141-1143.
69. Nakatani, M.; Abdelgaleil, S. A. M.; Saad, M. M. G.; Huang, R. C.; Doe, M.; Iwagawa, T. *Phytochemistry* **2004**, *65*, 2833-2841.
70. Wikipedia: <http://en.wikipedia.org/wiki/Entandrophragma>, as accessed on 2007/12/25.
71. Hall, J. S.; Medjibe, V.; Berlyn, G. P.; Ashton, P. M. S. *Forest Ecology and Management* **2003**, *179*, 135-144.
72. Adesida, G. A.; Taylor, D. H. A. *Phytochemistry* **1967**, *6*, 1429-1433.
73. Taylor, D. H. A. *J. Chem. Soc.* **1965**, 3495-3496.
74. Mulholland, D. A.; Osborne, R.; Roberts, S. L.; Taylor, D. H. A. *Phytochemistry* **1994**, *37*, 1417-1420.
75. Mulholland, D. A.; Schwikkard, S. L.; Sandor, P.; Nuzillard, J.-M. *Phytochemistry* **2000**, *53*, 465-468.
76. Hanni, R.; Tamm, C.; Gullo, V.; Nakanishi, K. *J. Chem. Soc., Chem. Comm.* **1975**, 563-564.
77. Guex, M.; Tamm, C. *Helvetica Chimica Acta* **1984**, *67*, Fasc. 3, Nr 99.
78. Tchouankeu, J. C.; Tsamo, E.; Sondengam, B. L.; Connolly, J. D. *Phytochemistry* **1989**, *28*, 2855-2857.



79. Koul, O.; Daniewski, W. M.; Multani, J. S.; Gumulka, M.; Singh, G. *J. Agric. Food Chem.* **2003**, *51*, 7271-7275.
80. Gullo, V. P.; Miura, I.; Nakanishi, K.; Cameron, A. F.; Connolly, J. D.; Harding, A. E.; McCrindle, R.; Taylor D. A. H. *J. Chem. Soc. Chem. Commun.* **1975**, 345-346.
81. Lukacova, V.; Polonsky, J.; Moretti, C.; Pettit, G. R.; Schmidt, J. M. *J. Nat. Prod.* **1982**, *45*, 288-294.
82. Arndt, R. R.; Baarschers, W. H. *Tetrahedron* **1972**, *28*, 2333-2340.
83. Bevan, C. W. L.; Ekong, D. E. U; Halsall, T. G.; Toft, P. *J. Chem. Soc. (C)* **1967**, 820-822.
84. Connolly, J. D.; Labbe, C.; Rycroft, D. S. *J. Chem. Soc. Perkin Trans. I* **1978**, 285-288.
85. Ansell S. M; Taylor, D. H. A. *Phytochemistry* **1988**, *27*, 1218-1220.
86. Daniewski, W. M.; Anczewski, W.; Gumulka, M.; Danikiewicz, W.; Jacobsson, U.; Norin, T. *Phytochemistry* **1996**, *43*, 811-814.
87. Ngnokam, D.; Massiot, G.; Nuzillard, J. M.; Tsamo, E. *Phytochemistry* **1995**, *37*, 529-531.
88. Chan, W. R.; Forsyth, W. G. C.; Hassall, C. H. *J. Chem. Soc.* **1958**, 3174-3179.
89. (a) Chan, W. R.; Taylor, D. R.; Yee, T. *J. Chem. Soc. (C)* **1970**, 311-314. (b) Chan, W. R.; Taylor, D. R.; Yee, T. *J. Chem. Soc. (C)* **1971**, 2663-2667.
90. Ngnokam, D.; Massiot, G.; Nuzillard, J. M.; Connolly, J. D.; Tsamo, E.; Morin, C. *Phytochemistry* **1993**, *34*, 1603-1607.
91. Ngnokam, D.; Nuzillard, J. M.; Bliard, C. *Bulletin of the Chemical Society of Ethiopia* **2005**, *19*, 227-231.
92. Connolly, J. D.; Phillips, W. R.; Mulholland, D. A.; Taylor, D. H. A. *Phytochemistry* **1981**, *20*, 2596-2597.
93. Harrison H. R.; Hodder, O. J. R. *Chem. Commun.* **1970**, 1388-1389.
94. Okorie, S. A.; Taylor, D. H. A. *Phytochemistry* **1977**, *16*, 2029-2030.
95. Tchouankeu, J. C.; Tsamo, E.; Sondengam, B. L.; Connolly, J. D.; Rycroft, D. S. *Tetrahedron Letters* **1990**, *31*, 4505-4508.
96. Daniewski, W. M.; Gumulka, M.; Pankowska, E.; Bloszyk, E.; Jacobsson, U.; Norin, T.; Szafranski, F. *Polish J. Chem.* **1994**, *68*, 499-504.
97. Daniewski, W. M.; Gumulka, M.; Danikiewicz, W.; Sitkowski, J.; Jacobsson, U.; Norin, T. *Phytochemistry* **1995**, *40*, 903-905.
98. Tchouankeu, J.-C.; Nyasse, B.; Tsamo, E.; Sondengam, B. L.; Morin, C. *Phytochemistry* **1992**, *31*, 704-705.
99. Garcia, J.; Morin, C.; Nyasse, B.; Sondengam, B.-L.; Tchouankeu, J.-C. *J. Nat. Prod.* **1991**, *54*, 136-142.
100. Tchouankeu, J. C.; Nyasse, B.; Tsamo, E.; Connolly, J. D. *J. Nat. Prod.* **1996**, *59*, 958-959.
101. Daniewski, W. M.; Gumulka, M.; Danikiewicz, W.; Gluzinski, P.; Krajewski, J.; Pankowska, E.; Bloszyk, E.; Jacobsson, U.; Norin, T.; Szafranski, F. *Phytochemistry* **1993**, *33*, 1534-1536.
102. Daniewski, W. M.; Gumulka, M.; Danikiewicz, W.; Gluzinski, P.; Krajewski, J.; Sitkowski, J.; Bloszyk, E.; Drozd, B.; Jacobsson, U.; Szafranski, F. *Phytochemistry* **1994**, *36*, 1001-1003.
103. Bevan, C. W. L.; Powell, J. W.; Taylor, D. A. H.; Halsall, T. G.; Toft, P.; Welford, M. *J. Chem. Soc.*

- (C) **1967**, 163–170.
104. Orisadipe, A. T.; Adesomoju, A. A.; D'Ambrosio, M.; Guerriero, A.; Okogun, J. I. *Phytochemistry* **2005**, *66*, 2324–2328.
  105. Bickii, J.; Tchouya, F. G. R.; Tchouankeu, J. C.; Tsamo, E. *African Journal of Traditional, Complimentary and Alternative Medicines* **2007**, *4*, 135-139.
  106. Amos, S.; Orisadipe, A.; Binda, L.; Emeje, E.; Adesomoju, A.; Okogun, J.; Akah, P.; Wambebe, C.; Gamaniel, K. *Pharmacology & Toxicology* **2002**, *91*, 71-76.
  107. Bevan, C. W. L.; Ekong, D. E. U.; Taylor, D. H. A. *Nature* **1965**, *206*, No 4991, 1323-1325.
  108. Chudnoff, M. *Tropical Timbers of the World* **1984**. USDA Forest Service. Ag. Handbook No. 607.
  109. Connolly, J. D.; McCrindle, R.; Overton, K. H.; Warnock, W. D. C. *Tetrahedron* **1967**, *23*, 4035-4039.
  110. Kadota, S.; Marpaung, L.; Kikuchi, T.; Ekimoto, H.; *Chem. Pharm. Bull.* **1989**, *37*, 1419-1421.
  111. Kokpol, U.; Chavasiri, W.; Tip-Pyang, S.; Veerachato, G.; Zhao, F.; Simpson, J.; Weavers, R. T. *Phytochemistry* **1996**, *41*, 903-905.
  112. Adesida, G. A.; Adesogan, E. K.; Okorie, D. A.; Styles, B. T. *Phytochemistry* **1971**, *10*, 1845-1853.
  113. Saewan, N.; Sutherland, J. D.; Chantrapromma, K. *Phytochemistry* **2006**, *67*, 2288-2293.
  114. Khalid S.A, Duddeck, H., Gonzalez-Sierra, M. *J. Nat Prod.* **1989**, *52*, 922-926.
  115. Mitsui, K.; Saito, H.; Yamamura, R.; Fukuya, H.; Hitotsuyanagi, Y.; Takeya, K. *J. Nat. Prod.* **2006**, *69*, 1310-1314.
  116. Connolly, J. D.; MacLellan, M.; Okorie, D. A.; Taylor, D. A. H. *J. Chem. Soc. Perkin Trans. 1* **1976**, 1993-1996.
  117. Abdelgaleil, S. A. M.; Okamura, H.; Iwagawa, T.; Doe, M.; Nakatani, M. *Heterocycles* **2000**, *53*, 2233-2240.
  118. Connolly, J. D.; Henderson, R.; McCrindle, R.; Overton, K. H.; Bhacca, N. S. *J. Chem. Soc.* **1965**, 6935-6948.
  119. Mootoo, B. S.; Ali, A.; Motilal, R.; Pingal, R.; Ramlal, A.; Khan, A.; Reynolds, W. F.; McLean, S. *J. Nat. Prod.* **1999**, *62*, 1514-1517.
  120. Abdelgaleil, S. A. M.; Doe, M.; Morimoto, Y.; Nakatani, M. *Phytochemistry* **2006**, *67*, 452-458.
  121. Olmo, L. R. V.; da Silva, M. F. G. F.; Fo, E. R.; Vieira, P. C.; Fernandes, J. B.; Pinheiro, A. L.; Vilela, E. F. *Phytochemistry* **1997**, *44*, 1157-1161.
  122. Saad, M. G. M.; Iwagawa, T.; Doe, M.; Nakatani, M. *Tetrahedron* **2003**, *59*, 8027-8033.
  123. Randrianarivelojosia, M.; Kotsos, M. P.; Mulholland, D. A. *Phytochemistry* **1999**, *52*, 1141-1143.
  124. Klaus Klumpp, K. *Expert Opin. Ther. Patents* **2004**, *14*, 1153-1168.
  125. Wang, G. T. *Expert Opin. Ther. Patents* **2002**, *12*, 845-861.
  126. Oxford, J. S.; Bossuyt, S.; Balasingam, S.; Mann, A.; Novelli, P.; Lambkin, R. *Clin. Microbiol. Infect.* **2003**, *9*, 1-14.
  127. Farina V.; Brown, J. D. *Angew. Chem. Int. Ed.* **2006**, *45*, 7330-7334
  128. Laver, G. ; Garman, E. *Science* **2001**, *293*, 1776-1777.
  129. Okamura, H. ; Nagaike, H. ; Nsiama, T. K. ; Iwagawa, T. ; Nakatani, M. *Heterocycles* **2006**, *68*, 2587-2594.

130. Taylor, N.R.; von Itzstein, M. *J. Med. Chem.* **1994**, *37*, 616-624.
131. Kim, C. U.; Lew, W.; Williams, M. A.; Liu, H.; Zhang, L.; Swaminathan, S.; Bischofberger, N.; Chen, M. S.; Mendel, D. B.; Tai, C. Y.; Laver, V. G.; Stevens, R. C. *J. Am. Chem. Soc.* **1997**, *119*, 681-690.
132. Rohloff, J. C.; Kent, K. M.; Postich, M. J.; Becker, M. W.; Chapman, H. H.; Kelly, D. E.; Lew, W.; Louie, M. S.; McGee, L. R.; Prsibe, E. J.; Schultze, L. M.; Yu, R. H.; Zhang, L. *J. Org. Chem.* **1998**, *63*, 4545-4550.
133. Federspiel, M.; Fischer, R.; Hennig, M.; Mair, H.-J.; Oberhauser, T.; Rimpler, G.; Albiez, T.; Bruhin, J.; Estermann, H.; Gandert, C.; Göckel, V.; Götzö, S.; Hoffmann, U.; Huber, G.; Janatsch, G.; Lauper, S.; Röckel-Stäbler, O.; Trussardi, R.; Zwahlen, A. *Org. Proc. Res. & Dev.* **1999**, *3*, 266-274.
134. Karpf, M.; Trussardi, R. *J. Org. Chem.* **2001**, *66*, 2044-2051.
135. Harrington, P. J.; Brown, J. D.; Foderaro, T.; Hughes, R. C. *Org. Proc. Res. & Dev.* **2004**, *8*, 86-91.
136. Abrecht, S.; Harrington, P.; Iding, H.; Karpf, M.; Trussardi, R.; Wirz, B.; Zutter, U. *Chimia* **2004**, *58*, 621-629.
137. Fukuta, Y.; Mita, T.; Fukuda, N.; Kanai, M.; Shibasaki, M. *J. Am. Chem. Soc.* **2006**, *128*, 6312-6313.
138. Mita, T.; Fukuda, N.; Roca, F. X.; Kanai, M.; Shibasaki, M. *Org. Lett.* **2007**, *9*, 259-262.
139. Yamatsugu, K.; Kamijo, S.; Suto, Y.; Kanai, M.; Shibasaki, M. *Tetrahedron Letters* **2007**, *48*, 1403-1406.
140. Cong, X.; Yao, Z.-J. *J. Org. Chem.* **2006**, *71*, 5365-5368.
141. Yeung, Y. Y.; Hong, S.; Corey, E. J. *J. Am. Chem. Soc.* **2006**, *128*, 6310-6311.
142. Satoh, N.; Akiba, T.; Yokoshima, S.; Fukuyama, T. *Angew. Chem. Int. Ed.* **2007**, *46*, 5734-5736.
143. Bromfield, K. M.; Graden, H.; Hagberg, D. P.; Olsson, T.; Kann, N. *Chem. Commun.* **2007**, *38*, 3183-3185.
144. (a) Nicolau, K. C.; Snyder, S. A.; Montagnon, Y.; Vassilikogiannakis, G. *Angew. Chem. Int. Ed.* **2002**, *41*, 1668-1698. (b) Diels, O.; Alder, K. *Justus Liebigs Ann. Chem.* **1928**, *460*, 98-122.
145. Brocksom, T. J.; Nakamura, J.; Ferreira, M. L.; Brocksom, U. *J. Braz. Chem. Soc.* **2001**, *12*, 597-622.
146. Corey, E. J. *Angew. Chem. Int. Ed.* **2002**, *41*, 1650-1667.
147. Okamura, H.; Nagaike, H.; Iwagawa, T.; Nakatani, M. *Tetrahedron Letters* **2000**, *41*, 8317-8321.
148. Okamura, H.; Nagaike, H.; Nsima, T. K.; Iwagawa, T.; Nakatani, M. *Heterocycles* **2006**, *68*, 2587-2594.
149. Posner, H. G.; Vinader, V.; Afarinkia, K. *J. Org. Chem.* **1992**, *57*, 4088-4097.
150. Luche, J.-L. *J. Am. Chem. Soc.* **1978**, *100*, 2226-2227.
151. Kan, T.; Fukuyama, T. *Chem. Commun.*, **2004**, 353-359.
152. Chankeshwara, S. V.; Chakraborti, A. K. *Org. Lett.*, **2006**, *8*, 3259-3262.